

This thesis has been submitted in fulfilment of the requirements for a postgraduate degree (e. g. PhD, MPhil, DClinPsychol) at the University of Edinburgh. Please note the following terms and conditions of use:

- This work is protected by copyright and other intellectual property rights, which are retained by the thesis author, unless otherwise stated.
- A copy can be downloaded for personal non-commercial research or study, without prior permission or charge.
- This thesis cannot be reproduced or quoted extensively from without first obtaining permission in writing from the author.
- The content must not be changed in any way or sold commercially in any format or medium without the formal permission of the author.
- When referring to this work, full bibliographic details including the author, title, awarding institution and date of the thesis must be given.

EXPLORING NOVEL DATA STORAGE APPROACHES FOR LARGE-SCALE NUMERICAL WEATHER PREDICTION

NICOLAU MANUBENS GIL



Submitted for the degree of Doctor of Philosophy

THE UNIVERSITY OF EDINBURGH

2025

Abstract

Driven by scientific and industry ambition, HPC and AI applications such as operational Numerical Weather Prediction (NWP) require processing and storing ever-increasing data volumes as fast as possible. Whilst POSIX distributed file systems and NVMe SSDs are currently a common HPC storage configuration providing I/O to applications, new storage solutions have proliferated or gained traction over the last decade with potential to address performance limitations POSIX file systems manifest at scale for certain I/O workloads.

This work has primarily aimed to assess the suitability and performance of two object storage systems —namely DAOS and Ceph— for the ECMWF’s operational NWP as well as for HPC and AI applications in general. New software-level adapters have been developed which enable the ECMWF’s NWP to leverage these systems, and extensive I/O benchmarking has been conducted on a few computer systems, comparing the performance delivered by the evaluated object stores to that of equivalent Lustre file system deployments on the same hardware. Challenges of porting to object storage and its benefits with respect to the traditional POSIX I/O approach have been discussed and, where possible, domain-agnostic performance analysis has been conducted, leading to insight also of relevance to I/O practitioners and the broader HPC community.

DAOS and Ceph have both demonstrated excellent performance, but DAOS stood out relative to Ceph and Lustre, providing superior scalability and flexibility for applications to perform I/O at scale as desired. This sets a promising outlook for DAOS and object storage, which might see greater adoption at HPC centres in the years to come, although not necessarily implying a shift away from POSIX-like I/O.

Lay summary

All consumer-level computers and cellphones nowadays keep data such as images and text in what are commonly known as files and directories, and these are in turn kept in hard disk drives (HDDs) and solid-state drives (SSDs) in computers, or in internal flash memory in cellphones. Files and directories were invented in the early years of computer systems and are both a necessary concept for computer systems to function, and a practical way for us humans to interact with computers.

Larger computers, for example in big research institutions, also use files and directories, but because the data volumes involved are so large, these are kept across many dedicated computers with several HDDs or SSDs each. The problems that need to be solved in such large computers have progressively become more ambitious and difficult, and scientists and programmers are struggling to move the data fast enough in and out between the large computer system and the dedicated storage computers. This is the case for example at the European Centre for Medium-Range Weather Forecasts (ECMWF), where very large simulations of the Earth system are run to predict the weather.

Different approaches to this issue are being taken in all fields of research and industry, such as producing and storing less data where possible, compressing them, and improving the programs or applications running on the large computer as well as those managing the the dedicated storage computers to make the most of the available resources. Some experts say that this slow data movement issue is in part due to using files and directories, which were designed for small computers in the early days, and are now not suitable anymore. Some have worked on a new alternative way of encapsulating and storing data in so called *objects*,

leaving behind the files and directories and all the associated standards and legacy programs, which they deemed a limiting factor. One well-known example of this was the early adoption of object-based storage by the Amazon company, in 2006, to manage and provide access to huge amounts of data distributed across their data centers.

Both file systems and object storage systems are very complex, with many moving parts, and it is therefore not easy to estimate the benefits of using one over the other, least when object storage requires carefully adapting the existing programs or applications to the mechanisms provided by this new paradigm.

This work has adapted the ECMWF’s operational weather forecasting software to function on two open-source object storage solutions —namely DAOS and Ceph—, and evaluated their suitability and performance benefits, both for the ECMWF’s use case and for other applications similarly entailing large data movement. While both were found to be suitable and able to provide advantages with respect to file systems, DAOS stood out reaching higher performance levels. This work shed some light on the performance aspect of object storage, and opened new doors for the ECMWF for future computer and storage system acquisitions.

Declaration

I declare that this thesis has been composed solely by myself, and that it contains only my work except where otherwise specified, or where the work is explicitly indicated below to have formed part of a jointly-authored publication. This work has not been submitted for any other degree or professional qualification.

Nicolau Manubens Gil

July 2025

Acknowledgements

This work has been conducted as part of a collaboration between the ECMWF and the EPCC at The University of Edinburgh. I am very grateful to both institutions for this unique opportunity.

Special thank you to Adrian Jackson for his constant guidance and patience during all these years, his invaluable insight, and his very substantial technical and paper contributions, as well as seeking systems where to conduct the analysis. It has been a privilege and a pleasure to have such an involved supervisor.

Special thank you to Tiago Quintino and Simon Smart; Tiago, for proposing this research idea and making this project possible, and for his invaluable guidance, insight, and contributions during these years; Simon, for his guidance, brilliant insight, and substantial contributions to the published papers and technical developments — particularly, the implementation of the FDB DAOS backends.

Thank you to Emanuele Danovaro for his insight, contributions, and dedication to the software infrastructure surrounding the FDB backends, without which this research would not have been possible.

Thank you to all the above and the rest of my colleagues at the ECMWF, from whom I have had the privilege of learning so much, and have all contributed to an ideal atmosphere for technical discussion and professional growth.

Thank you to the DAOS development team, especially Johann Lombardi and Mohamad Chaarwi, for their invaluable help and inputs provided for the development and evaluation of the FDB DAOS backends.

Thank you to Google Cloud and Dean Hildebrand for providing resources to conduct large part of the analysis, and for their help and insight.

Thank you to David Henty and Michele Guidolin for thoroughly examining this thesis and for their very valuable feedback, and thank you to Michael Bareford for his follow-up and feedback.

Last but most subjectively important, thank you to my parents, siblings, and close friends for their support and patience during these challenging years. Special thank you to my mother Isabel Gil González, my father Domingo Manubens Bertran, and my brother Domingo Manubens Gil.

Contents

List of Figures	xi
List of Tables	xix
1 Introduction	1
1.1 Contributions	6
1.2 Outline	8
2 Background	11
2.1 State of The Art	11
2.2 POSIX file systems	13
2.2.1 Lustre	17
2.3 DAOS	19
2.4 Ceph	22
2.5 Comparison of object storage and file system features	27
2.6 NWP at the ECMWF	30
2.7 The FDB	32
2.7.1 Store and Catalogue Interfaces	37
2.7.2 POSIX I/O backends	41
3 Object Storage Backends	65
3.1 DAOS backends	65
3.1.1 The DAOS Store	72
3.1.2 The DAOS Catalogue	75
3.1.3 Operational NWP I/O pattern on DAOS	81
3.1.4 fdb-hammer I/O pattern on DAOS	84
3.2 Ceph backends	86
3.2.1 The Ceph Store and Catalogue	93
3.2.2 Operational and fdb-hammer I/O patterns on Ceph	95
3.3 S3 Store	95

4 Performance Assessment	101
4.1 Methodology	103
4.1.1 Type of I/O operations and benchmarks	108
4.1.2 I/O patterns of interest	112
4.1.3 Parameter optimisation	113
4.1.4 Scaling the system and benchmark runs	114
4.1.5 Performance metrics	114
4.2 DAOS and Lustre on SCM	116
4.2.1 The NEXTGenIO system	116
4.2.2 Hardware performance measurements	118
4.2.3 IOR performance	120
4.2.4 Field I/O performance	125
4.2.5 FDB backend performance	129
4.2.6 Summary	139
4.3 DAOS, Ceph, and Lustre on NVMe SSDs	140
4.3.1 The Google Cloud Platform	140
4.3.2 Hardware performance measurements	144
4.3.3 IOR performance	144
4.3.4 FDB backend performance	149
4.3.5 Small object size performance	159
4.3.6 DAOS and Ceph data redundancy	160
4.3.7 DAOS interfaces	164
4.3.8 Summary	168
5 Conclusion	171
5.1 Future work	176
Bibliography	181
Appendix A – Performance Comparison of DAOS and Lustre for Object Data Storage Approaches	187
Appendix B – DAOS as HPC Storage: a View from Numerical Weather Prediction	195
Appendix C – Reducing the Impact of I/O Contention in Numerical Weather Prediction Workflows at Scale Using DAOS	209
Appendix D – Exploring DAOS Interfaces and Performance	223

List of Figures

2.1	Illustration of the high-level APIs provided by libdaos.	20
2.2	Illustration of the high-level APIs provided by librados.	24
2.3	Comparison of features provided by Lustre, DAOS, and Ceph. .	28
2.4	Illustration of the FDB, a domain-specific object storage library abstracting away underlying storage systems, providing functionality to store and retrieve meteorological data objects.	32
2.5	Snapshot of the content of a dataset directory after a process has called FDB archive() four times for four meteorological objects for two different collocation keys. The archive() calls are shown at the top, using different colours for the dataset, collocation, and element keys. flush() has not been called yet, thus the index files are empty as the indexing structures are still held in memory at this point. The object data may or may not have been persisted into storage media at this point.	44
2.6	Content held in memory by a process after calling FDB archive() four times for four meteorological objects for two different collocation keys, before flush() is called.	48
2.7	Snapshot of the content of a dataset directory after a process has called FDB archive() four times for four meteorological objects for two different collocation keys, after flush() has been called. All data objects and indexing information required to access them has been persisted into storage media at this point. close() has not been called yet and therefore the full index files are still empty. .	50
2.8	Snapshot of the content of a dataset directory after a process has called FDB archive() a few times, then flush(), then archive() a few more times, and then flush() again. The partial indexing information for all archive() calls before a flush() call is appended to the partial index and sub-TOC files.	51

2.9	Content held in memory by a process after calling FDB archive() a few times, then flush(), then archive() a few more times, and then flush() again. The partial indexes and information are reset, and the full indexes and information accumulate new entries for all archive() calls during the lifetime of the process.	52
2.10	Snapshot of the content of a dataset directory after an archive()ing process has terminated and Catalogue close() has been called. New entries are appended to the TOC file pointing to the full indexes, and the sub-TOCs and partial indexes are masked.	53
2.11	Not based on real profiling. Illustration of a simplification of the ECMWF's operational NWP storage access pattern. Three I/O server nodes archive weather fields produced by the NWP model, using multiple parallel processes per node (p1-p6), for three simulation time steps. At the end of every simulation step the archived fields are flushed, and a post-processing job (PGEN) is launched for that step. The third PGEN job has been omitted. Every PGEN job runs on one node and lists and retrieves data using multiple processes per node (p1-p6). The proportions of the durations for the different types of operation in real operational runs might significantly differ from the ones displayed in this illustration. Real operational runs currently use 260 I/O nodes and 4 to 8 nodes per PGEN job, and archive data for 144 time steps.	56
2.12	Not based on real profiling. Illustration of a simplification of the storage access pattern of the fdb-hammer benchmark. One writer node archive()s weather fields for three time steps using multiple parallel processes per node (p1-p6). At the end of every step the archived fields are flushed. One reader node simultaneously retrieves pre-archived data using an equivalent set of parallel processes (p1-p6) performing equivalent sequences of retrieve() operations. Each reader process loads the content of the TOC file, then loads one full index from one index file, and reads all fields from a single data file — these index and data files have been written by the corresponding writer process. The proportions of the durations for the different types of operation in real fdb-hammer runs might significantly differ from the ones displayed in this illustration. Real fdb-hammer runs performed in this analysis employed up to 24 writer and 24 reader nodes, with up to 48 processes per node, and were run for 100 time steps.	61

3.1	Diagram of DAOS entities resulting from an FDB archive() call for one meteorological object. The archive() call is shown at the top, using different colours for the dataset, collocation, and element keys. The object data and indexing information are persisted immediately. A flush() call would result in no additional changes to these entities.	67
3.2	Diagram of DAOS entities resulting from four FDB archive() calls for four meteorological objects spanning two different collocation keys (one having levtype=sfc and the other levtype=pl) and two different element keys (one having step=1 and the other step=2).	78
3.3	Not based on real profiling. Illustration of a simplification of the ECMWF’s operational NWP storage access pattern using the FDB DAOS backends. The PGEN job for the third simulation step has been omitted. The proportions of the durations for the different types of operation in real operational runs might significantly differ from the ones displayed in this illustration.	82
3.4	Not based on real profiling. Illustration of a simplification of the storage access pattern of the fdb-hammer benchmark on DAOS. The proportions of the durations for the different types of operation in real fdb-hammer runs on DAOS might significantly differ from the ones displayed in this illustration. Real fdb-hammer runs performed in this analysis employed up to 24 writer and 24 reader nodes, with up to 48 processes per node, and were run for 100 time steps. . . .	86
3.5	Performance of the FDB Ceph/RADOS backends with different options enabled. Measured with fdb-hammer runs on 32 client nodes, using 16 processes per node, against a Ceph deployment on 16 OSD nodes with 6 TiB of NVMe SSDs each. RADOS pools were configured with 512 placement groups and no replication or erasure-coding. Every process archive()d or retrieve()d 10000 weather fields of 1 MiB each. The mean of the bandwidths obtained for 3 repetitions are shown for each configuration. Using a RADOS object per archive()d FDB object resulted in best performance. Using a RADOS object per archive() call and ensuring persistence on flush(), shown with patterned columns, did not fulfill the consistency requirements.	90
3.6	Diagram of Ceph/RADOS entities resulting from an FDB archive() call for one meteorological object. The archive() call is shown at the top, using different colours for the dataset, collocation, and element keys. The object data and indexing information are persisted immediately. A flush() call would result in no additional changes to these entities.	92

4.1	Plausible timeline of I/O operations and delays in a non-synchronised parallel I/O benchmark run. Only the writer phase of a run of the "no write+read contention" access pattern is represented. ©2023 IEEE.	115
4.2	NEXTGenIO architecture.	117
4.3	Example Lustre and DAOS configurations for comparison. An additional node was employed for Lustre MDTs.	118
4.4	Ideal write and read bandwidths of a NEXTGenIO node used as networked storage server.	120
4.5	Bandwidths for IOR runs against a 2+1-node Lustre deployment in NEXTGenIO. Every process accessed a separate file and performed 100 x 1MiB I/O operations. Tests were repeated 5 times.	121
4.6	Bandwidths for IOR runs against a 2-node DAOS deployment in NEXTGenIO. Every process wrote or read 100 x 1MiB objects. Tests were repeated 5 times.	122
4.7	IOR bandwidth scalability against increasingly large Lustre and DAOS deployments in NEXTGenIO. A ratio of 4-to-1 client-to-server nodes was used except for hollow dots, and 36 to 72 processes were run in each client node. Every process performed 100 x 1MiB I/O operations. Tests were repeated 5 times. ©2022 IEEE.	123
4.8	Bandwidth scalability of Field I/O runs, with no write+read contention, against increasingly large DAOS deployments in NEXTGenIO. A ratio of 2-to-1 client-to-server nodes was used except for hollow dots, and 36 to 48 processes were run in every client node. Every process wrote and indexed, or de-referenced and read, 2000 x 1MiB weather fields. Tests were repeated 10 times. ©2023 IEEE.126	
4.9	Bandwidth scalability of Field I/O runs, with write+read contention, against increasingly large DAOS deployments in NEXTGenIO. A ratio of 2-to-1 client-to-server nodes was used except for hollow dots, and 36 to 48 processes were run in each client node. Every process wrote and indexed (or de-referenced and read) 2000 x 1MiB weather fields. Tests were repeated 10 times.	127
4.10	Bandwidths of Field I/O runs on 16 client nodes, with no write+read contention, against a 8-node DAOS deployment in NEXTGenIO, varying field size and object sharding configuration. 36 processes were run in each client node. Every process wrote and indexed (or de-referenced and read) 100 x 1MiB weather fields. Tests were repeated 5 times.	128

4.11 Field I/O bandwidth scalability against increasingly large Lustre and DAOS deployments in NEXTGenIO. A ratio of 2-to-1 client-to-server nodes was used, and 24 to 48 processes were run in each client node. Every process wrote and indexed (or de-referenced and read) 2000 x 1MiB weather fields. Tests were repeated 5 times. ©2022 IEEE.	130
4.12 fdb-hammer and Field I/O bandwidth scalability, with no write+read contention, against increasingly large Lustre and DAOS deployments in NEXTGenIO. A ratio of 2-to-1 client-to-server nodes was used except for hollow dots, and 16 to 48 processes were run in each client node. Every process wrote and indexed (or de-referenced and read) 10000 x 1MiB weather fields. Tests were repeated 3 times.	131
4.13 fdb-hammer and Field I/O bandwidth scalability, with write+read contention, against increasingly large Lustre and DAOS deployments in NEXTGenIO. A ratio of 2-to-1 client-to-server nodes was used except for hollow dots, and 16 to 48 processes were run in each client node. Every process wrote and indexed (or de-referenced and read) 10000 x 1MiB weather fields. Tests were repeated 3 times.	134
4.14 Profiling results for fdb-hammer/DAOS runs without (top row) and with (bottom row) write+read contention, using 10 server and 20 client nodes; 32 processes per client node. Every process wrote and indexed (or de-referenced and read) 10000 x 1MiB weather fields.	136
4.15 Profiling results for fdb-hammer/Lustre runs without (top row) and with (bottom row) write+read contention, using 10 server and 20 client nodes; 32 processes per client node. Every process wrote and indexed (or de-referenced and read) 10000 x 1MiB weather fields.	137
4.16 VM types used for benchmarking on GCP.	141
4.17 Example Lustre, Ceph, and DAOS configurations for comparison. An additional node was employed for Lustre MDTs and Ceph Monitors.	142
4.18 Ideal write and read bandwidths of a GCP VM of type n2-custom-36-153600 used as networked storage server.	145
4.19 Bandwidths for IOR runs against Lustre, DAOS, and Ceph deployments on 16 VMs (+1 for Lustre and Ceph). Every process performed 10000 x 1MiB I/O operations (100 x 1MiB for Ceph). Tests were repeated 3 times.	146

4.20 IOR bandwidth scalability against increasingly large Lustre, Ceph, and DAOS deployments on GCP. A ratio of 2-to-1 client-to-server nodes was used for all tests, and 16 to 32 processes were run in each client node. Every process performed 10000 x 1MiB I/O operations (100 x 1 MiB for Ceph). Tests were repeated 3 times.	148
4.21 fdb-hammer bandwidth scalability, with no write+read contention, against increasingly large Lustre, Ceph, and DAOS deployments on GCP. A ratio of 2-to-1 client-to-server nodes was used for all tests, and 16 to 32 processes were run in each client node. Every process wrote and indexed (or de-referenced and read) 10000 x 1MiB weather fields. Tests were repeated 3 times.	149
4.22 fdb-hammer bandwidth scalability, with write+read contention, against increasingly large Lustre, Ceph, and DAOS deployments on GCP. A ratio of 2-to-1 client-to-server nodes was used for all tests, and 16 to 32 processes were run in each client node. Every process wrote and indexed (or de-referenced and read) 10000 x 1MiB weather fields. Tests were repeated 3 times.	151
4.23 Profiling results for fdb-hammer/DAOS runs without (top row) and with (bottom row) write+read contention, using 20 server and 40 client nodes; 24 processes per client node. Every process wrote and indexed (or de-referenced and read) 10000 x 1MiB weather fields.	154
4.24 Profiling results for fdb-hammer/Ceph runs without (top row) and with (bottom row) write+read contention, using 20 server and 40 client nodes; 24 processes per client node. Every process wrote and indexed (or de-referenced and read) 10000 x 1MiB weather fields.	155
4.25 Profiling results for fdb-hammer/Lustre runs without (top row) and with (bottom row) write+read contention, using 20 server and 40 client nodes; 12 processes per client node. Every process wrote and indexed (or de-referenced and read) 10000 x 1MiB weather fields.	156
4.26 Bandwidths for fdb-hammer runs with small object size on 8 client VMs against Lustre, DAOS, and Ceph deployments on 4 VMs (+1 for Lustre and Ceph). Every process performed 10000 x 1KiB I/O operations. Tests were repeated 3 times.	160
4.27 fdb-hammer bandwidth scalability, with no write+read contention, against increasingly large Ceph, and DAOS deployments on GCP, using a replication factor of 2. A ratio of 2-to-1 client-to-server nodes was used for all tests, and 16 to 32 processes were run in each client node. Every process wrote and indexed (or de-referenced and read) 10000 x 1MiB weather fields. Tests were repeated 3 times.	162

4.28	fdb-hammer bandwidth scalability, with no write+read contention, against increasingly large Ceph, and DAOS deployments on GCP, using 2+1 erasure-coding. A ratio of 2-to-1 client-to-server nodes was used for all tests, and 16 to 32 processes were run in each client node. Every process wrote and indexed (or de-referenced and read) 10000 x 1MiB weather fields. Tests were repeated 3 times.	163
4.29	Bandwidths for IOR/HDF5 runs against DAOS and Lustre deployments on 16 VMs (+1 for Lustre). Every process performed 10000 x 1MiB I/O operations. Tests were repeated 3 times.	166
4.30	Bandwidths for Field I/O runs using dummy libdaos against DAOS and Lustre deployments on 4 VMs (+1 for Lustre). Every process performed 1000 x 1MiB I/O operations. Tests were repeated 3 times.	167

List of Tables

2.1	Comparison of the dimension of ECMWF's operational NWP runs and fdb-hammer runs performed in Chapter 4.	61
4.1	Process-to-process transfer rates with PSM2 and TCP.	119

Chapter 1

Introduction

Driven by scientific and industry ambition, computer systems have steadily and rapidly evolved since their inception nearly eight decades ago, with frontline High-Performance Computing (HPC) systems currently providing on the order of one exaFLOPS (10^{18} floating-point operations per second) of processing power and tens of TB/s (10^{12} bytes per second) of storage bandwidth[1, 2, 3, 4]. Traditionally, HPC practitioners have striven to adopt new hardware technology and adapt software and applications to efficiently leverage the increasingly capable resources, facing new challenges along the way as the technology landscape evolved.

As we enter the Exascale era, one of the most prominent challenges, besides handling the unprecedented high degree of complexity and heterogeneity of HPC systems, is that of handling the extremely large and ever-increasing data volumes that the greater processing power now makes possible to process and produce. Although this challenge was also present to an extent in previous epochs, it is more marked this time due to a bigger leap in processing power unmatched by storage capability, and due to certain data access patterns becoming more commonly used, mainly by Artificial Intelligence (AI) applications, which can add significant strain on current storage systems[5].

In consequence, HPC systems —both large and small— now need to be more carefully designed to achieve the right balance between processing and storage capability, maximizing overall system performance while minimizing total cost of ownership. This requires exploring best ways of combining the storage hardware options available in the market, as well as ensuring the software layer of the storage system —typically a parallel file system nowadays— is aware and makes efficient use of the hardware topology. Simultaneously, an additional effort is required to ensure HPC and AI applications make the most of the available storage resources by revisiting and if necessary optimizing their Input-Output (I/O) logic, or even shifting to new I/O approaches both at the application and storage software levels.

Regarding storage hardware, despite the current gap between processing and storage capability, there certainly have been advances in the recent years impacting the design of modern-day HPC systems. Most remarkably, there were upgrades in the Peripheral Component Interconnect Express (PCIe) standard and in network technologies such as Ethernet and Infiniband, enabling large sets of storage devices such as Solid-State Drives (SSDs) distributed over a high-performance network to provide higher aggregate I/O throughput than ever before. Currently, SSDs are usually attached to a set of nodes in the HPC system devoted to high-performance storage and exposed as a single view to compute nodes, but are also often used in other configurations including compute-node-local storage, fast caching tiers interfacing slower storage devices such as Hard Disk Drives (HDDs), or pools of disaggregated fast storage devices which can be mounted and exploited individually by any one node in the network. HDDs, on the other hand, were relegated to providing affordable capacity in high-performance storage systems with fast SSD-based cache tiers, as well as providing fast caching themselves in slower tape-based data archives[6].

Also noteworthy, a new non-volatile memory technology, namely 3D Xpoint,

was developed and marketed in PCIe and Dual Inline Memory Module (DIMM) form factors, offering a new latency and capacity trade-off and thus filling the gap in the storage hierarchy between Dynamic Random-Access Memory (DRAM) and SSDs[7]. Storage devices within this echelon of the hierarchy are also commonly referred to as Storage Class Memory (SCM). 3D Xpoint, however, was unfortunately discontinued in 2022 due to a lack of demand.

Regarding storage software, parallel file systems such as Lustre and IBM Storage Scale remained the most widespread software-level approach for high-performance storage in HPC systems. These file systems also evolved in recent years with new capability and performance enhancements, and were made able to exploit fast storage hardware tiers as those became available. Despite their popularity, parallel file systems can manifest performance limitations at scale for certain I/O workloads due to fundamental design aspects (see Chapter 2), calling for I/O optimization at the application level—which is often challenging—or even consideration of alternative or complementary storage software approaches to ensure efficient usage of the hardware resources.

In that respect, of particular relevance to this work, the past two decades have seen the object storage paradigm flourish, giving way to technologies such as the S3 (Amazon Simple Storage Service) protocol and the Ceph and DAOS object stores, which all gained traction both in Cloud and HPC environments. Object stores break away from the parallel file system standards, implementations, and approaches, and offer new Application Programming Interfaces (APIs) and semantics revolving around objects, which hold blobs of data of any size and are lightweight in metadata. They also generally provide key-value or dictionary objects such that entries can be inserted—each associating a key to a value—and queried with strong consistency guarantees. To varying extents, on a case-by-case basis, object stores are designed in ways which potentially enable them to overcome

the performance limitations of parallel file systems at scale.

All these hardware and software developments facilitated storage tiering and boosted the storage capability per node and per cost unit, ultimately providing means to combat the imbalance relative to processing power. Nevertheless, the challenge still persists and requires constant review of the I/O logic and exploration of new storage approaches at HPC centres.

One exemplar HPC application this work has particularly focused on is large-scale Numerical Weather Prediction (NWP) as conducted operationally at the European Centre for Medium-Range Weather Forecasts (ECMWF). The application produces large amounts of time-critical forecast data which need to be stored into the distributed file system that is currently part of their HPC system, and simultaneously read back and processed during an operational run to then be disseminated to stakeholders within strict deadlines. The large scale of the simulation and the high degree of write-read contention require the various components of the application to be implemented following certain I/O programming best practices to ensure high performance and data consistency.

Over the past decades, the ECMWF has developed and used operationally a middleware I/O library, namely the FDB, which abstracts away the I/O programming complexity and reduces the overall software complexity of the application. The FDB has been iteratively and aggressively optimised to make as efficient use as possible of the storage resources available. Notwithstanding these efforts, at present, a significantly large and costly storage system is still necessary to handle the operational I/O workload with enough margin to avoid performance issues that can manifest under excessive contention.

Looking forward, the ECMWF plans to increase the resolution of the operational simulations in the coming years[8], likely giving continuity to the so far exponential growth in data volumes and further exacerbating the I/O performance

issue. Because the ECMWF newly procures its HPC system every four years, there might be opportunities in the future to increase I/O capability and re-balance the system, potentially mitigating this.

In light of these facts, exploration and evaluation of new storage hardware and alternative or complementary storage software approaches have become paramount duties for the success of the ECMWF's mission.

Latest generations of storage hardware should be evaluated and adopted, even though new generations of processing hardware may potentially offset the benefits of the former. Regarding storage software, given parallel file systems can manifest performance limitations at scale, simply procuring one of larger size than the current might be less cost-effective than adopting other more efficient storage software approaches, if there were any.

This dissertation work has primarily aimed to evaluate the suitability and performance of the Ceph and DAOS object stores, both specifically for the ECMWF's operational NWP as well as for HPC applications in general. This work has also aimed at evaluating, on one hand, the performance of 3D Xpoint DIMM devices and, on the other hand, the options and challenges of porting the ECMWF's NWP to the S3 storage protocol for additional compatibility with other storage solutions.

In the course of this work, new software-level adapters have been developed which enable the FDB, and by extension the ECMWF's NWP workflows, to operate on the evaluated storage systems and protocols. Extensive benchmarking has been conducted on two HPC systems where Ceph and DAOS were deployed, using both generic and NWP I/O benchmarks, and the observed performance has been compared to that of equivalent Lustre parallel file system deployments on the same hardware. The challenges and advantages of porting to object storage have been evaluated along the way.

1.1 Contributions

The contributions of this work consist of:

A Documentation of the ECMWF’s storage software stack: The ECMWF’s operational systems, applications, and access patterns have been further documented, primarily focusing on the FDB library and its techniques to make efficient use of parallel file systems at scale. Whilst already covered in existing literature[9, 10, 7], this thesis has more thoroughly documented these matters with additional information collated from discussion with a number of the ECMWF’s staff members, review of internal documentation, and analysis of the FDB’s source code and applications. This will provide useful information and guidance for future I/O-related developments at the centre.

Part of this work has been presented as a poster at a technical meeting[11].

B Object storage adapters for the ECMWF’s NWP workflows: New adapters, or backends, have been developed which enable the FDB, and by extension the ECMWF’s NWP workflows, to operate on the DAOS and Ceph object stores, as well as on storage systems conforming to the S3 storage protocol. This has opened new doors for the ECMWF to consider and exploit these storage solutions if made available in future systems, projects, or collaborations. The different options and challenges encountered in the course of these developments have been discussed, providing insight of relevance to other HPC practitioners needing to port applications to these storage systems and protocols.

Best practices for porting HPC applications to object stores have been documented and presented at a technical user meeting[12] and as part of a conference tutorial[13]. The development of the FDB DAOS backend has been documented

and published in a conference paper[14], and presented in a scientific workshop[15] and a technical user meeting[16]. The development of the other FDB backends has been documented in this dissertation, and the source code of all backends has been made publicly available in the ECMWF’s FDB GitHub repository[17].

C I/O performance assessment methodology: A methodology has been defined for the performance assessment of I/O systems and applications, which provides guidance on how to approach exploration and optimization of the extensive parameter domain in this type of assessments. It is sufficiently general that it can be used to guide assessment of other I/O systems and developments.

D Suitability and performance assessment of Ceph and DAOS for the ECMWF’s operational NWP: A comprehensive analysis of the Ceph and DAOS object stores including functionality, consistency, and performance aspects has been conducted, aiming to determine the suitability of these stores for operational NWP at the ECMWF. The types of storage hardware tested included Non-Volatile Memory Express (NVMe) SSDs and 3D Xpoint DIMMs. This analysis has resulted in relevant insight for the ECMWF to consider for future HPC system procurements or other acquisitions.

Part of this work has been published in a conference paper[18] and a workshop paper[19], and the rest has been documented in this dissertation.

E Fair performance comparison of DAOS, Ceph, and Lustre: The DAOS, Ceph, and Lustre storage systems have been deployed on the same hardware and exercised both with generic and NWP I/O benchmarks, and their performance and scalability have been measured and compared. This had not been documented previously in such a rigorous apples-to-apples comparison,

and will provide insight to the HPC community and I/O practitioners.

Part of this work has been published in the workshop paper mentioned in the second contribution and in another workshop paper[20], and presented at a technical user meeting[21]. The rest has been documented in this dissertation.

1.2 Outline

Chapter 2 provides background information on the storage systems evaluated in this work, and compares them in terms of their features and limitations. It also provides a detailed explanation of the ECMWF’s operational systems, workflows, and storage software stack, particularly focusing on the FDB library and its backend for efficient operation on parallel file systems.

Chapter 3 describes the newly developed FDB backends that enable operation on the selected object stores and storage protocols, including discussion on the options and challenges encountered along the development process.

Chapter 4 presents an I/O performance assessment of the DAOS and Ceph object stores, including performance and scalability results obtained from running various benchmarks against these object stores deployed on two different HPC systems. The performance of the object stores is compared to that of equivalent Lustre file system deployments on the same hardware. The analysis includes a performance evaluation of the data redundancy features in DAOS and Ceph, and an analysis of the performance impact of using different I/O interfaces provided by DAOS.

Chapter 5 concludes with a summary of the most relevant findings and higher-level conclusions, and suggests avenues for future work.

The conference and workshop papers mentioned in 1.1 Contributions have been inserted in this dissertation as Appendix A[20], Appendix B[18], Appendix C[14],

and Appendix D[19], as these document a substantial part of the accomplished work and contributions. The most relevant material and results in these papers have been included and discussed again in the body of this dissertation, and the dissertation further expands those with additional results and discussion. The rest of the results in the papers have been referenced where relevant with a pointer to the corresponding paper and section.

Chapter 2

Background

This chapter introduces concepts relevant to the understanding of the contributions of this dissertation, ranging from file systems, through high-performance object stores, to the ECMWF’s current storage libraries used for operational NWP. This also includes a comparison of features and limitations across file systems and object stores, as well as a review of related work.

Part of this chapter therefore addresses the first contribution of the dissertation, *"Documentation of ECMWF’s storage software stack"*.

Beyond the concepts introduced in this chapter, this dissertation also assumes prior knowledge of high-performance computer and storage systems. An excellent overview of some of the most relevant introductory concepts is given in Section 2 of Sarah Neuwirth’s PhD. dissertation[22].

2.1 State of The Art

There have been several research works on how to exploit and utilise novel storage technology such as SCM and object storage on the path to adapting I/O to Exascale.

Some have focused on the benefits of object storage as opposed to commonly used file systems and their limitations[23, 24, 25]. Others have focused on adapting I/O middleware to exploit object storage, with some reports of satisfactory performance[26, 27, 28, 29]. There have also been reports of successful outcomes using object storage via file system[30] and block device interfaces[31].

Some have gone beyond file system and I/O middleware APIs and developed domain-specific object stores building on top of general-purpose object stores and low-level non-volatile memory (NVM) storage libraries, and verified the benefits of that approach[32]. This includes the ECMWF’s previous work on the FDB[9], which originally exploited POSIX file systems, and was later adapted to make native use of SCM[10] and the Ceph RADOS and Cortx Motr object stores. Part of the conclusions of the ECMWF’s work were that a PMEM (Persistent Memory) backend was difficult to maintain, and RADOS did not at the time provide sufficient performance. Of the remaining storage options, Motr was discontinued in 2023.

The Intel’s Optane Data Center Persistent Memory Module (DCPMM) —the only ever relevant SCM option in the market— was unexpectedly discontinued in 2022 due to a lack of demand. Object stores, nevertheless, have continued to gain traction, and this is also true for DAOS despite the fact that it originally required SCM to function — it shifted to supporting NVMe-only systems shortly after Optane was discontinued[33]. A few object stores became increasingly present in IO-500 performance rankings[4], with a few large institutions at the top after adopting object storage often as a backend for the file system APIs commonly used by their applications[34].

The work in this dissertation describes newly developed FDB backends which enable native FDB operation on DAOS and Ceph, and discusses the implementation and performance differences between running realistic NWP I/O workflows

with the new object storage backends vis-à-vis the traditional POSIX backend on Lustre. This research significantly advances the understanding of the place of object storage in the storage landscape for HPC systems and discusses some of the features, configurations, and challenges this approach presents both for the ECMWF’s NWP and for HPC applications in general.

2.2 POSIX file systems

In the early years of computer systems, standard subroutines were developed to facilitate data I/O from and to persistent storage, and these I/O developments were integrated and continued as part of the UNIX family of operating systems —first released in the 70s— and the C programming language —first released in 1972—, crystallizing eventually as the standard file system API, largely as we know it today. This API revolves around the file and directory concepts, which enable encapsulation and organisation of data.

The file system API was included as part of the ISO POSIX.1 (Portable Operating System Interface) standard, first published in 1990[35, Chapter 2]. POSIX was broadly adopted by most computer vendors, and the file system API thus became tightly integrated with most operating systems and programming languages, paving the way for the development of vast amounts of applications relying on this API in the following decades. To this day it is still the most widely used I/O API for persistent storage.

POSIX defined a standard interface for file and directory operations such as `open`, `close`, `write`, `read`, `stat`, and so forth, but left flexibility for file systems to implement these as desired. Since the publication of POSIX, file systems have evolved significantly to support growing storage capacities and provide higher performance, resulting in the creation of a range of file systems designed for

specific operating systems, workloads, and hardware configurations.

Early file systems relied on relatively simple mechanisms. File data was stored in fixed-size *blocks* —the smallest unit of allocation; typically 4 KiB or smaller—, and an *inode* data structure was maintained for every file, containing file metadata and pointers to the corresponding data blocks. The blocks corresponding to a file could be contiguous or scattered in storage media depending on fragmentation and allocation strategy.

A region at the beginning of the storage medium —the superblock— was usually reserved for metadata describing the overall file system layout and contained a table of inodes and directory entries mapping file names to inode structures. When a file was accessed, the operating system typically cached its inode and block mappings in memory to accelerate subsequent operations. Blocks were fetched from storage as atomic units and mapped and cached into system memory via pages —typically 4 KiB in size—, although some systems also supported hugepages —larger memory pages from a few MiBs up to a few GiBs in size— to reduce the overheads associated to the management of many small pages for large file access.

As file systems matured, new mechanisms were introduced to improve reliability and performance. One major development was the introduction of log-structured file systems. These systems treated storage as a circular log, appending all updates sequentially. This minimized disk seeks and allowed fast writes, especially on spinning disks. However, log-structured systems often required complex garbage collection logic to reclaim space and suffered from write overheads as the system was further populated with data.

Journaled file systems later emerged as a solution to the problem of data corruption due to unexpected shutdowns. In these systems a journal —or log— records metadata updates before they are applied to the file system. This allows the system to recover to a consistent state after a crash by replaying the journal.

The journal is typically held in a dedicated area on disk and is managed by the file system. Some implementations —e.g. ext3— only journal metadata, while others —e.g. NTFS and XFS— can optionally journal both metadata and data. Among local file systems, ext4 is one of the most widely used in Linux. It is a journaled file system and provides features for efficient block allocation and reduced fragmentation.

More recent innovations include copy-on-write (COW) file systems like Btrfs and ZFS, which enhance reliability by never overwriting existing data. Instead, updates are written to new blocks, and only after success are block pointers updated. Also, these systems use advanced techniques for more efficient block indexing.

In parallel to local file systems, the need for shared access in distributed computing led to the development of networked file systems. One of the earliest and most influential was the Network File System (NFS), developed by Sun Microsystems. NFS enables clients to mount remote directories over a network as if they were local. It relies on caching and periodic refreshes to maintain consistency across clients and servers, with the drawbacks that this can lead to consistency issues and cause significant overheads in highly concurrent workloads. Its successor, NFSv4, provides solutions to some of these issues, although it is still in the process of being fully implemented and adopted.

For HPC and data-intensive workloads, specialized distributed file systems such as Lustre and GPFS emerged. These file systems combine storage resources distributed across multiple networked nodes, leveraging local file system instances on each node to manage the local resources, and expose these as a single view while preserving the POSIX semantics and consistency guarantees of a single-node local file system. This enables distributed file systems to scale to larger capacities while providing higher throughput by concurrently serving data and I/O operations

from multiple storage nodes.

Typically, distributed file systems are deployed as separate metadata and data servers. When a client requires accessing a file, it first establishes a connection with a metadata server, which handles file namespaces and access control, and is then redirected to the relevant data servers where file data is to be written or read from.

To avoid the communication overheads when repeatedly accessing the same file, or when accessing a recently written file, most distributed file systems by default cache written and read data pages in client memory. In turn, this implies that written data is by default not persisted immediately on storage media, and applications need to issue an explicit system call or close the open file to ensure data persistence.

Due to this caching approach, maintaining strict consistency across clients and servers and fully complying with the POSIX semantics is one of the most challenging aspects of the design of distributed file systems. POSIX mandates that all write and read operations must be consistent. That is, a read operation initiated right after a write operation on the same file extent must see the data being written by the write operation, and a write operation initiated right after a read operation must not modify the original data before it is fully returned to the reader. Distributed file systems commonly accomplish this by implementing a distributed locking mechanism such that every client process opening a file for write or read must request a lock from a lock server —involving a network round-trip— for the target file extent before writing or reading that extent from storage, and in case of conflicting I/O the last racing process blocks until it obtains the lock it requested. Any issued set of conflicting write and read operations is thus guaranteed to be consistent and free of interruptions or failures due to I/O conflicts, although this can result in large lock communication overheads on the

client nodes for highly contentious workloads[36, 37, 38].

To mitigate this, some recent distributed file systems such as GlusterFS, GFS, or VAST —when accessed via its file system interface—, have given up some of the POSIX consistency guarantees, often deemed as excessive for write-once-read-many workloads, in favor of performance.

2.2.1 Lustre

Lustre[39] is a fully POSIX-compliant distributed file system widely used nowadays in HPC environments which can exploit HDDs and SSDs as well as Remote Direct Memory Access (RDMA) networks. Lustre has been used in this work as a reference for performance comparison vis-à-vis other storage approaches due to its popularity and the fact that it is currently being used and has been used operationally at the ECMWF for more than a decade.

Lustre is deployed as a set of Metadata Servers (MDSs) and Object Storage Servers (OSSs) on the available storage nodes, with either an MDS or an OSS typically deployed on every storage node. An MDS handles metadata aspects such as file namespaces and access control, and can often benefit from being deployed on a faster storage hardware tier if available. An OSS, on the other hand, is usually deployed on a node with large-capacity storage hardware, and serves bulk file data and handles negotiation of locks on local files with the clients. Both the MDSs and the OSSs leverage underlying local file systems, such as `ldiskfs` or `ZFS`, to manage the storage hardware.

While Lustre deployments in most cases encompass multiple OSSs on multiple —often several— storage nodes, a single MDS on a single node can be sufficient for small to medium-scale instances. Nevertheless, multiple MDSs can be deployed on multiple nodes for larger instances if required, and the metadata workload can be distributed over the available MDSs by utilizing the Lustre’s Distributed Name

Space (DNE) feature. DNE supports two different modes of operation; DNE1, which allows system administrators to delegate metadata handling for a selected file system directory—or sub-tree—to a specific MDS other than the first; and DNE2, which allows the user to enable balanced distribution of the metadata workload for a given directory over a configurable number of MDSs.

Clients interact with both the MDSs and OSSs to write and read files in parallel. Lustre does not implement algorithmic placement, and this implies that for every metadata operation performed, such as a file `open`, `stat`, `unlink`, or `mkdir`, a client needs to interact with an MDS. Once a file is opened, `write` and `read` operations are performed directly against the corresponding OSSs.

Every OSS manages a set of Object Storage Targets (OSTs) deployed on the same node, with every OST serving data for a separate local file system deployed on a subset of the storage resources in the node. Files in Lustre can be sharded—or *striped*—, such that the file is split in parts—or *stripes*—and every stripe is placed in a separate OST. The size of the stripes to split the file into and the number of OSTs to distribute the resulting stripes over can be configured at a per-directory or file level. Striping enables parallel and therefore faster access to a same file, exploiting the aggregate bandwidth of the storage devices and network interfaces of multiple storage nodes.

Lustre does not currently provide software-level fault tolerance mechanisms such as erasure-coding. For that purpose, either specialised hardware can be employed, or `mdadm` used at the local file system level to create RAID setups.

2.3 DAOS

The Distributed Asynchronous Object Store (DAOS)[40] is an open-source high-performance object store designed for massively distributed NVM, including SCM—which resides in the memory domain of a compute node—and NVMe SSDs. DAOS was originally developed by Intel but was recently transferred to the DAOS foundation, with HPE—one of the founding members—actively maintaining and developing it.

DAOS provides low-level key-value storage functionality on top of which other higher-level APIs, also provided as part of DAOS, are built. DAOS's features include transactional non-blocking I/O, fine-grained I/O operations with zero-copy I/O to SCM, end-to-end data integrity, and advanced data protection. The OpenFabrics Interfaces (OFI) library is used for low-latency communications over a wide range of network backends.

DAOS is deployable as a set of I/O processes or *engines*—generally one per physical socket in a server node—, each managing access to NVM devices associated with the socket. Graphical examples of how engines, storage devices, and network connections can be arranged in a DAOS system can be found at [41].

An engine partitions the storage it manages into *targets* to optimize concurrency, each target being managed and exported by a dedicated group of threads. DAOS allows reserving space distributed across targets in *pools*, a form of virtual storage. A pool can serve multiple transactional object stores called *containers*, each with their own address space and transaction history.

The low-level key-value DAOS API is provided in the `libdaos` library, and it exposes what is commonly known as a map or dictionary data structure, with the feature that every value indexed in it is associated to two keys: the distribution key (*dkey*) and the attribute key (*akey*). All entries indexed under a same dkey are collocated in the same target, and the akeys identify the different entries under

a same dkey. Listing dkeys and akeys is supported. This is an advanced API and not commonly used by third-party libraries using DAOS.

High-level key-value and array APIs are also provided as part of `libdaos`, both building on top of the low-level API. These are illustrated in Fig. 2.1.

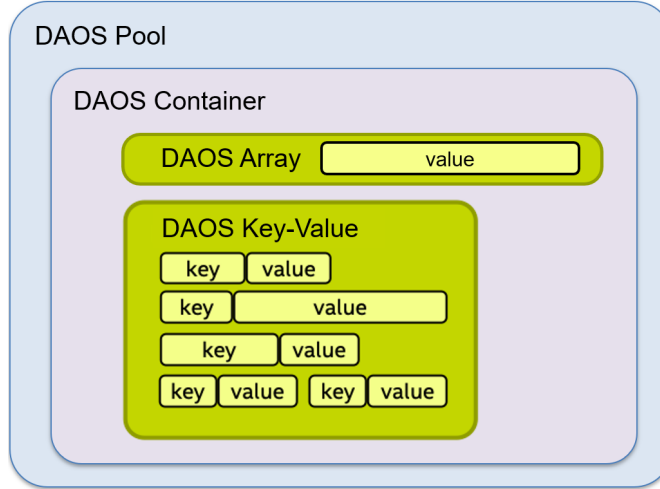


Figure 2.1: Illustration of the high-level APIs provided by libdaos.

The high-level key-value API exposes a single-key dictionary structure, where limited-length character strings (the *keys*) can be mapped onto byte strings of any length (the *values*). Entries can be added or queried with the transactional `daos_kv_put` and `daos_kv_get` API calls. Querying the size of an entry and listing keys is also supported.

The array API is intended for bulk-storage of large one-dimensional data arrays. An in-memory buffer can be stored into DAOS or populated with data retrieved from DAOS with the transactional `daos_array_write` and `daos_array_read` API calls. These operations support targeting one or multiple byte ranges with arbitrary offset and length.

Upon creation, key-value and array objects are assigned a 128-bit unique object identifier (OID), of which 96 bits are user-managed. These objects can be configured for replication, erasure-coding, and striping across pool targets by

specifying their *object class*. If configured with striping, for instance, they are transparently stored by parts in different low-level dkeys and thus distributed across targets, enabling concurrent access analogous to Lustre file striping.

DAOS also provides a `libdfs`[42] library which implements POSIX directories, files and symbolic links on top of the described APIs, such that an application including this library can perform common file system calls—with slightly different function names—which are transparently mapped to DAOS. `libdfs` is, however, not fully POSIX-compliant and does not support features such as the atomicity of `mkdir`, appending to a file after opening it with the `O_APPEND` flag, and advisory locks. A File System in User Space (FUSE) daemon—namely DFUSE—and interception library are also distributed as part of DAOS for use by existing applications using the POSIX file system API without modification.

Other interfaces provided by DAOS include S3 and NVMe-oF.

An important feature of DAOS, if compared to POSIX distributed file systems, is that contention between writer and reader processes is resolved server-side with Multi-version Concurrency Control (MVCC) rather than via distributed locking on the clients. When a write operation is issued, it is immediately persisted by the server in a new region or object in storage, with no read-modify-write operations. The new object is then atomically indexed in a persistent index kept in low-latency SCM or in a write-ahead log on NVMe, and the write operation returns successfully. Any subsequent read operation for that object triggers visitation of the index and returns the associated data from the corresponding storage regions across the servers. This way, writes always occur in new regions without modifying data potentially being read, and reads always find the latest fully written version of the requested object in the corresponding index entry. This mechanism not only ensures strong consistency guarantees but also avoids the use of locks and the associated overheads.

Another relevant feature of DAOS is that it implements algorithmic placement—that is, algorithmically determining which server node an object should be written to or read from before any interaction with the storage system occurs—and this means metadata operations are performed against all server nodes in DAOS, rather than on dedicated metadata servers which can potentially bottleneck and hinder performance at scale.

In terms of authentication and authorisation, the DAOS pools and containers can be configured via Access Control Lists (ACLs) to allow read-only or write-read access to different users. The client processes attach their effective UNIX user and group in every I/O operation sent to the server, and these are used to determine access permissions according to the ACLs.

2.4 Ceph

Ceph[43, 44] is an open-source distributed storage system designed to operate on commodity hardware, with a focus on resilience and data safety to support failures of such hardware. Although data safety was prioritised over high performance, Ceph was designed to scale up to large amounts of storage resources.

It became popular in Cloud environments mainly due to the fact that, among other purposes, it can be used as a backend to provide virtual machine images, in a way that the resources used for compute and storage can be detached and managed independently. Also, the fact that it can be accessed via the S3 object storage protocol contributed to its popularity in Cloud.

Ceph is software-defined. It can be deployed on any commodity hardware and is not dependent on specific hardware. The types of storage device it can exploit include HDDs, SATA or SAS SSDs, and NVMe SSDs. Regarding networking, it can only exploit TCP/IP networks out of the box, although there are ongoing

developments to support native operation on low-latency networks with DPDK and RDMA[45].

Ceph was architected as a set of services or daemons that can be deployed on different nodes and scaled independently, and these services provide the core storage functionality. Additional daemons can be deployed on additional nodes or on top of the existing ones to provide additional functionality. A minimal Ceph cluster has at least one Object Storage Daemon, or OSD, one Monitor daemon, and one Manager daemon.

An OSD daemon manages storage devices in a storage node. One or more OSDs may be deployed in a single node, each managing a subset of the devices. OSDs can exploit raw devices directly without the need of an intermediate local file system. The OSD daemon stores object data and maintains a metadata index in the devices it manages. Each OSD requires between 2 and 4 GiB of DRAM to function, and can be configured to build the index on faster storage hardware if available.

A Monitor daemon keeps an up-to-date map of the state of the cluster —also known as *OSD map*—, which describes which OSDs are available in the system and which are down, and how they are organised in nodes, racks, and so forth. The Monitor serves the OSD map to clients when required. For high availability, multiple Monitors should be deployed in a Ceph system, from 3 to 7. The different Monitor replicas reach agreement on a consistent view of the OSD map with the Paxos algorithm. The monitor also acts as manager for the other daemons in the system, and acts as the central authority for authentication. A Ceph monitor node requires 32 GiB of DRAM for small clusters, and up to 128 GiB for very large ones.

The Manager daemon aggregates and exposes system metrics. Two instances should be deployed for high availability, and each requires approximately 32 GiB

of DRAM.

A system with these three daemons is also referred to as a Reliable Autonomous Distributed Object Store (RADOS), or also as a Ceph Storage Cluster.

RADOS exposes an object storage API, and client applications can interact with it via the `librados` library[46]. Every object in RADOS is identified with a name, and can have attributes. There are two types of objects: regular objects, which are similar to files or DAOS arrays in the sense that they store a string of bytes, and `Omaps`, which provide key-value functionality akin to the DAOS key-values. These are illustrated in Fig. 2.2.

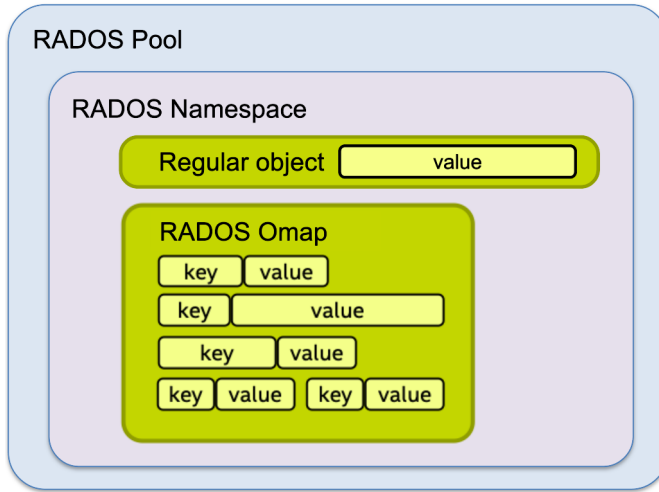


Figure 2.2: Illustration of the high-level APIs provided by librados.

Objects are stored within *pools*, which are a form of partitioning of the storage often used to contain data for different applications. For example, one pool could contain virtual machine images for Cloud infrastructure, another could contain media or data files, and so forth. Pools are identified by name, and by default span all OSDs in the system, although they can be assigned to specific subsets of OSDs on creation.

Pools can be configured to replicate or erasure-code the objects they contain, resulting in replicas or chunks of the objects distributed across multiple OSDs.

In contrast to DAOS, RADOS objects cannot be replicated or erasure-coded individually as it is a per-pool setting. Also, RADOS objects cannot be sharded other than by enabling erasure-coding, and Omaps cannot be erasure-coded.

Objects in a RADOS pool can be placed in *namespaces*, such that the names of the objects in a given namespace do not collide with the names of those in another namespace, akin to DAOS containers.

Like DAOS, RADOS implements algorithmic placement and achieves strong consistency with a mechanism similar to MVCC. When an object write is performed, the client first retrieves an up-to-date copy of the OSD map if it does not have one already, and then calculates a list of OSDs the object should be written to based on the object name and the OSD map. The first OSD in the list is selected as primary. The client then transfers the object data directly to the calculated primary OSD without prior roundtrips to a centralised set of metadata servers. Once the OSD has persisted the data in storage media, it sends copies to any other OSDs that should keep replicas or erasure-coding chunks, and only after all replicas or parts are persisted the index on the primary OSD is updated and the write operation is acknowledged. A reader requesting that same object does the same calculations to determine the primary OSD, which is then queried to retrieve the object data, finding always the latest version made available in the index. Since RADOS does not implement client-side caching, there are no concerns regarding consistency of any such caches.

To achieve efficient recovery in case of hardware failures, RADOS does not determine the placement of every object individually. Instead, objects in a pool are internally grouped in *placement groups* (PGs), and all objects assigned to a same PG end up being placed by the algorithm in the same set of OSDs. Why this grouping is necessary is further explained in [47].

By default, RADOS automatically adjusts how many PGs are used —always

aiming to have 100 PGs per OSD—, although the PG count can also be set manually on pool creation. The overall RADOS performance can be very sensitive to this parameter.

A drawback of the PG concept is that, because OSDs usually manage storage devices of a few TiB of capacity, PGs usually end up being a few GiB in size, thus the objects in them cannot be very large. In fact, RADOS is designed to handle objects of up to a few MiB in size, and it imposes an object size limit of 128 MiB by default. This limit can be adjusted when deploying a RADOS cluster, but using larger sizes is discouraged and results in low performance. Because of this, if a large data element such as a video file of a few GiB needs to be stored in RADOS, the application must first split it in parts, and assign a different name to each part.

Ceph provides a few higher-level interfaces or layers which build on top of RADOS, and this includes the Rados Gateway, or RGW, providing S3 object storage functionality; the Rados Block Device, or RBD, which tightly integrates RADOS with the Linux kernel to provide virtual machine images and block devices; and the Ceph File System, or CephFS, which provides POSIX distributed file systems.

Both the S3 and POSIX layers solve the limitation of small objects in RADOS in a transparent way, allowing applications to use S3 objects and POSIX files as large as desired and breaking them down into small RADOS objects under the hood. However, when using any of these, the key-value functionality that RADOS Ommaps provide if using `librados` directly is lost.

2.5 Comparison of object storage and file system features

Fig. 2.3 summarises and compares the most relevant features of Lustre —the exemplar distributed file system chosen for this analysis—, DAOS, and Ceph — the two open-source high-performance object stores considered. From top to bottom:

- Lustre delegates metadata serving to a set of designated nodes separate from the bulk storage nodes, whereas both DAOS and Ceph implement algorithmic placement such that clients communicate directly with the relevant storage nodes which also serve the associated metadata. Object stores therefore have potential to more efficiently handle large-scale metadata-intensive workloads.
- Lustre implements client-side caching and it is enabled by default, whereas the object stores do not implement it in their core, although their corresponding file system interfaces do implement caching. This means Lustre can provide a performance advantage for small-scale applications that do not overflow the caches, which object stores could never provide if accessed natively.
- Lustre is tightly ingrained in the operating system, and this implies many context switches between user space and the kernel are required both on the client and server sides while performing I/O, both for file operations and network communications. DAOS, instead, was carefully implemented to operate fully user-space to avoid these overheads. If using TCP communications over the fabric, however, DAOS will involve the kernel. Ceph is also largely designed to run user-space, but it does not currently support RDMA networks, and therefore always involves the kernel to a certain degree for TCP communications.

Feature	Lustre	DAOS	Ceph
Algorithmic placement		●	●
Centralised metadata	●		
Client-side caching	●	●	●
Kernel involved	●		●
Strictly consistent	●	●	●
Immediately persistent	●	●	●
Provides POSIX files/directories	●	●	●
Provides objects		●	●
Provides key-values		●	●
Software-level data safety		●	●
High-performance networks	●	●	
Byte-addressable		●	
Zero-copying		●	
Can exploit fast storage tier	●	●	●
Supports HDDs	●		●
Can scale to O(10k) nodes	●	●	●
High perf. for GiB objects	●	●	
High perf. for MiB objects		●	●
High perf. for KiB objects		●	

● Yes ● Can do ■ No

Figure 2.3: Comparison of features provided by Lustre, DAOS, and Ceph.

- In terms of consistency, all storage systems provide strong guarantees. Lustre achieves this via distributed locking, and DAOS and Ceph do so with MVCC.
- Lustre does not by default guarantee immediate persistence of writes, although there are flags and system calls available for applications to ensure persistence. DAOS and Ceph, instead, persist all I/O operations before returning unless using their file system interfaces.
- While Lustre provides file and directory APIs, and DAOS and Ceph provide

object and key-value APIs, the latter storage systems also provide file and directory APIs for POSIX I/O access with varying degrees of compliance.

- DAOS and Ceph provide software-level redundancy and erasure-coding, whereas Lustre does not.
- Lustre and DAOS can exploit high-performance fabrics natively out of the box, whereas Ceph can not.
- Lustre builds on top of the block device infrastructure and therefore fetches data from storage in entire blocks even if requesting only one or a few bytes. DAOS, instead, is designed to provide byte-level access to data. Ceph, at least if accessing erasure-coded objects, currently fetches the full object extent even if a partial range is accessed.
- DAOS is the only storage system carefully implemented to avoid unnecessary copies between storage media, intermediary library buffers, and kernel and network buffers. Data is transferred directly from storage media to client memory.
- The three storage systems can exploit low-latency storage hardware, if available, for superior overall performance.
- DAOS cannot exploit HDDs—it is exclusively designed for NVM—whereas Lustre and Ceph can.
- The three storage systems are designed to scale to tens of thousands of storage nodes.
- Regarding performance at different I/O sizes, DAOS is the only storage system that provides high performance for small, medium, and large object sizes, as demonstrated in Chapter 4. Lustre does not perform well when spreading data

across many small or medium files, and Ceph does not perform well when using a few large objects nor large amounts of very small objects.

2.6 NWP at the ECMWF

The ECMWF is an intergovernmental organization aiming, among other duties, to provide its member and cooperating states with global weather forecasts of time periods ranging from a few days to a few weeks into the future[48]. The states —specifically their national meteorological and hydrological services— then use these global forecasts as boundary conditions for their own regional NWP models which are run periodically to produce localized forecasts and take action accordingly.

As part of the ECMWF’s operational procedure, their NWP models are run in an in-house HPC system composed of thousands of compute nodes and a Lustre parallel file system providing 1.5 PiB of SSD-based storage[49]. During an operational run, which lasts approximately one hour —but cannot last longer than that as per committed deadlines—, the models presently produce approximately 95 TiB of forecast data, which are stored into the parallel file system. Those data are read back from storage, while the models continue to run, and post-processed to generate derived products, of much smaller size, to be delivered to member states together with the forecast data[7].

This application presents two challenges. On one hand, the large problem size requires partitioning the model domain into sub-domains which are processed in parallel across the compute nodes. In turn, every node employs several parallel processes for the execution of its corresponding model sub-domain to fully exploit the computing resources, and all these processes need to store their output into the parallel file system as it is produced, concurrently. This high degree

of I/O parallelism needs to be supported by the file system while maintaining high performance, and requires I/O to be performed in particular ways at the application level to minimize strain on the file system. In practice, at the ECMWF, this is addressed in part by funneling I/O through a set of designated I/O nodes to reduce the degree of parallelism before I/O hits the storage system—a technique also known as I/O forwarding—but also by adhering to certain best practices for high-performance I/O on parallel file systems[50] such as employing a separate file per writer process and configuring large files to be distributed across multiple storage nodes—also known as sharding or striping—to unlock their aggregate bandwidth. These approaches ensure writing of model output is performed as fast as the file system allows, causing the least possible impact on the progress of model processes, which sit in the critical path of an operational run.

On the other hand, post-processing of model output cannot be performed on the fly in the compute nodes where model sub-domains are run, and this is because post-processing requires visibility of the full model domain. Instead, model output is forwarded to I/O servers as it is produced and written into the storage system, and separate post-processing jobs read data back for the full domain from storage while model processes continue to produce and write output. This results in a highly contentious write-read access pattern where every post-processing job reads data across a large number of files being continually written into by model processes. Again, the storage system needs to be able to handle such contention and large number of file access operations without deteriorating performance, and I/O needs to be performed—and is performed—in particular ways at the application level to avoid data and metadata corruption and minimize performance impact.

The ECMWF developed an I/O library over the past few decades, namely the FDB[10], which exposes a scientifically meaningful API for applications to easily

write and read forecast data, abstracting away the underlying file system and the associated I/O programming complexity. A significant effort was made over the years to optimize the FDB’s internal I/O logic and mechanisms, maximizing I/O performance and reducing strain on the parallel file system during operational runs whilst ensuring data consistency under contention.

2.7 The FDB

The FDB[9, 10] is a domain-specific object store for meteorological data, which sits between various data producing and consuming components in wider NWP workflows. In practice, it is a software library which is compiled into these components, and provides them with functionality to easily and efficiently store and retrieve meteorological data elements or objects into and from persistent storage systems. The library is provided along with a set of management command-line tools, and configurations and data governance rules allowing adjustment of the patterns in which the storage is accessed. The FDB exists to abstract away the specific behavioural details of various underlying storage systems, and to provide a standardised API for high-performance data use.

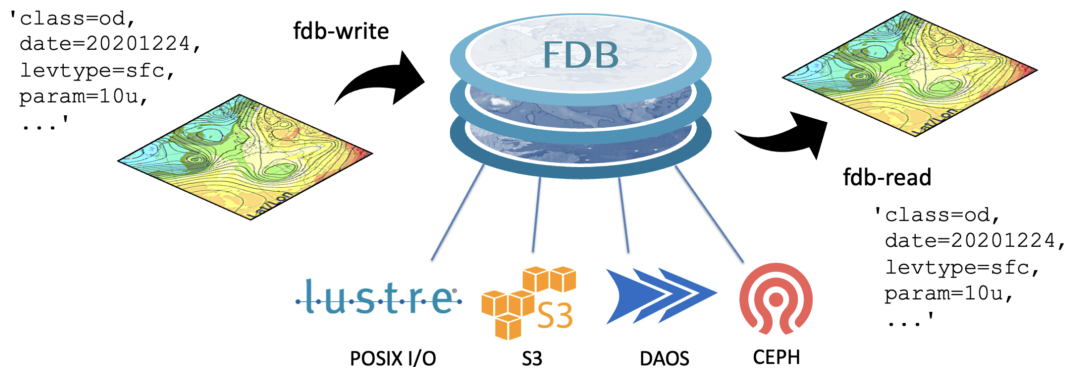


Figure 2.4: Illustration of the FDB, a domain-specific object storage library abstracting away underlying storage systems, providing functionality to store and retrieve meteorological data objects.

The FDB, under the hood, creates and maintains an index of stored objects in persistent storage. The need for this index stems from the fact that it is usually not possible to map small meteorological data objects one-to-one to the APIs or storage units (e.g. files) provided by storage systems whilst maintaining high performance, and therefore objects need to be collocated in shared storage units. Discovery and querying of stored objects —a necessary feature for ECMWF’s operational workflows— would be too expensive to perform without an index.

The FDB API is metadata-driven, that is, all API actions are invoked using scientifically-meaningful metadata describing the data to be acted upon. All data objects —usually weather fields— are identified by a globally unique metadata identifier, formed as a set of key-value pairs conforming to a user-defined schema. An example identifier for a weather field from an operational ensemble forecast is illustrated in Listing 2.1.

Listing 2.1: An example metadata identifier of a weather field in the FDB.

```
class = od,           expver = 0001,           stream = oper,
date = 20231201,     time = 1200,             type = ef,
levtype = sfc,       step = 1,                 number = 13,
levelist = 1,         param = v
```

The schema defines not only the valid object identifier keys and values, but also how the FDB will internally split the identifiers provided by the user application into three sub-identifiers which control how the FDB storage logic lays out data within the storage system, and therefore control the storage access patterns:

1. **Dataset key:** describes the dataset an object belongs to. For instance, a forecast produced today starting at midday. For example, if the schema is configured to recognise `class`, `stream`, `expver`, `date` and `time` as dataset

dimensions, the following dataset key would result for Listing 2.1:

```
class = od,           expver = 0001,
stream = oper,        date = 20231201,
time = 1200
```

2. **Collocation key:** the object should be collocated in storage with other objects sharing the same collocation key. E.g.:

```
type = ef,           levtype = sfc
```

3. **Element key:** identifies the object within a collocated dataset. E.g.:

```
step = 1,           number = 1,
levelist = 1,       param = v
```

Aside from a number of administrative functions, there are four primary functions in the FDB API, namely `archive()`, `flush()`, `retrieve()`, and `list()`. Their signatures, with some simplification, are shown in Listing 2.2.

Listing 2.2: Simplified signatures of the primary FDB API methods.

```
void archive(const Identifier& id, DataHandle& data);

void flush();

DataHandle* retrieve(const IdentifierList& query);

IdentifierIterator list(const PartialIdentifier& query);
```

Applications can use the `archive()` method to request archival—that is, writing and indexing—of a meteorological data object by providing its metadata identifier

together with a data handling object which manages a pointer to the object data in memory. Usually, data producers have multiple objects available for archival simultaneously, and in that case a more efficient variant of the `archive()` method can be used which accepts as only input a single data handling object managing the full set of data objects and identifiers. Producer applications are expected to `archive()` data for one or a few dataset keys, on the order of ten collocation keys, and up to millions of element keys.

`flush()` must be called to ensure any previously `archive()`d objects are persisted into storage and made visible to consumers. This method should typically be called as infrequently as possible, as persisting small amounts of data separately and frequently may cause large overheads. For example, in the ECMWF’s operational workflow, `flush()` is called by I/O servers only at the end of a simulation step, to ensure the step data is made visible before signaling the workflow manager to trigger execution of the post-processing task for that step.

Consumers call the `retrieve()` method providing as only input a list of identifiers of the objects to be read back. This only fetches information from the index on the location of the objects in storage, and that information is encapsulated in a data handling object and returned to the application. The actual object data can then be read from storage through this data handle.

The `list()` method enables applications to query which objects are available in storage with identifiers matching a provided partial identifier.

The FDB API has precisely determined semantics. In particular[10]:

1. Data is either visible, and correctly indexed, or not. The FDB adheres to the ACID[51] (Atomicity, Consistency, Isolation, and Durability) semantics commonly used to define database transactions.
2. `archive()` blocks until the FDB has taken control of (a copy of) the data.

Data is not necessarily visible to consumers or persisted in storage devices at this point, but it is permitted to be.

3. `flush()` blocks until all data `archive()`d from the current process is persisted into the underlying storage medium, correctly indexed, and made visible and accessible to any reading process via `retrieve()` and `list()`.
4. Once data is made visible, it is immutable.
5. Data can be replaced by `archive()`ing a new piece of data with the same metadata. This second `archive()` shares the semantics of the first, such that the old data is visible until the new data is fully persisted and indexed.

The FDB provides adapters or backends for operation on a range of storage systems. These backends are responsible for ensuring that the described semantics are correctly implemented on top of whatever provisions are made by the underlying storage system.

The FDB internally implements indexing functionality in what is known as a Catalogue backend, and functionality for storage —bulk write and read— of meteorological objects in a Store backend. The FDB defines abstract interfaces for these backends, such that specific Catalogue or Store instances can be implemented to operate on top of a given type of storage system. If backends conform to the established interfaces and semantics, the FDB will guarantee its external API semantics. Any pair of conforming Catalogue and Store backends can then be used in conjunction even if they operate on different underlying storage systems.

When an FDB API method is called, the FDB library determines which Store and Catalogue backends to use according to configuration provided by the FDB administrator at deployment time.

2.7.1 Store and Catalogue Interfaces

Both the Store and Catalogue backend interfaces define `archive()`, `flush()` and `retrieve()` methods. Leaving aside some complexity, the Catalogue interface also defines `list()` and `axis()` methods. A call to the high-level FDB API will result in internal calls to the corresponding methods in the lower-level backend interfaces. Specifically:

- an FDB `archive()` call internally calls Store `archive()` and then Catalogue `archive()`.
- `flush()` calls Store `flush()` and then Catalogue `flush()`.
- `retrieve()` calls Catalogue `axis()` and `retrieve()`, and then Store `retrieve()`.
- `list()` calls Catalogue `list()` (neglecting some complexity).

The Store Interface

archive()

A Store backend must implement an `archive()` method accepting, as arguments, a pointer to in-memory data, a dataset key, and a collocation key. The data is taken control of and optionally persisted into storage before the method returns. An object location descriptor —equivalent to a Uniform Resource Identifier (URI)— is returned describing where the data is to be persisted. This location should be collocated with other fields sharing the same collocation key. The storage location must be unique, avoiding collisions with concurrent processes — `archive()` will potentially be called repeatedly with the same dataset and collocation key, and previously archived objects must not be overwritten or modified.

flush()

The `flush()` method blocks until all data which has been `archive()`d has been persisted to permanent storage and made accessible to external reading processes.

retrieve()

Given an object location descriptor, the Store `retrieve()` method builds and returns a `DataHandle` —a backend-specific instance of an abstract reader object—, allowing the calling process to read the object from storage without knowledge of the backend implementation.

When multiple objects are requested via the top-level FDB `retrieve()` method, that method may merge the `DataHandles` returned by the corresponding Store `retrieve()` calls, such that as few I/O operations as possible are issued to the storage system when reading data from the merged `DataHandle`. This can help avoiding unnecessary overheads if the requested objects are collocated within a same storage data structure (e.g. a same file or object) or placed in consecutive regions in storage. For this, the `DataHandles` returned by Store `retrieve()` must support merging.

The Catalogue Interface

A Catalogue backend has more complexity than a Store backend, not only because it addresses a more complex problem —that of maintaining a consistent index under contention— but also because it is involved in more operations, including archival, retrieval, removal, and listing. The Catalogue interface comprises more than ten methods, but only the ones required for field archival, retrieval, and listing are covered here, with some simplification.

archive()

Catalogue backends require an `archive()` method such that, given a dataset key, a collocation key, an element key, and an object location descriptor (from an

earlier `Store archive()` call), an entry is inserted in an indexing structure, either in local memory or shared storage, mapping the element key to the provided location descriptor. Once the entry is inserted, the method returns with no return value. This may be a local in-memory operation, and is not guaranteed to be persistent or visible to reading processes on return. The backend may make use of the dataset and collocation keys, and knowledge of the process performing the write operation, to index related information together, or separately, as makes most sense for performance on the targeted storage system.

flush()

`flush()` must also be implemented, which blocks until all indexing information has been persisted and made visible to any external `retrieve()`ing processes.

One of the requirements of Catalogue archival is that all indexing information `archive()`d and `flush()`ed by any parallel writers should be accessible to `retrieve()`ing and `list()`ing processes in a reasonably efficient manner. This may require helper data structures to be present, such as summaries of the indexed data which can be retrieved from a superficial layer of the index. If `archive()`ing processes persist indexing information in separate data structures or storage units (e.g. files), higher level shared indexing structures may be required such that all indexing information can be discovered and reached from a single entry point.

The index must always be consistent from the perspective of an external reading process, even under read and write contention. If multiple `archive()` calls with same dataset, collocation, and element keys occur, the older data should be replaced by newer in a transactional manner from the perspective of any reading processes.

axis()

Although not captured by Listing 2.2 due to oversimplification, the identifiers provided to the top-level FDB `retrieve()` method can contain expressions to

request retrieval of multiple objects matching one such expression. When called, the FDB `retrieve()` method first expands those expressions into fully specified object identifiers, using both the schema definition and the output from Catalogue `axis()` calls, and forwards those identifiers to the Catalogue `retrieve()` method.

The `axis()` method accepts as inputs a dataset key, a collocation key, and the name of one element key dimension, and returns a vector with all indexed values for that dimension for the given dataset and collocation keys. As suggested earlier, this information should ideally be made available and retrieved from a superficial summary rather than requiring a deep scan of the entire indexing structure.

retrieve()

The Catalogue `retrieve()` method must return the object location descriptor of an object given its dataset, collocation, and element keys. Due to the potential for the use of the FDB as a cache in a larger data infrastructure, failing to find a field is not an error and results only in no data being returned. The returned location descriptor, if any, can then be passed as an argument to the Store `retrieve()` method to obtain a `DataHandle` through which the actual data can be read.

list()

The Catalogue `list()` method must return a list of all `archive()`d object identifiers and location descriptors for a given dataset matching a partial identifier provided as input. The partial identifier represents a span of the domain of possible object identifiers, and the information for all indexed objects within this span must be returned.

When the FDB `list()` method is called, the FDB scans a registry of possible storage systems and locations within them where FDB datasets may be found. This registry is maintained by the FDB administrator and must be previously made available to applications using the FDB API. The Catalogue `list()` method

is then called internally for every dataset found within the registered storage systems and locations which matches the dataset key part of the partial identifier provided as input, and the results of all calls are merged and returned.

2.7.2 POSIX I/O backends

The logic for the FDB to operate on file systems originally constituted the core of the library. As the ECMWF’s HPC systems evolved over the years, the FDB was adapted to operate on the new file systems made available. The POSIX standard was first released in 1990, and in the late 90s and early 2000s POSIX distributed file system software such as the GPFS (today known as IBM Storage Scale) and Lustre gained traction and were adopted by HPC centres including the ECMWF. When the FDB Catalogue and Store abstractions were put in place in 2020, the logic of the FDB to operate on POSIX file systems was encapsulated as the POSIX I/O Catalogue and Store backends.

These backends aim to make as efficient use as possible of the file and directory APIs provided by POSIX distributed file systems to implement the required meteorological object indexing and bulk storage functionality. To that end, the backends were designed following two guiding principles. The first lay in adhering to I/O programming best practices for high performance on file systems, and this included avoiding use of many small files, reducing the number of I/O operations, and avoiding file contention where possible. The second principle lay in favoring write performance at the expense of read performance where there was the choice, to avoid throttling model progress as much as possible.

The POSIX backends store data and indexing information in a directory per dataset key. That is, all `archive()`d objects identified with a same dataset key are placed, together with their indexing information, under a same directory. For example, in the ECMWF’s operational case, all weather fields for an operational

run use the same dataset key and are therefore placed in a same directory along with indexing information.

For every parallel process performing FDB `archive()` operations for data objects for a same dataset and collocation key pair, four files are created within the dataset directory. One contains the data of the objects `archive()`d, and the other three contain indexing information for those objects. To avoid immediately persisting many small objects and indexing information very frequently, which would slow down the writing, these objects are only made persistent in storage—in the per-process files—when `flush()` is called.

Also, a high-level shared indexing file is created in the dataset directory which contains an index of all per-process indexing files, binding them together and making them easily and efficiently discoverable.

Fig. 2.7 illustrates the directory and files created for an example case where a single process calls `archive()` four times for four different objects—all sharing a same dataset key—and then calls `flush()` once. The same collocation key is used for the first two `archive()` calls, and another collocation key is used for the other two calls.

How these files are populated in a consistent and efficient way and used for retrieval and listing is explained in the following.

The FDB POSIX I/O Store

archive()

When the POSIX Store `archive()` method is called, the dataset directory is created, if it does not exist, using a stringified representation of the input dataset key as directory name. This is done with a `mkdir` system call which guarantees atomicity of the operation even if multiple processes call `archive()` for an object with a new dataset key concurrently.

Also, the first time `archive()` is called by a process for a new dataset and collocation key pair, the backend creates a unique file within the dataset directory where all data objects `archive()`d by that process for that key pair will be written. To ensure the file is unique, it is named as a function of the input collocation key, current system time, host name, process ID, and a process-local counter. The data file is then opened in append mode (using the `O_APPEND` flag of the `open` system call) and kept open for the lifetime of the `archive()`ing process.

Every time `archive()` is called, the object data provided as input is written at the end of the data file. However, this is not done directly. To avoid the overheads of performing large amounts of small write operations if a long sequence of small data objects are `archive()`d by a process—as the I/O servers do in the ECMWF’s operational runs—, the data is buffered in process memory, and only written in large bursts as the buffer becomes full. To that end, streamed I/O as provided by the `stdio` library is employed (i.e. using the `fopen`, `setvbuf`, and `fwrite` functions). Furthermore, if the operating system is configured in write-back mode, the data may be temporarily held in the kernel’s page cache before it is sent to the storage system and persisted. The `archive()`d data is therefore not guaranteed to be persisted immediately as it may be held in process or kernel memory.

A location descriptor for the object is finally returned, composed of the path name of the containing data file, the file offset the object data was written at (but not necessarily persisted), and the object data length. Because the file is exclusive to the process, the file region allocated for a new object is guaranteed to be only allocated for that object.

If the underlying POSIX file system is a Lustre distributed file system, the POSIX I/O backends by default configure the data files with a sharding factor of 8 and a shard size of 8 MiB, such that the data is written to or read from

multiple Lustre OSTs simultaneously, resulting in network and server saturation, and therefore best performance, in `archive()` or `retrieve()` workloads at scale.

Fig. 2.5 shows an example of the state of a dataset directory after a process has called FDB `archive()` a few times for two different collocation keys, before `flush()` has been called. The data files may or may not yet contain the object data, and this is illustrated with dotted edges for the objects.

```
FDB.archive(
  Key({"class": "od", "expver": "0001", "stream": "oper", "date": "20231201", "time": "1200",
    "type": "ef", "levtype": "sfc", "step": 1, "number": 1, "levelist": 1, "param": "v1"}),
  buffer, len)

FDB.archive(
  Key({"class": "od", "expver": "0001", "stream": "oper", "date": "20231201", "time": "1200",
    "type": "ef", "levtype": "sfc", "step": 1, "number": 1, "levelist": 2, "param": "v1"}),
  buffer, len)

FDB.archive(
  Key({"class": "od", "expver": "0001", "stream": "oper", "date": "20231201", "time": "1200",
    "type": "ef", "levtype": "pl", "step": 1, "number": 1, "levelist": 1, "param": "v2"}),
  buffer, len)
```

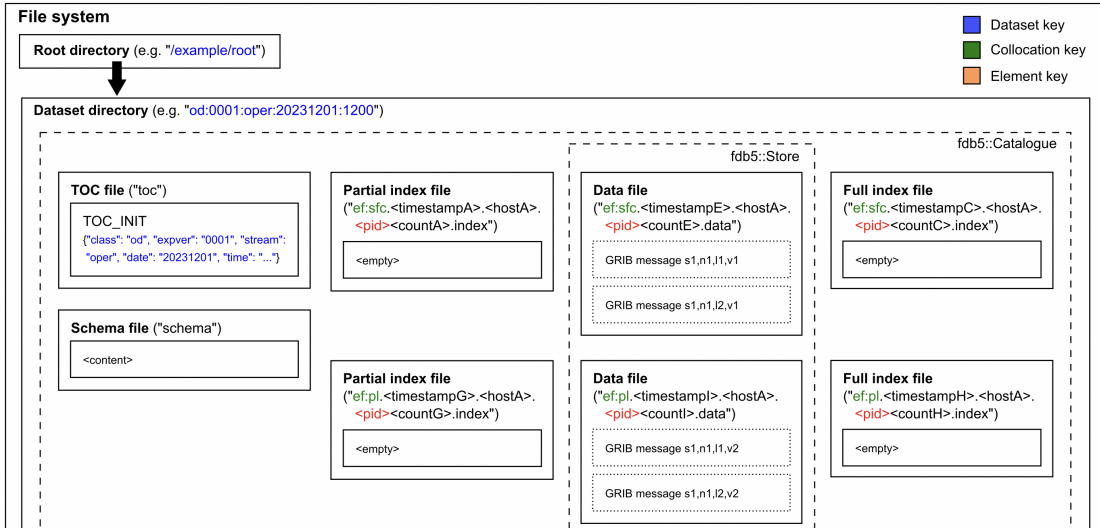


Figure 2.5: Snapshot of the content of a dataset directory after a process has called FDB `archive()` four times for four meteorological objects for two different collocation keys. The `archive()` calls are shown at the top, using different colours for the dataset, collocation, and element keys. `flush()` has not been called yet, thus the index files are empty as the indexing structures are still held in memory at this point. The object data may or may not have been persisted into storage media at this point.

`flush()`

`flush()` ensures all object data `archive()`d by the calling process is made persistent with `fflush` and `fdatasync` function calls for each data file written by the process — one per dataset and collocation key.

retrieve()

When `retrieve()` is called, the input field location descriptor is used to build —without performing any I/O operation— and return a `DataHandle` object which enables the application to transparently read data from file range specified in the descriptor. The `DataHandle` internally uses the `open`, `seek`, and `read` system calls for reading.

This handle supports merging with other handle instances returned by the POSIX Store `retrieve()` method. When FDB `retrieve()` is called for multiple objects which are located in sparse ranges within a same data file, a merged handle is returned which internally opens the file only once even if the application reads all data ranges. Also, if multiple requested objects are collocated in adjacent ranges in the file, a single `read` operation is performed.

The FDB POSIX I/O Catalogue

archive()

When the Catalogue `archive()` method is called, the dataset directory is created if it does not exist, in the same way as described for Store `archive()`. The top-level shared index file —also referred to as the *TOC* (Table Of Contents) file—is also created within the directory if it does not exist, and some header data is written in it. A copy of the schema —previously made available to applications by the FDB administrator— is written in a file within the dataset directory. Because multiple concurrent processes may race to perform the first `archive()` operation for a given dataset key, mechanisms were put in place to ensure consistency of these dataset initialisation operations under contention.

Also, the first time `archive()` is called by a process for a new dataset and collocation key pair, a pair of unique files are created within the dataset directory where the indexing information for all data objects `archive()`d by that process

for that key pair will be written. The two index files are ensured to be unique with the same mechanisms as in Store `archive()`, and both are opened and kept open for the lifetime of the `archive()`ing process.

One of the index files is used to store small indexes of the objects `archive()`d between the last two `flush()` calls —that is, one indexing structure per `flush()` call—, and the other index file is used to store, at the end of the process lifetime, a single index of all objects `archive()`d by the process. Although both files eventually contain equivalent indexing information, they have different characteristics. The indexing structures in the first file are made available sooner, on `flush()`, but are be slower to use for retrieval and listing as many more files need to be accessed —this is explained below— and multiple indexing structures need to be visited. The indexing structure in the second file is faster and requires fewer file accesses, but it is only made available at the very end of the producer application lifetime.

Every time FDB `archive()` is called, the Catalogue `archive()` method associates the element key of the archived object with the location descriptor returned by Store `archive()` within a pair of B*-Tree indexes built in memory. One of the indexes holds the indexing information for a given dataset and collocation key pair between two `flush()` calls. On `flush()`, this index is written to the first index file, and the instance in memory is reset. The other index holds the full indexing information for the same key pair, and is eventually written to the second index file at the end of the process lifetime.

It is likely that many of the location descriptors inserted in these B*-Trees will point to regions within a same data file, as producer applications usually `archive()` many objects for a given dataset and collocation key pair. These descriptors will all be identical except for the offset and length of the objects they point to. To avoid repeatedly inserting that common part of the location

descriptors and unnecessarily enlarging the indexes, a helper data structure is built in memory, referred to as the *URI store*, such that every file URI is mapped to an integer, and that integer is inserted in the index in place of the URI.

Also on every `archive()` call, the values of the element key are recorded into another set of helper data structure in memory, referred to as the *axes*, such that a summary is kept of all values inserted in an index for every element key dimension. These axes enable the `retrieve()` method to quickly skip indexes that do not contain the targeted objects.

As the producer processes continue to `archive()` more objects, these in-memory structures will grow. Processes issuing many consecutive `archive()` calls—as is done in operational runs—should not result in any I/O performance issues caused by this indexing mechanism as all the work is done in memory.

Fig. 2.5 shows an example of the state of a dataset after `archive()` has been called but before `flush()` is called. Most indexing files are empty, and sub-TOC files have not been created yet. Fig. 2.6 illustrates the data structures held in process memory after these `archive()` calls.

flush()

The POSIX Catalogue `flush()` method writes all partial B*-Tree indexes held by a process, potentially for multiple dataset and collocation key pairs, at the end of the corresponding partial index files. For every index, the associated URI store and axes are written at the end of a separate per-process file—referred to as *sub-TOC* file—which is first created if it does not exist. The collocation key associated to the index and a descriptor of the location of the index within the index file (composed of a file URI, offset, and length) are also written in the sub-TOC file.

On creation of a sub-TOC file—which occurs only on the first `flush()` call for a given process and dataset key—a pointer to that file is appended to the shared

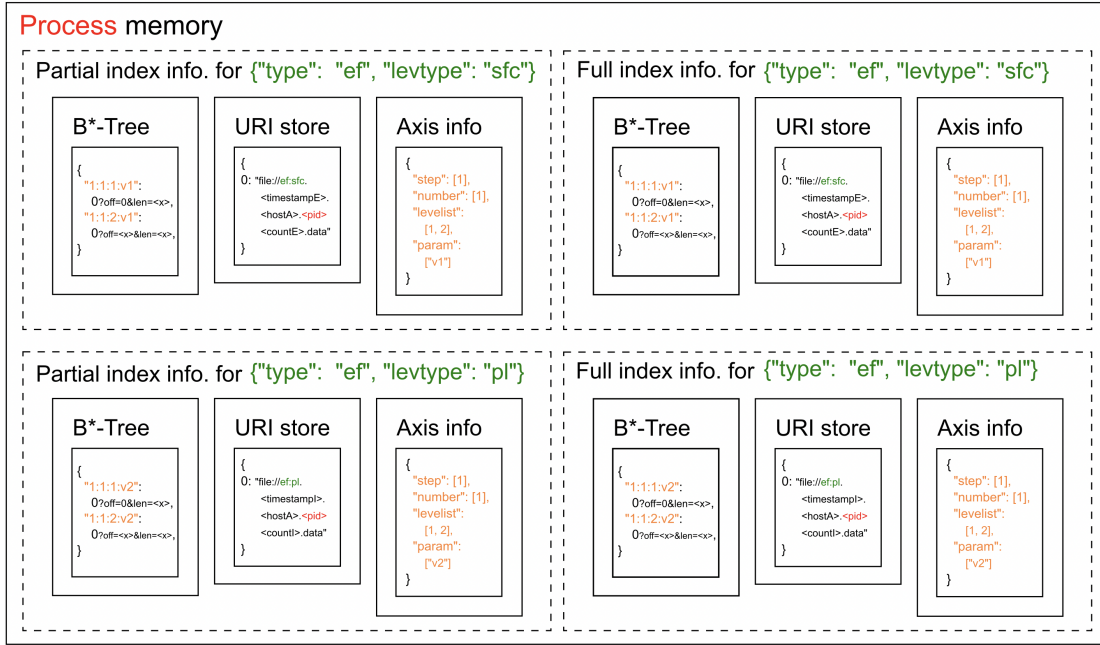


Figure 2.6: Content held in memory by a process after calling FDB archive() four times for four meteorological objects for two different collocation keys, before flush() is called.

TOC file, making all sub-TOC and index files easily discoverable by `list()`ing and `retrieve()`ing processes. Given the TOC file was opened with `O_APPEND`, this is simply done with a `write` system call. Multiple concurrent process may race to append their pointers to the TOC file on their first `flush()` call, but POSIX guarantees atomicity and therefore consistency as long as the contending `write` operations are for data buffers smaller than the configured system block size, as is the case here.

The sub-TOC files exist separately from the index files to make high-level indexing information efficiently accessible without requiring scanning of the index data. Because every process writes exclusively to its own index and sub-TOC files, there is no contention or room for inconsistency when writing data at the end of these files.

After the indexing information has been persisted and the pointers appended

to the TOC file, the partial in-memory indexes are reset, the full indexes are kept intact, and `flush()` returns.

If more objects are `archive()`d after a `flush()` call, a subsequent Catalogue `flush()` call will only result in indexing information being appended to the corresponding index and sub-TOC files, as long as no objects are previously archived for new dataset and collocation key pairs.

Fig. 2.7 shows the state of the example dataset from Fig. 2.5 after `flush()` is called, with the mentioned indexing information persisted in storage media.

Fig. 2.8 shows part of the dataset state after additional objects are archived and flushed, using a value of 2 instead of 1 for the `step` element key.

Fig. 2.9 shows the structures held in memory after such second flush. Full indexes have grown, and partial indexes are empty.

`close()`

At the end of the lifetime of an `archive()`ing process, the Catalogue `close()` method is called, which persists the full indexes into the corresponding files created on the first `archive()` call. The URI store and axes associated to every full index are encapsulated together with the collocation key and a pointer to the corresponding full index file, and appended as an entry to the shared TOC file using the same mechanisms as in `flush()` to ensure consistency.

An additional `TOC_MASK` entry is appended to the TOC file after every full index entry. This entry signals any `retrieve()`ing or `list()`ing processes to skip the pointers to sub-TOC files made obsolete by the new full index. Consumer processes are therefore expected to read the TOC file in reverse order to ensure any masking entries are found before scanning unnecessary sub-TOCs.

Fig. 2.10 shows the state of the dataset after `close()` is called, with new full index entries present in the TOC file, and with the sub-TOC file masked.

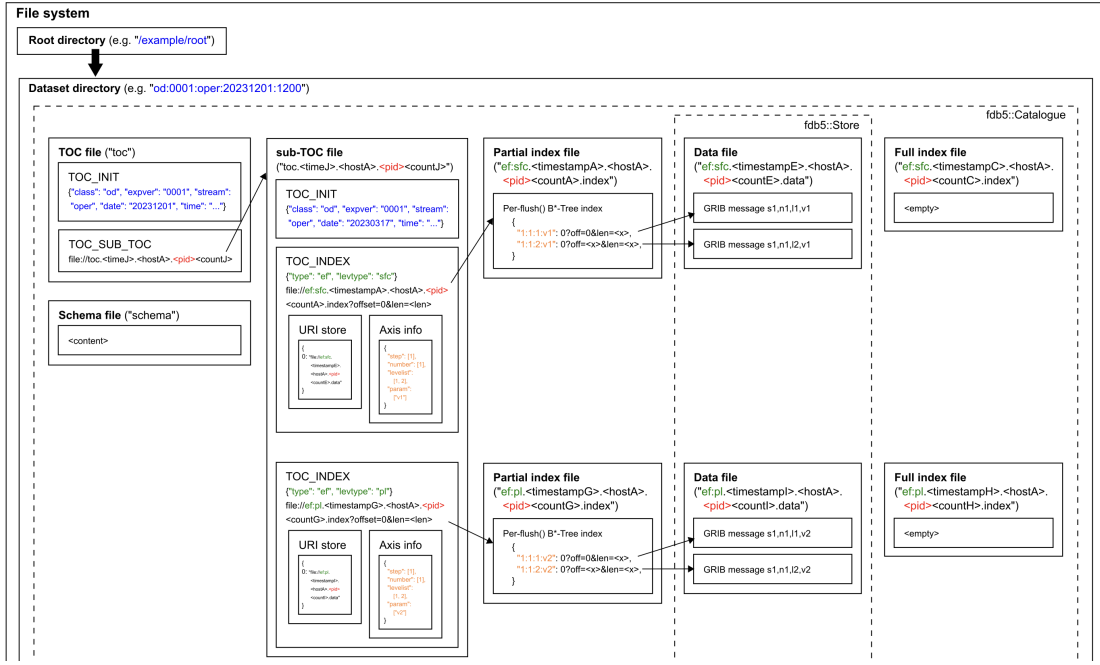


Figure 2.7: Snapshot of the content of a dataset directory after a process has called FDB `archive()` four times for four meteorological objects for two different collocation keys, after `flush()` has been called. All data objects and indexing information required to access them has been persisted into storage media at this point. `close()` has not been called yet and therefore the full index files are still empty.

TOC pre-loading

The first time a process calls FDB `retrieve()` or `list()` for a given dataset key, the POSIX Catalogue backend reads the dataset TOC file, scans it in reverse order, and reads all sub-TOC files —except for the masked ones—, rebuilding all URI stores and axes in memory. The TOC and sub-TOC files are loaded entirely with a single `read` system call per file.

This loading and scanning in advance of the full content of all TOC and non-masked sub-TOC files is necessary for `list()` to provide consistent results, and desirable for `retrieve()` as otherwise, if loading the sub-TOC files only when strictly necessary, the loading would potentially happen in many sparse `read` system calls, not benefiting from I/O parallelism.

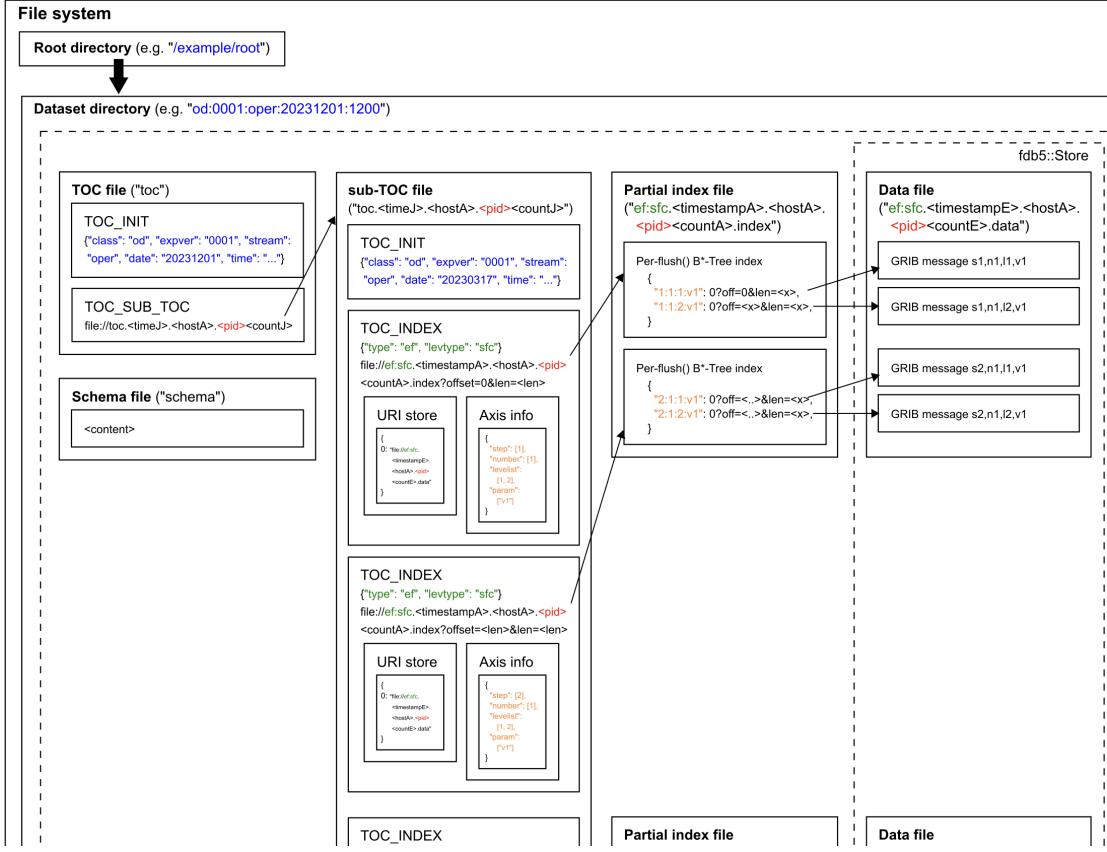


Figure 2.8: Snapshot of the content of a dataset directory after a process has called `FDB archive()` a few times, then `flush()`, then `archive()` a few more times, and then `flush()` again. The partial indexing information for all `archive()` calls before a `flush()` call is appended to the partial index and sub-TOC files.

One caveat of this pre-loading mechanism is that, if a consumer application `retrieve()`s a dataset using multiple parallel processes —as is the case in operational runs—, all of them will read all TOC and sub-TOC files on the first `retrieve()` call, potentially adding significant strain on the file system if many processes are used. This can be addressed by using threads instead of processes or, as done in operational runs, by calling `retrieve()` from a single process and node for the full set of identifiers of objects to be retrieved, and distributing the resulting location descriptors or `DataHandles` to other nodes and processes.

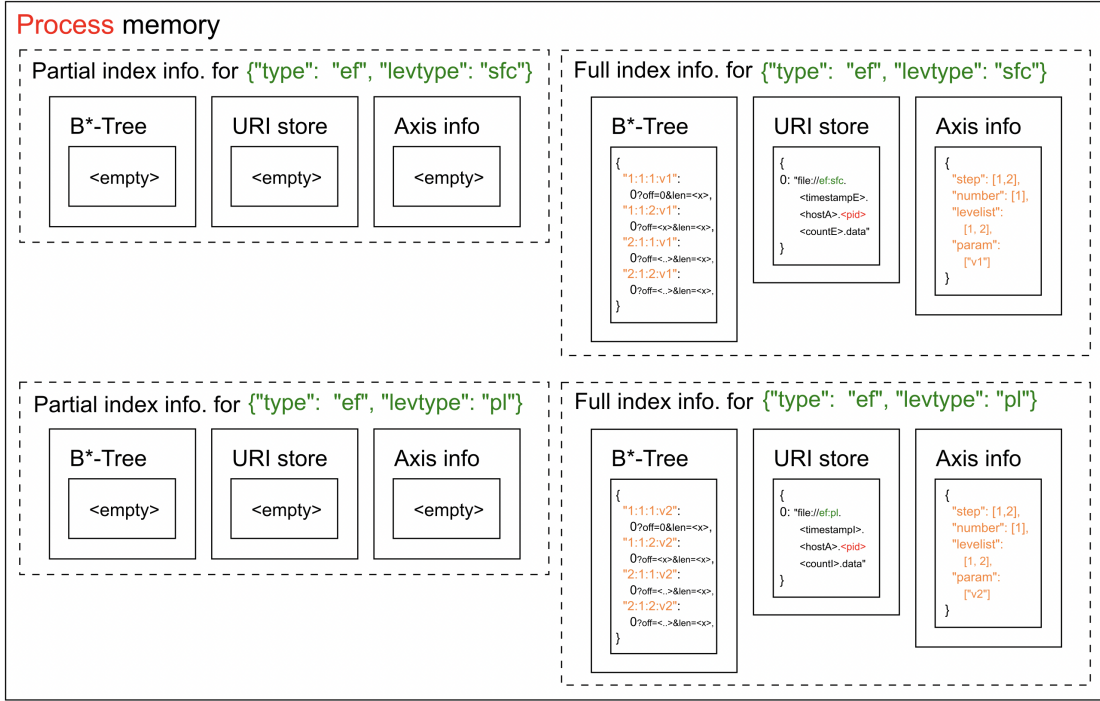


Figure 2.9: Content held in memory by a process after calling FDB archive() a few times, then flush(), then archive() a few more times, and then flush() again. The partial indexes and information are reset, and the full indexes and information accumulate new entries for all archive() calls during the lifetime of the process.

axis()

As explained in the Catalogue interface introduction, the `axis()` method is called by FDB `retrieve()` in a preliminary step to expand any multi-object expressions provided as input.

When `axis()` is called, a dataset key, collocation key, and the name of an element key dimension are provided as inputs. Also, due to TOC pre-loading, all axes of the dataset are available in memory for the `axis()` method to use. The method visits the axes of all indexes matching the input dataset and collocation keys, extracts the values for the specified dimension from each of them, and merges the obtained values. This results in a single set containing all values indexed across all indexes in the dataset for the specified dimension, and this set is returned.

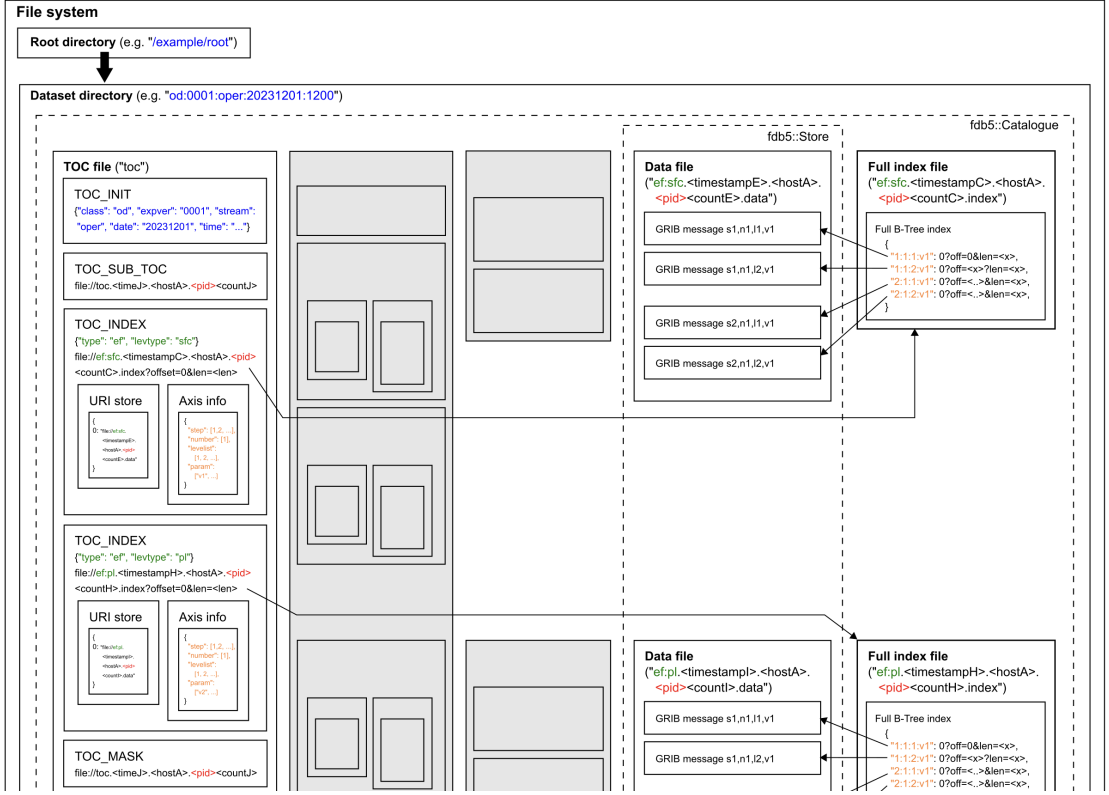


Figure 2.10: Snapshot of the content of a dataset directory after an archive()ing process has terminated and Catalogue close() has been called. New entries are appended to the TOC file pointing to the full indexes, and the sub-TOCs and partial indexes are masked.

This operation should be relatively fast, as it is performed entirely in memory and does not require scanning the content of the B*-trees.

retrieve()

The `retrieve()` method visits all index entries pre-loaded from the TOC and sub-TOC files which have a collocation key matching the one provided as input. For every index entry visited, the axes are queried to determine whether the B*-tree index may contain a match for the element key provided as input. If so, the B*-tree index is then loaded from the corresponding index file, and this is done with multiple `read` system calls. The B*-tree index is then queried to obtain an object location descriptor associated to the element key. If not found, visiting

of other index entries is resumed. If found, the descriptor is expanded using the information in the URI store and returned.

A `retrieve()` operation only has visibility of the index entries and axes pre-loaded on first call of a `retrieve()` or `list()` operation for any objects with the same dataset key. Any newly `archive()`d or `flush()`ed objects will not be visible.

Leaving TOC pre-loading aside, a `retrieve()` operation usually requires accessing the file system to load the matching B*-Tree, and this is likely to dominate the latency of this operation. However, the in-memory visiting of the TOC and sub-TOCs can also impact performance, particularly if the number of indexes—and therefore number of parallel `archive()`ing processes—is large, or if the `archive()`ing processes have not yet finalized and persisted the full indexes. For isolated `retrieve()` operations for one or a few object identifiers, TOC pre-loading will likely dominate the latency if full indexes are not yet available.

list()

The `list()` method loads the B*-tree indexes, for a given dataset, which have a collocation key matching the partial identifier provided as input. Multiple `read` system calls are used to load each index. For every index, all of its entries are visited, and those matching the partial identifier are added to a list which is returned at the end of the visiting.

Like `retrieve()`, a `list()` operation only has visibility of the pre-loaded indexing information of the dataset, and will suffer from the same TOC pre-loading performance impact if full indexes are not available. Aside from TOC pre-loading, the latency of a list operation will largely vary depending on the number of indexes matched and loaded.

Operational NWP I/O pattern

Currently, operational runs at the ECMWF consist of an ensemble of 52 NWP model members. For each member, 5 HPC nodes are allocated to forward I/O from model processes to HPC storage, adding up to a total of 260 I/O nodes for all members. 2600 I/O server processes run across these nodes, each performing long sequences of FDB `archive()` calls. During a model time step, every I/O server process receives and `archive()`s 65 weather fields of an average size of 4.3 MiB, and calls FDB `flush()` at the end of the archival of the data for that step. This is repeated for 144 time steps. A full operational model run produces approximately 24 million fields, which are distributed as approximately 9300 fields per I/O server process. The same dataset and collocation keys are used for the identifiers of most of the `archive()`d fields.

On first `archive()` call, the I/O server processes would normally contend to initialise the dataset directory, including directory and TOC file creation, TOC file initialisation, and schema writing. This is avoided, however, by manually initializing the directory in advance. Therefore, the first operation performed by `archive()`ing processes is the creation of their per-process data and index files. This means several file create operations are issued simultaneously, putting metadata operation strain on the file system, although this is a one-off event. This initialisation phase is illustrated with orange stripes at the start of the parallel processes, on the left end in Fig. 2.11.

Writing of field data into per-process data files then begins. Object data is first written into memory buffers and kernel page caches, which start becoming full after a few `archive()` calls, and their content is then written to storage in large transfers in the background. Because objects are first written in memory, the internal Store `archive()` calls return location descriptors quickly, without waiting for the file system to persist the data, and these descriptors are passed

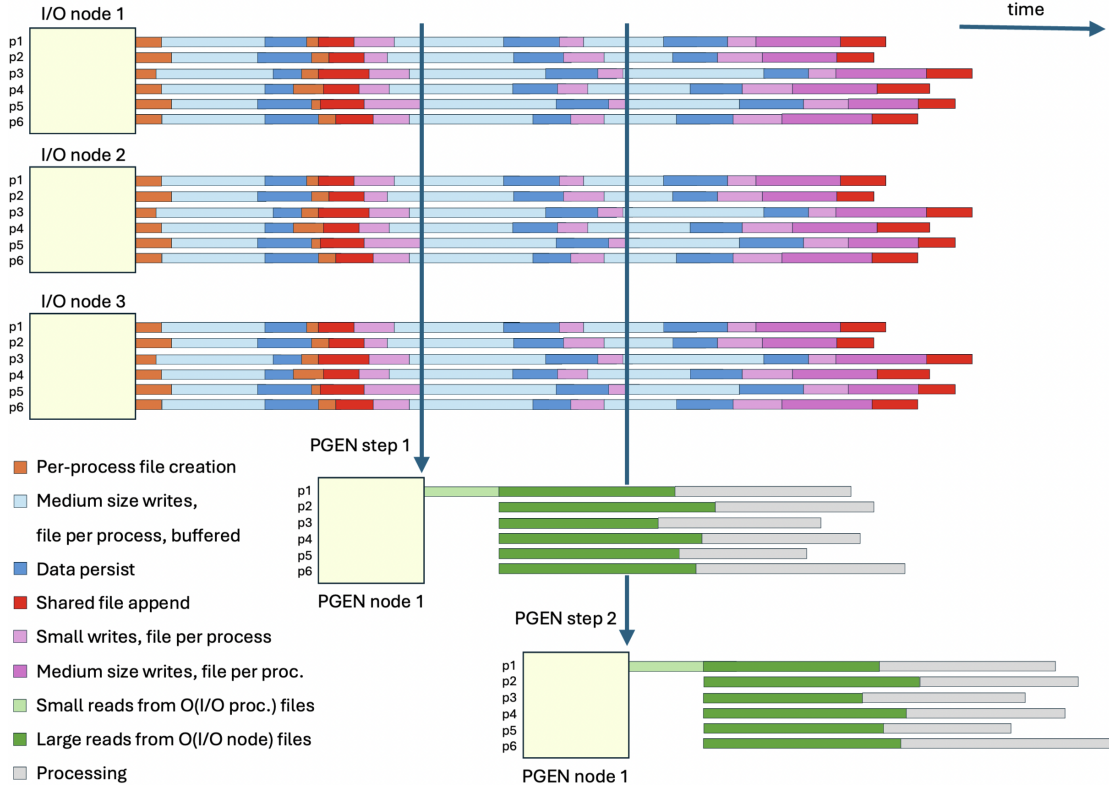


Figure 2.11: Not based on real profiling. Illustration of a simplification of the ECMWF’s operational NWP storage access pattern. Three I/O server nodes archive weather fields produced by the NWP model, using multiple parallel processes per node (p1-p6), for three simulation time steps. At the end of every simulation step the archived fields are flushed, and a post-processing job (PGEN) is launched for that step. The third PGEN job has been omitted. Every PGEN job runs on one node and lists and retrieves data using multiple processes per node (p1-p6). The proportions of the durations for the different types of operation in real operational runs might significantly differ from the ones displayed in this illustration. Real operational runs currently use 260 I/O nodes and 4 to 8 nodes per PGEN job, and archive data for 144 time steps.

to the Catalogue `archive()` method, which performs in-memory indexing of the location descriptors. This phase lasts as long as required for all processes to archive and index their 65 assigned fields, and combines writing object data to buffers and in-memory indexing work, while, in the background, some of the data is being transferred from buffers to storage. This phase is illustrated with light blue stripes in Fig. 2.11.

As soon as processes have archived their fields for a step, they call FDB `flush()`, where the data buffers are flushed and persisted into storage. This adds bulk I/O pressure on the system, and processes wait for this to complete. Once object data is persisted, partial indexes are then written into the per-process partial index files, and processes also wait for this operation to be fully persisted. This blocking write phase is illustrated with dark blue stripes in Fig. 2.11.

Still as part of `flush()`, processes then create a per-process sub-TOC file, adding metadata pressure on the system —illustrated with orange stripes—, then contend to append an entry to the shared TOC file —illustrated with red stripes—, and finally write the sub-TOC index entries, including the axes and URI store, at the end of their sub-TOC file, and wait for the write to be persisted — illustrated with purple stripes.

Processes continue to `archive()` and `flush()` fields for subsequent simulation steps. For these, only the light blue, dark blue, and purple phases are performed.

At the end of the model run, Catalogue `close()` is called and all processes write their full indexes into the per-process full index files, waiting for the writing to be fully persisted —illustrated with dark purple stripes—. Finally, they contend to append the corresponding index and mask entries to the shared TOC file — illustrated with red stripes.

At the end of most model steps, as soon as the straggler I/O process has `flush()`ed its data for the step, the workflow manager is signaled to execute a post-processing job —also referred to as Product Generation (PGEN) job— for that step.

Post-processing jobs run each on 4 to 8 HPC nodes, using 8 processes per node. First, the entire indexing information for the step is loaded from a single node and process by calling FDB `list()`, providing a partial request which matches all weather fields `archive()`d for that step. This reads the full content of the

TOC and the several sub-TOC files, as well as the last partial index in all index files, adding I/O pressure to the system as many files —two per `archive()`ing process— need to be accessed and many I/O operations are performed. This can create write-read contention with any `flush()`ing processes appending entries to the sub-TOC files or indexes to the partial index files. The listing process then calls FDB `retrieve()` for all field identifiers, which efficiently extracts the full set of location descriptors from the indexes made available in memory by `list()`. This phase, dominated by the retrieval of indexing information, is illustrated with light green stripes in Fig. 2.11.

The location descriptors are then distributed across all job nodes and processes such that each process is assigned descriptors of fields for a subset of parameters across all ensemble members, as the full ensemble data is required for the generation of derived products. The processes then build `DataHandles` for their assigned descriptors, merge the handles into one, and read the data from storage through that handle. This results in many read operations being issued. Although the size of the data transfers is large —thanks to handle merging—, these operations hit all data files written by I/O servers, adding significant I/O pressure on the file system. Additionally, write-read contention may occur between these and any `flush()`ing processes appending data to the data files. This phase, characterised by several large reads, is illustrated with dark green stripes in Fig. 2.11.

The processes then apply computations as required to generate the derived products. This is illustrated with grey stripes.

fdb-hammer I/O pattern

`fdb-hammer` is an FDB performance benchmarking tool provided as part of the FDB Git repository[17], which can be built alongside the other FDB command-line tools.

`fdb-hammer` takes a single weather field as input, supplied as argument on the command line, and uses its encoded metadata as a template to generate a sequence of field identifiers which are then archived —alongside a copy of the field data—, retrieved or listed. By default, `fdb-hammer` runs independently as a single process, without synchronisation with any other parallel processes. However, multiple instances of `fdb-hammer` can be executed in parallel mimicking the ECMWF’s operational I/O behaviour, where model I/O server processes `archive()` independent streams of data, and post-processing processes `retrieve()` subsets of the archived data. `fdb-hammer` creates an “I/O-pessimised” benchmark, that is, a worst possible case for I/O as all relevant computation that would occur in the operational workflows has been removed.

For the performance analysis in this dissertation, `fdb-hammer` has been run in two phases: a write phase, and a read phase. In each phase, multiple parallel processes are launched across a set of nodes with access to the storage system to benchmark against.

During the write phase, each parallel process issues a sequence of FDB `archive()` calls. A sequence of weather field identifiers corresponding to a range of NWP model parameters and levels —adjusted via the `--nparams` and `--nlevels` options— is iterated, and every identifier is passed as input to an FDB `archive()` call along with a fixed weather field used as data object for archival.

The `number` key of the identifiers, which identifies the ensemble member a field belongs to, is set to a fixed value depending on the node the writer process runs on. This is to mimic operational behavior, where an I/O server node `archive()`s several fields for a single member. Although in operations the data for a given member is managed by multiple I/O server nodes, `fdb-hammer` is designed to have each writer node `archive()` fields for a single member.

Initially, every parallel writer process sets the `step` key of the identifiers to

a value of 1. When the full range of identifiers for the different parameters and levels has been iterated, `flush()` is called. The `step` value is then increased by 1, and another sequence of `archive()` calls is issued for all parameters and levels, followed by a `flush()`. This is repeated for as many steps as configured via the `--nsteps` option, and the write phase ends with a Catalogue `close()` call after the `flush()` call for the last step.

The `param`, `levelist`, `number`, and `step` keys are therefore the only field identifier keys adjusted by `fdb-hammer` and, when run on POSIX file systems —using the default FDB schema described in the introduction of Section 2.7—, this results in the benchmark `archive()`ing fields with unique element keys which all share the same dataset and collocation key.

Overall, the write phase issues a set of FDB API calls and produces a storage access pattern very similar to that of operational runs of similar size. Fig. 2.12 illustrates the storage access pattern of a simple `fdb-hammer` run using one writer node and one reader node. The write pattern is very similar to that of operational runs, shown in Fig. 2.11.

Despite the write phase being very similar to operational runs, it is worth noting that all `fdb-hammer` runs performed in Chapter 4 were configured to produce a different number of fields than would be produced operationally. As shown in table 2.1, `fdb-hammer` runs were configured to simulate not only fewer members and steps, but also fewer parameters and levels per step. This resulted in less data being written per step — that is, in `fdb-hammer` runs having proportionally shorter light and dark blue stripes compared to operational runs.

The read phase is run on as many nodes and using as many processes as the write phase. The processes in the read phase issue sequences of `retrieve()` calls equivalent to those in the write phase.

This phase can be run either independently once the write phase has ended,

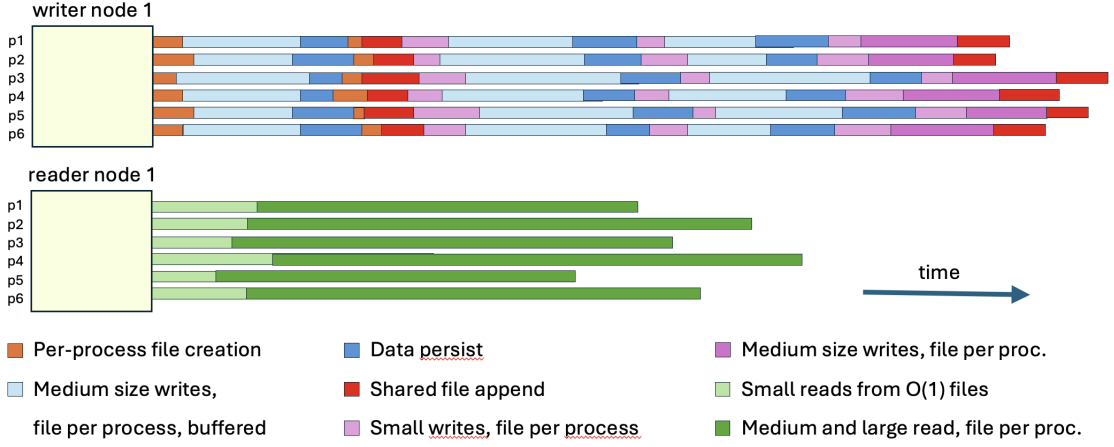


Figure 2.12: Not based on real profiling. Illustration of a simplification of the storage access pattern of the fdb-hammer benchmark. One writer node archive()s weather fields for three time steps using multiple parallel processes per node (p1-p6). At the end of every step the archived fields are flushed. One reader node simultaneously retrieves pre-archived data using an equivalent set of parallel processes (p1-p6) performing equivalent sequences of retrieve() operations. Each reader process loads the content of the TOC file, then loads one full index from one index file, and reads all fields from a single data file — these index and data files have been written by the corresponding writer process. The proportions of the durations for the different types of operation in real fdb-hammer runs might significantly differ from the ones displayed in this illustration. Real fdb-hammer runs performed in this analysis employed up to 24 writer and 24 reader nodes, with up to 48 processes per node, and were run for 100 time steps.

Table 2.1: Comparison of the dimension of ECMWF’s operational NWP runs and fdb-hammer runs performed in Chapter 4.

	operational run	fdb-hammer
members	52	1 to 24
steps	144	100
levels	150	10
parameters	20	10

or concurrently with the write phase on a separate but equally sized set of nodes, although the latter option requires previously running the write phase once in isolation to populate the storage system for the readers to always find data in case they are faster than the writers. Both modes have been employed for the performance analysis in this dissertation.

The reader processes by default check that all previously written and indexed fields are found and can be de-indexed and their data retrieved. If this consistency check is not fulfilled, the benchmark execution fails with an error. Additionally, the readers can optionally be configured to verify that the read data matches exactly the data that was originally written. This requires readers to load and process the read data in memory, which can impact benchmark performance, and it is therefore advisable to execute the benchmark separately, with this option enabled, to fully test storage system consistency.

The `retrieve()` calls issued during the `fdb-hammer` read phase load a set of field location descriptors equivalent to the set loaded by all `list()`ing PGEN processes in an operational run of the same size. However, the timing and the storage access pattern generated are different in a few ways.

The first difference is that all `fdb-hammer` reader nodes and processes start issuing `retrieve()` calls and fetching data at the very beginning of the read phase. On one hand, this implies that `fdb-hammer` readers mostly hit data files and full indexes from a previously completed write phase. Therefore, there is no write-read contention on sub-TOC or data files. This is in contrast to operational readers, which are started in a staggered way, one subset of processes at a time after the data for each step has been `flush()`ed and before the full indexes have been made available, and this results in write-read contention on sub-TOC and data files. On the other hand, this means that all the index accesses occur at the beginning of the `fdb-hammer` read phase, making the first part of a run more challenging

in terms of metadata operations than the rest of the run. In operational runs, instead, indexes are accessed in multiple bursts, one at the beginning of every PGEN job, thus having the index access workload spread more evenly along the duration of the run.

Also, although TOC pre-loading is performed by every `fdb-hammer` reader process on the first `retrieve()` operation, it involves very few or no partial indexes, resulting in a small number of `read` system calls overall for TOC pre-loading. In operational runs, instead, many sub-TOC files are `read` during TOC pre-loading, and although only a single process in every PGEN job pre-loads, the total number of `read` system calls performed for pre-loading is larger than in `fdb-hammer` runs.

Another difference is that, because every `fdb-hammer` reader process issues a sequence of `retrieve()` calls for the entire set of fields `archive()`d by its corresponding writer process —for a single member and the full sequence of steps—, every reader process only loads the full index made available by the corresponding writer process from a previously completed write phase. This means as many `read` system calls are issued overall for index loading as there are reader process. In operational runs, instead, every PGEN job has a single `list()`ing process load the last partial index from every index file for every writer process, thus issuing as many `read` system calls as the number of writer processes times the number of PGEN jobs. This is a larger number of `read` operations for index loading than in `fdb-hammer`, by approximately two orders of magnitude.

Every `retrieve()` call performed by an `fdb-hammer` reader processes returns a location descriptor wrapped as a `DataHandle`, which is then merged into one with subsequent `DataHandles`. The resulting merged handle is then used to read the entire content of the data file written by the corresponding writer process. This results in a few large `read` system calls per reader process. In operational

runs, instead, the processes in a PGEN job read data of fields for a single step for all ensemble members, resulting in many `read` system calls hitting all data files at every step. The amount of data read is the same as in `fdb-hammer` runs of equivalent size, but data is read using a much larger number of `read` system calls, by approximately one order of magnitude.

The read phase is illustrated at the bottom of Fig. 2.12. All processes first load the TOC file —represented with light green stripes—, and then load the full content of a single index file and a single data file — illustrated with dark green stripes.

In summary, whereas the write access pattern of `fdb-hammer` very closely mimics that of the operational runs, the read phase has a few differences, the main ones being that all reading starts simultaneously at the beginning of the run, and that the transposed access of operational runs is not reproduced. This results in `fdb-hammer` producing a more condensed I/O workload at the beginning of the run and an easier I/O workload overall, as write-read contention is partly not captured, fewer small `read` operations are performed for index access, and fewer and larger `read` operations are performed for bulk data reading.

Despite these differences, `fdb-hammer` is still challenging, as it performs only I/O —excluding all processing—, and is representative of operational runs, as it captures well the I/O in terms of FDB API calls and reproduces the operational contention in terms of volume of data being stored and retrieved simultaneously from the file system. Also, `fdb-hammer` has other advantages such as being a much simpler tool to configure and run than other more sophisticated benchmarks like Kronos or real operational workflows, and not requiring large amounts of nodes to meaningfully reproduce the desired contentious patterns.

This analysis has informed further developments at the ECMWF to make `fdb-hammer` more representative of operational runs.

Chapter 3

Object Storage Backends

This chapter describes newly developed FDB backends for operation on the DAOS and Ceph object stores, as well as backends to support other storage solutions implementing the S3 storage protocol. The options these storage approaches provided and the challenges encountered during the development are discussed.

This addresses the second contribution of the dissertation — the development of *"Object storage adapters for the ECMWF's NWP workflows"*.

3.1 DAOS backends

Before the DAOS Catalogue and Store backends for the FDB were developed, a preliminary assessment was conducted to determine whether DAOS provided sufficient functionality for the implementation of both backends, as well as the required consistency guarantees and performance. This assessment, which resulted in positive answers to all these questions, is presented in Appendix B. As part of the assessment, a proof-of-concept library named Field I/O was developed which provides a pair of functions to write and read weather fields from DAOS, including creation and use of an internal index. During this development, best practices for

high performance on DAOS were identified[18, 12] and implemented in the Field I/O library.

The implementation of the DAOS backends was heavily informed by the preliminary assessment and the design of the Field I/O functions. Essentially, the DAOS backends store object data and indexing information in a container per dataset key. Every `archive()`d meteorological object is written into a new DAOS array—with its own object identifier—within the corresponding dataset container, and a network of key-value objects is created and populated in the container which in conjunction form an index of all objects `archive()`d, enabling efficient discovery and access on `retrieve()` and `list()`. The transactionality of the `daos_kv_put` and `daos_kv_get` operations on the DAOS key-value objects is critical to ensuring consistency of the index under `archive()` and `retrieve()` contention, and such contention is resolved on the DAOS servers rather than by negotiating locks between clients and servers as is the case in the POSIX I/O backends.

The consistent behavior of DAOS and the FDB backends was verified by executing the `fdb-benchmark` at scale, with the consistency check option enabled, on both computer systems employed for the performance analysis in Chapter 4.

The end-to-end implementation of the FDB DAOS backends spanned a period of one to two years. This was in part due to the need to familiarise with the DAOS libraries and systems, and to assess any overall consistency or performance limitations—covered in detail in the preliminary assessment—; but also due to the need to fully analyse and map the FDB’s internals onto the object storage paradigm for the first time; the need for developing auxiliary unit testing libraries—discussed in Appendix A—; the multiple required iterations of performance testing at scale and optimisation—discussed in this section and in Chapter 4—; and the fact that the developments were tested initially on a system with novel

storage and network hardware, which posed a number of challenges.

A graphical representation of the different DAOS entities involved in an FDB `archive()` call is shown in Fig. 3.1.

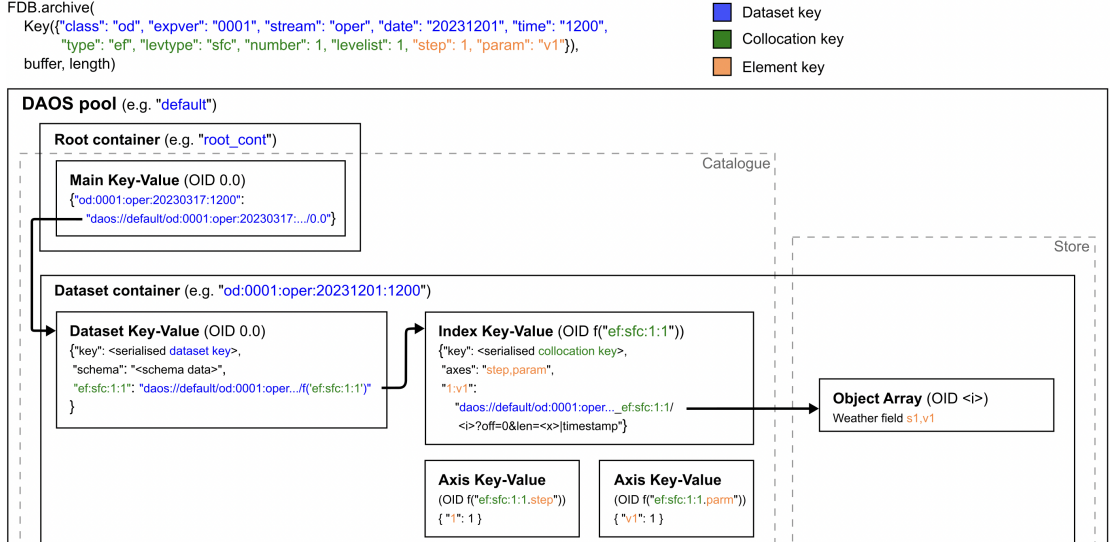


Figure 3.1: Diagram of DAOS entities resulting from an FDB `archive()` call for one meteorological object. The `archive()` call is shown at the top, using different colours for the dataset, collocation, and element keys. The object data and indexing information are persisted immediately. A `flush()` call would result in no additional changes to these entities.

At the deepest layer of the key-value hierarchy, an *index key-value* is created for every collocation key, holding an index of all objects `archive()`d for that key within the dataset. A few ancillary key-values, referred to as *axis key-values*, hold summaries of the entries inserted into each index key-value for increased efficiency of the `retrieve()` calls. One layer above, a *dataset key-value* is created within every dataset container, which holds an index of collocation keys for which objects were `archive()`d, associating every collocation key to a pointer to the corresponding index key-values. Finally, a top-level index of the available datasets, also implemented with a DAOS key-value, is kept in a separate *root container*. By default, all containers created by the DAOS backends are placed within a same

DAOS pool configured by the FDB administrator at deployment time.

By default, all key-values and arrays created by the DAOS backends are configured with no sharding, that is, with an object class of `OC_S1`, which results in them being stored each in a single DAOS storage target. In the preliminary assessment, this configuration was found to result in best performance for `archive()`al and `retrieve()`al at scale, as shown in Appendix B - Figure 8. This choice assumes `archive()` and `retrieve()` are mainly used operationally and performed in parallel on multiple nodes and several processes per node, with every process writing or reading several small objects, on the order of 1 MiB. In such a scenario, because the several DAOS arrays are evenly distributed across DAOS targets, all targets are hit by all client nodes at all times, resulting in network and server saturation, and therefore good performance, despite the arrays not being sharded.

Sharding arrays might nevertheless be desirable for other use cases, for example if using a single process or working with larger objects. To that end, the FDB user can override the object class used for indexing key-values or object arrays, separately, choosing values such as `OC_S2` to shard over two targets or `OC_SX` to shard across all targets. Depending on the type of storage hardware managed by the DAOS servers, and the power failure resilience mechanisms of the system, it might also be desirable to replicate or erasure-code the key-values or arrays over multiple storage targets, and this can be attained with object classes such as `OC_RP_2G1` or `OC_EC_2P1G1`. The performance of these DAOS data redundancy options is briefly analysed in 4.5 DAOS and Ceph data redundancy.

Regarding the overall design of the DAOS backends, as discussed in the preliminary assessment, a slightly different design was first considered such that the objects for every dataset and collocation key pair were placed in a separate container, as this mapped more closely to the design of the POSIX I/O backends. However, the use of so many containers was found to significantly deteriorate

performance, and the design was revisited to make use of a single container per dataset, plus one container for the top-level index of datasets, which addressed the performance issue. This final design assumes applications will `archive()` meteorological objects for only one or a few dataset keys, therefore resulting in only a few containers and thus avoiding deteriorating performance. This assumption is valid for an operational NWP run at the ECMWF, where objects are `archive()`d for a single dataset key.

A potential alternative design to completely eliminate this issue would consist in using a single container for all datasets, also including the top-level dataset index. However, having each dataset in a separate container is desirable as it simplifies maintenance tasks such as removing a specific dataset, which can be done with a simple DAOS container destroy operation, that is, without requiring knowledge and manipulation of the internal structures of the FDB backends. Due to this, together with the fact that some performance tests revealed that using on the order of a few tens of containers did not significantly deteriorate performance, the current design was considered to be the best compromise.

Given every `archive()`d FDB object is assigned a unique meteorological metadata identifier on `archive()`, and given every object is stored in a separate DAOS array, the indexing component of the DAOS backends—that is, the network of key-values—could seem unnecessary, as every array could simply be created with an OID resulting from applying a hash function to the metadata identifier, and any consumer process requiring to `retrieve()` a particular object could calculate the same hash to determine the corresponding OID, and read the object content directly without the need of querying an index to determine the OID. However, without an index, it would be impossible to implement efficient listing of objects matching a partial identifier, or functionality to request retrieval of large sets of objects based on compact expressions with special features such as

wildcards. If this type of functionality is required, as is the case in the ECMWF’s operational NWP, an index must be built on `archive()`al. Nevertheless, even if an index is implemented, as is the case in the current DAOS backend design, the arrays could still be assigned OIDs based on hashes of the identifiers, and this would allow further optimisation in `retrieve()` and `list()`. This optimisation was not pursued and remains as potential future work.

Differences w.r.t. the POSIX I/O backends

One major difference with respect to the POSIX I/O backends is that no per-process structures are created in the DAOS backends, neither for storage of object data nor for indexing. Regarding storage of object data, as demonstrated in the preliminary assessment, DAOS supports creating a DAOS array for every object —that is, several objects per process— without deteriorating performance, whereas using a file per object instead of a file per process in POSIX file systems would have resulted in an excessive strain on the metadata servers. Regarding indexing, DAOS provides key-value objects which enable easy implementation of efficient, persistent, and strictly consistent indexes shared across processes, removing the need for building in-memory per-process indexes or implementing custom mechanisms to persist these and ensure their consistency under contention, as was done in the POSIX I/O backends. These DAOS features resulted in notably simpler logic and thus better readability and maintainability of the code base with respect to the POSIX I/O backends.

The preliminary assessment showcased the implementation of an index based on DAOS key-values, and demonstrated this approach does not deteriorate performance as long as excessive multi-process contention on same key-value objects is avoided — the performance impact of such contention is shown in Appendix B - Figures 6 and 7.

The root and dataset key-values are not sensitive to contention as, although concurrent producer and consumer processes interact with them, this interaction generally happens only shortly at the beginning of the processes' lifetimes. Index key-values are the most sensitive to contention. Because all objects `archive()`d by all concurrent writers for a same collocation key are indexed in the same index key-value, avoiding contention on these key-values requires avoiding `archive()`ing objects for a same collocation key from many parallel processes simultaneously. This can be attained, if necessary, either by modifying the application accordingly, or by adjusting the FDB schema to recognize as part of the collocation key those object identifier components that vary the most across parallel processes. As an example, in the ECMWF's operational case, the default FDB schema used in conjunction with the POSIX I/O backends defines that a collocation key is formed by the `type` and `levtype` components of an identifier, as illustrated in Listing 2.1. As explained in 2.7.2, many parallel processes use the same collocation key in the operational case, and this is not an issue when using the POSIX I/O backends as a separate set of index and data files are created for every process, however this would be problematic if using the DAOS backends. To avoid contention on indexing key-values, a modified schema is used in conjunction with the DAOS backends which recognises the `number` and `levelist` components as part of the collocation key. This results in every parallel processes `archive()`ing objects for a different collocation key, thus never contending with other processes. The use of this modified schema is illustrated in Fig. 3.1.

One last noteworthy difference with respect to the POSIX I/O backends is that, because DAOS does not implement client-side caching and provides high performance despite performing many small I/O operations, all object writes and key-value updates are always persisted immediately on the server side, without the need for buffered I/O. Objects are available for consumers to `retrieve()`

or `list()` on return of `archive()`, and the `flush()` implementation does not perform any operation internally. Although this does not immediately benefit operational runs at the ECMWF, it opens doors to explore further optimisation of the operational workflows, and may be beneficial for other FDB use cases. Nevertheless, this also suggests that the current implementation of the DAOS backends may be excessively conservative, and there might be room for further performance gains if implementing a buffered and persistent-on-`flush()` approach.

Similarly, because DAOS performs well for small I/O operations, only the strictly necessary information is extracted from the indexing key-values for `retrieve()` and `list()`, rather than loading and caching large chunks of indexing information as is done in the POSIX I/O backends. Due to this, the DAOS backends have different performance behaviour for these two operations, providing lower latency for retrieval or listing of one or a few meteorological objects, but higher latency when listing many of them.

3.1.1 The DAOS Store

archive()

Data is stored in the DAOS backends in containers identified by a stringified representation of the dataset key. When the DAOS Store `archive()` method is called, the corresponding dataset container is created if it does not exist within the DAOS pool. This is done with the `daos_cont_create_with_label` function of the `libdaos` API, which guarantees atomicity of the operation even if multiple processes call `archive()` for objects with a same new dataset key concurrently. Once opened for use, the pool and dataset container handles are cached for the process lifetime.

Every `archive()`d object is written into a new DAOS array object. A new unique OID is first obtained from DAOS with the `daos_cont_alloc_oids` function

to avoid collisions with any concurrent processes. This requires a round trip to the DAOS server and, as such, a large set of OIDs are pre-allocated in a single call and cached by a process before object creation. The array is then created and opened with the `daos_array_open_with_attr` function, which in fact does not perform any Remote Procedure Call (RPC). This was found to improve write performance at scale in contrast to using `daos_array_create` which does perform an RPC. Once the array is created, the input object data is written in it with `daos_array_write` and the array is closed. A unique location descriptor to this array is finally returned, composed of the pool name, the dataset container name, the OID of the array containing the written object, the offset the object data was written at within the array —always zero given the array-per-object design—, and the object data length.

Note that the collocation key provided as input to this method has not been used to determine data placement. In a previous version of the backend this key was used to create separate containers that collocated data, but the additional containers resulted in significant performance overheads and they were removed. As such, all the object data associated with a single dataset key is collocated in the same container. The collocation key is nonetheless still used in the Catalogue backend for structuring the indexing information.

Another choice that had to be made for the implementation of this method was whether to store multiple FDB objects into a single DAOS array, as this would reduce the number of I/O operations with respect to the initial design and potentially result in better backend performance. This could be attained by either collocating all objects for a same collocation key in a same array, which would require any concurrently `archive()`ing processes to atomically append to such array, or writing any objects `archived()` by a same process at the end of a per-process array, either individually and immediately on `archive()`, or in

batches on `flush()`. However, DAOS does not currently implement atomic array appends, and the first option was therefore discarded. The approach of writing immediately at the end of a per-process array would result in the same number of I/O operations being issued as in the initial design with an array per FDB object, and it was thereby discarded as well. And writing in batches on `flush()` would require `archive()`ing processes to accumulate all data in memory until `flush()` is called and, particularly if using multiple processes within a node, these would easily run out of memory. Given these limitations and the good performance of the array-per-object approach observed in the preliminary assessment, these alternatives were not further pursued.

`flush()`

By contrast to the POSIX I/O backend implementation, as the DAOS API immediately persists objects and makes them available, the DAOS Store makes objects available to external readers immediately on `archive()`, and there is no further action to be taken in the `flush()` method.

In the future, the `flush()` method may be useful if, for example, the non-blocking DAOS APIs are used in `archive()` to write object data, in which case the `flush()` method would block until those operations were complete.

`retrieve()`

When `retrieve()` is called, the input object location descriptor is used to build —without performing any I/O operation— and return a `DataHandle` object which enables the application to transparently read data from the corresponding DAOS array. The `DataHandle` internally uses the `daos_array_read` function when the application requests data content.

Note that `daos_array_read` does not fail if the requested length to read is larger than the object and does not report back the actual number of bytes read. Due to this, `daos_array_get_size` must be called first to discover the

array size. However, in this case, because the object length is encoded in the location descriptor on `archive()`, no call needs to be made to obtain the array size. Removing unnecessary `daos_array_get_size` calls was found to have a noticeable positive impact on the performance of the backends at scale.

By contrast to the POSIX I/O backend, the handles returned by the DAOS Store `retrieve()` method do not support merging because there would be no benefit in this case. Every FDB object is stored in a separate DAOS array and it is therefore not possible to merge `daos_array_read` calls or avoid `daos_array_open_with_attr` calls.

3.1.2 The DAOS Catalogue

archive()

Fig. 3.1 can be used as visual guidance to follow the steps described here. When the Catalogue `archive()` method is called, a connection to the DAOS pool is opened, and the *root container* —whose name is configured by the FDB administrator at deployment time— is created if it does not exist, and opened. The container creation is performed with the `daos_cont_create_with_label` function, which guarantees it is created only once even if multiple process race on their first `archive()` call. As there is a significant overhead in opening pools and containers, once any have been opened they are cached for the lifetime of the process.

A key-value object with OID 0.0 is then opened in the root container with the `daos_kv_open` function. This issues no RPCs and does not fail if the key-value does not exist yet. In fact, objects are generally always considered to exist in DAOS, although they might have no content associated yet. This key-value will hold an index of dataset keys for which objects have been `archive()`d, associating each dataset key with a pointer to the corresponding dataset key-value.

If the dataset key provided as input is not found in the root key-value—queried using the `daos_kv_get` function—, a new dataset container is created in the same way as described for the Store backend. A dataset key-value is then created in the container, again at OID 0.0, where the dataset key and the schema are inserted as new entries. An entry is then inserted in the root key-value which maps the dataset key to (the URI of) the dataset key-value just created. These insertions are performed with the `daos_kv_put` function. Any processes racing on their first `archive()` call for a same dataset key may insert the same key-value entry in the root key-value, but this does not break the consistency of the Catalogue.

The collocation key is handled in the same manner. If the supplied collocation key is not found in the dataset key-value, a new index key-value is created with an OID generated as a function of the collocation key, and an entry is added to the dataset key-value mapping the collocation key to (the URI of) the new index key-value. Otherwise, the found index key-value is used.

Finally, an entry is added to the index key-value mapping the element key to the supplied object location description, and the axis key-values are built if not yet present, which will describe the span of values indexed in this index key-value. To avoid collision between axes for different collocation keys, the axis key-value OIDs are generated as a function of the collocation key and the name of the element key dimension they store values for. For every dimension of the `archive()`d element key, an entry is inserted into the axis key-value for that dimension, where the keyword is the value of the element key for that dimension, and a placeholder value of 1 is used. This way, racing processes `archive()`ing objects for a same element key dimension will consistently register their dimension values as keywords of the corresponding axis key-value, and repeatedly inserted values will only be present once, resulting in a concise summary of the values indexed. This information will be available for consumers to use by calling the `daos_kv_list` function on the

relevant axis key-value.

Every `archive()`ing process keeps an in-memory history of values inserted into the axis key-values to avoid repeatedly inserting the same value in the same axis key-value in the likely case that multiple objects with similar identifiers are `archive()`d.

Note that the URIs inserted into the dataset and index key-values share identical roots, and the size of these entries could be significantly reduced by implementing a mechanism similar to the URI store used in the POSIX I/O Catalogue. This would reduce the latency of the `daos_kv_put` function calls and free up valuable space in the fast storage tier of the DAOS servers.

As producer processes continue to `archive()` more objects, new arrays are written and new entries inserted into the index and axis key-values. If objects are `archive()`d for new collocation keys, new sets of index and axis key-values are created, and new entries added to the dataset key-value. An example of the state of a dataset container after four different objects have been `archive()`d for two different collocation keys is shown in Fig. 3.2.

flush()

After `archive()` has returned, the indexing information has already been persisted and the indexed objects have been made visible to reader processes. There is no further action to be taken in the `flush()` method.

close()

By contrast to the POSIX I/O Catalogue, where `close()` appended full indexes to the TOC file and masked out previously inserted partial indexes, the DAOS Catalogue takes no action on `close()`. Therefore, consumer processes will use the same indexing structures for accessing objects regardless of producers being still active or not, resulting in more uniform `retrieve()` and `list()` performance.

Connection caching and axis pre-loading

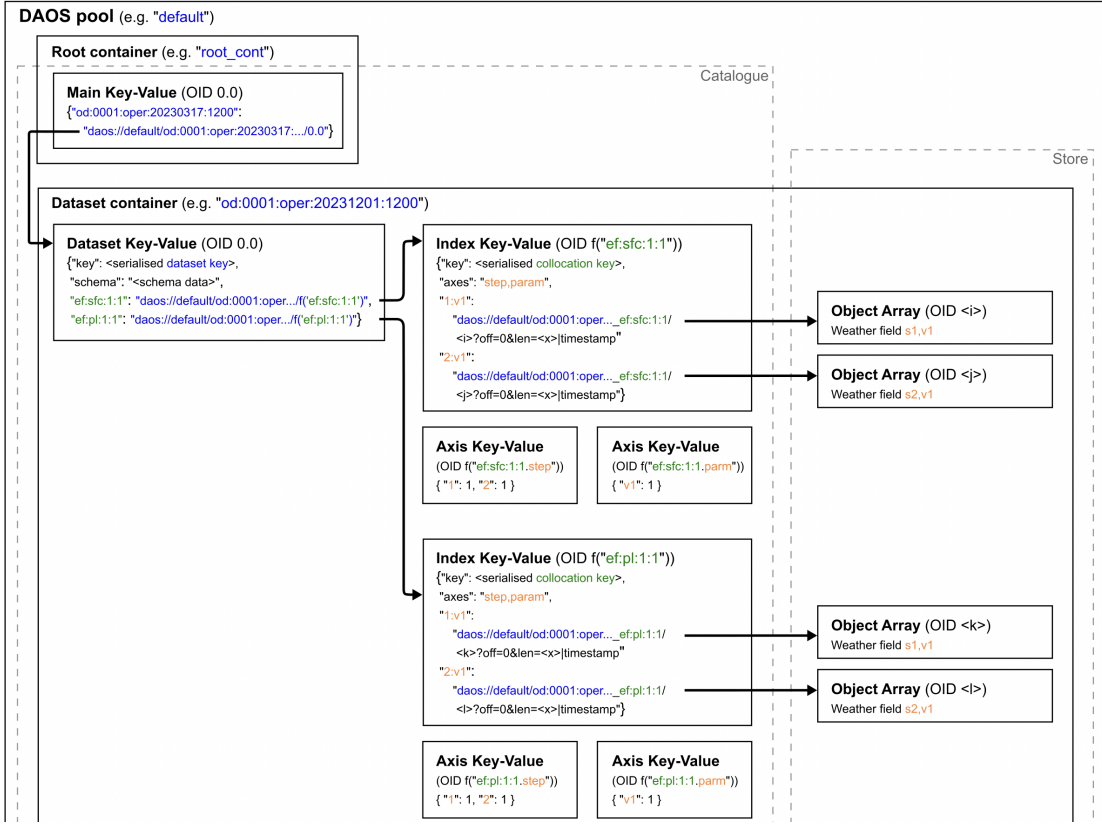


Figure 3.2: Diagram of DAOS entities resulting from four FDB archive() calls for four meteorological objects spanning two different collocation keys (one having levtype=sfc and the other levtype=pl) and two different element keys (one having step=1 and the other step=2).

The first time a process calls FDB `retrieve()` or `list()` for a given dataset key, the DAOS pool and the root container are opened. The root key-value is then queried to obtain the URI(s) of the corresponding dataset key-value(s), and the dataset container is opened. Once any pools or containers are opened, they are kept open for the lifetime of the process.

The first time a process calls FDB `retrieve()` for a given dataset and collocation key pair, the DAOS Catalogue backend queries the dataset key-value to obtain the location of the corresponding index key-value, and then retrieves the values associated to the `key` and `axes` keywords from it. The `axes` entry contains

a list of the names of all axes available for that index. The OIDs for all axis key-values are calculated using these names, and a `daos_kv_list` function call is then issued to retrieve the values from each axis key-value. The obtained axis data is stored in memory for use in the Catalogue `axis()` and `retrieve()` methods.

axis()

The Catalogue `axis()` method is called internally at the beginning of every FDB `retrieve()` call — more detail on this is given in the Catalogue interface description. A dataset key, collocation key, and the name of an element key dimension are supplied as inputs. This method extracts the list of values from the pre-loaded axis corresponding to the element key dimension and collocation key provided as inputs, and returns this list.

retrieve()

This method queries the pre-loaded axes corresponding to the supplied dataset and collocation keys to determine whether the index key-value for these keys may contain a match for the element key provided as input. If so, a `daos_kv_get` operation is issued on the index key-value to obtain the object location descriptor associated to the element key and, if found, the descriptor is returned.

Although `retrieve()` has immediate visibility of any `archive()`d objects, if a new object is `archive()`d for a given dataset and collocation key pair after a process has `retrieve()`d any object for that key pair, a subsequent `retrieve()` call by that process for the newly `archive()`d object may determine the object does not exist based on the pre-loaded axis information on first `retrieve()`.

By contrast to the POSIX I/O Catalogue, the DAOS Catalogue only loads the strictly necessary bits of information from the indexing structures in storage as needed. The POSIX backend pre-loads all TOC and sub-TOC files —including all axes and URI stores— on first `retrieve()` call for a dataset key, and loads the entire index when `retrieve()` is called for a given collocation key. The

DAOS backend, instead, only pre-loads the axes on first `retrieve()` call for a given collocation key, but performs a few `daos_kv_get` I/O operations on the dataset and index key-values on each `retrieve()` call. This means `retrieve()` of location descriptors for small sets of few FDB objects spread across different dataset and collocation keys should be more efficient on DAOS than on POSIX file systems, but less so for requests of large spans of objects for one or a few dataset and collocation key pairs.

list()

This method loads all entries from the dataset key-value corresponding to the dataset key provided as input. To that end, a `daos_kv_list` function call is first issued, followed by a `daos_kv_get` call for each entry in the key-value, resulting in a list of index key-value URIs. Ideally, this loading should be performed in a single I/O operation, but DAOS currently does not provide the option of loading all key-value keys and values in a single operation.

The collocation key present in each index key-value (under the `key` keyword) is then retrieved with a `daos_kv_get` call, and if it matches the partial identifier provided as input to this method, all keywords of the corresponding index key-value are loaded with a `daos_kv_list` call. All found keywords are turned into element keys, and for every one matching the input partial identifier, the associated object location descriptor is retrieved from the index key-value with a `daos_kv_get` call. All found location descriptors are finally returned by `list()`.

The DAOS `list()` method fetches indexing information from storage slightly more selectively than the POSIX I/O backends do, but performs many more I/O operations. This means `list()`ing on DAOS might be more efficient for requests of one or a few FDB objects, but less efficient for requests of large sets of objects.

This method has immediate visibility of any `archive()`d objects without exception.

3.1.3 Operational NWP I/O pattern on DAOS

If a DAOS system and the new DAOS backends were used for an operational run at the ECMWF, the type of I/O operations issued and the I/O patterns generated would significantly differ from those in operational runs using the POSIX I/O backends.

Consider the operational workflow described in 2.7.2.

At the end of the first simulation step, on first `archive()` call, the I/O server processes would contend to connect to the DAOS pool, open the root container—likely already created in previous runs—, create and open the dataset container, populate the dataset key-value, and insert the corresponding entry in the root key-value. The straggler processes would directly find the dataset key-value indexed in the root key-value. The processes would then allocate a wide range of OIDs each before writing begins. This initialisation phase, likely dominated by the more expensive pool and container connection operations, is represented with red stripes in the diagram in Fig. 3.3.

Writing of field data into DAOS arrays—one per field—would then begin as part of Store `archive()`. For every field to be archived, a writer process would pick the next available OID, and call `daos_array_write` which, on return, would make the field data available for consumers to access via the relevant OID. Store `archive()` would then return a location descriptor, pointing to the new array, which would be passed on to Catalogue `archive()`.

As part of Catalogue `archive()`, the process would attempt getting a match for the collocation key from the dataset key-value. On first `archive()` call no match would be found, and the process would initialise an index key-value and insert corresponding entries in the dataset key-value. In subsequent `archive()` calls a match would be found and this initialisation would be skipped. In both cases, the process would then insert the new field location descriptor into the

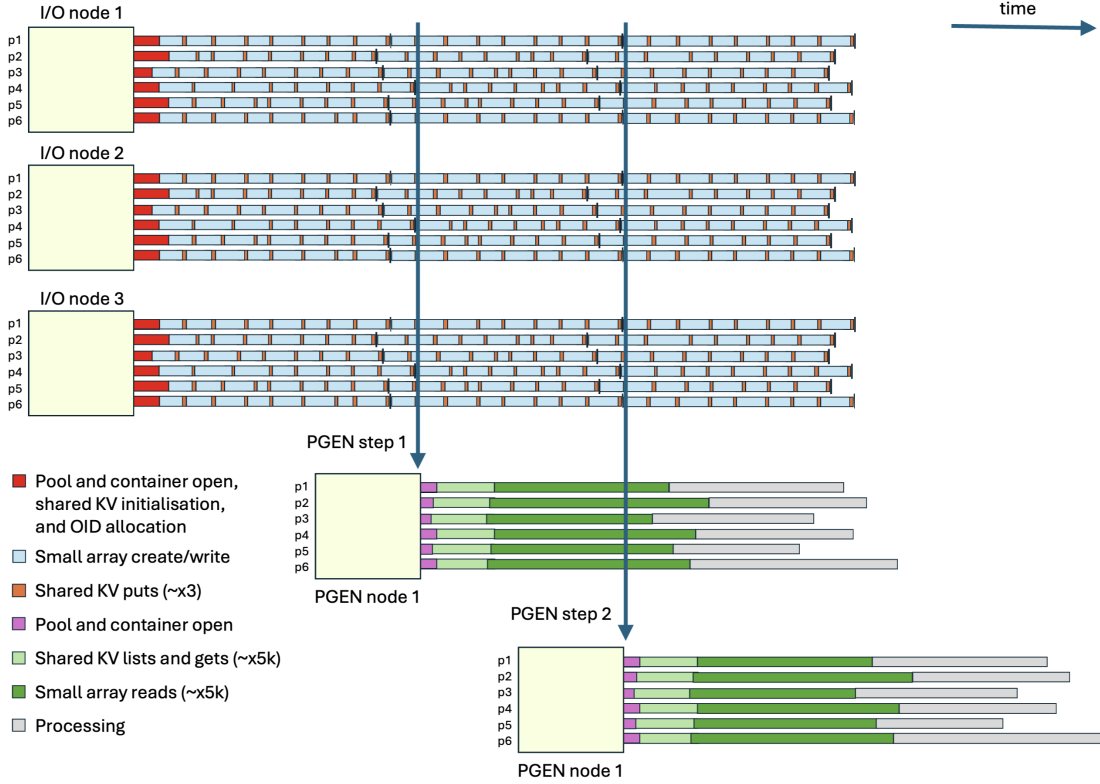


Figure 3.3: Not based on real profiling. Illustration of a simplification of the ECMWF's operational NWP storage access pattern using the FDB DAOS backends. The PGEN job for the third simulation step has been omitted. The proportions of the durations for the different types of operation in real operational runs might significantly differ from the ones displayed in this illustration.

index key-value with a `daos_kv_put` call, and insert the relevant axis elements into the axis key-values with one `daos_kv_put` call per dimension in the element key. Due to the FDB being configured to recognize the `number` and `levelist` components of the object identifiers as part of the collocation key, processes would never contend to insert entries into the same index and axis key-values.

Every process would repeat these archival operations for each of their 65 assigned step fields, for 144 simulation steps. At the end of every step `flush()` would be called, although it does not perform any operation in the DAOS backend implementation.

This writing plus indexing phase, with long sequences of `daos_array_write` calls followed by a few `daos_kv_put` calls, is represented in Fig. 3.3 with blue stripes for the object writing and orange stripes for the indexing. `flush()` calls are represented with small black segments.

At the end of every simulation step, once the straggler `archive()`ing process `flush()`ed, the workflow manager would be signaled to trigger execution of a PGEN job.

The entire indexing information for the step could first be loaded by a single node and process via `list()`, as done with the POSIX I/O backends. This would entail opening the pool and the relevant dataset container, then listing all keys of the dataset key-value and getting the content for each (there would be on the order of 8000 keys), then getting the collocation key from each index key-value and listing its keys, and finally getting the content for each key matching the current step (there would be on the order of 20 matching keys per index key-value). This would amount to a total of approximately 8000 `daos_kv_list` and 175000 `daos_kv_get` operations.

However, in this case it would be preferable to have each reader process `retrieve()` directly its corresponding subset of weather fields to be processed, which would result in a similar number of `daos_kv_list` and `daos_kv_get` operations being performed in parallel, and would not incur large per-process initialisation overheads — distributing the retrieval or listing workload over multiple processes had to be avoided with the POSIX I/O backends as all processes would perform TOC pre-loading, resulting in significant overheads.

Every `daos_kv_list` and `daos_kv_get` operation performed on an index key-value by a reader process would contend with up to one writer process performing a `daos_kv_put` operation on the same key-value.

This parallel `retrieve()` phase, likely dominated by key-value operations, is

represented in Fig. 3.3 with purple stripes for pool and container connection, and light green stripes for `daos_kv_list` and `daos_kv_get` operations.

Every PGEN process would obtain a subset of field location descriptors from the previous phase, and would then read the data from these locations issuing a sequence of on the order of 5000 `daos_array_read` operations — that is, approximately as many as the total number of fields `archive()`d per step (2600 times 65) divided by the number of processes per PGEN job (4 times 8). The reading of these arrays would not cause contention with writer processes as any newly `archive()`d objects would be written into separate new arrays. This bulk read phase is represented with dark green stripes in Fig. 3.3.

3.1.4 `fdb-hammer` I/O pattern on DAOS

The `fdb-hammer` benchmark can be executed against DAOS storage systems by configuring the FDB to use the DAOS backends. The various benchmark processes `archive()` or `retrieve()` sequences of weather fields exactly as described in Section 2.7.2, with the only notable difference being that, because the FDB schema used for operation on DAOS systems recognises the `number` and `levelist` identifier components as part of the collocation key, the benchmark writes or reads fields not only for different element keys, but also for different collocation keys.

The write phase of `fdb-hammer` on DAOS produces a storage access pattern very similar to that of an operational run on DAOS, with the only significant differences being the configured dimension sizes —as summarised in Table 2.1—, the timing of the operations, and their distribution across processes.

Regarding timing of operations, all reader nodes and processes immediately start fetching their assigned subset of fields at the beginning of the run. Every process first issues a sequence of `retrieve()` calls for all the relevant fields, to obtain their location descriptors. Overall, this results in a large number of pool and

container connection operations, as well as index key-value list and get operations, all taking place at the beginning of the read phase. Therefore, during this part of the read phase, `fdb-hammer` creates more contention on the index key-values than there would be in an operational run, but no contention is created during the rest of the `fdb-hammer` run. For the rest of the read phase, reader processes build `DataHandles` from the obtained location descriptors and read data from the corresponding arrays — one per field. There is no write-read contention on access to these arrays, just as in an operational run.

Regarding distribution, every process reads exactly the subset of fields its corresponding writer process `archive()`d for the full sequence of simulation steps and for a single member, rather than reading fields for a single step across multiple members. In consequence, a smaller number of key-value operations per reader process are performed than in operational runs, but the total set of index key-value operations performed across all processes does not change.

An illustration of an example `fdb-hammer` run on DAOS, employing a single node for each phase, is shown in Fig. 3.4.

All in all, `fdb-hammer` on DAOS is more representative of operational runs on DAOS than `fdb-hammer` on POSIX is representative of operational runs on a POSIX file system, and this is mainly due to the fact that the writer processes in `fdb-hammer` on DAOS do access and reuse the indexing data structures created on the preliminary write phase, thus reproducing contention with readers. When using the POSIX backends, instead, `fdb-hammer` writer processes mostly create new indexing structures which the readers do not access, thus partly not capturing the contention of operational runs.

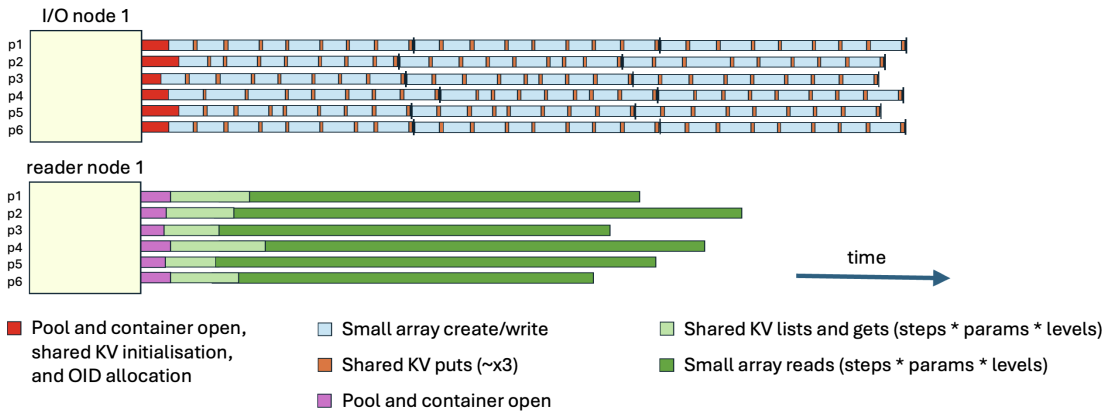


Figure 3.4: Not based on real profiling. Illustration of a simplification of the storage access pattern of the fdb-hammer benchmark on DAOS. The proportions of the durations for the different types of operation in real fdb-hammer runs on DAOS might significantly differ from the ones displayed in this illustration. Real fdb-hammer runs performed in this analysis employed up to 24 writer and 24 reader nodes, with up to 48 processes per node, and were run for 100 time steps.

3.2 Ceph backends

Ceph’s RADOS provides functionality, APIs, and semantics similar to those of DAOS. Most relevant, RADOS provides regular objects where byte strings can be stored—similar to DAOS’s arrays—, and Omap objects for key-value functionality, very similar to DAOS’s key-values.

In 2019, the ECMWF attempted implementing FDB RADOS backends due to Ceph’s increasing popularity in cloud environments and its adoption in part of the ECMWF’s cloud infrastructure. A RADOS Store backend was implemented which used large RADOS regular objects, each containing multiple weather fields, and as new weather fields were `archive()`d and the objects reached the RADOS object size limit—usually 128 MiB—these were expanded with additional objects which were linked to the previous ones using object attributes. The backend implementation at that time resulted in lower I/O performance than expected, potentially due to the overheads caused by attribute manipulation, and was in

consequence discontinued, with the implementation of a RADOS Catalogue never being pursued.

A few years later, as part of this thesis, new RADOS Store and Catalogue backends were implemented heavily based on the design of the DAOS backends, requiring only replacing DAOS API calls by RADOS API calls for large part of the development thanks to the similarities between DAOS and RADOS. In turn, this resulted in an end-to-end implementation and evaluation time of only 3 to 6 months. Nevertheless, there were significant differences between the two storage systems and APIs, which raised a few questions regarding the overall design of the new backends, and required further evaluation, decision making, and modifications in the backend code base with respect to the DAOS backends.

The first question was related to data organization. Encapsulating all data and indexing information for a given dataset key within a separate logical division is desirable as it makes some administrative tasks easier, such as removing entire datasets without knowledge of the backend internals. This was achieved with containers in the DAOS backends, but RADOS does not provide containers. Instead, RADOS provides the option of creating namespaces within pools, akin to DAOS containers. Although RADOS namespaces seemed an ideal resource for encapsulation, pools were also an option worth exploring as it is more difficult to accidentally remove a RADOS pool than a namespace. Also, the data redundancy of RADOS objects can only be configured at the pool level, and having a pool per dataset would allow more flexibility in that regard. Conversely, one strong advantage of RADOS namespaces is that these are lightweight and should in principle have a smaller performance impact than pools.

The next question concerned data collocation and object size. Using a RADOS object per meteorological object, just as with the DAOS backends, seemed a more natural and easier way of implementing the Store backend than storing multiple

meteorological objects in a single RADOS object. However, the RADOS Store backend attempt a few years earlier resulted in insufficient performance despite using large RADOS objects where multiple meteorological objects were collocated, suggesting that using a RADOS object per meteorological object could potentially result in even worse performance as a larger number of small operations would be performed over the network between RADOS servers and clients.

In turn, if choosing the approach involving large RADOS objects, there were two options. The first —and the one followed in the existing RADOS Store implementation— consisted in having each process write all meteorological objects `archive()`d for a same dataset and collocation key into a single RADOS object, but spanning additional objects as needed if exceeding the default maximum object size of 128 MiB. The second option consisted in enlarging the maximum permitted object size on the RADOS servers —at deployment time— to a value large enough to fit all meteorological objects to be `archive()`d for a same dataset and collocation key by a single process, thus avoiding spanning multiple medium-sized objects. Although altering this setting is not possible in third-party-managed Ceph systems, it might be an option worth of consideration if using a Ceph system solely devoted to the application at hand.

The last question was whether to immediately persist `archive()`d objects and indexing information —as done in the DAOS backends—, or deferring ensuring persistence until `flush()` is called —as done in the POSIX I/O backends—, potentially resulting in better backend performance. RADOS provides options to implement both approaches. Regular objects can be written either immediately on `archive()` with `rados_write`, or asynchronously with `rados_aio_write` and have their persistence ensured later on `flush()` with `rados_aio_wait_for_complete`. Omap entries could also be inserted asynchronously, but this feature is not necessary as, if object data is written asynchronously, index Omap insertions must be performed

in blocking mode on `flush()` to ensure a consistent view is provided to consumers at all times. If object data is written immediately, Omap insertions —much cheaper than the data writing— should preferably be performed immediately on `archive()`.

Given no in-depth preliminary assessment was conducted for RADOS —unlike for DAOS— and there was no insight available as to which of these options would result in better performance, all of them were implemented in the new RADOS backends, with the possibility of enabling or disabling them via compilation flags. All options were then tested at scale with the `fdb-hammer` benchmark, with the consistency check option enabled, to determine their performance level and verify their consistent behavior. The results are shown in Fig. 3.5.

The first test set, shown in the left-most column, had the Ceph backends configured to use a single pool with multiple namespaces in it — one per dataset key. All objects `archive()`d by a same process for a same dataset and collocation key spanned multiple RADOS objects of default size (128 MiB), and all Omap insertions and object writes were persisted immediately.

The second test set was identical except a pool per dataset key was used instead of namespaces. Specifically, two pools were created by these tests instead of just one. The achieved bandwidths were slightly lower than with the previous configuration likely due to the fact that RADOS is sensitive performance-wise to the total number of placement groups (PGs) in the system. Having an additional pool meant there were double as many PGs, which could have caused the performance downgrade. This performance issue could potentially be mitigated by enabling PG auto-scaling or manually adjusting the PG count per pool to an appropriate value as a function of the number of pools in the system. Although the pool-per-dataset configuration was deemed valid and suitable, all following tests were configured to use a single pool and a namespace per dataset key as this avoided the complexity

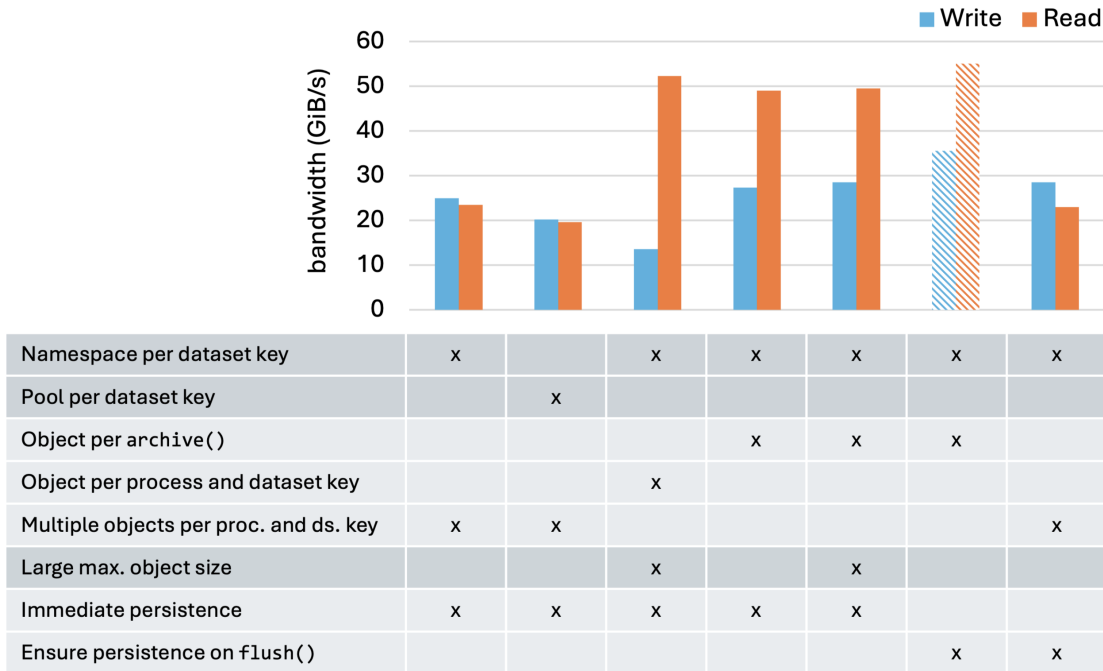


Figure 3.5: Performance of the FDB Ceph/RADOS backends with different options enabled. Measured with `fdb-hammer` runs on 32 client nodes, using 16 processes per node, against a Ceph deployment on 16 OSD nodes with 6 TiB of NVMe SSDs each. RADOS pools were configured with 512 placement groups and no replication or erasure-coding. Every process archive()d or retrieve()d 10000 weather fields of 1 MiB each. The mean of the bandwidths obtained for 3 repetitions are shown for each configuration. Using a RADOS object per archive()d FDB object resulted in best performance. Using a RADOS object per archive() call and ensuring persistence on flush(), shown with patterned columns, did not fulfill the consistency requirements.

associated with PG counts and resulted in slightly better performance.

The third set of tests were configured to use a single large object per process and collocation key. Although this resulted in significantly better read performance, the write performance halved, implying this option would be inconvenient for applications such as the ECMWF’s operational runs where write performance is critical.

The fourth set used a RADOS object per `archive()`d FDB object. This resulted in write performance as high as with the approach using multiple objects per process and collocation key, and read performance nearly as high as with

a single large object per process and collocation key. The object-per-archive-call approach thus provided the best performance balance among the tested configurations. The high read bandwidths obtained with this configuration — using several objects per process and collocation key —, in combination with the high read bandwidths in the third set of tests — using a single object per process and collocation key — suggested there might be inefficiencies potentially worth addressing, impacting read performance, in the option employing multiple objects per process and collocation key — tested in the first, second, and seventh sets. Nevertheless, even if removing such inefficiencies, the read performance would unlikely exceed the bandwidths observed in the third test set — which used as few objects as possible —, and the configuration with an object per `archive()` call would therefore remain as one of the best performing options.

The fifth set was identical to the fourth except a larger maximum object size (1024 instead of 128 MiB) was set on the RADOS servers. The performance did not vary significantly with respect to the previous test set, suggesting that enlarging the maximum object size should enable applications requiring storing larger objects without deteriorating performance for smaller objects.

The sixth set used an object per `archive()` and the default maximum object size, just as the fourth set, but was configured to use the asynchronous family of functions in `librados` and ensured persistence of Omap and object operations on `flush()`. This configuration performed better than the rest, but unfortunately the objects `archive()`d by writers were not always accessible to readers if attempting `retrieve()`al shortly after `flush()`. This did not fulfill the consistency guarantees expected from the RADOS asynchronous API, and this configuration was therefore discarded as a viable option. Nevertheless, further analysis would be required to confirm the asynchronous RADOS APIs were not misused in the backend implementation.

The seventh and last set of tests used multiple objects per process and collocation key, just as in the first set, but this time using the asynchronous APIs and ensuring persistence on `flush()`. This configuration did provide the expected consistency guarantees, and resulted in slightly higher write performance than equivalent tests using the blocking APIs.

Among all tested configurations, the one using a namespace per dataset key, an object per `archive()` call, and blocking I/O with immediate persistence, was the one that performed best. These options were thereby fixed as defaults for the Ceph backends, and used for all `fdb-hammer` runs on Ceph in Chapter 4.

A diagram of RADOS entities resulting from an FDB `archive()` call using the Ceph backends with the selected configuration is shown in Fig. 3.6.

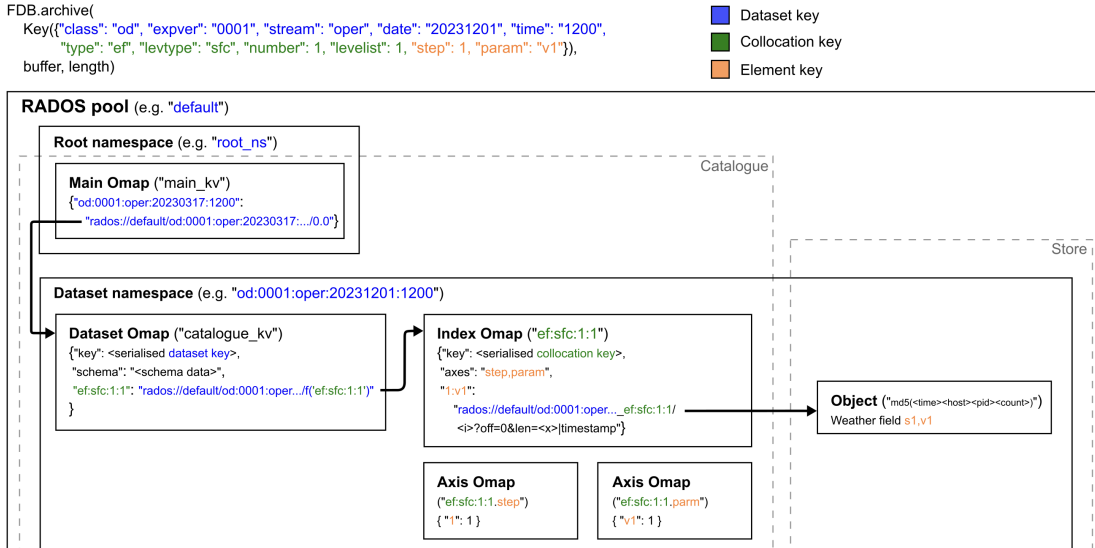


Figure 3.6: Diagram of Ceph/RADOS entities resulting from an FDB `archive()` call for one meteorological object. The `archive()` call is shown at the top, using different colours for the dataset, collocation, and element keys. The object data and indexing information are persisted immediately. A `flush()` call would result in no additional changes to these entities.

Due to the design of the Ceph backends —with the chosen configuration— being nearly identical to that of the DAOS backends, the overall object layout

and logic of both backends are very similar, and most of the explanations and discussion in Section 3.1 concerning the DAOS backends are directly applicable to the Ceph backends.

All in all, more design options were explored and tested for the Ceph backends than for DAOS, and this was justified partly because the previous work on the DAOS backends paved the way for a more in-depth exploration on Ceph, but also because past backend attempts on Ceph resulted in insufficient performance, making such deeper exploration necessary to ensure a well-performing design was found for the Ceph backends. Nevertheless, the main findings —i.e. the fact that using an object per `archive()` performs very well, and the fact that using asynchronous I/O and ensuring persistence on `flush()` may perform slightly better than persisting immediately— should also be applicable to the DAOS backends, meaning that the current object per `archive()` design of the DAOS backends probably performs equally or better than a hypothetical alternative design using large per-process objects, and that DAOS asynchronous I/O might be worth exploring in the future to achieve slightly higher performance with the DAOS backends.

Eventually, the design of the backends for both DAOS and Ceph have used the same design approaches, making them a suitable tool to fairly compare the performance of both storage systems.

3.2.1 The Ceph Store and Catalogue

The logic of the developed Ceph Store and Catalogue backends is very similar to that of the DAOS backends, described in Section 3.1, with only the following differences:

- Namespaces are used instead of containers. Namespaces are more lightweight and do not require creation or opening.

- RADOS regular objects are used instead of DAOS arrays. The `rados_write_full` and `rados_read` calls are used instead of `daos_array_write` and `daos_array_read`. Arrays are richer in the ways they provide to access the data in them, but these features were not used in the DAOS backends and are not necessary either for the Ceph backends.
- Omaps are used instead of key-values. The `rados_write_op_omap_set2` and `rados_read_op_omap_get_vals_by_keys2` calls are used instead of `daos_kv--_put` and `daos_kv_get`. The functionality they provide is very similar. Omaps require creation with `rados_op_write_create` before use.
- Omaps are richer than DAOS key-values in the ways they provide to retrieve, query, and filter entries. Most relevant, `rados_read_op_omap_get_vals_by_keys2` allows retrieving the full set of keys and values for an Omap in a single RPC, which was not possible in DAOS. This resulted in a more efficient FDB `list()` implementation in the Ceph backends.
- RADOS regular objects and Omaps are identified with character strings instead of 128-bit OIDs.
- DAOS containers provided functionality for the DAOS backends to allocate a set of unused OIDs. In the Ceph backends, instead, allocating a new object name is done by creating unique character strings based on the technique used for per-process file creation in the POSIX I/O backends. An MD5 checksum of the unique character string is then calculated and used as object name to avoid objects being placed repeatedly in the same OSD if the character strings share a common root.

3.2.2 Operational and `fdb-hammer` I/O patterns on Ceph

Both the operational NWP and `fdb-hammer` I/O patterns using the Ceph backends are very similar to those described for the DAOS backends, illustrated in Fig. 3.3 and Fig. 3.4, with only the following differences:

- There are no container connection nor OID allocation overheads at the beginning of operational nor `fdb-hammer` writers or readers — the red and purple stripes in both Fig. 3.3 and Fig. 3.4 would be shorter if using the Ceph backends.
- Since `list()`ing is more efficient with the Ceph backends, the operational workflows on Ceph might benefit from the approach used for operational runs with the POSIX I/O backends, illustrated in Fig. 2.11, where a single process per PGEN job first lists the full set of FDB objects to be read.

`fdb-hammer` on Ceph is more representative of operational runs on Ceph than `fdb-hammer` on POSIX is representative of operational runs on a POSIX file system.

3.3 S3 Store

S3 is a very popular object storage protocol which originated as a Representational State Transfer (REST) Hypertext Transfer Protocol (HTTP) API for Amazon to expose their cloud object storage services. Although it is mainly used in Cloud rather than HPC setups, and there are challenges associated to using it for high-performance[25], many high-performance storage systems such as DAOS, Ceph, VAST, Weka, and MinIO, provide S3 interfaces.

Due to the relevance of this protocol, the development of S3 backends for the FDB was explored with the aim of broadening the range of storage systems

supported by the FDB rather than assessing S3 as a potential HPC storage candidate for the more highly demanding operational workloads at the ECMWF.

S3-compatible storage systems serve a REST HTTP API which conforms to the S3 API[52], exposing endpoints for applications to request GET, POST, PUT and DELETE operations to be performed on buckets —storage partitions with their own namespace— or objects — independent data blobs belonging to a bucket. Both buckets and objects are identified with a name.

Credentials for authorisation are typically negotiated first through dedicated endpoints (see the CreateSession S3 operation) and these credentials can then be provided in further S3 API requests via HTTP headers.

Buckets and objects can be created, listed and deleted, among others. Of most relevance here, are the object write and read operations.

An object can be created with a PUT request specifying, in the headers, the name of an existing target bucket and the desired object name —also referred to as *key*— for the object to be created, and attaching the desired object data in the body. According to the S3 semantics, either the PUT operation will succeed and result in the object being fully written, or the operation will fail. If multiple concurrent PUT operations are submitted for a same bucket and object, the last racing operation prevails, replacing the object data for the previous operations. An object cannot be modified or updated. An object can be locked such that further PUT operations on it fail, or configured for versioning such that old versions of the object are preserved and identified with a version number.

While it is not possible to expand or append data to an object, multipart uploads are supported. A multipart upload must first be initiated with a POST operation specifying the desired key for the full object upon completion. This returns an upload ID which must then be provided in subsequent part upload PUT operations, each returning a part ID. Finally, a multipart upload completion

operation must be POSTed, containing the upload and part IDs. Upon success, the full assembled object is made available to readers.

An existing object can be read with a GET request specifying, in the headers, the name of the containing bucket and the object key. The current version of the object is fully returned by default. Partial byte ranges of the object can be requested via the HTTP Range header.

S3 defines many other operations, each with its semantics, and with multiple options and variants. Implementing a fully compliant HTTP client can be a challenging task. Many S3 client libraries exist to make this easier, with the Amazon Web Services (AWS) S3 Software Development Kit (SDK) being the one used by the ECMWF to implement higher-level S3 functionality which was then leveraged for the development of the S3 FDB backends.

Implementation of an S3 Catalogue backend was considered but eventually discarded due to a lack of features in S3 to do so easily. The previously described POSIX I/O and object storage Catalogue backends relied on the atomic append and the key-value features to implement a consistent and expandable index of archived objects. S3, however, did not provide these features. It should theoretically be possible to implement an S3 Catalogue backend very similar to the POSIX I/O one by simply replacing index and sub-TOC files by S3 objects, and using S3 object listing features to provide an inventory of available sub-TOC and index objects in place of the TOC file. However, this would have likely resulted in an excessive and non-well-performing use of such listing features, and was therefore not pursued.

Conversely, it was possible to implement an S3 Store backend such that each FDB meteorological object is stored in a separate S3 object, and all objects for a same dataset key are stored in a same bucket.

Every time `archive()` is invoked, it generates a unique ID based on the current

time, hostname, and ID of the process invoking it. That ID is used as key for a new S3 object which is created and populated with the meteorological object data with an S3 PutObject operation. `archive()` blocks until the S3 operation returns successfully, and therefore until the data is made available to reader processes.

`flush()` performs no operation as the data is already ensured to be persistent upon `archive()`.

`retrieve()` creates and returns a `DataHandle` object which wraps the S3 object containing the requested field. `DataHandle` provides methods for reading the data which issue GetObject operations under the hood.

Two major design options arose while developing the S3 Store backend. The first was whether to use a single bucket to contain all fields or objects for all dataset keys, as opposed to using a separate bucket for each. The single-bucket approach is more convenient for Cloud environments where the number of buckets a user can have is usually limited, or where a single bucket with a name chosen by the system administration is provided. The bucket-per-dataset approach seems cleaner as the data structures and data are kept separately for each dataset key, which not only makes it easier and safer wipe a specific dataset, but also makes the backend code simpler. The bucket-per-dataset approach was chosen, although code for the single-bucket approach was also drafted and should be easy to fully implement if necessary.

The second design option was whether to store every FDB object in a separate object, as opposed to having a common object for all FDB objects sharing dataset and collocation keys, where newly archived objects would be "appended" with a part upload operation and the resulting multipart object would be aggregated and made visible upon `flush()`. The object-per-field approach was chosen due to ease of implementation, although the multipart upload approach would likely result in better performance as it would substantially reduce the number of S3

objects — and this is known to have a significant overhead in S3 stores. The code infrastructure required for the multipart upload approach was also drafted and should equally be easy to fully implement if needed.

The developed S3 Store backend was verified to work consistently against local deployments of Ceph —via the Object Gateway interface— and MinIO.

Although this was not pursued due to lack of time, the FDB S3 Store backend should be tested against high-performance DAOS and Ceph deployments exposing an S3 API, and the performance results compared to equivalent tests operating against the storage systems natively. Some performance loss would be expected for tests using the S3 backend due to the inherent overheads of the HTTP protocol, and also due to HTTP servers and clients not necessarily being designed for optimal performance in HPC environments.

Chapter 4

Performance Assessment

So far, this work has looked mainly into the functionality and consistency of the DAOS and Ceph object stores. However, performance and scalability are also key factors to determine the overall suitability of these object stores for the ECMWF’s operational NWP and for HPC and AI applications in general.

This chapter presents performance and scalability measurements obtained by running certain I/O-intensive applications, also referred to as benchmarks, against both object stores and the Lustre distributed file system deployed on the same hardware, and discusses the observed differences. A range of I/O benchmarks were employed, some of which perform generic I/O workloads, and some others perform NWP-specific I/O workloads. Among the latter, some make use of the FDB library and the backends described in Chapters 2 and 3.

The benchmarks were run in two different systems with different storage hardware. One of them —the NEXTGenIO system— was equipped with Intel’s Optane DCPMM, and the other —the Google Cloud Platform (GCP)— provided Virtual Machines (VMs) equipped with NVMe SSDs.

This addresses the third, fourth, and fifth contributions of this dissertation: *"I/O performance assessment methodology"*, *"Suitability and performance as-*

essment of Ceph and DAOS for the ECMWF's operational NWP", and "Fair performance comparison of DAOS, Ceph, and Lustre".

4.1 Methodology

The main question this assessment aimed to address is whether object storage systems and approaches are suitable and can provide an advantage, in terms of performance, over traditional POSIX file systems both for the ECMWF's operational NWP as well as for HPC and AI applications in general.

The adopted methodology consisted in conducting I/O benchmarking experiments against DAOS and Ceph object storage systems as well as against Lustre file systems deployed on the same hardware, and comparing the resulting performance measurements.

I/O benchmarking consists in measuring how a given storage system performs under the I/O workload of a given application or benchmark where I/O operations usually predominate. This has several degrees of freedom, described below, which need to be navigated and adjusted in function of the benchmarking context and aims to ensure that the benchmark configuration and the produced I/O workloads are as representative as possible of a real production setup, and that the resulting bandwidth measurements are actually and fairly indicative of what performance the storage system can provide under these I/O workloads.

- **The type of I/O operations issued by the benchmark.** These can include metadata operations such as file or object creation, deletion, listing, writing, or reading, among others. Write and read operations, in turn, may be larger or smaller in size, and this can have a significant impact on performance. Which I/O benchmark is selected largely determines the type of I/O operations that will be issued, although many benchmarks provide parameters to modulate, to varying extents, the composition of the I/O workload.
- **The I/O patterns produced by the benchmark.** Some benchmarks issue I/O operations from all client nodes and processes for the entire duration of

the run, and some others have different subsets of nodes or processes start issuing I/O operations at different times. Some have all processes issue I/O operations in a synchronised fashion, all at the same instant, and some others have the processes issue sequences of operations independently. Some combine I/O operations with client-side sleeping or processing, and some do not. Some have all processes perform the same type of I/O operation at any one time (e.g. write operations only), and some combine different types of potentially contending I/O (e.g. writes and reads simultaneously). Some access large regions of contiguous data in storage, and some access small data units at random locations. All these aspects characterise the I/O patterns produced by a benchmark. Again, what I/O patterns are produced is largely determined by the selected benchmark, but can often be modified through parameters.

- **The degree of parallelism of the benchmark.** While some real applications (as opposed to I/O benchmarks) run massively in parallel, some others are constrained to one or a few processes or daemons, and the I/O benchmark should capture this aspect according to the intended use of the storage system. If the intended use is for massively parallel applications, the degree of parallelism of the benchmark can repeatedly be altered and the benchmark rerun to discover the optimal configuration and the performance potential of the storage system.
- **The size of the storage system used for benchmarking.** It is often not possible to access and benchmark against a storage system large enough and therefore representative of a production setup. Instead, I/O benchmarking can be conducted against increasingly large partitions of the storage resources available for testing to determine the scalability behaviour of the storage system, and this result extrapolated to estimate the performance of a system of a scale as large as required for production.

- **The size and duration of the I/O workload produced by the benchmark.**

A benchmark may run for a very short time period if intending to test the performance of applications performing small one-off queries or updates where low latency is desirable, or for a long time period if intending to test the performance of parallel applications writing or reading large data volumes where high throughput is more important than low latency. In the latter case, the duration of a run may be modulated by adjusting the I/O size, process count, and number of I/O operations performed per process. This degree of freedom is therefore tightly linked to the previously described ones. If the size of the storage system is varied to determine scalability, the I/O workload can be scaled together with the storage system if aiming to test weak scaling —that is, the ability of the storage system to deliver higher performance as more storage resources are added given a proportionally large I/O workload—, or fixed to a constant size if aiming to test strong scaling —that is, the ability to deliver higher performance given a fixed I/O workload—, although in the latter case the duration of the I/O workload will usually reduce when run against larger and faster storage system deployments.

- **The amount of client resources used for benchmarking.** Similarly to the parallelism degree of freedom, some applications are designed to run on a single machine with a single network adapter, whereas some others are designed to run on as many machines and exploiting as many network adapters as necessary to obtain the highest performance the storage system can deliver. These resources may be scaled weakly or strongly relative to the storage system, independently of how the I/O workload is scaled.

- **Other client and server-side configuration.** I/O performance can be very sensitive to a wide array of other client and server-side settings, both at the

operating system and application levels. Determining when and which such settings exactly may be negatively impacting I/O performance, and what might be their optimal values, can be one of the most challenging aspects of I/O benchmarking. Some examples of relevant settings are the operating system block size both on the client and server sides (mostly relevant when operating against a parallel file system), the network maximum transmission unit (MTU), whether storage devices in the server machines are interleaved or arranged as a redundant array of independent disks (RAID) configuration, how many processes are deployed on these machines to serve such devices, how parallel processes are pinned to CPU cores both client and server-side, whether client-side caches are utilized or bypassed, and whether the storage system and the benchmark are configured to stripe and/or create redundant copies of the files or objects. These are often set to their default, or a guess made as to which might be the best value, and their optimal value is then explored by readjusting and rerunning the benchmark.

- **The events to log and performance metrics to use.** At the very least, an I/O benchmark should record timestamps when I/O starts and when it ends so that the total elapsed time can be calculated and used to compare the performance of different benchmark runs against different storage systems or using different configuration. For simple benchmarks issuing only a single metadata operation or one-off query this measurement is referred to as *latency*, and for more complex benchmarks issuing multiple operations, potentially concurrently, this is referred to as *wall-clock time*. If the benchmark runs as multiple non-synchronised processes, all processes must record start and end timestamps for it to be possible to calculate the overall wall-clock time.

The wall-clock time metric has the disadvantage that when the degree of parallelism or the size of the I/O workload are repeatedly altered and the

benchmark is rerun, the wall-clock time measurements for the successive runs may not be indicative of how well the storage system and the benchmark performed. For instance, a benchmark run taking 10 seconds to perform a single I/O operation performs worse than a benchmark run taking 12 seconds to complete 10 of the same I/O operations in parallel in terms of work accomplished per unit of time, but the wall-clock time measurement does not capture this. In these cases, calculating the rate of I/O operations per time unit —also referred to as *IOPS*— or bytes transferred per time unit —referred to as *bandwidth*— is preferable.

Often, mainly due to the high degree of complexity of I/O systems, variance can occur among latency, wall-clock time, IOPS, or bandwidth measurements for subsequent runs of a same I/O benchmark on a same system with identical configuration. It is therefore advisable to perform multiple benchmark runs and calculate the average, maximum, or any other suitable statistic across the set of obtained measurements.

This methodology defined ways to fix or narrow down a few of these degrees of freedom, and ways to explore and optimise the rest of degrees of freedom, such that the I/O benchmarking experiments would result in meaningful measurements of the performance the different storage systems can provide for operational NWP at the ECMWF as well as for other similar data-intensive HPC applications.

The methodology —particularly the parameter optimisation and scaling strategies described below— is sufficiently generic that it can be used for other storage and I/O performance analyses looking into similar applications issuing many I/O operations with a high degree of parallelism.

4.1.1 Type of I/O operations and benchmarks

Regarding the type of I/O operations, this analysis mainly focused on file or object write and read operations of 1 MiB in size. This operation size was selected because, at the time the first part of this performance assessment was conducted, operational runs at the ECMWF wrote and read data elements — weather fields — from storage of approximately 1 MiB in size. The operational model resolution was later increased, resulting in fields of an average size of 4.3 MiB, but given both the previous and the new field sizes were within the same order of magnitude, the performance assessment adhered to the previous one for consistency and comparability across results. A set of I/O benchmarks were selected which produce I/O workloads where these types of operation predominate.

As described earlier, operational NWP at the ECMWF not only performs bulk writing and reading but also requires creating an index of written meteorological data objects. Some of the selected benchmarks also exercise the storage systems with the necessary operations to implement the index — these operations include small file writes and reads, file appends, and key-value or Omap gets and puts.

The selected benchmarks are described in the following.

IOR

IOR[53] is a popular open-source I/O benchmark developed by the HPC community, originally intended to measure the I/O performance of parallel file systems, but expanded over time with new I/O backends to support operation on other storage systems like DAOS and Ceph.

IOR runs as a parallel MPI application where the concurrent processes create a file or object each, wait for each other, and commence issuing a sequence of write or read operations against their corresponding file or object. This mode, where processes do not contend for access to a same file, is known as *IOR easy*[54].

IOR can also be configured such that all processes operate against a single shared file or object, and this is known as *IOR hard*. For this analysis, only the IOR easy mode was used as it is more representative of what a domain-specific object store like the FDB would do, avoiding multi-process contention on the same files or objects.

IOR provides parameters to adjust the number and size of the I/O operations performed by each process as well as their distribution in the file. The following algorithm shows a simplification of the logic and I/O operations performed by IOR easy, highlighting some of the parameters.

Algorithm 1: IOR easy main loop

Inputs: nIterations, nSegments, blockSize, transferSize

```

for i in 1..nIterations do
    barrier
    create and open per-process file or object
    for s in 1..nSegments do
        for transfer in 1..(blockSize / transferSize) do
            | write/read transferSize consecutive bytes from segment s
        end
    end
    close
    barrier
end

```

For all IOR tests in this analysis, a single iteration (`-i 1`), multiple segments (`-s > 1`), and equal block and transfer size (`-b = -t`) were used. This means every process performed a single barrier, a single create and open operation, and multiple write or read I/O operations. Therefore, I/O operations across processes were not synchronised.

HDF5

The IOR benchmark provides a backend for operation via Hierarchical Data Format 5 (HDF5). HDF5[55] is an I/O middleware library for efficient storage of complex and voluminous datasets used in a range of disciplines, and supports features such as data compression and encryption. HDF5 operates, by default, on POSIX file systems, but has adapters to support operation on other storage systems including DAOS[27].

When IOR is run with the HDF5 backend on POSIX, a file is created per writer process where the process metadata, indexing information, and data are stored. If the DAOS adapter is enabled, a DAOS container is created per writer process, and the data from every write operation stored in a separate object in the container and an index created using key-value objects. This results in IOR and the HDF5 backend producing a more complex set of I/O patterns —both on POSIX and on DAOS— than those produced by IOR and its POSIX or DAOS backends.

Field I/O

Field I/O is a standalone I/O benchmark developed as part of this research to evaluate the performance a DAOS system can provide for operational NWP at the ECMWF without involving the full complexity of the operational I/O stack. It runs as a set of independent processes, each writing and indexing a sequence of weather variables, or fields, into DAOS with a combination of array and key-value operations. If configured in read mode, the processes retrieve the same sequence of fields by querying the key-values and reading the array data. Field I/O processes write each field in a separate array, and store indexing information in a set of key-values — some of them exclusive to the process, and some of them shared among all processes.

The Field I/O benchmark is described and discussed in more detail in Appendix B - Section IV.

Although Field I/O was designed to run on DAOS only, it can also be run on POSIX file systems via a mock `libdaos` library, also developed as part of this research, which implements the `libdaos` API using files and directories under the hood. More detail on this library is provided in Appendix A - Section IV.

fdb-hammer

`fdb-hammer` is an FDB performance benchmarking tool provided as part of the FDB source repository which can be built alongside the other FDB command-line tools. In the same way as Field I/O, `fdb-hammer` runs as a set of independent processes, each archiving, retrieving, or listing—depending on supplied arguments—a sequence of weather fields via the FDB.

When run with the POSIX I/O FDB backends, `fdb-hammer` writer processes create a few dedicated files each, which are expanded incrementally with indexing information and field data, respectively. Reader processes then open and read these files to retrieve the written weather fields. This is described thoroughly at the end of Section 2.7.2, including a discussion of the differences between the I/O workload and patterns generated by `fdb-hammer` and those of operational NWP runs at the ECMWF.

When run with the DAOS or Ceph FDB backends, `fdb-hammer` writers use a set of arrays (or regular objects) and key-values (or Omaps) to store and index the weather fields, which are then accessed by readers. This is described thoroughly at the end of Section 3.1.

4.1.2 I/O patterns of interest

Three generic I/O patterns of interest were identified and defined, and the benchmarks configured where relevant to adhere to these.

- **No write+read contention.** A writing phase is run first, where the benchmark is run in parallel from a number of parallel processes, and each process writes (and indexes, if relevant) a sequence of 1 MiB data units. Following this, a reading phase is run where the benchmark is executed from as many processes, with each process reading back the same sequence of data units its corresponding writer process wrote. There is no contention between writers and readers as they run separately, optionally on separate sets of nodes. If run on the same set of nodes, the readers in a node must read data written from a different node to avoid accessing locally cached data, if any. This I/O pattern is suitable to determine the performance potential of the storage system for either writing or reading in isolation and in parallel.
- **Write+read contention.** A writing phase is run initially to populate the storage, and then a writer and a reader phase —as described in *no write+read contention*— are run simultaneously. In this variant there is contention between writers and readers. This I/O pattern is intended to mimic the I/O patterns of the ECMWF’s operational NWP, where parallel processes independently write and read sequences of meteorological objects.
- **Contending repeated writes and reads.** A writing phase is run initially to populate the storage, and then a writer and a reader phase are run simultaneously where every process repeatedly writes or reads a same data unit, with the same identifier. Every parallel process uses a different identifier. This aims to test a slightly more aggressively contentious I/O pattern, although this was seldom used as this is not representative of the ECMWF’s operational NWP.

These I/O patterns do not fully specify all properties of an I/O pattern mentioned earlier. Beyond the specified constraints, all selected benchmarks were used with their default settings. This meant all benchmarks issued I/O operations from all parallel processes for the entire duration of the run, without synchronisation, and avoided non-I/O overheads.

Given the non-synchronised nature of the benchmarks, significant delays could occur between the start times of the parallel processes of a phase, as well as between the start times of the write and the read phases in the contentious patterns. Such delays would result in unfair performance measurements, and should therefore be monitored and corrected if they occur. A methodology to characterise and determine whether delays require correcting was defined in Appendix B - Section V - F.

4.1.3 Parameter optimisation

A procedure was defined to explore and fix the "Size and duration of the I/O workload", "Degree of parallelism", "Amount of client resources", and "Other client and server-side configuration" degrees of freedom.

Firstly, an appropriate run length is determined. The benchmark is run against a fixed-size system with fixed configuration, only varying the number of I/O operations per process, which is increased progressively until the variability in bandwidth measurements becomes small (less than 5%). This helps balance test reproducibility whilst also keeping run times as short as possible.

After this, the client-to-server node ratio and the number of benchmark processes per client node are varied to find the point of diminishing returns, where the server connections approach saturation and adding additional client nodes or processes has little benefit. Note that each additional process added increases the overall size of the I/O workload as number of I/O operations per process is now

fixed.

Once these parameters are fixed, the I/O startup timestamps are then analysed to ensure that all processes in the benchmark are really working in parallel. If this is not true, the startup processes of the benchmark should be modified, the number of I/O operations per process needs to be increased further to minimise the impact of startup time, or explicit I/O startup synchronisation needs to be implemented.

Following this, any other client and server-side configuration parameters can be tested and optimised.

4.1.4 Scaling the system and benchmark runs

Once the previous procedure is completed, the number of storage nodes employed for the storage system can be progressively increased, and the benchmark run at each scale with a corresponding number of client nodes —according to the previously determined client-to-server-node ratio—, with all I/O patterns of interest. The bandwidths obtained for the sequence of steps will provide insight into the scaling behaviour for the different access patterns. This approach effectively scales the I/O workload and client resources weakly relative to server size.

This addresses the "Size of the storage system" degree of freedom.

4.1.5 Performance metrics

All selected benchmarks report per-process I/O start and end timestamps. Bandwidths are calculated as the ratio between the total volume of data written or read —that is, bytes transferred between the benchmark processes and the storage system— and the time elapsed between the start time of the first I/O operation performed by the benchmark and the end time of the last operation. This ratio,

measured in bytes per second, is referred to as *global timing bandwidth* in some of the appendices but referred to as *bandwidth* hereunder.

Fig. 4.1 shows a plausible timeline of I/O operations in a parallel benchmark run with no synchronisation between processes, highlighting how the I/O wall-clock time is measured.

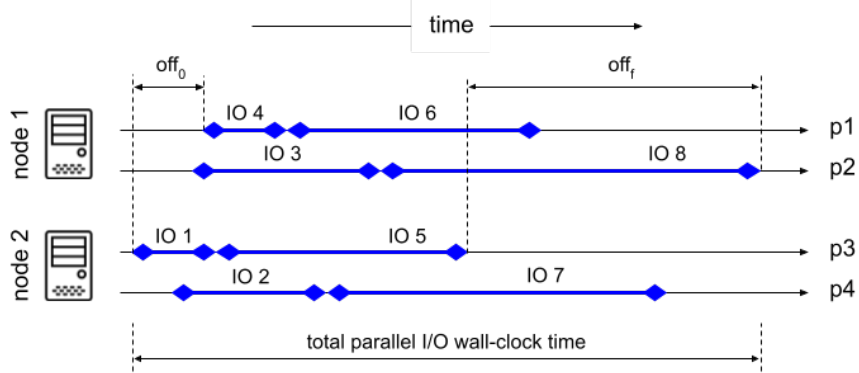


Figure 4.1: Plausible timeline of I/O operations and delays in a non-synchronised parallel I/O benchmark run. Only the writer phase of a run of the "no write+read contention" access pattern is represented. ©2023 IEEE.

To account for potential variation in system performance, the benchmark is rerun at least three times for any given configuration, and the average of the bandwidths is calculated.

4.2 DAOS and Lustre on SCM

This section presents I/O benchmarking experiments conducted against DAOS and Lustre deployments in a HPC system with SCM.

4.2.1 The NEXTGenIO system

NEXTGenIO[56] is a research HPC system composed of 34 dual-socket nodes with Intel Xeon Cascade Lake processors, with 48 cores and 192 GiB of DRAM per node. Each socket has six 256 GiB first-generation Intel Optane DCPMMs configured in App Direct interleaved mode, amounting to 3 TiB of SCM per node. There are no NVMe SSDs.

As shown in Fig. 4.2, each processor is connected via its own integrated network adapter to a low-latency OmniPath fabric, with each of these adapters providing a maximum bandwidth of 12.5 GiB/s. The fabric is configured in dual-rail mode. That is, there are two separate high-performance networks — one connecting the first processor sockets of all nodes via an OmniPath switch, and the other connecting the second processor sockets via another OmniPath switch.

The system nodes use a CentOS7 operating system, and batch jobs can be submitted to the nodes via a Slurm workload manager.

For the DAOS benchmarking, DAOS v2.4 was deployed on different numbers of nodes and configured to execute a single DAOS engine per socket (i.e. two per node), with each engine using an ext4 file system spanning the entire SCM for the corresponding socket. Each engine was configured to use the full set of cores, fabric interface, and interleaved SCM devices associated to its corresponding socket, and was configured to create 12 DAOS targets to manage these resources. DAOS did not support using PSM2 — a low-latency communication protocol implementing RDMA on OmniPath. Instead, it was configured to use the TCP

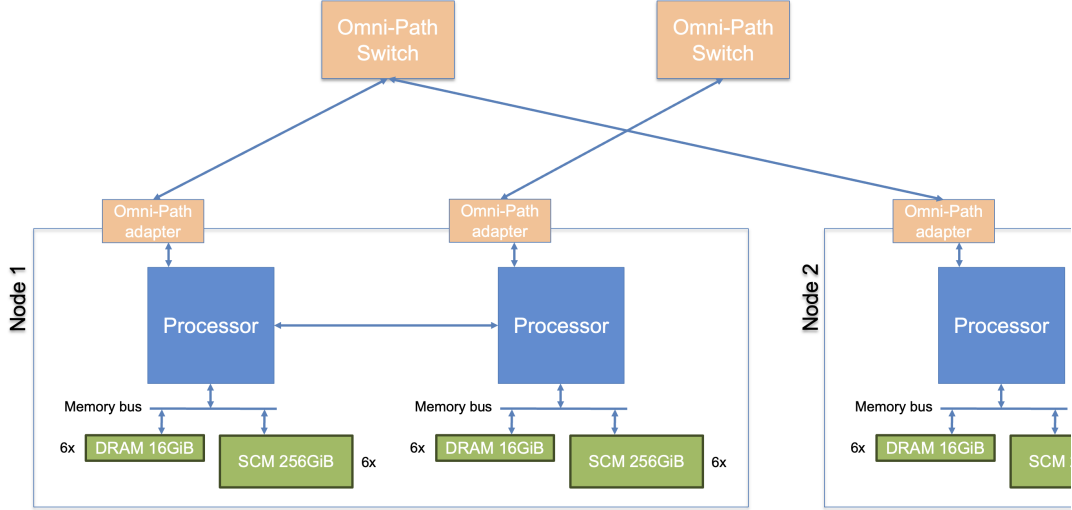


Figure 4.2: NEXTGenIO architecture.

protocol.

For the Lustre benchmarking, Lustre was deployed as well on different numbers of nodes, with one node always devoted exclusively to the metadata service, and the rest having one OST deployed per socket. Both the OSTs and the MDTs mounted an ext4 file system on the SCM attached to their respective sockets, providing 1.5 TiB of high-performance storage per OST and MDT, with servers and clients connected using the high-performance PSM2 protocol.

Lustre deployments used one more node than corresponding DAOS deployments. For instance, to compare to a Lustre deployment on two OST nodes—with 4 OSTs overall—and one MDT node—with 2 MDTs—, a two-node DAOS deployment—with 4 engines—was also provisioned and benchmarked. This example is illustrated in Fig. 4.3.

DAOS and Lustre deployments were made on an ad-hoc basis, having them deployed on the desired number of nodes as needed and removed once all relevant tests were completed. Part or all of the remaining system nodes were used to run the benchmarks. Up to 20 nodes were employed as clients to execute the

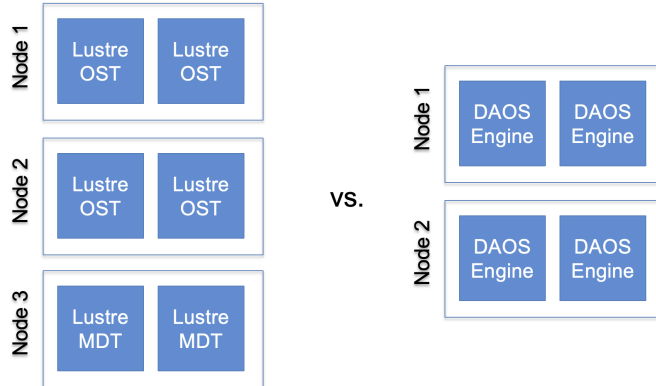


Figure 4.3: Example Lustre and DAOS configurations for comparison. An additional node was employed for Lustre MDTs.

benchmark processes, exploiting both sockets and network interfaces in each node. The SCM in the client nodes was not used and did not have any effect on I/O performance.

4.2.2 Hardware performance measurements

Measuring the raw bandwidths the network and storage devices can provide is a crucial first step in any I/O benchmarking experiment, as these bandwidths can later be used to determine whether any software-level storage system managing and providing access to these devices is being able to use them efficiently.

The raw bandwidth of the SCM devices in this system was analyzed thoroughly in [57]. As shown in Table 2, Figure 3, and Figure 4 in the referenced paper, the SCM devices in one NEXTGenIO node can provide approximately up to 10 GiB/s of write bandwidth and 80 GiB/s of read bandwidth, although these bandwidths can be much lower depending on the I/O size and how often data persistence is enforced.

Network bandwidth was determined by measuring data transfer rates between a pair of MPI processes, each pinned to the first socket of a different node to

ensure only a single network adapter on each node was utilized. Having MPI configured to use the PSM2 high-performance communication protocol, and using transfer sizes of 4 MiB or larger, the observed transfer rates were of approximately 12 GiB/s — very close to the 12.5 GiB/s the OmniPath network adapters should provide according to specifications. This result is shown in the first row of Table 4.1 below. However, because DAOS did not support PSM2, measuring network performance with the TCP protocol was also relevant. The measured bandwidths with TCP were of approximately 3 GiB/s between a single pair of processes, much lower than with PSM2. Nevertheless, using 8 process pairs simultaneously, with all processes pinned to the first socket of a single node pair, resulted in transfer rates of up to 9.5 GiB/s, much closer to the PSM2 bandwidths.

Table 4.1: Process-to-process transfer rates with PSM2 and TCP.

fabric provider	process pairs	optimal transfer size (MiB)	bandwidth (GiB/s)
PSM2	1	8	12.1
TCP	1	2	3.1
TCP	2	1	4.1
TCP	4	2	6.9
TCP	8	16	9.5
TCP	16	2	9.0

This meant that, for a storage system such as DAOS, which did not support PSM2, having multiple processes transferring data both on the server and client sides could largely, albeit not entirely, mitigate the performance downgrade caused by the use of TCP. The performance impact of using TCP versus PSM2 was further analysed in Appendix B - Section VI C.

All in all, assuming optimal transfer size, amount of multiprocessing, and persistence horizon were used by a software-level networked storage system deployed

in NEXTGenIO using the TCP protocol, every additional node used as server should provide approximately 10 GiB/s of write bandwidth, limited by SCM, and 19 GiB/s of read bandwidth, limited by the two network interfaces. These bottlenecks are illustrated in Fig. 4.4. If using PSM2, the read bandwidth per node should be 5 GiB/s higher. However, the assumption that such storage system would consistently use optimal values for all the parameters is very optimistic — significant variation is likely to occur for any of these, which would result in significantly lower bandwidths per server node.

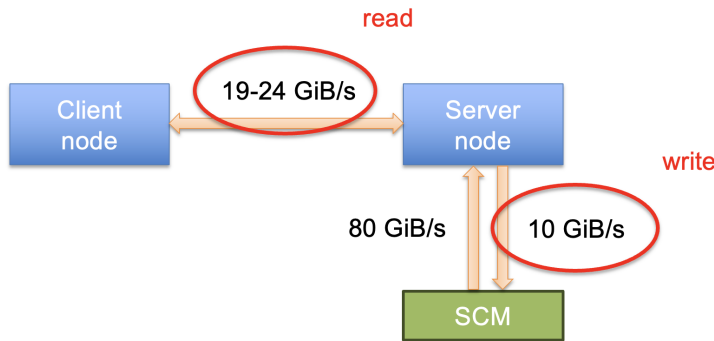


Figure 4.4: Ideal write and read bandwidths of a NEXTGenIO node used as networked storage server.

4.2.3 IOR performance

Due to its simplicity, IOR was the first benchmark used to measure I/O performance of the DAOS and Lustre deployments in NEXTGenIO, with the expectation that close-to-ideal bandwidths would be reached. This benchmark produces an I/O access pattern with *no w+r contention*.

The full parameter optimisation and scaling strategy, as defined in the methodology, was followed for the IOR benchmark. The procedure is explained in the following.

IOR was configured to have every parallel process perform 100 I/O operations,

of 1 MiB each, within a dedicated per-process file or object. This required setting `-b` and `-t` to `1m`, `-s` to 100, and `-i` to 1, and specifying `-F`. The 1 MiB I/O size was motivated by the order of magnitude of the size of weather fields currently produced in operational runs at the ECMWF. The amount of 100 operations per process was selected as part of the first step of the parameter optimisation strategy — i.e. determining an appropriate run length. This value was found to result in little variability in bandwidths across consecutive benchmark runs, both for Lustre and DAOS, whilst resulting in short benchmark run times. Files for IOR runs on Lustre were sharded across all OSTs using the `setstripe` command on the parent directory, but objects for IOR runs against DAOS were not sharded across engines as their object class was set to `OC_S1`.

The next step consisted in determining the optimal benchmark process count and client-to-server node ratio. For this, Lustre was deployed on 2 NETXGenIO nodes plus one node for the MDTs, and IOR was run on 2, 4, and 8 client nodes using a range of different process counts. The results are shown in Fig. 4.5. Every test was repeated 5 times, and the average and standard deviation are shown for each test with a dot and a segment around it.

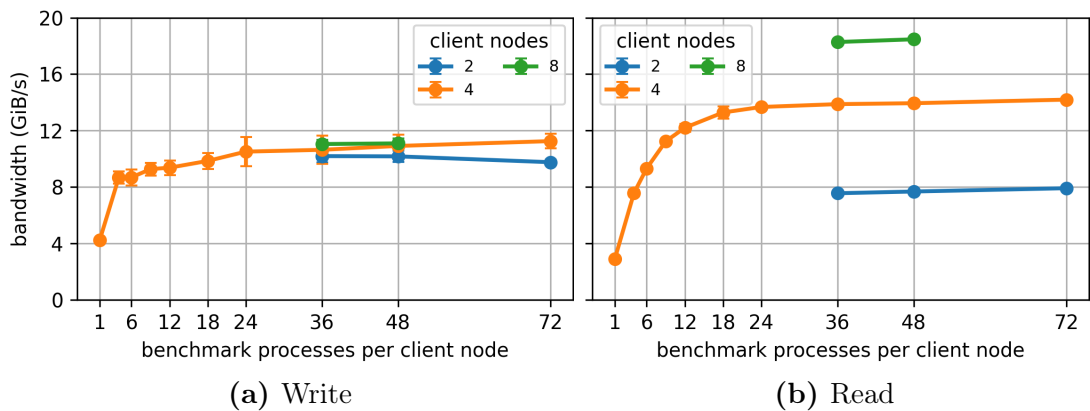


Figure 4.5: Bandwidths for IOR runs against a 2+1-node Lustre deployment in NETXGenIO. Every process accessed a separate file and performed 100 x 1MiB I/O operations. Tests were repeated 5 times.

As shown in the orange curve, 24 processes per client node or more resulted in best bandwidths. Employing 8 client nodes resulted in best bandwidths, reaching approximately 12 GiB/s for write and 19 GiB/s for read. A client-to-server node ratio of 4 was therefore found to be optimal for IOR on Lustre, although a ratio of 2 was also acceptable at the expense of a 25% of read bandwidth.

The same client count optimisation steps were followed for IOR runs against a DAOS system deployed on 2 NEXTGenIO nodes. The results are shown in Fig. 4.6.

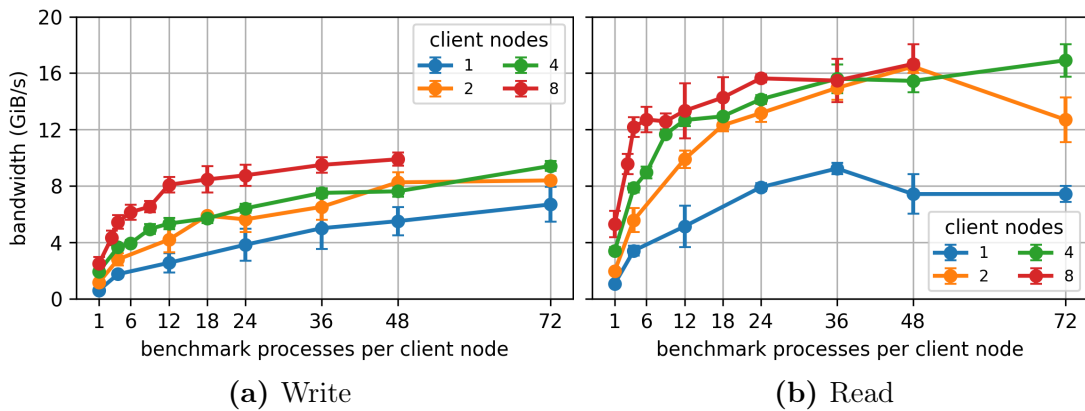


Figure 4.6: Bandwidths for IOR runs against a 2-node DAOS deployment in NEXTGenIO. Every process wrote or read 100 x 1MiB objects. Tests were repeated 5 times.

These results showed DAOS could reach bandwidths similar to Lustre's, approaching 11 GiB/s for write and 18 GiB/s for read, although with a smaller client-to-server node ratio of 2. Even with a ratio of 1 DAOS could reach bandwidths within the higher range. Large process counts were found to be more beneficial for DAOS than for Lustre, and this was likely due to the fact that DAOS did not use the PSM2 protocol.

The achieved IOR bandwidths, both for Lustre and DAOS, were notably far from the ideal bandwidths two NEXTGenIO nodes should provide — that is, 20 GiB/s for write and 38 to 48 GiB/s for read. This gap was likely mostly due to the high sensitivity of the hardware to small variations in transfer size, process count,

and persistence horizon, as this seemed to affect both storage systems equally. In hindsight, fully sharding the per-process objects across storage servers —i.e. using an **SX** object class instead of **S1**— for IOR runs on DAOS might have resulted in better utilisation of the network interfaces, and therefore higher bandwidths.

Following the scaling strategy, further tests were conducted having Lustre and DAOS deployed on increasing numbers of server nodes, up to 8 server nodes, and running IOR using the optimal process counts (i.e. 36 to 72) and a client-to-server node ratio of 4 where possible. The results are shown in Fig. 4.7. Hollow dots indicate where it was not possible to test with a client-to-server node ratio of 4 due to the limited size of the system. Instead, a ratio of 2 was used in these cases.

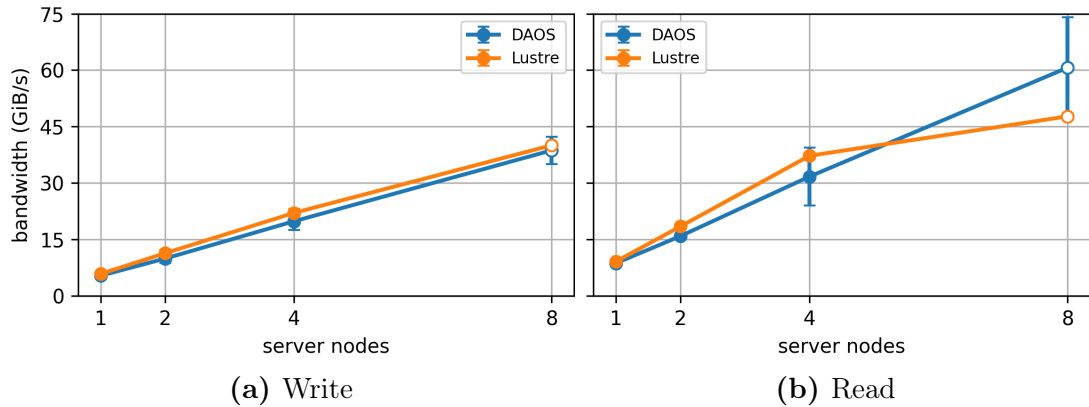


Figure 4.7: IOR bandwidth scalability against increasingly large Lustre and DAOS deployments in NEXTGenIO. A ratio of 4-to-1 client-to-server nodes was used except for hollow dots, and 36 to 72 processes were run in each client node. Every process performed 100 x 1MiB I/O operations. Tests were repeated 5 times. ©2022 IEEE.

Both Lustre and DAOS showed very good linear scalability both for write and read. For write, their performance was nearly identical, reaching 40 GiB/s in both cases. For read, DAOS showed significant variance in the achieved bandwidths, whereas Lustre consistently reached bandwidths at the top of the bandwidth range achieved by DAOS up to 4 server nodes, likely due to Lustre using RDMA instead of TCP. Beyond 4 server nodes, Lustre showed a scalability decline for read due

to the fact that, as observed previously, IOR on Lustre requires a client-to-server node ratio of 8 to fully saturate the storage servers for read-intensive workloads, but it was only possible to test with a ratio of up to 2 for configurations with 8 server nodes.

The fact that both systems showed similar performance behavior was a good sign indicating that both were equally configured to make use of the available storage and network resources. This was verified by monitoring resource usage during some of the test runs.

Given DAOS was able to reach high performance with a client-to-server node ratio of 2 or even 1 in some cases, the scalability curve for IOR on DAOS was further expanded with more tests at larger scales. The results are shown in Appendix B - Section VI B.

Overall, despite the gap relative to hardware bandwidths, these IOR results were encouraging as they showed DAOS could perform and scale well, at a level very similar to Lustre, at least for easy IOR workloads in this system.

One relevant setting that required adjustment before the bandwidths shown here were reached, was the pinning of server and client process across available cores for optimal network use. This was found to have substantial impact in I/O performance, with up to 50% reduction in performance when DAOS server engines were not optimally pinned across processors in a node, and up to 90% reduction when benchmark client processes were not optimally pinned. For best performance, each DAOS engine was configured to pin engine processes to a single socket, and to target the corresponding fabric adapter. This was achieved via the `pinned_numa_node` DAOS server configuration item. On the client side, processes were distributed in a balanced way across sockets in each client node with the `mpirun` option `--bind-to socket`.

4.2.4 Field I/O performance

Field I/O was the next benchmark used. Field I/O was developed aiming to mimic and perform the ECMWF’s operational I/O patterns against DAOS systems in a minimalist way, without involving the complexity of the ECMWF’s software stack. This would provide insight on the performance potential as well as the options and challenges of porting to DAOS.

Field I/O has each parallel process write or read a sequence of weather fields of 1 MiB into or from DAOS via the `libdaos` API, using a separate DAOS array for every field. The writer processes create a hierarchy of key-value objects where the stored fields are indexed, and these key-values are accessed by reader processes to locate the field array before reading it. For every field in the sequence, a few key-value operations are performed and one array object is written or read.

The parameter optimisation and scaling strategy, as defined in the methodology, was followed from scratch for Field I/O. This was documented thoroughly in Appendix B. One of the most relevant results, also shown here in Fig. 4.8, were the scalability curves obtained for Field I/O runs with *no write+read contention* against DAOS deployments on up to 16 NEXTGenIO nodes. As shown with different curve colours, Field I/O was tested with different configuration options. The *full* mode, in blue, used several indexing key-value objects and had the array and key-value objects distributed across several DAOS containers. The *no containers* mode, in green, was identical except it placed all objects in a single container. The *no index* mode, in orange, skipped the creation and use of indexing key-values. Hollow dots indicate where the optimal client-to-server node ratio of 2 could not be fulfilled due to resource limitations. Every process stored and indexed, or de-referenced and read, a sequence of 2000 fields.

These results showed that DAOS and Field I/O, if configured to use a single container, scaled linearly and reached IOR bandwidths despite using several small

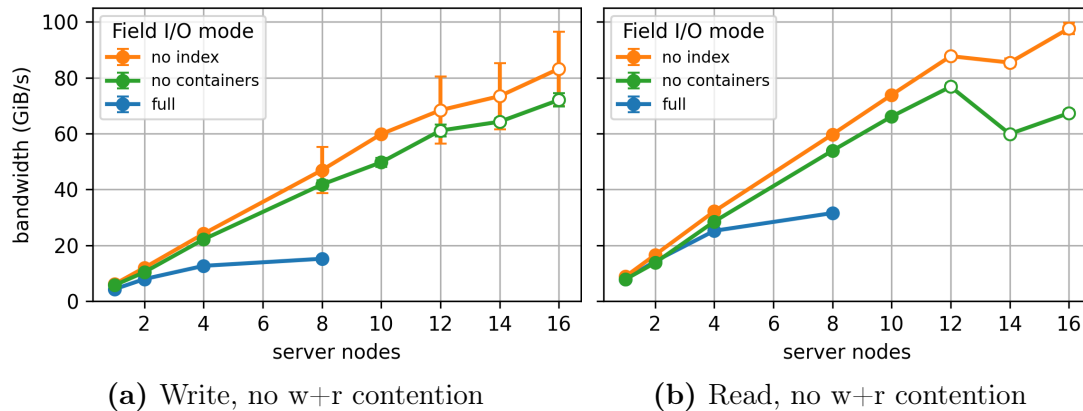


Figure 4.8: Bandwidth scalability of Field I/O runs, with no write+read contention, against increasingly large DAOS deployments in NEXTGenIO. A ratio of 2-to-1 client-to-server nodes was used except for hollow dots, and 36 to 48 processes were run in every client node. Every process wrote and indexed, or de-referenced and read, 2000 x 1MiB weather fields. Tests were repeated 10 times. ©2023 IEEE.

objects and performing several key-value operations per process. Also, the results demonstrated that the implementation of an index based on DAOS key-value objects had little impact on overall performance and scalability, whilst using several containers did have a significant impact.

These and other findings materialised as a set of recommendations for the development of high-performance DAOS applications, which were presented in [12].

The work in Appendix B - Section VI D also measured the Field I/O performance and scalability under *contending repeated writes and reads*. This result demonstrated the advantages of implementing domain-specific object stores on top of general-purpose object stores for such type of access pattern. The work in Appendix B, however, did not analyse *write+read contention* patterns, which are more representative of the ECMWF's operational workloads.

Field I/O was later run with *write+read contention*, and the measured bandwidths are shown here in Fig. 4.9. These runs were configured to use a half of the allocated client nodes to execute Field I/O writer processes, and the other

half to execute reader processes simultaneously. For example, for a run against a 8-node DAOS deployment, 16 client nodes were allocated according to the optimal client-to-server node ratio of 2 —determined earlier in the analysis—, and 8 of these nodes were used to run writer processes and the other 8 to run reader processes. This means the bandwidths for a given test in graphs a) and b) of Fig. 4.9 can be added to determine the total aggregate bandwidth the system delivered during the execution of that test.

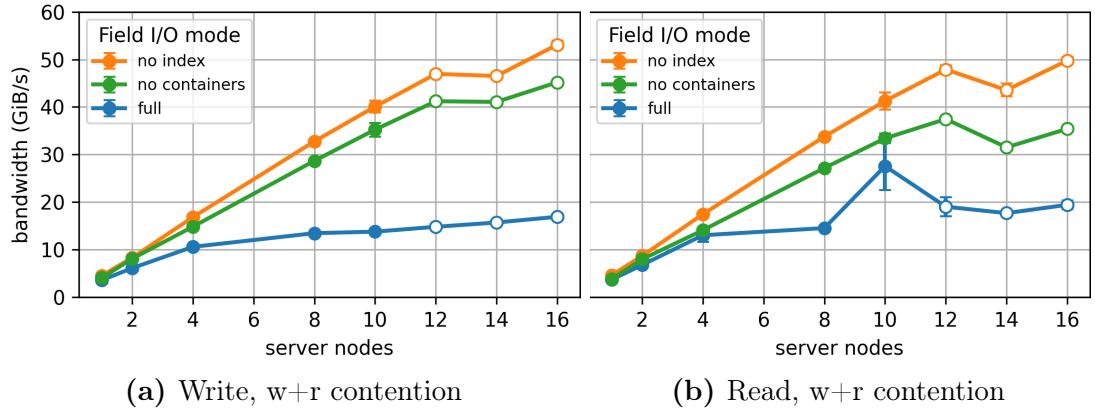


Figure 4.9: Bandwidth scalability of Field I/O runs, with write+read contention, against increasingly large DAOS deployments in NEXTGenIO. A ratio of 2-to-1 client-to-server nodes was used except for hollow dots, and 36 to 48 processes were run in each client node. Every process wrote and indexed (or de-referenced and read) 2000 x 1MiB weather fields. Tests were repeated 10 times.

The Field I/O mode using a single container —i.e. the *no containers* mode—, scaled linearly under operational-like contention both for write and read, providing aggregate (write plus read) bandwidths of up to 70 GiB/s in the configuration with 10 NEXTGenIO nodes employed as DAOS servers. This was an outstanding result. For reference, the ECMWF’s operational Lustre file system at that time, composed of 300 OST nodes, provided approximately 50 GiB/s of sustained aggregate throughput under operational workloads.

Another relevant set of results from the benchmarking reported in Appendix B (Section VI D 4) were the bandwidths measured for Field I/O runs configured

to write and read weather fields of larger sizes, beyond 1 MiB, and use different sharding configurations for the key-value and array objects. These runs were performed on 4 client nodes, against a 2-node DAOS deployment. Similar runs are shown here, in Fig. 4.10, but performed at larger scale on 16 client nodes, against a 8-node DAOS deployment.

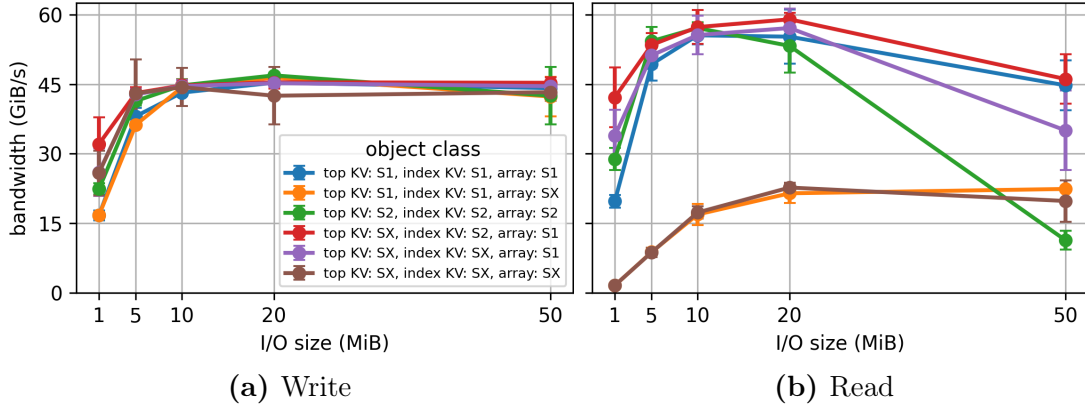


Figure 4.10: Bandwidths of Field I/O runs on 16 client nodes, with no write+read contention, against a 8-node DAOS deployment in NEXTGenIO, varying field size and object sharding configuration. 36 processes were run in each client node. Every process wrote and indexed (or de-referenced and read) 100 x 1MiB weather fields. Tests were repeated 5 times.

These results show that using an object class of S1 for DAOS arrays (i.e. no sharding across DAOS engines) results in best performance, and increasing field size beyond 1 MiB —as would be required for future resolution increases at the ECMWF— improves rather than deteriorates performance.

Overall, the results and findings from Field I/O runs against DAOS deployments in NEXTGenIO were very promising, and justified and informed the later development of a DAOS backend for the ECMWF’s FDB.

Field I/O on Lustre

One shortcoming of Field I/O was that, because it is designed to operate natively only on DAOS via `libdaos`, there was no direct way of running this benchmark

against Lustre deployments for comparison.

However, a dummy `libdaos` library was developed for Continuous Integration and Continuous Development (CI/CD) purposes at the ECMWF. Dummy `libdaos` implements the `libdaos` API on top of POSIX file systems by mapping DAOS concepts such as pools, containers, key-values, and arrays, to POSIX directories and files. This enabled running Field I/O against Lustre deployments in NEXTGenIO by linking Field I/O to dummy `libdaos` instead of proper `libdaos`.

Appendix A describes this approach in more detail, including bandwidth measurements of Field I/O runs against Lustre deployments of various sizes. The results showed Field I/O on DAOS performed and scaled much better than on Lustre, and this was not surprising because dummy `libdaos` made a rather abusive use of the POSIX file and directory APIs, e.g. by mapping every DAOS array to a separate file, or by mapping every key in a DAOS key-value to a separate file. This did not comply with some of the most important programming best practices for high-performance on POSIX file systems. A selection of the results comparing Field I/O performance and scalability on DAOS and Lustre is shown here in Fig. 4.11. Lustre deployments used one more node than the corresponding DAOS deployments, for the MDTs.

Despite this comparison being unfair due to the POSIX I/O API abuse in dummy `libdaos`, this provided evidence of the limitations of POSIX I/O and, more importantly, established that Field I/O in combination with dummy `libdaos` were a representative example of non-well-behaved POSIX I/O. This benchmark was used again later in this work.

4.2.5 FDB backend performance

With the insight from Field I/O experiments, a pair of DAOS backends for the FDB —described in Section 3.1— were developed. The `fdb-hammer` benchmark,

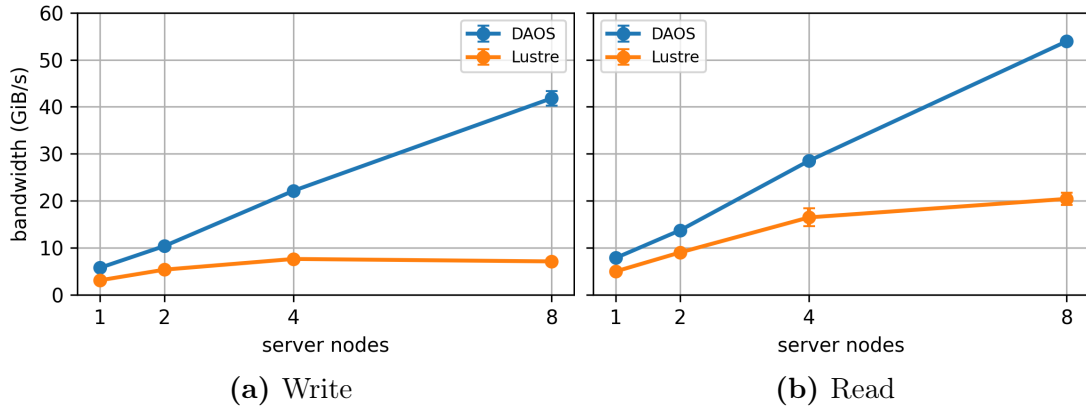


Figure 4.11: Field I/O bandwidth scalability against increasingly large Lustre and DAOS deployments in NEXTGenIO. A ratio of 2-to-1 client-to-server nodes was used, and 24 to 48 processes were run in each client node. Every process wrote and indexed (or de-referenced and read) 2000 x 1MiB weather fields. Tests were repeated 5 times. ©2022 IEEE.

which performs I/O via the FDB library, was then run in NEXTGenIO against DAOS and Lustre deployments using the respective FDB backends. Because these backends were both carefully designed to make efficient use of DAOS and Lustre systems, `fdb-hammer` allowed for direct and fair comparison of the performance potential of both systems for the ECMWF’s NWP as well as for any other HPC applications performing similar I/O patterns.

`fdb-hammer` runs as a set of parallel processes which write or read a sequence of weather fields using the FDB library. Just as in Field I/O, for every field written or read, a few key-value operations are performed and one array object is written or read.

The first set of `fdb-hammer` tests aimed to address the parameter optimisation part of the methodology. The optimisation procedure was followed separately for `fdb-hammer` on DAOS and for `fdb-hammer` on Lustre. The results were covered thoroughly in Appendix C - Section 5.1. One result worth noting is that, in contrast to the IOR runs reported earlier, the optimal client-to-server node ratio was found to be 2 both for `fdb-hammer` on Lustre and on DAOS. This meant there

were sufficient nodes in the system to run scalability curves for Lustre deployments on up to 10 server nodes, unlike in earlier IOR scalability tests on Lustre where a client-to-server node ratio of 4 was required to fully saturate the system.

After several rounds of adjusting the benchmark configuration, optimising the FDB DAOS backends, and testing performance at scale—which was covered in detail in Appendix C - Sections 5.1 to 5.3—, scalability curves were produced for `fdb-hammer` runs with *no write+read contention*, shown in Fig. 4.12 here. Field I/O scalability curves produced earlier were included in the graphs as well for direct comparison. Hollow dots indicate where the optimal client-to-server node ratio of 2 was not fulfilled, therefore not fully saturating the system.

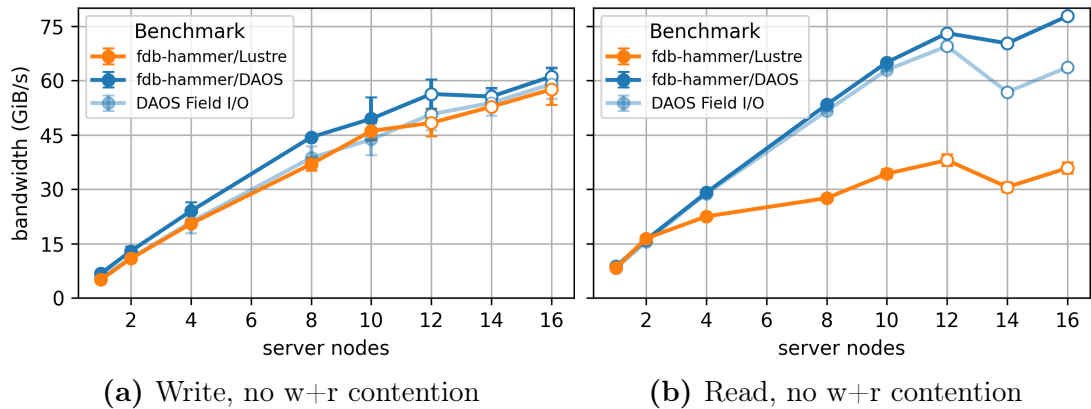


Figure 4.12: `fdb-hammer` and Field I/O bandwidth scalability, with no write+read contention, against increasingly large Lustre and DAOS deployments in NEXTGenIO. A ratio of 2-to-1 client-to-server nodes was used except for hollow dots, and 16 to 48 processes were run in each client node. Every process wrote and indexed (or de-referenced and read) 10000 x 1MiB weather fields. Tests were repeated 3 times.

The write performance results in (a) showed both DAOS and Lustre performed similarly and scaled linearly for write up to 10 server nodes, reaching IOR bandwidths. As in Fig. 4.7 (a), this suggested both storage systems were properly configured to exploit the underlying hardware, and both backends were properly configured to efficiently access the storage systems and optimised for best write performance. The write performance of DAOS at 10 server nodes showed variance

and cast some doubt on the ability of DAOS to hold the linear scaling pattern at larger node counts. However, tests in the upper part of the range of variation did fall on the projected straight line, suggesting additional fine-tuning of DAOS and the benchmark might allow consistently reaching these bandwidths, although this was not pursued. Tests beyond 10 server nodes resulted in good performance despite not using enough client nodes to fully saturate the system, also suggesting that the linear scaling would likely hold at these scales if sufficient nodes were available.

For read, in (b), DAOS performed remarkably well and scaled linearly, in line with previous Field I/O results, whereas Lustre showed a marked decline in scalability beyond 2 server nodes and reached only a half of the read performance of DAOS at larger scales. The sub-optimal performance of **fdb-hammer** on Lustre was first thought to be due to the design of the POSIX I/O backends, which favours write performance at the expense of read performance. However, as discussed earlier, **fdb-hammer** does not initiate reader processes in a staggered way, as operational runs do, nor reproduces the transposed data access of operational readers, resulting in I/O workloads easier than the operational ones if using the POSIX I/O backends. The significant gap in read performance for **fdb-hammer** runs on Lustre relative to IOR was therefore a slightly surprising result.

For both DAOS and Lustre, read performance continued scaling with 12 server nodes despite not fulfilling the optimal 2-to-1 client-to-server node ratio. This was due to the fact that 20 client nodes were used for that configuration and this was not far from the optimal ratio. Performance dropped significantly at 14 and 16 nodes because a ratio of 1-to-1 was used for these configurations. Conversely, write performance did not drop as much at these scales because write is less sensitive to sub-optimal client-to-server node ratios, as shown in Appendix C - Section 5.1.

It is worth noting that **fdb-hammer** on DAOS slightly exceeded IOR and Field

I/O bandwidths, and this was explained by the fact that a few optimisations were implemented in the FDB DAOS backends which were not implemented in the IOR `libdaos` backend nor in Field I/O. Specifically, these optimisations consisted in using DAOS arrays without attributes, which allow ditching array creation calls on write (see the documentation of `daos_array_open_with_attrs`), and avoiding unnecessary `daos_array_get_size` calls on read.

`fdb-hammer` was also run in its `list()` mode for some of the configurations after the read phase completed, to compare the listing performance of both backends. The benchmark was configured to list all fields `archive()`d by all writer processes during the write phase for the first simulation step —1 out of 100 steps—, and executed from a single node. Listing with the POSIX I/O backends was consistently twice as fast as with the DAOS backends, for all server node counts. This was in line with expectations as, as explained in Section 3.1, the POSIX I/O backends load all required indexing information in only a few `read` calls, whereas the DAOS backends issue a `daos_kv_get` operation for every matching entry, making the former backends more efficient for listing large sets of fields as done in this test. The performance of FDB `list()` with the DAOS backends was not further investigated or improved, as `list()` would not be involved in operational runs on DAOS, as discussed in Section 2.7.2.

Scalability curves were also produced for `fdb-hammer` runs with *write+read contention*, shown in Fig. 4.13. This access pattern more closely mimicked the I/O patterns of an operational NWP run at the ECMWF. As in Field I/O runs with contention, half of the allocated client nodes executed writer processes and the other half executed readers, simultaneously. Bandwidths for a given test in graphs (a) and (b) can be added to determine the total aggregate bandwidth the system delivered.

In this case, DAOS and Lustre showed different write performance behavior

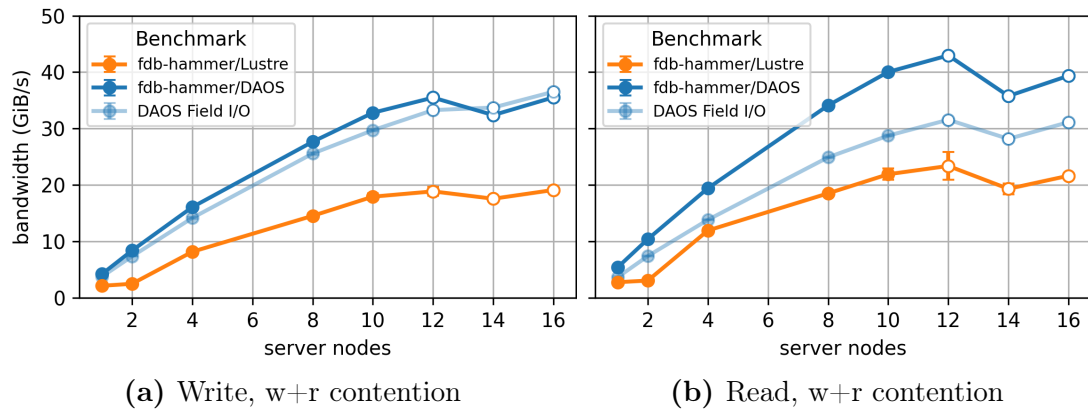


Figure 4.13: fdb-hammer and Field I/O bandwidth scalability, with write+read contention, against increasingly large Lustre and DAOS deployments in NEXTGenIO. A ratio of 2-to-1 client-to-server nodes was used except for hollow dots, and 16 to 48 processes were run in each client node. Every process wrote and indexed (or de-referenced and read) 10000 x 1MiB weather fields. Tests were repeated 3 times.

from each other. DAOS scaled nearly linearly, close to the expectations set by Field I/O under *write+read contention*, although with a gentle decline as more server nodes were added. Remarkably, although Lustre scaled linearly for write —neglecting the lack of performance increase at 2 server nodes, which was not investigated—, it reached significantly lower write bandwidths relative to DAOS. This was despite the POSIX I/O FDB backends being optimised for write, and despite the Lustre’s write performance being very similar to DAOS’s in the benchmark runs with *no write+read contention*. This clearly indicated that the concurrent read workload was negatively impacting write performance on Lustre, effectively as though the writes and reads were mutually exclusive and never overlapped, while they fully overlapped on DAOS.

This low write performance on Lustre under contention was at first thought to be due to the Lustre’s locking mechanisms engaging to ensure strong consistency of data and metadata across client-side caches and servers. However, as described in Section 2.7.2, **fdb-hammer** with *write+read contention* produces a type of write-read contention that should not result in intensive involvement of such locking

mechanisms. On one hand, this meant write bandwidth might be even lower if operational contention were fully reproduced. On the other hand, this also meant the low write performance was an unexpected result.

For read, in (b), the general performance behavior of both systems was similar to the write behavior, that is, with a gentle decline in DAOS’s scalability and significantly lower but linearly scaling bandwidths for Lustre. The inferior read performance on Lustre was a slightly surprising result, for the same reasons as in the *no write+read contention* case. Also in (b), **fdb-hammer** on DAOS performed significantly better than Field I/O, again likely due to the optimisation put in place in **fdb-hammer** to avoid unnecessary array size checks.

To gain further insight on the behavior of both backends and the reasons why Lustre struggled under contention, **fdb-hammer** and the DAOS and POSIX I/O backends were instrumented to report the amount of time spent on some of the most relevant operations performed. Fig. 4.14 and Fig. 4.15 summarise the profiling information obtained for **fdb-hammer** runs against 10-node DAOS and Lustre deployments, respectively, both with and without write+read contention.

The profiling results for DAOS, in Fig. 4.14, showed that most of the time was spent in array write and read operations, which was a good sign as it meant DAOS and the FDB backends were able to prioritise data movement and persistence without being interfered by the surrounding metadata management, thus providing close-to-hardware bandwidths. The fact that the profiling results with write+read contention —at the bottom row— were very similar to the results without contention was an excellent result, meaning that neither writing nor reading on DAOS suffered a noticeable performance impact despite the benchmark fully reproducing the contention of a hypothetical operational run using the FDB DAOS backends.

The profiling results for Lustre, in Fig. 4.15, showed most of the time of the

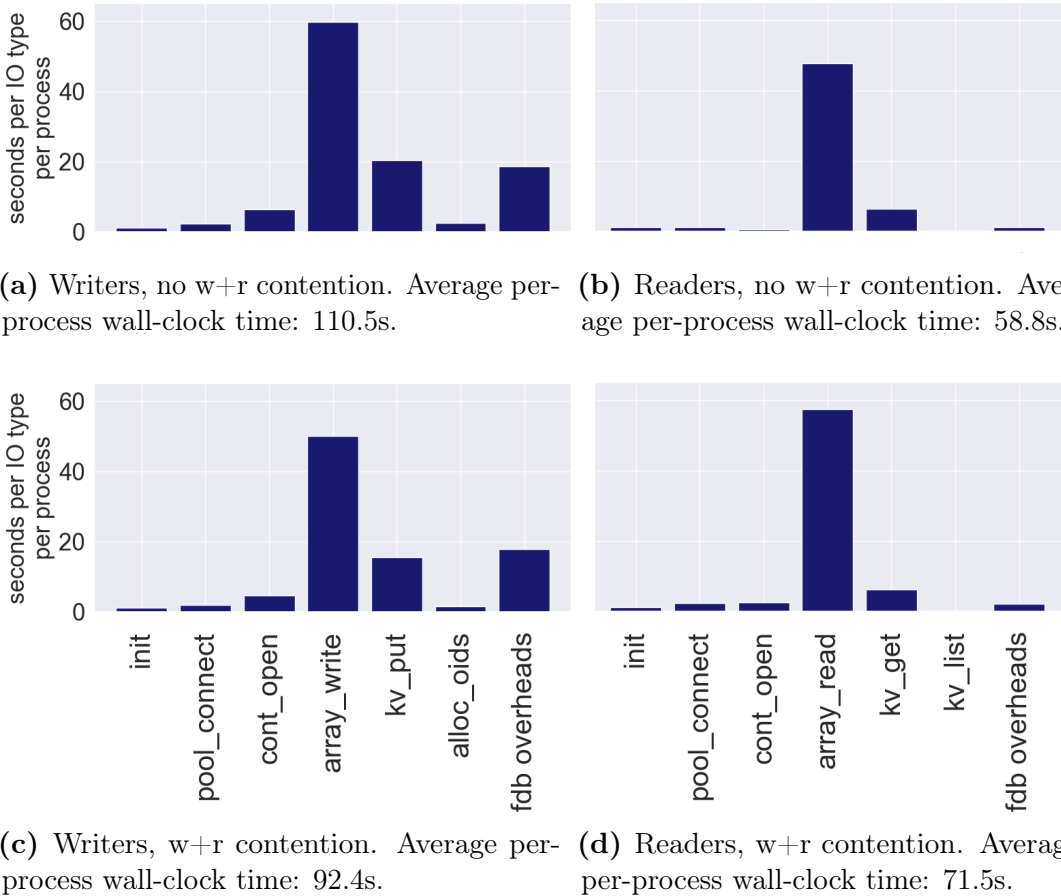


Figure 4.14: Profiling results for fdb-hammer/DAOS runs without (top row) and with (bottom row) write+read contention, using 10 server and 20 client nodes; 32 processes per client node. Every process wrote and indexed (or de-referenced and read) 10000 x 1MiB weather fields.

write phase —both with and without contention— was spent in the Store `flush()` and Catalogue `flush()` methods, and this was in line with expectations as these methods persist data or wait for data to be persisted into storage.

The fact that a similar portion of time was spent in Store `archive()` and Catalogue `flush()` for both patterns demonstrated that the contentious pattern was in fact not suffering from the Lustre’s locking mechanisms. If the contentious pattern had captured the full operational contention, the Store `archive()` and Catalogue `flush()` methods would have issued `write` calls —on the data, sub-

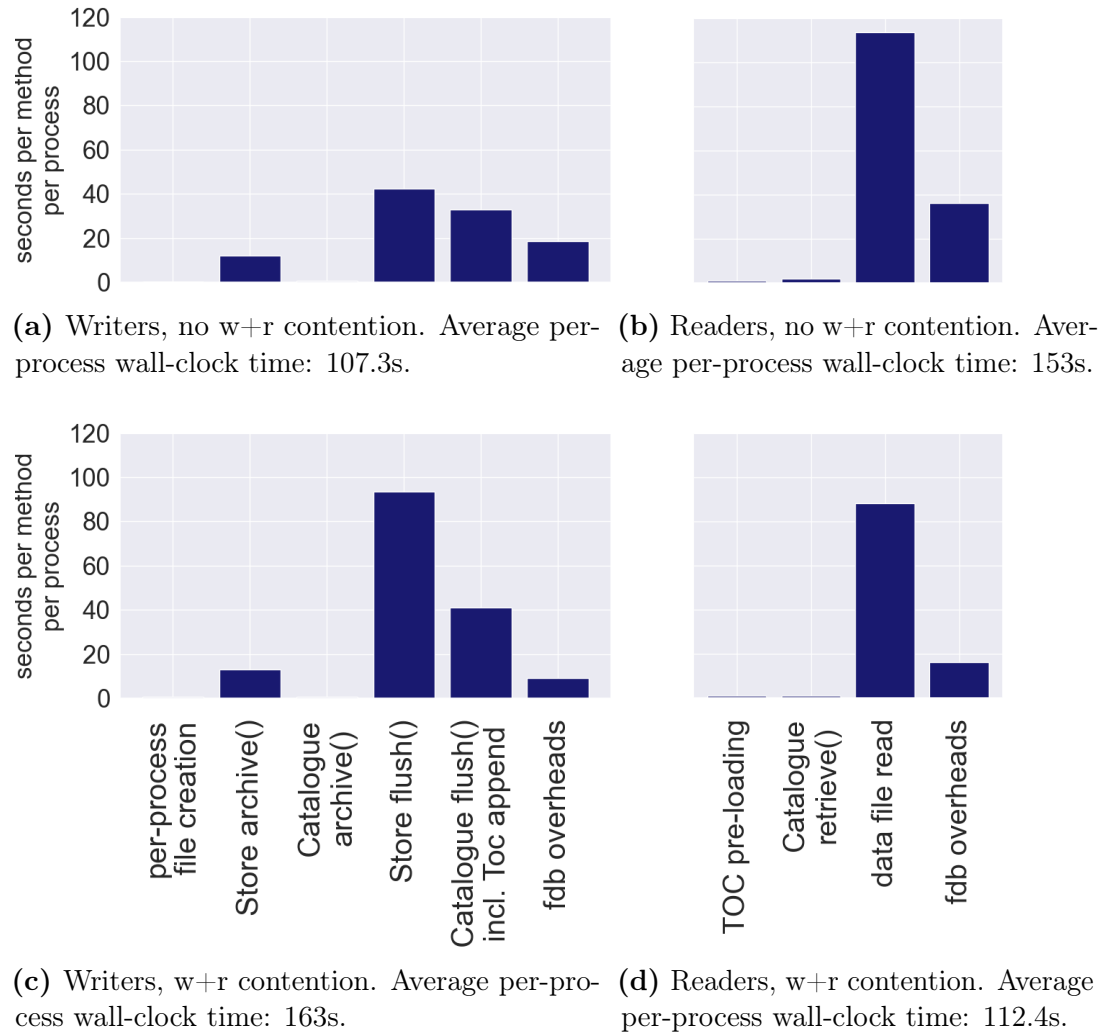


Figure 4.15: Profiling results for fdb-hammer/Lustre runs without (top row) and with (bottom row) write+read contention, using 10 server and 20 client nodes; 32 processes per client node. Every process wrote and indexed (or de-referenced and read) 10000 x 1MiB weather fields.

TOC, and index files—which would have contended with `read` calls on the same files issued as part of TOC pre-loading and the bulk data reading in the read phase, thus engaging the distributed locking mechanisms and resulting in higher wall-clock times for `Store archive()` and `Catalogue flush()`, but this was not the case. Instead, surprisingly, `Store flush()`—which only waits for the bulk

data to be transferred to the Lustre servers and persisted into storage media— took more than double the time in the contentious pattern. This suggested that, possibly, the network or the storage media were not properly handling concurrent writes and reads, resulting in longer than expected persist wall-clock times. Given this issue did not occur in equivalent runs on DAOS, a possible explanation could be that Lustre might not be optimised to perform concurrent writes and reads on SCM, or alternatively that the PSM2 protocol used by Lustre did not properly handle concurrent transfers in both directions.

Regarding the read phase on Lustre, in Fig. 4.15 (b) and (d), most of the time was spent on bulk reading from a single data file per process, in line with expectations. However, the bulk reading time for runs with *no write+read contention* seemed excessive, particularly if compared to the time spent on array reads in equivalent runs on DAOS, which overall read the exact same amount of data from storage. This slowness in bulk reading was the main contributor to the inferior Lustre read performance observed in Fig. 4.12 and 4.13, and was potentially due to Lustre not handling well the relatively large number — albeit not as large as in operational runs— of `read` operations issued per process. Another possible cause could be an undiscovered issue or inefficiency in the logic for merging `DataHandles` returned by the sequence of FDB `retrieve()` calls issued by a reader process, such that the same data file is re-opened and closed or its size queried several times unnecessarily.

A substantial amount of time was spent on FDB overheads — that is, time spent by the FDB library on non-I/O operations such as calculations or in-memory operations. Although this was not investigated, as it was shadowed by the bulk read inefficiencies, this is discussed in more detail later on.

Neither the lower-than-expected read performance nor the write performance deterioration under contention for runs on Lustre were further investigated.

4.2.6 Summary

The I/O benchmarking so far has shown both Lustre and DAOS were capable of reaching similarly high and linearly scaling bandwidths for easy I/O workloads on a system with SCM.

The system has an Omni-Path fabric which DAOS could not exploit natively —i.e. not bypassing the operating system for communications via the fabric—, but DAOS nevertheless achieved performance levels as high as Lustre —which did natively exploit the fabric— provided large parallel process counts were used.

Both storage systems showed an equally substantial gap in performance relative to hardware limits, and this was possibly due to the high sensitivity of the SCM storage hardware to small variations in I/O sizes and persistence horizon.

Both Lustre and DAOS, and the respective FDB backends, performed and scaled very well for NWP I/O workloads without write+read contention, although DAOS stood out reaching twice as high read bandwidths. For contentious NWP workloads, DAOS reached twice as high write and read bandwidths. DAOS's performance advantage should have been even more marked if the benchmark runs on Lustre had fully captured the operational access pattern and contention.

These results were encouraging as they showed DAOS can provide similar performance to Lustre for simple I/O workloads, and superior performance for complex applications requiring storage and indexing of relatively small data objects. This suggested DAOS has potential both for HPC storage in general as well as for the ECMWF's operational NWP. The results, however, had to be taken with caution as, on one hand, the root cause of DAOS's advantage in read performance was not well identified and, on the other hand, the write performance advantage under contention seemed to be due to Lustre not being able to optimally exploit the specific hardware at hand, and might therefore not be entirely applicable to other systems with different hardware.

4.3 DAOS, Ceph, and Lustre on NVMe SSDs

All benchmarking so far was conducted in a system with Optane SCM and an Omni-Path network, but these hardware options became a less likely choice for new production systems after Omni-Path was temporarily discontinued in 2019 and 2020, and Optane was permanently discontinued in mid 2022. This section presents I/O benchmarking experiments conducted against DAOS, Ceph, and Lustre systems deployed on machines with NVMe SSDs — a commonplace storage hardware option nowadays.

4.3.1 The Google Cloud Platform

The experiments were conducted on Google Cloud Platform (GCP)[58] infrastructure. DAOS, Ceph, and Lustre systems were deployed on VMs —also referred to as *instances*— of a custom type[59], `n2-custom-36-153600`, each with 36 logical cores, 150 GiB of DRAM, 6 TiB of local NVMe SSDs distributed in 16 logical devices, and a 50 Gbps network adapter. On the client side, the benchmarks were run in VMs of type `n2-highcpu-32`, each with 32 logical cores, 32 GiB of DRAM, and a 50 Gbps network adapter. These VM types are illustrated in Fig. 4.16.

Because the network adapters did not provide RDMA capability, the TCP protocol was used for all communication over the network. To exploit all available network bandwidth, the VMs had to be configured with Simultaneous Multi-Threading (SMT)[60] enabled, and the benchmark processes pinned evenly across all available cores.

To minimise running costs, all VMs were provisioned with a *spot* provisioning model[61], implying these might not be immediately available during periods of high demand, and could be evicted at any time. This required putting mechanisms in place both client and server-side to wait for availability of spot resources and

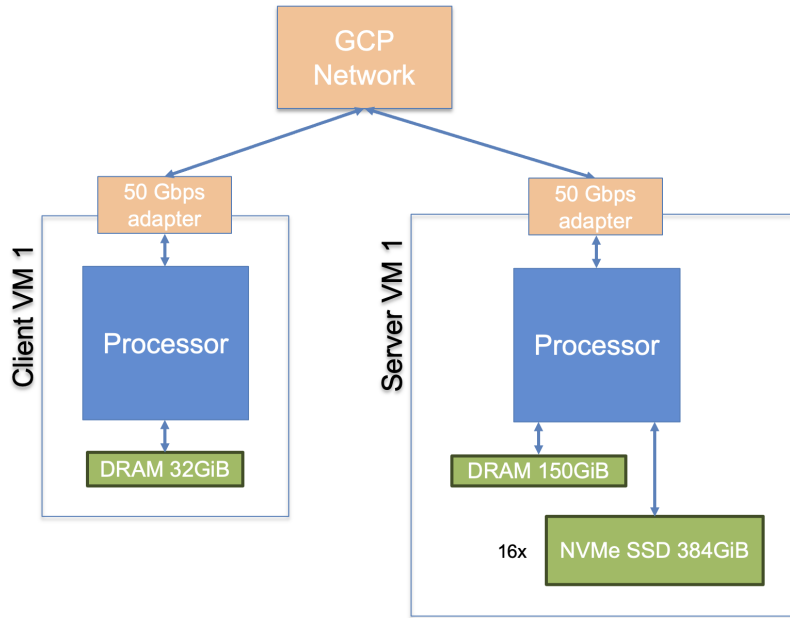


Figure 4.16: VM types used for benchmarking on GCP.

gracefully handle eviction.

For the server side, a few scripts were developed which programmatically provision VMs with SSDs and deploy one of the storage systems evaluated on these VMs. Upon eviction of one of the VMs, the scripts properly tear down the storage system and the rest of server VMs, wait for spot resources to be re-provisioned, and redeploy the storage system.

For the client side, an auto-scaling Slurm cluster was created with the help of `cluster-toolkit`[62] — a tool to declare and provision HPC and AI infrastructure-as-code on Google Cloud. The auto-scaling Slurm cluster automatically provisioned new spot client VMs as required upon submission of new I/O benchmarking jobs, thus ensuring the jobs did not run until enough spot resources were available, and automatically tore down the VMs if no new jobs were submitted. These client VMs were properly configured for high-performance access to the previously deployed storage systems.

Whenever any of the server or client VMs were evicted during a benchmark run, the described mechanisms engaged to re-provision as needed, and the test was re-run.

The infrastructure-as-code and scripts used to deploy the different storage systems —except for DAOS, as these are property of Google Cloud— and the `cluster-toolkit` blueprints of the auto-scaling Slurm cluster are available in [63].

All provisioned client and server VMs ran images of the Rocky Linux 8 operating system.

Ceph and Lustre deployments used one more VM than corresponding DAOS deployments. For instance, to compare to a DAOS deployment on two VMs —each hosting one DAOS engine and 16 targets—, a Ceph deployment on two OSD VMs —with 32 OSDs overall— plus one Monitor VM was used, and a Lustre deployment on two OST VMs —with 32 OSTs overall— plus one MDT VM was used. This example is illustrated in Fig 4.17

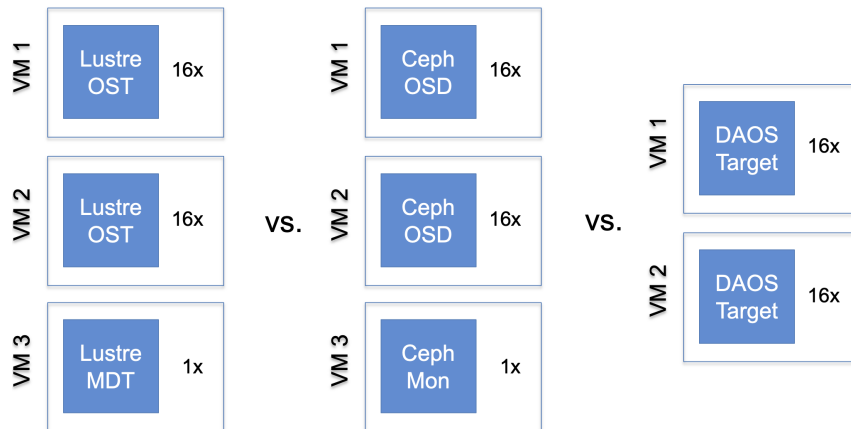


Figure 4.17: Example Lustre, Ceph, and DAOS configurations for comparison. An additional node was employed for Lustre MDTs and Ceph Monitors.

This meant Ceph and Lustre had an advantage in terms of allocated resources, although DAOS had the advantage that it was configured to use the DRAM in

the server VMs for metadata storage —including any I/O operations smaller than 4 KiB—, whereas the other two persisted all metadata and small I/O into NVMe SSDs. DAOS currently provides the option to persist metadata into SSDs in the absence of SCM, but this feature was not yet available at the time the experiments were carried out.

Data protection mechanisms —i.e. erasure-coding and replication— were disabled for the three storage systems except for a few particular tests where the use of data protection is explicitly noted. Furthermore, the storage devices in the server VMs were not configured as RAID arrays for any of the storage systems.

As a consequence of not using RAID setups, it was necessary to deploy a daemon —be it a Lustre OST, a Ceph OSD, or a DAOS target— to manage each storage device in every server VM, and this was done equally for the three storage systems. Deploying several daemons per server VM can cause DRAM or CPU overheads with respect to creating RAID arrays and deploying only one or a few daemons per VM, although in this case the number of daemons deployed was small enough that the overheads were not expected to significantly impact I/O performance. Also, high OST/OSD/target counts usually improve rather than deteriorate performance with respect to RAID configurations in highly parallel I/O workloads like the ones produced by the benchmarks in this analysis. For reference, the OST-to-OSS ratio used for the Lustre deployments in this analysis is within Lustre’s practical range and close to that of a few high-performance production instances[38].

Although Google Cloud provides VMs deployed on generic hardware, not necessarily tailored purely for HPC, it makes an excellent standard and neutral testbed enabling the analysis of software-level performance and scalability of the various storage systems being evaluated. While the analysis may not map directly to specialised systems, the same overall behavior should be expected on

systems using similar storage and network technology. Regarding contention with other users and performance stability, Google Cloud is committed to ensure the CPU, storage, and network specifications requested upon VM creation are fulfilled. Google Cloud should therefore not be perceived as a contended and fluctuating system. However, some fluctuation in performance can occur if running on spot instances, as done in this analysis, and for this reason the benchmarks were run multiple times to capture any performance variance.

4.3.2 Hardware performance measurements

The raw bulk I/O bandwidth of the NVMe SSDs on server instances was measured by mounting each of the 16 drives in one of the instances as an ext4 file system and then running the `dd` command in parallel for all of them, first writing and then reading 1000 blocks of 100 MiB. The measurements showed 3.86 GiB/s of aggregate write bandwidth and 7 GiB/s of aggregate read bandwidth.

`iperf` was used to measure raw network bandwidth between client and server instances, which was found to match the expected 50 Gbps (6.25 GiB/s) in both directions. The `--parallel` option was necessary for `iperf` to run multiple parallel streams and reach optimal bandwidths.

These measurements indicated that every additional server instance employed for a DAOS, Ceph, or Lustre deployment could at best provide an additional 3.86 GiB/s for write, limited by the SSD bandwidth, and 6.25 GiB/s for read, limited by the network. This is represented in Fig. 4.18.

4.3.3 IOR performance

DAOS, Ceph, and Lustre were deployed on 16 VMs (plus one for Ceph and Lustre), and the IOR benchmark was run using various amounts of client VMs and processes with the aim of determining the optimal client-to-server node ratio

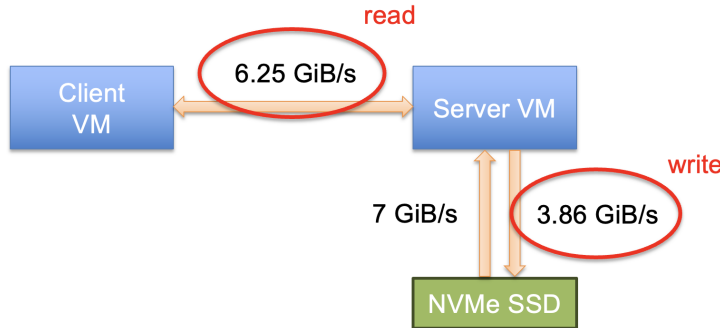


Figure 4.18: Ideal write and read bandwidths of a GCP VM of type n2-custom-36-153600 used as networked storage server.

and process count, as per the parameter optimisation strategy, for every storage system. In this case, in contrast to IOR runs on NEXTGenIO, every process was configured to perform 10000 I/O operations of 1 MiB each, also within a dedicated per-process file or object. Ceph objects, however, are by default limited to 128 MiB, and IOR runs on Ceph were consequently limited to 100 I/O operations per process. Moreover, DAOS objects and Lustre files were sharded across all storage servers, whereas Ceph objects could not be sharded. The results are shown in Fig. 4.19.

Based on the hardware bandwidth measurements earlier, 16 server VMs should ideally provide approximately 62 GiB/s for write and 100 GiB/s for read. As shown in the first two rows of Fig. 4.19, Lustre and DAOS reached close to these values, providing up to 50 GiB/s for write and 80 GiB/s for read.

Ceph, however, reached only a half of that write bandwidth, and up to 55 GiB/s for read. One relevant aspect worth of scrutiny in regard to Ceph's performance, which one might think could be behind these far-from-optimal results, is the Placement Group (PG) configuration. However, in this case—and in all following benchmark runs on Ceph—PG auto-scaling was disabled, and several different PG counts were manually set and tested to determine the optimal value, thus leading to the PG configuration being discarded as a potential cause. For this

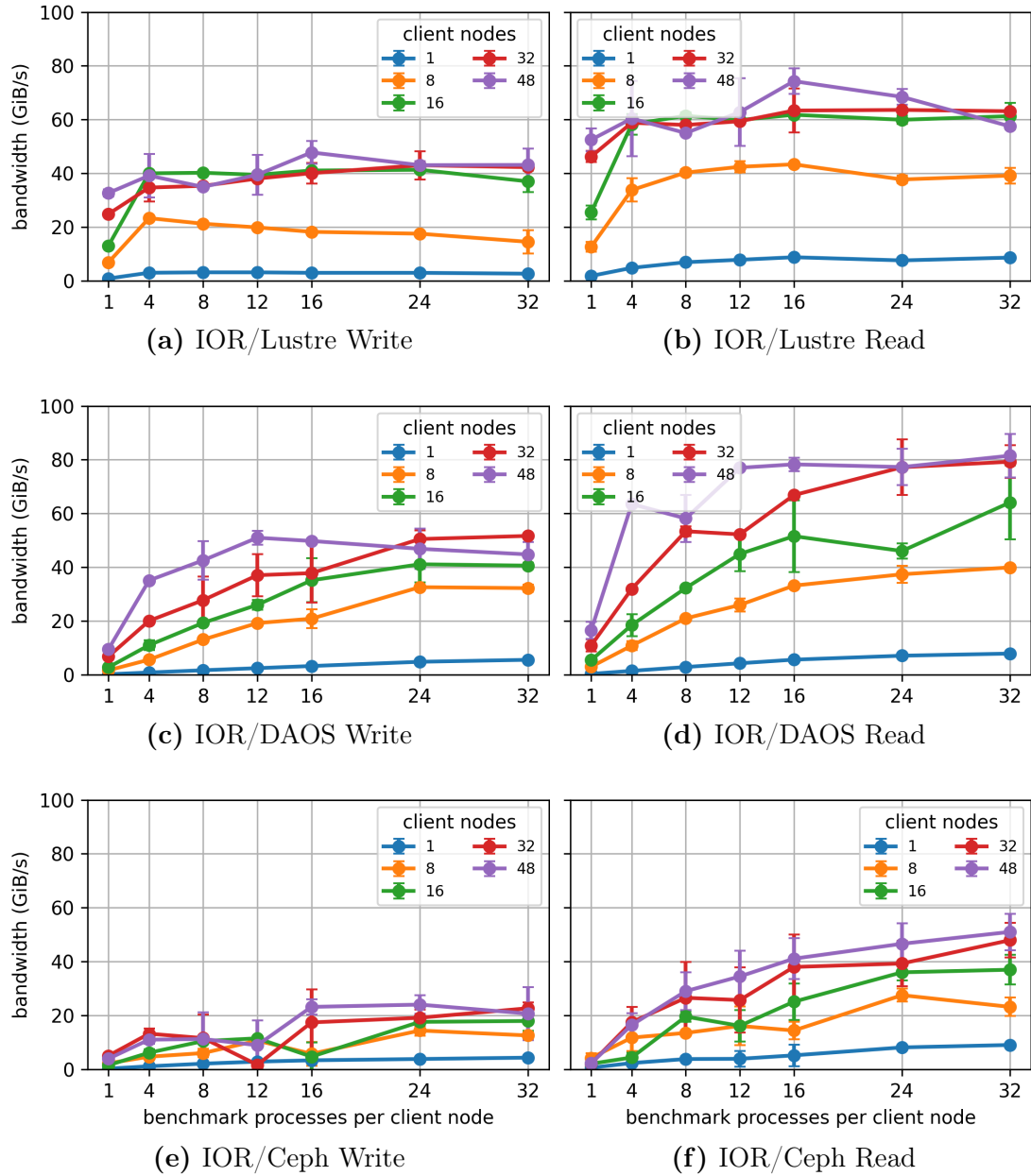


Figure 4.19: Bandwidths for IOR runs against Lustre, DAOS, and Ceph deployments on 16 VMs (+1 for Lustre and Ceph). Every process performed 10000 x 1MiB I/O operations (100 x 1MiB for Ceph). Tests were repeated 3 times.

particular test set, the optimal PG count was found to be 8192.

Instead, the observed sub-optimal performance was likely due to Ceph objects not being sharded, making it impossible for a single client VM to target all 256 OSDs, and less likely for the whole set of client processes to target all OSDs in a balanced way. Also, the small number of I/O operations issued per process prevented IOR processes from sustaining I/O to their corresponding objects for a long time period, thus likely not saturating the network nor the servers.

Some of the IOR runs on Ceph were repeated having Ceph configured with a large maximum object size—which is discouraged—and IOR configured to issue 10000 I/O operations per process. This option resulted in even lower write performance and was thereby discarded. This could seem contradictory with the result in the 5th column of Fig. 3.5, where the performance of the FDB Ceph backends was not impacted despite having Ceph configured with a large maximum object size. However, in that case, the objects were kept small, never actually approaching the maximum permitted size.

In fact, the results in Fig. 3.5 demonstrated that using multiple objects per process or even an object per I/O would result in better write performance—presumably due to client processes targeting OSDs in a more balanced way—but IOR did not support these arrangements.

Regarding client count optimisation, the three storage systems generally performed best in tests using 16 or 32 client VMs—i.e. a client-to-server node ratio of 1 or 2—and 16 to 32 benchmark processes per VM.

The results for DAOS and Lustre demonstrated that despite using the TCP protocol, which involves the operating system in all network communications both client and server-side, high performance levels could be achieved if using large process counts in combination with a large enough transfer size, just as observed in NEXTGenIO.

The client count optimisation procedure was repeated for deployments of the three storage systems on 4 server VMs (plus one for Ceph and Lustre), resulting in similar optimal client-to-server node ratios and process counts. IOR was then run against deployments on increasing amounts of server VMs, using these optimal client counts. The results are shown in Fig. 4.20.

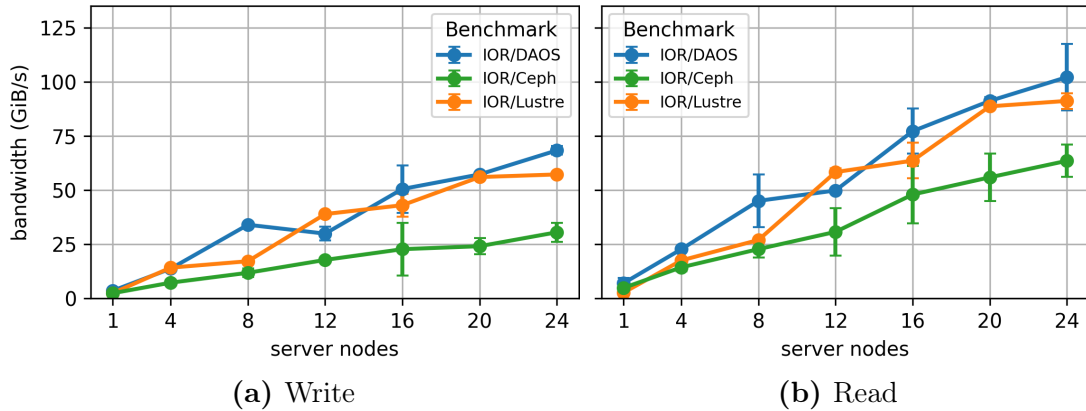


Figure 4.20: IOR bandwidth scalability against increasingly large Lustre, Ceph, and DAOS deployments on GCP. A ratio of 2-to-1 client-to-server nodes was used for all tests, and 16 to 32 processes were run in each client node. Every process performed $10000 \times 1\text{MiB}$ I/O operations ($100 \times 1\text{ MiB}$ for Ceph). Tests were repeated 3 times.

These encouraging results demonstrated all storage systems were able to scale roughly linearly on NVMe SSDs, at least for IOR workloads. At the largest scales tested, both DAOS and Lustre reached 80% of the write bandwidth and 66% of the read bandwidth the hardware could provide, whereas Ceph reached approximately a third of the write bandwidth and two thirds of the read bandwidth achieved by the other two storage systems.

The gap between the hardware bandwidths and the bandwidths for runs against DAOS or Lustre was significant, particularly for read, but this was not investigated further. The difference in performance between Ceph and the other two was due to the same reasons discussed in the client count optimisation tests.

Despite the good scalability, all storage systems showed a slight decline beyond

16 server VMs, and this was more noticeable for Lustre than for the rest.

4.3.4 FDB backend performance

The methodology was followed again to produce scalability curves for `fdb-hammer` runs against the three storage systems, using the respective FDB backends.

The client count optimisation process was documented in Appendix D - Section III - B, E, and F, and the results shown in Figures 3 (g) and (h), 7, and 8 in that paper. Similar to IOR, a client-to-server node ratio of 2 and 16 to 32 processes per node resulted in best performance.

`fdb-hammer` was then run using the optimal client counts against deployments on increasing amounts of VMs. The resulting scalability curves are shown in Fig. 4.21.

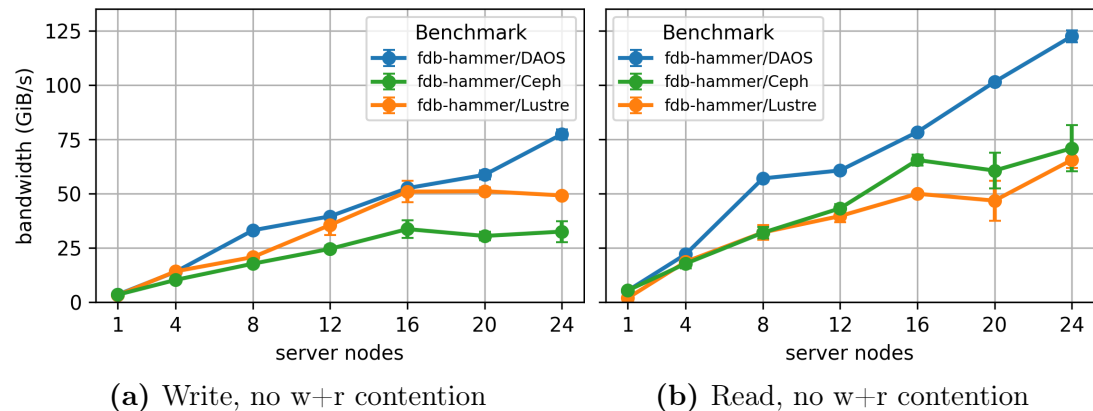


Figure 4.21: `fdb-hammer` bandwidth scalability, with no write+read contention, against increasingly large Lustre, Ceph, and DAOS deployments on GCP. A ratio of 2-to-1 client-to-server nodes was used for all tests, and 16 to 32 processes were run in each client node. Every process wrote and indexed (or de-referenced and read) 10000 x 1MiB weather fields. Tests were repeated 3 times.

DAOS and the respective backends scaled roughly linearly both for write and read, with bandwidths spiking above the trend for tests against 8 server VMs. The read bandwidths slightly exceeded those of previous IOR tests, just as observed in

NEXTGenIO, likely due to the additional optimisations put in place in the DAOS backends. These excellent results demonstrated that DAOS can achieve close to hardware performance at scale for complex I/O workloads such as the ECMWF’s NWP I/O workloads, even if a large number of array and key-value operations are issued. Also, these demonstrated high performance on DAOS is not an exclusive result of SCM, but can be achieved as well in systems with common NVMe SSDs.

fdb-hammer runs on Ceph scaled linearly both for write and read up to 16 server VMs, reaching two thirds of the hardware write bandwidth and close to hardware read bandwidths, but plateaued at larger server counts. The runs against up to 16 server VMs performed notably better than corresponding IOR runs, presumably due to the object per `archive()` approach of the FDB Ceph backends—as opposed to the object per process approach in IOR—, which resulted in a more balanced distribution of objects across OSDs and in turn allowed for longer benchmark runs with 10000 I/O operations per process. Beyond 16 server VMs, write bandwidths plateaued, and read bandwidths seemed to continue scaling in line with the trend excluding a spike at 16 VMs.

For Lustre, the **fdb-hammer** write bandwidths scaled linearly up to 16 server VMs, reaching close to DAOS and hardware bandwidths, but markedly plateaued at 50 GiB/s for larger server counts. This plateauing was an unexpected result, on one hand because the POSIX I/O FDB backends are optimised for write performance, and on the other hand because equivalent tests in NEXTGenIO showed better write scalability.

Read bandwidths on Lustre scaled almost linearly throughout, with a slight decline beyond 12 server VMs and a spike under the trend for 20 server VMs, and were notably lower than those observed in corresponding IOR tests. This gap relative to IOR was slightly surprising as **fdb-hammer** produces a relatively easy read workload, involving only a few files per process. A similar unexpected

gap had been observed for runs in NEXTGenIO, and this strongly suggested that the lower `fdb-hammer` performance was likely unrelated to the hardware of either system and was rather caused by a potential software or configuration issue at the storage system level or in the POSIX I/O FDB backends, such as Lustre not handling well the relatively large number of `read` operations, or an undiscovered issue in the logic for merging `DataHandles`.

Scalability curves for `fdb-hammer` runs with *write+read contention* were also produced. One half of the client nodes ran writer processes, and the other half ran reader processes. These are shown in Fig. 4.22.

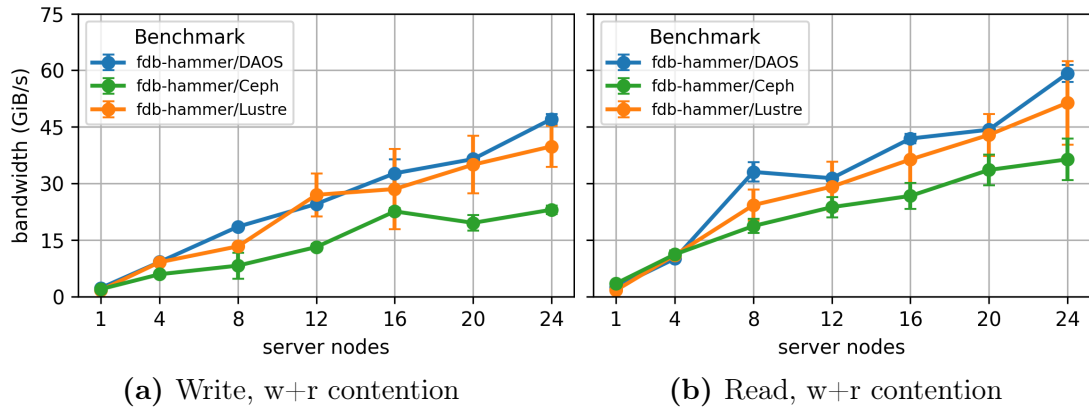


Figure 4.22: `fdb-hammer` bandwidth scalability, with *write+read contention*, against increasingly large Lustre, Ceph, and DAOS deployments on GCP. A ratio of 2-to-1 client-to-server nodes was used for all tests, and 16 to 32 processes were run in each client node. Every process wrote and indexed (or de-referenced and read) 10000 x 1MiB weather fields. Tests were repeated 3 times.

Just as observed previously in NEXTGenIO, DAOS and the respective backends scaled roughly linearly both for write and read —omitting a few spikes—, thus were not significantly impacted in terms of scalability by operational contention, which was fully captured by `fdb-hammer` in this case. In terms of performance, writing performed better than initially expected — runs with *no write+read contention*, in Fig. 4.21, reached up to 75 GiB/s using 24 server and 48 client VMs, and therefore the runs here, which had writers running on only a half of

the client VMs presumably being served by a half of the server resources, were expected to reach up to a half of these bandwidths. Instead, writers exceeded these bandwidths, reaching up to 45 GiB/s, and this was due to readers ending sooner and releasing server resources which immediately proceeded to serve writers.

Ceph also scaled roughly linearly, although with a progressive decline in read performance. The bandwidths achieved were significantly lower than with DAOS, but this was within expectations based on previous tests with *no write+read contention*. The results here demonstrated that, just as DAOS, Ceph’s performance was not significantly impacted by operational contention levels, although the performance would very likely plateau at larger server VM counts based on tests with *no write+read contention*. These results were moderately encouraging. Although Ceph does not provide optimal performance, it ought not to be discarded as an option for high-performance storage for small to medium-scale applications.

fdb-hammer runs on Lustre scaled nearly linearly, reaching bandwidths similar to DAOS, although the performance would have likely plateaued or declined at larger server VM counts based on tests with *no write+read contention*, and would have further deteriorated if **fdb-hammer** on Lustre had more precisely captured the operational contention and read transposition. Nevertheless, the positive results here contrasted with equivalent tests on NEXTGenIO, where both the write and read bandwidths on Lustre halved under contention. This reinforced the idea that Lustre did not properly exploit the specialised hardware in NEXTGenIO for contentious workloads, whereas it did for the more commonplace hardware in GCP.

To gain further insight on the behaviour of the storage systems tested, and particularly on why Ceph and Lustre performed and scaled worse than DAOS, some of the **fdb-hammer** runs at scale —with and without write-read contention— were profiled and the results summarised in Fig. 4.23, 4.24, and 4.25.

For runs against DAOS, in Fig. 4.23, most of the time was spent on array write and read operations, which permitted bandwidths to reach close to hardware limits. In contrast to equivalent runs on NEXTGenIO, a nearly negligible amount of time was spent on key-value **gets** and **puts**, likely due to the fact that DAOS deployments in GCP exploited DRAM for storage of metadata and small I/O operations such as index key-value **gets** and **puts**, whereas deployments in NEXTGenIO used SCM. DAOS’s performance might be lower or plateau at larger scales if enabling the feature to persist metadata and small I/O into NVMe SSDs, although previous analysis has shown that, due to its write-ahead-log (WAL) approach, the impact of this feature should only be noticeable for extremely metadata-operation-intensive workloads[33].

For runs with *write+read contention* on DAOS, the portion of time spent on array write operations —in Fig. 4.23 (c)— was significantly smaller than for runs without contention —in Fig. 4.23 (a)—, and this was again due to the read phase ending sooner and releasing server resources which immediately proceeded to handle pending writes. This occurred to some extent as well for runs against Ceph and Lustre, but occurred to a much lesser extent for equivalent runs in NEXTGenIO as the write and read performance levels were closer to each other in that system, resulting in closer end times for the write and read phases.

For runs on Ceph, summarised in Fig. 4.24, most of the time was similarly spent on object writes and reads, although a more significant portion was spent on Omap **sets** and **gets**, likely due to Ceph being configured to persist all metadata and Omaps into NVMe SSDs instead of holding these in DRAM.

Smaller-scale runs on Ceph —the profiling results of which have been omitted in favour of conciseness— spent a less significant portion of time on object **write** operations, which indicated that the plateauing observed in Fig. 4.21 was caused by such **write** operations rather than by Omap **sets** and **gets**. The Omap

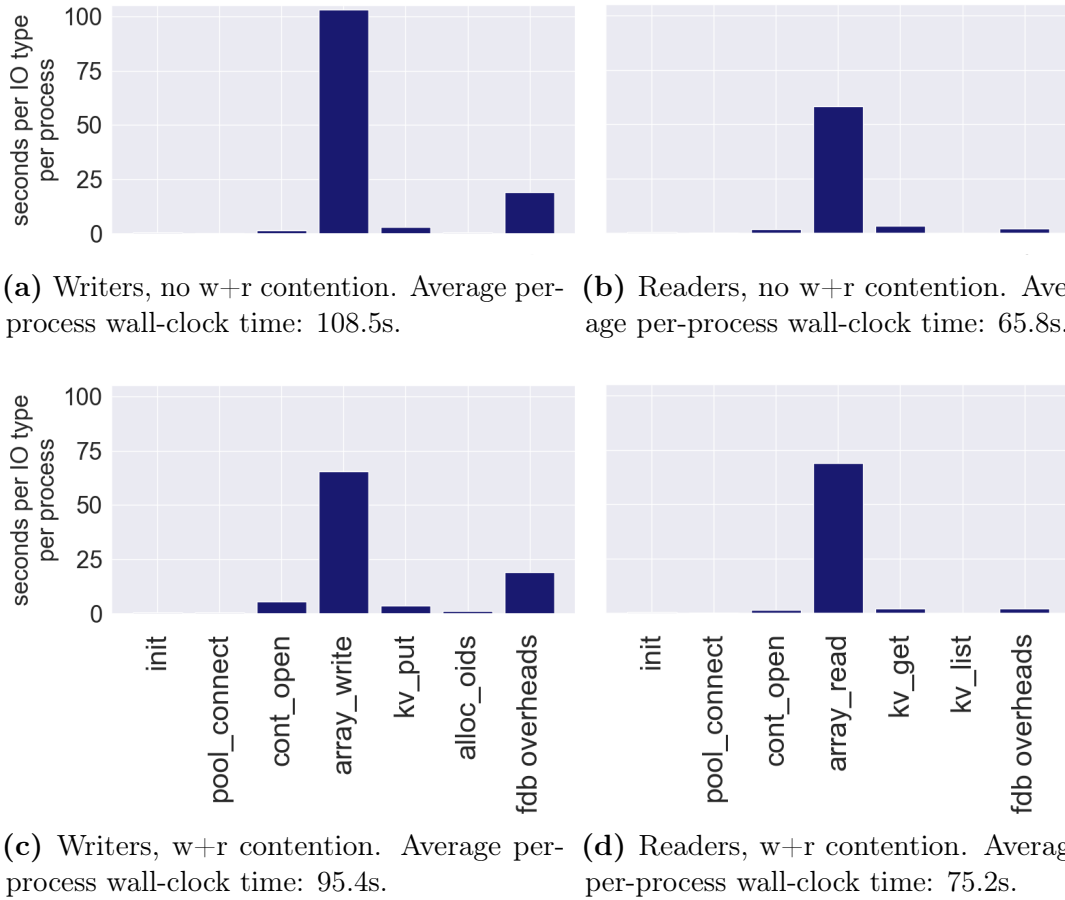
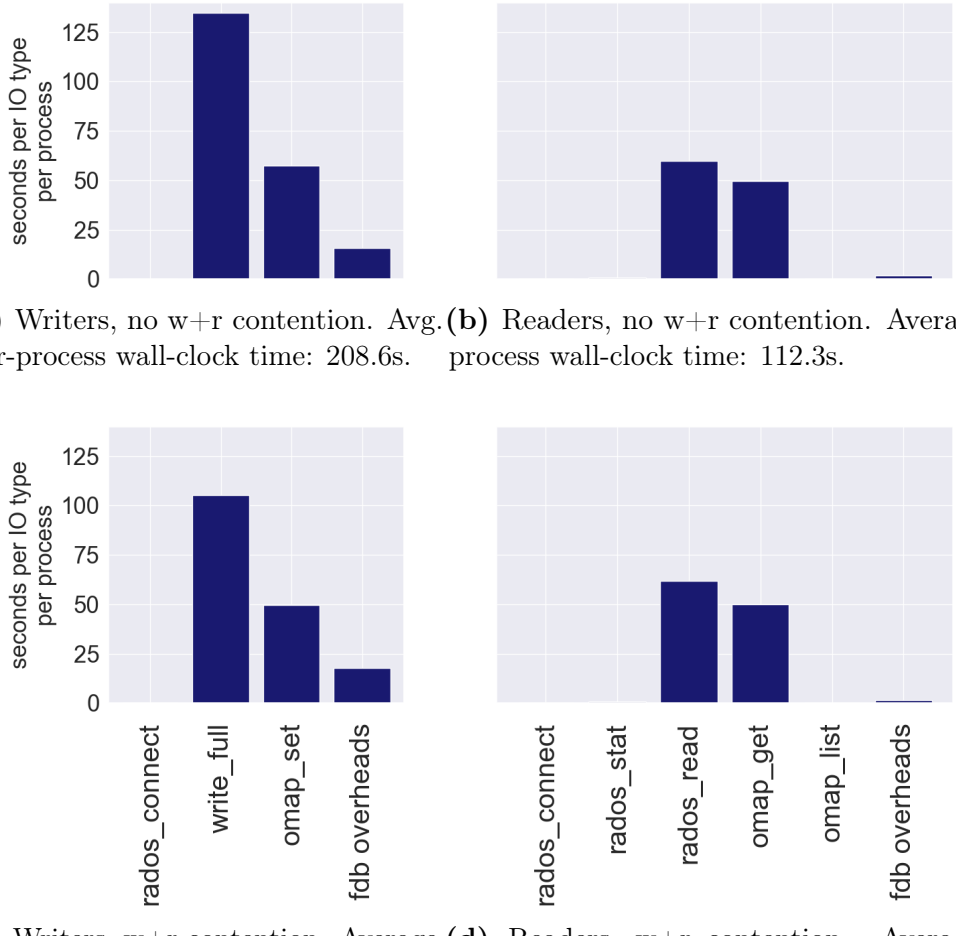


Figure 4.23: Profiling results for fdb-hammer/DAOS runs without (top row) and with (bottom row) write+read contention, using 20 server and 40 client nodes; 24 processes per client node. Every process wrote and indexed (or de-referenced and read) 10000 x 1MiB weather fields.

overheads, instead, were equally significant in smaller-scale runs, and hence were the main contributor to the consistently inferior performance levels reached by Ceph in the experiments in Fig. 4.21 and 4.22.

This suggested that Ceph could potentially have reached performance levels as high DAOS at small scales if Ceph had been configured to hold Omaps in DRAM, although even in that case, and even in the best-case scenario that the time spent on Omap operations on DRAM were negligible, Ceph would have likely suffered a scalability decline beyond 16 server VMs due to object writes —which



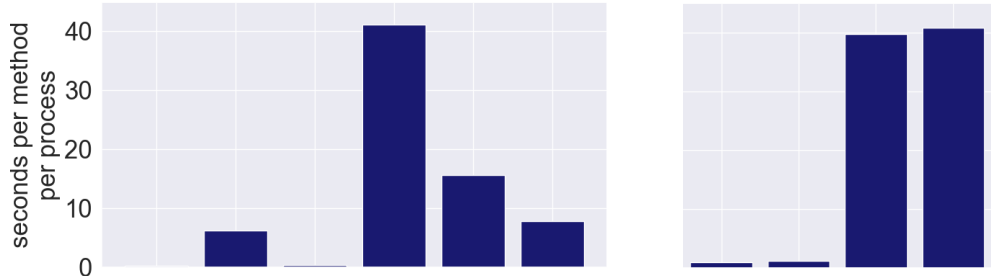
(c) Writers, w+r contention. Average per-process wall-clock time: 172.7s. (d) Readers, w+r contention. Average per-process wall-clock time: 114.5s.

Figure 4.24: Profiling results for fdb-hammer/Ceph runs without (top row) and with (bottom row) write+read contention, using 20 server and 40 client nodes; 24 processes per client node. Every process wrote and indexed (or de-referenced and read) 10000 x 1MiB weather fields.

are persisted on NVMe SSDs both by Ceph and DAOS— being slow at scale.

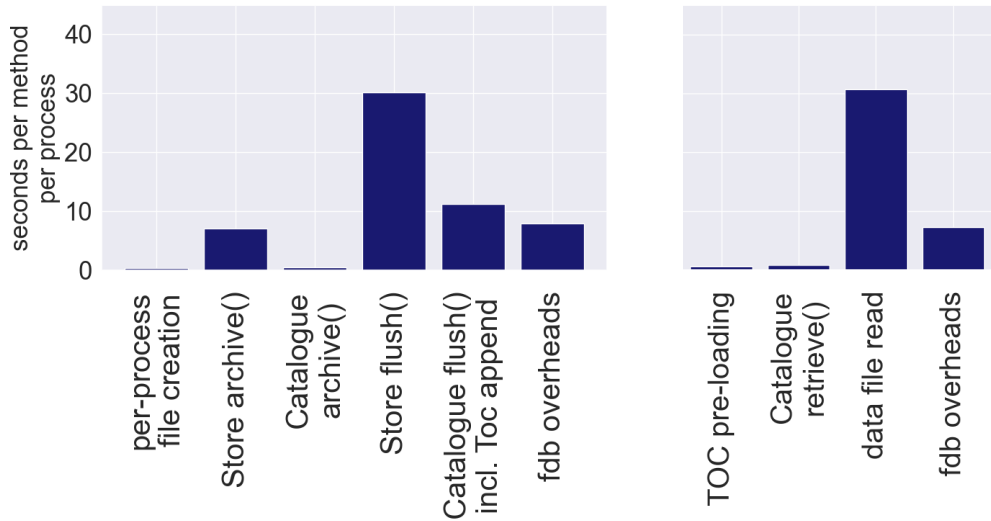
The profiling for runs with *write+read contention*, in Fig. 4.24 (c) and (d), did not significantly differ, except for the slightly lower portion of time spent on object write operations — again due to the server resources that served readers being released earlier. This demonstrated that, like DAOS, Ceph is not sensitive to contention, at least for the type of I/O workload tested here.

Profiling results for runs on Lustre are shown in Fig. 4.25. Lower client counts had to be used on Lustre for optimal performance, which resulted in smaller I/O workloads being issued than in previous tests, hence the wall-clock times shown for Lustre runs cannot be directly compared to previous results.



(a) Writers, no w+r contention. Average per-process wall-clock time: 71.8s.

(b) Readers, no w+r contention. Average per-process wall-clock time: 82.8s.



(c) Writers, w+r contention. Average per-process wall-clock time: 57.4s.

(d) Readers, w+r contention. Average per-process wall-clock time: 39.6s.

Figure 4.25: Profiling results for fdb-hammer/Lustre runs without (top row) and with (bottom row) write+read contention, using 20 server and 40 client nodes; 12 processes per client node. Every process wrote and indexed (or de-referenced and read) 10000 x 1MiB weather fields.

The results in (a) and (b) correspond to runs with *no write+read* contention

against 20 server VMs, for which both write and read bandwidths plateaued or diverged from DAOS, as shown in Fig. 4.21. These results should therefore reflect any overheads causing the performance deterioration on Lustre.

For write, in (a), the proportions of time spent on the different methods were reasonable and within expectations, with most of the time being spent on writing —in Store `archive()` and the first part of Catalogue `flush()`— and waiting for persistence — in Store `flush()` and the last part of Catalogue `flush()`. However, profiling results for runs at smaller scale, not included here, showed a less prominent portion of time being spent on Catalogue `flush()`, and the write scalability decline was therefore attributed to Lustre not handling well the large number of small per-process file `writes` issued by that method. If Lustre had been configured to hold metadata and small I/O operations in DRAM, as done for the DAOS system, this decline might have been alleviated.

Compared to equivalent runs in NEXTGenIO, the distribution of time over the different methods was similar, except that a larger portion of time was spent on Store `flush()` relative to the other methods. This was likely due to the different characteristics of the storage devices, with NVMe SSDs being slower to persist the data than SCM.

For read, in (b), two aspects stood out. The first one was the large amount of time spent on data file reads. In the write phase, approximately 45 seconds were spent on bulk data writes —in Store `archive()` and `flush()`—, and in the read phase 40 seconds were spent on the bulk data reads. However, the bulk reading should have been ideally twice as fast as the writing, based on the profiling of `array_writes` and `array_reads` for runs against DAOS. A similar slowness was observed for equivalent runs in NEXTGenIO, although the slowness in that system was more marked — double the time was spent on bulk reading relative to bulk writing. This difference was again likely due to the different characteristics

of the hardware at hand — the hardware read bandwidths in GCP were higher than in NEXTGenIO, relative to hardware write bandwidths. This slowness was potentially due to inefficiencies in `DataHandle` merging, or due to Lustre not handling well the relatively large number —albeit not as large as in operational runs— of `read` operations issued per process.

The other aspect that stood out were the very substantial FDB overheads. That time was spent mostly in the `axis()` method of the POSIX I/O backends described in 2.7.2, essentially manipulating in-memory metadata. These overheads were less prominent for runs at smaller scale, and grew exponentially as a function of the number of reader processes used for benchmarking. This pointed out that there was room for further optimisation in the POSIX I/O backends, and the `fdb-hammer` read performance at scale on Lustre, in Fig. 4.21, would have been closer to DAOS if these inefficiencies had been addressed. Runs with *no write+read contention* were not noticeably affected by this issue because in these cases only a half of the client VMs were used to run reader processes, preventing the excessive `axis()` overheads from manifesting. Similarly, these overheads were not as marked in `fdb-hammer` runs against Lustre on NEXTGenIO as these used only up to 20 client nodes.

Profiling results for runs with *write+read contention*, in Fig. 4.25 (c) and (d), showed smaller portions of time being spent on Store and Catalogue `flush()`. Just like for runs against DAOS and Ceph, this was due to part of the server resources being released as soon as the read phase ended. This was a positive sign indicating that Lustre was able to efficiently use the available resources under contention, and reaffirmed the hypothesis that it did not properly exploit the specialised hardware in NEXTGenIO, where contentious runs spent twice as much time in Store `flush()` as runs with *no write+read contention*.

For read, in (d), the portion of time spent on bulk data reads was smaller

than in (b), likely due to the smaller number of `read` operations issued which alleviated the RPC pressure on Lustre. Also, the `axis()` overheads reduced very significantly due to the smaller scale of the read workload, allowing `fdb-hammer` to scale better than in runs with *no write+read contention*.

4.3.5 Small object size performance

Tests so far issued medium size ($O(\text{MiB})$) I/O operations, and showed all system performed relatively well, with DAOS standing out reaching higher bandwidths. Many HPC applications, however, operate with object and I/O sizes orders of magnitude smaller or larger. While workloads with large I/O size are generally easier —due to the reduced metadata or RPC pressure— and should not negatively impact the performance observed so far, workloads with small I/O size might significantly affect the performance behaviour of the storage systems, and the analysis so far did not provide insight on whether such applications would benefit more from the POSIX I/O approach or the object storage one.

An additional set of `fdb-hammer` tests was run using small I/O size —1 KiB instead of 1 MiB— against deployments of the three storage systems on 4 VMs. The results are shown in Fig. 4.26.

For write, `fdb-hammer` on Lustre performed better than on the other storage systems, very likely due to the fact that the POSIX I/O backends use large files to contain all the small I/Os and this results in a much smaller metadata workload compared to the object storage backends which create a separate object per I/O operation. DAOS performed only slightly worse than Lustre, and although this was a very good result given the object per I/O approach, it was likely attributable to DAOS holding many —if not all— I/O operations on DRAM server-side given their small size.

For read, `fdb-hammer` on DAOS performed clearly better than the rest. Even

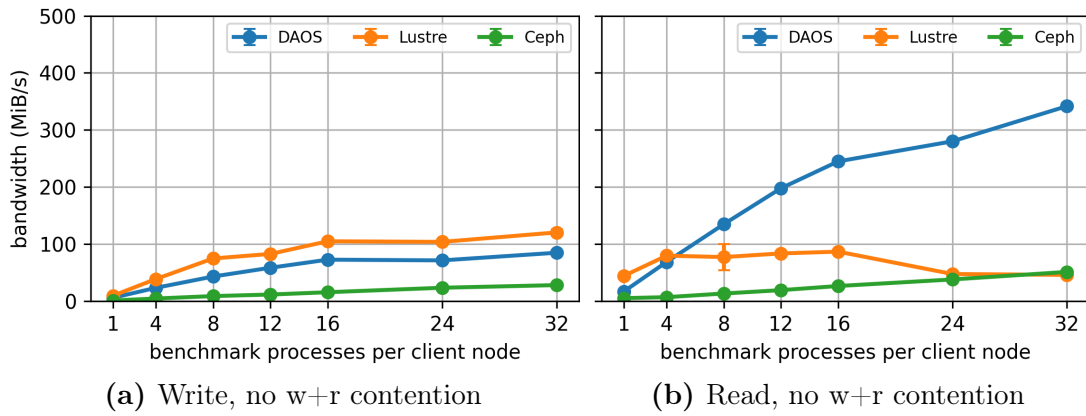


Figure 4.26: Bandwidths for fdb-hammer runs with small object size on 8 client VMs against Lustre, DAOS, and Ceph deployments on 4 VMs (+1 for Lustre and Ceph). Every process performed 10000 x 1KiB I/O operations. Tests were repeated 3 times.

if DAOS had been configured to persist metadata and small I/O operations into NVMe devices, it would have cached a copy of such operations on DRAM server-side for fast access, resulting in the same read performance as observed here. Lustre can similarly cache data server-side, but in this experiment the bandwidths on Lustre sharply plateaued again likely due to inefficiencies in FDB `DataHandle` merging or due to Lustre not handling well the large number of I/O operations issued. Ceph performed an order of magnitude worse than DAOS likely due to accessing NVMe devices on most Omap and regular object operations.

These results highlighted the importance of understanding whether the storage systems persist or cache metadata operations server-side or not, and hinted at DAOS’s superior capability for metadata-intensive read workloads.

4.3.6 DAOS and Ceph data redundancy

Data safety mechanisms such as replication and erasure-coding are paramount for storage systems to prevent permanent data loss as well as to minimise the impact on running applications in the event of various types of hardware failure or unexpected storage node reboots.

For storage systems intended as long-term permanent storage—for example backing home directories—, enabling such mechanisms is a must to prevent permanent data loss. If solely intended as high-performance storage for short-lived applications—also referred to as scratch storage—, however, enabling such mechanisms is not strictly necessary. In fact, not enabling data safety mechanisms for scratch storage can be a sensible choice to avoid the associated overheads, although if a failure occurs applications must detect or be made aware of it and start from scratch to regenerate any temporarily unavailable or permanently lost data. For short-lived and time-critical applications such as the ECMWF’s operational NWP, however, a rerun from scratch in the event of a hardware failure generally cannot be afforded, as the execution would likely overrun the operational deadlines. Data safety mechanisms are therefore a necessary choice for the ECMWF’s production setup and their performance impact should be assessed.

Data safety mechanisms can be implemented at a hardware or software level. Production Lustre setups usually rely on specialised storage hardware implementing such mechanisms, although Lustre can also leverage software-level disk arrays created with `mdadm`, with the disadvantage that these arrays cannot be configured to span multiple devices distributed over the network, and hence are a less likely configuration for production setups. DAOS and Ceph, conversely, do currently provide integrated production-ready software-level data safety options.

To gain insight on the performance impact of the data safety options provided by DAOS and Ceph, the `fdb-hammer` benchmark was run against deployments of the two storage systems on increasing amounts of VMs in GCP, as done in Fig. 4.21, this time having the systems configured to either replicate or erasure-code all objects.

Fig. 4.27 shows results for runs having the storage systems maintain one redundant replica for every object, be it a key-value or a bulk data object.

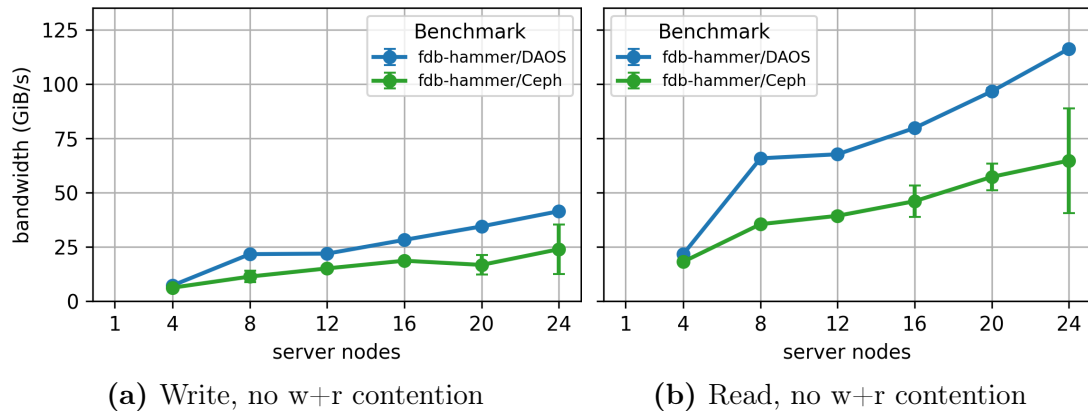


Figure 4.27: fdb-hammer bandwidth scalability, with no write+read contention, against increasingly large Ceph, and DAOS deployments on GCP, using a replication factor of 2. A ratio of 2-to-1 client-to-server nodes was used for all tests, and 16 to 32 processes were run in each client node. Every process wrote and indexed (or de-referenced and read) 10000 x 1MiB weather fields. Tests were repeated 3 times.

Relative to Fig. 4.21, the write performance of both DAOS and Ceph reduced by approximately 40%, and the scalability behavior did not change significantly. This decrease in performance was an expected result. Either storage system, if mostly idle, should be able to absorb write operations as fast as without replication since the replicas for a given write operation should be written concurrently on multiple storage devices. Nevertheless, when the I/O workload saturates the system —as done in the experiments here—, half of the storage devices are busy handling writes of redundant copies, therefore reducing the effective write bandwidth to a half if one replica is maintained for every object.

For read, performance was not significantly affected on either system, and this was in line with expectations — having redundant copies should improve rather than deteriorate performance, as reader processes can target more server VMs to retrieve data in parallel for a given object.

Results for runs with 2+1 erasure-coding —that is, with objects being split in two parts, an additional part with redundant data being created, and the three parts being stored in different devices— are shown in Fig. 4.28. Since Ceph

does not support erasure-coded Omaps, the Omaps were kept in a separate pool configured for replication just as in the previous experiment.

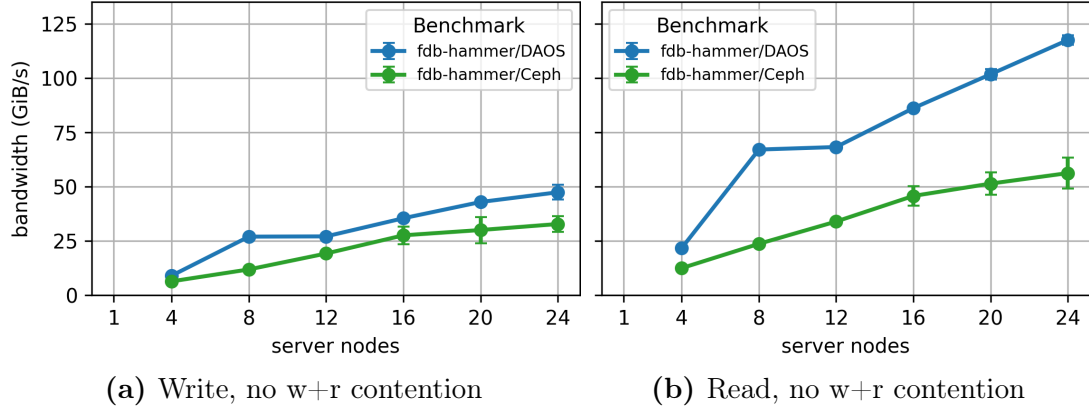


Figure 4.28: fdb-hammer bandwidth scalability, with no write+read contention, against increasingly large Ceph, and DAOS deployments on GCP, using 2+1 erasure-coding. A ratio of 2-to-1 client-to-server nodes was used for all tests, and 16 to 32 processes were run in each client node. Every process wrote and indexed (or de-referenced and read) 10000 x 1MiB weather fields. Tests were repeated 3 times.

Write bandwidths on both DAOS and Ceph were slightly higher than in the replication experiment. Runs on DAOS reached up to a 66% of the bandwidths measured for experiments without redundancy, in Fig. 4.21. This was again in line with expectations, as an erasure-coding factor of 2+1 implies 50% more data is written into storage devices, and therefore one third of the storage devices are busy handling these additional data. Runs on Ceph, however, reached similar bandwidths as without redundancy, and this was an indicator that Ceph was likely not being limited by the storage device bandwidth.

For read, bandwidths on DAOS were unaffected with respect to runs without erasure-coding, although Ceph suffered a noticeable decline in performance at larger scales.

These results showed both storage systems could perform well despite enabling their built-in data safety mechanisms, and this was particularly true for DAOS, which stood out reaching bandwidths as high as the hardware permitted.

4.3.7 DAOS interfaces

So far, DAOS demonstrated outstanding performance when used natively via libdaos. Porting existing POSIX I/O applications to libdaos, however, can be a daunting task —the API and semantics are radically different, and there are challenges associated to porting as showcased in this work—and is not always a viable option.

DAOS provides a FUSE module for transparent access via the standard POSIX I/O infrastructure, namely DFUSE, with potential to mitigate the challenges of porting to DAOS. DFUSE, however, is not a silver bullet as it is currently not fully POSIX-compliant. Among other limitations, it currently does not provide advisory locks, and does not support features such as the atomicity of `mkdir` or the `O_APPEND` flag of the `open` system call. For instance, due to these limitations, running `fdb-hammer` or any other application using the POSIX I/O FDB backends on DFUSE is not possible. Nevertheless, a large portion of existing POSIX I/O applications can run directly on DFUSE and, in fact, DAOS is often presented as a new type of file system, and is by default exposed as a file system in early-adopting production HPC systems such as Aurora.

This rises the question of what is the performance impact of accessing DAOS via DFUSE relative to native libdaos access, and how POSIX I/O applications perform on DAOS via DFUSE compared to a high-performance distributed file system deployed on the same hardware.

Appendix D - Section III - B and C looked into the performance and scalability of DFUSE compared to libdaos, and demonstrated that using DFUSE in conjunction with `libioil` —a POSIX I/O interception library distributed alongside DAOS— resulted in as good performance and scalability as accessing DAOS natively via libdaos, at least for IOR workloads.

The paper also tested a more involved HDF5 benchmark which provides back-

ends for native operation on DAOS via libdaos as well as for efficient operation on POSIX file systems. The benchmark was run in GCP against DAOS deployments on 16 server VMs, both natively and via DFUSE using the POSIX backend. The results have been included here in Fig. 4.29 (a), (b), (c), and (d).

Surprisingly, runs on DFUSE resulted in higher performance than via libdaos, but this was due to the HDF5 native backend making use of a large number of containers, which was shown to deteriorate performance earlier. In spite of this, these results suggested that DFUSE has potential to provide high performance also for complex POSIX I/O applications with zero porting effort.

To gain further insight on whether runs on DFUSE performed well or not, additional HDF5 tests were run against Lustre deployed on the same hardware, using HDF5’s POSIX I/O backend. The results, in Fig. 4.29 (e) and (f), showed that HDF5 on Lustre reached notably lower bandwidths than runs via DFUSE, both for write and read. Although write runs on DFUSE might have taken advantage to an extent of the fact that DAOS held metadata and small I/O operations in DRAM server-side instead of persisting these into NVMe devices, read runs both on DFUSE and Lustre benefited from the same amount of server-side DRAM available for caching data and optimising read operations. This was yet another indicator that DFUSE can provide high performance levels for complex POSIX I/O applications without porting, in this case higher than a high-performance file system could provide.

HDF5 and its POSIX I/O backend were designed to make efficient use of the underlying distributed file system. However, often the reality at HPC centres is that large part of the applications do not perform easy or well-behaved POSIX I/O, either because these do not adhere to programming best practices for high performance on distributed file systems, or because these, by nature, cannot be made to conform to well-behaved POSIX I/O patterns. One example of this are

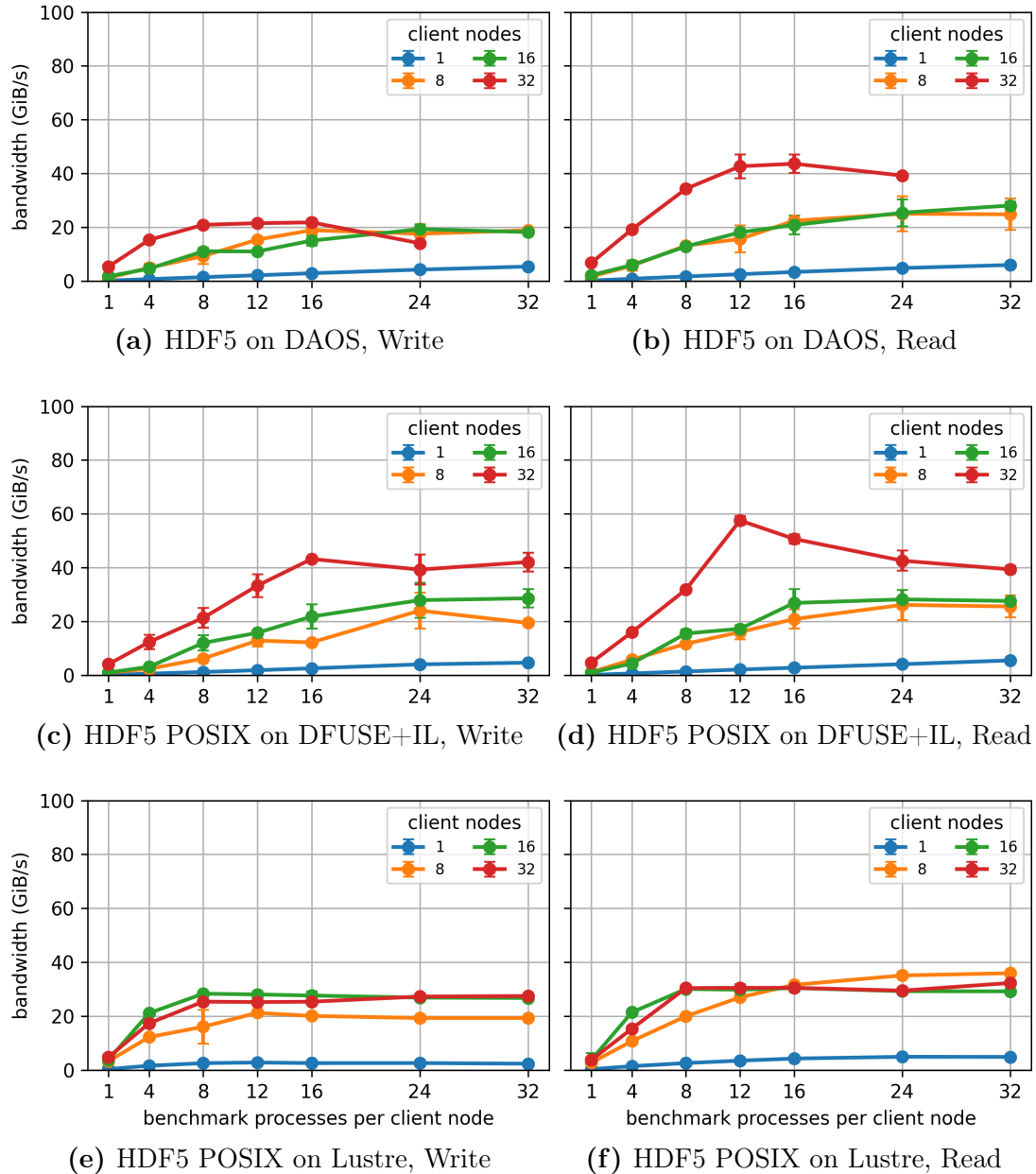


Figure 4.29: Bandwidths for IOR/HDF5 runs against DAOS and Lustre deployments on 16 VMs (+1 for Lustre). Every process performed $10000 \times 1\text{MiB}$ I/O operations. Tests were repeated 3 times.

some of the emerging AI applications, which require accessing many small and sparse subsets of the data domain.

To analyse the performance of DFUSE when exposed to this type of non-well-behaved applications, the Field I/O benchmark and the dummy DAOS library—which were shown to make an abusive use of the POSIX I/O APIs in Section 4.2.4—were rescued and run against DAOS (via DFUSE) and Lustre deployments on 4 server VMs in GCP. The resulting bandwidths for Field I/O runs on DFUSE are shown at the top row of Fig. 4.30, and bandwidths for equivalent runs on Lustre are shown at the bottom row.

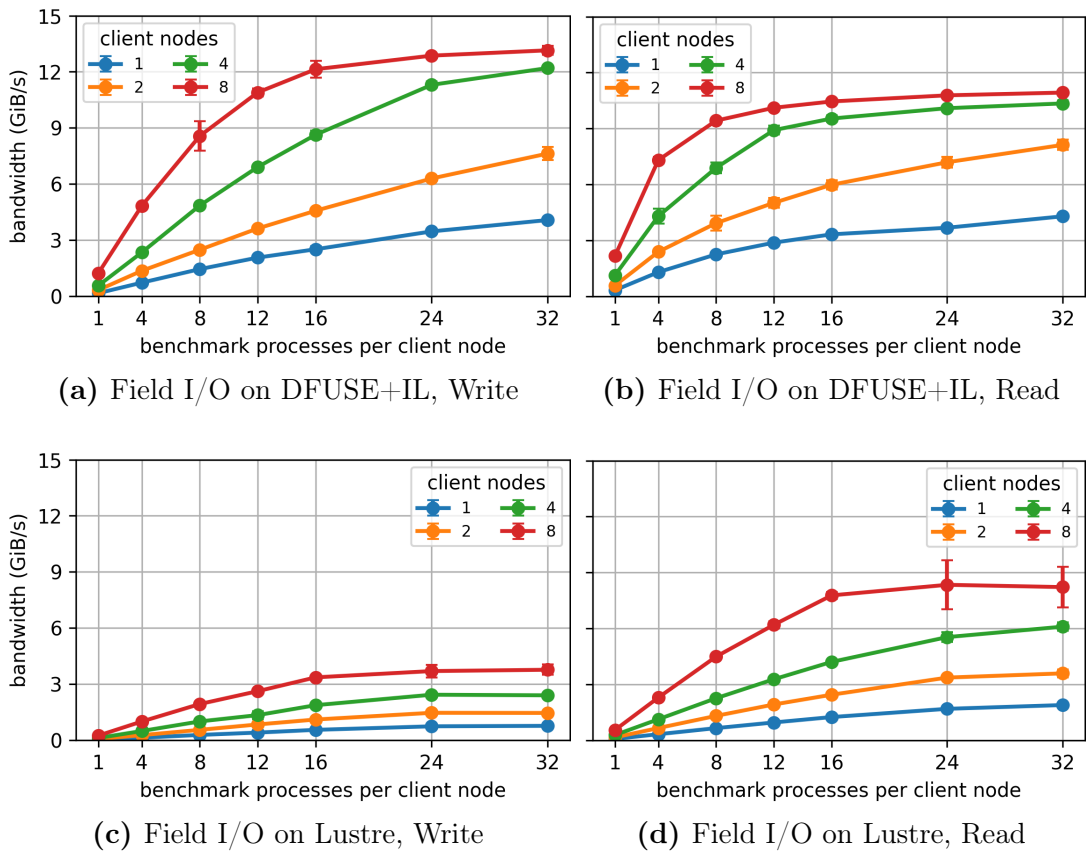


Figure 4.30: Bandwidths for Field I/O runs using dummy libdaos against DAOS and Lustre deployments on 4 VMs (+1 for Lustre). Every process performed 1000 x 1MiB I/O operations. Tests were repeated 3 times.

The write bandwidths for runs on DFUSE were significantly higher than for runs on Lustre, this time likely mostly due to DAOS holding metadata and small I/O operations on DRAM server-side. For read, both storage systems reached similar bandwidths, although DAOS was slightly ahead.

These results suggested that DAOS and DFUSE do not harm performance or can even result in slight performance improvements for non-well-behaved POSIX I/O applications without porting effort. In turn, this meant that the POSIX I/O APIs and semantics might not be a causing factor of the known performance limitations of POSIX file systems at scale, and these limitations might instead be a result of the design and implementation of the internals of the file systems so far backing such APIs and semantics.

4.3.8 Summary

The I/O benchmarking in GCP revealed that the three storage systems evaluated—Lustre, DAOS, and Ceph—were capable of scaling nearly linearly in performance for IOR workloads if deployed on NVMe SSDs, albeit with a slight decline at the largest scales tested. Ceph reached significantly lower bandwidths than the other two, but this was partly due to the lack of a feature for IOR to use multiple objects per process.

In contrast to previous experiments in NEXTGenIO, the three storage systems used the TCP protocol this time. Using large client process counts unlocked high performance, although tests at larger scales showed a significant gap relative to hardware limits, particularly for read, and the reasons of this were not investigated.

For NWP I/O workloads, DAOS and the respective FDB backends performed remarkably well, scaling nearly linearly both for write and read despite the benchmark closely capturing the access pattern and contention of an operational run at the ECMWF.

Ceph and the respective backends scaled linearly up to a certain point, reaching higher bandwidths than equivalent IOR tests due to I/O being performed over several objects per process. Nevertheless, the bandwidths were significantly lower than for DAOS, and this was likely partly due to Ceph immediately persisting metadata and Omaps into NVMe SDDs, whereas DAOS held these in DRAM. Also, more importantly, the write bandwidths plateaued in the larger tests due to object `write` operations not scaling well on Ceph, which conversely did scale well on DAOS despite being equally persisted into SSDs.

Lustre and the respective backends performed and scaled very well for write up to a certain point, but bandwidths plateaued at the largest scales tested due to large amounts of small `write` operations being issued periodically by the backends and `synced` into NVMe SSDs. For read, Lustre scaled relatively well but reached significantly lower performance than DAOS, although this was largely due to inefficiencies in the POSIX I/O backends, and if these had been addressed, read bandwidths on Lustre would have been close to DAOS's. One aspect worth noting, however, is that, unfortunately, the `fdb-hammer` benchmark did not capture well the operational contention nor the read access transposition when run on Lustre with the POSIX I/O backends. If these had been captured, both the write and read performance—but particularly the read performance—would have likely been lower on Lustre.

All things considered, the performance curves in Fig. 4.21 fairly represented the performance potential of the different storage systems on NVMe, with a few exceptions:

- DAOS's write performance might be lower at larger scales if enabling DAOS's feature to persist metadata and small I/O operations into NVMe SSDs.
- Lustre's write and particularly read performance would likely be lower, with a potential scalability deterioration, if the benchmark fully captured the operational

contention and read transposition.

- Lustre’s read performance would likely be higher if the inefficiencies identified in the POSIX I/O backends were addressed. Combined with the previous exception, the resulting read performance on Lustre would likely be slightly higher than in the graphs.

These results were moderately positive for Ceph, which performed and scaled relatively well both for contentious and non-contentious workloads, and demonstrated it ought not be discarded for high-performance at small to medium scales.

The results were also moderately positive for Lustre, as these demonstrated Lustre on NVMe can perform better than it did in NEXTGenIO, and showed it can provide competitive bandwidths and scalability relative to DAOS, with the exception that it can suffer scalability issues for writing at scale.

The results were very positive for DAOS, as these demonstrated that the outstanding performance and scalability was not exclusive of SCM or other specialised hardware, and further consolidated DAOS as the evaluated storage system with the most potential to handle the ECMWF’s operational NWP or other similar HPC I/O workloads at scale.

This benchmarking in GCP also looked into the data safety mechanisms provided by DAOS and Ceph, and showed that both systems can provide replication and erasure-coding without significantly harming performance or scalability, although DAOS stood out reaching bandwidths close to hardware limits despite the data safety mechanisms being enabled.

Finally, the performance of DFUSE —an interface provided by DAOS for transparent POSIX-like access, although not fully POSIX compliant— was shown to reach close to hardware performance for simple POSIX I/O workloads, and slightly higher performance than Lustre for POSIX I/O applications performing well-behaved and non-well-behaved I/O patterns.

Chapter 5

Conclusion

Driven by scientific and industry ambition, HPC and AI applications such as operational NWP require processing and storing ever-increasing data volumes as fast as possible. Whilst POSIX distributed file systems and NVMe SSDs are currently a common HPC storage configuration providing I/O to applications, new storage solutions have proliferated or gained traction over the last decade with potential to address performance limitations POSIX file systems manifest at scale for certain I/O workloads.

This work has primarily aimed to assess the suitability and performance of two object storage systems —namely DAOS and Ceph— for ECMWF’s operational NWP as well as for HPC and AI applications in general. New software-level adapters have been developed which enable ECMWF’s NWP to leverage these systems, and extensive I/O benchmarking has been conducted on a few computer systems, comparing the performance delivered by the object stores to that of equivalent Lustre file system deployments on the same hardware. Challenges of porting to object storage and its benefits with respect to the traditional POSIX I/O approach have been discussed and, where possible, domain-agnostic performance analysis has been conducted, leading to insight also of relevance to I/O

practitioners and the broader HPC community. This work has also investigated the options and challenges the S3 storage protocol provides by porting the ECMWF’s NWP to it. This allowed direct comparison to the object storage approaches that have been the main focus of this research, and in turn broadened the range of storage solutions supported by the ECMWF’s NWP.

The main findings and conclusions drawn from this work are summarised in the following.

Both DAOS and Ceph were found to provide enough features for a full porting of the ECMWF’s NWP, which was ultimately demonstrated with the development of the mentioned adapters. Also, both were shown to provide strong consistency, free of data corruption or inconsistencies when exercised with the ECMWF’s highly contentious I/O workloads.

Porting to these object stores was not trivial. Whilst using their native programming APIs was initially not particularly complicated, unlocking the highest performance the stores could provide required making non-obvious configuration and development choices, and several rounds of adjustment and performance evaluation at scale. This was more marked for DAOS than for Ceph. Some examples included choosing the right granularity of objects, properly pinning DAOS server processes to available cores, finding the optimal number of Ceph placement groups, distributing the data across the right number of DAOS containers or Ceph pools, and selecting the optimal DAOS object classes. This experience led to the production of recommendations, encapsulated in documentation and training material made openly available to the community.

Nevertheless, atomic key-values stood out as a particularly useful feature available in both object stores to implement well-performing indexing of NWP data elements, which is currently difficult to achieve in POSIX file systems. The programming APIs and features offered by the DAOS and Ceph object stores

enabled a more flexible and natural expression of I/O patterns, in turn resulting in simpler code for the newly developed object storage adapters than for the previously-existing POSIX ones.

Both object stores and the respective adapters performed well or very well under NWP I/O workloads, but DAOS stood out reaching higher performance than Lustre and Ceph and scaling linearly up to the largest scale tested, whereas Lustre and Ceph showed signs of a write scalability decline at the largest scales. Specifically, in a system with up to 24 server nodes equipped with NVMe SSDs, DAOS performed slightly better than Lustre for write workloads and notably better (40%) for read, whereas Ceph performed notably worse (40%) than Lustre for write, and slightly better for read. The write scalability of Lustre and Ceph declined starting at 16 server nodes, with write bandwidths plateauing beyond that scale. In another system with Intel’s Optane SCM devices —Optane is unfortunately discontinued now—, both Lustre and DAOS scaled linearly throughout, although DAOS reached significantly higher bandwidths particularly under contentions I/O workloads. Nevertheless, this was in part due to Lustre not efficiently exploiting the specialised hardware in that system.

Remarkably, both object stores achieved such performance despite being exercised with operational-like NWP workloads, and despite very frequently persisting a large number of small (1 MiB) objects and performing several persistent key-value operations to index and de-index those objects. This type of storage access pattern would have been too expensive to perform at scale with POSIX file systems, and this demonstrated object stores, and DAOS in particular, enable new access patterns at scale involving many I/O operations and small-sized data elements.

Furthermore, DAOS was found to also perform well for both large and very small objects, making it the only evaluated storage system able to provide high

performance at KiB, MiB, and GiB object sizes. This emphasized DAOS’s unique flexibility, unlocking a wider range of access patterns whilst preserving high performance for traditional ones.

Regarding software-level data redundancy, of relevance for production setups, neither DAOS nor Ceph showed significant deterioration of their baseline performance or scalability when enabling replication of objects, although DAOS stood out maintaining its superior performance levels despite the redundancy mechanisms being engaged.

Further performance tests demonstrated that DFUSE —DAOS’s POSIX interface— can provide native performance for simple, large-file-per-process POSIX I/O applications without porting, showing no significant performance differences relative to Lustre. Other more complex applications, performing more involved POSIX I/O patterns, showed slightly better performance when run on DFUSE without porting compared to equivalent runs on Lustre. Although for some of the tests DAOS benefited from holding small I/O operations on DRAM server-side, these encouraging results strongly suggested that DAOS, via DFUSE, can provide performance levels as high or slightly higher than Lustre both for easy or well-behaved POSIX I/O workloads as well as for workloads not adhering to well-behaved I/O patterns. Nevertheless, this can only be taken advantage of if the application does not use certain POSIX I/O features that are currently not supported by DFUSE.

Overall, both evaluated object stores were found to be suitable and beneficial for the ECMWF’s NWP as they both provided sufficient functionality, consistency guarantees, and performance. Due to their different performance behavior, however, they were deemed suitable for different purposes. Where a Ceph system is available —not uncommon in Cloud environments— it can provide high-performance read access to applications such as NWP data services at small

to medium scale. DAOS, instead, has potential for operational NWP due to its superior performance at scale.

More broadly, this work characterized and shed some light on the performance differences between DAOS, Ceph, and Lustre, which had not been previously documented in such a rigorous apples-to-apples comparison. On one hand, it demonstrated the advantage and potential of DAOS as HPC storage, enabling a wide range of access patterns and providing better performance and scalability, and, on the other hand, it showed Ceph is also an option worth of consideration, enabling new patterns as well, although providing lower write performance and suffering from scalability limitations similar to Lustre.

These positive results do not mean object stores can easily replace POSIX file systems in HPC centres as typically, in these contexts, several existing applications using POSIX I/O must continue to be supported whilst minimizing performance impact if the storage system is replaced. Ceph can provide fully POSIX-compliant access via CephFS, and therefore is able to support existing applications without disruption, but may provide significantly lower performance than Lustre, as seen in this work. In the DAOS case, DFUSE is not currently fully POSIX compliant, and porting all unsupported POSIX I/O applications to object storage is generally not an option. Nevertheless, where a complementary DAOS system is provisioned, any applications ported natively may see an increase in performance and scalability, as observed with the ECMWF’s NWP I/O benchmark. Furthermore, any POSIX I/O applications supported by DFUSE may see a notable performance increase if they perform complex I/O workloads that were not optimized for POSIX file systems or do not fit well-behaved POSIX I/O patterns — as is usually the case in AI applications.

All evaluated storage systems, however, are continually evolving, and the view may change in the years to come. For instance, there are ongoing efforts in

Ceph and Lustre to address some of their performance limitations, as there are in DAOS’s DFUSE to extend POSIX compliance.

The feasibility of porting the ECMWF’s NWP to the storage systems and protocols evaluated in this work was a great result. This demonstrated that these offer enough features to implement consistent indexing and bulk-storage functionality on top of them, and was an indicator of the good quality of the design and abstractions put in place in the FDB —the ECMWF’s I/O middleware for NWP applications— allowing easy implementation of new adapters. This work has contributed enabling the FDB and the ECMWF’s NWP to leverage additional storage solutions and opening doors for the ECMWF to consider these in future HPC system procurements.

5.1 Future work

One relevant result of this work has been the demonstration of the advantage and potential of DAOS as HPC storage, and this has been based on its observed superior performance and scalability, compared to Ceph and Lustre, in systems with NVMe SSDs or SCM. There are a few factors that could potentially modify or even disprove this result, and should therefore be examined thoroughly with additional performance tests.

In the first place, only up to 24 server nodes were employed for the scalability analysis. Additional tests should be conducted at scales more representative of production HPC setups, ideally using up to hundreds of server nodes, to determine whether the scalability behaviors observed so far hold at such larger scales. This should include running the ECMWF’s Kronos benchmark, or even running full operational NWP workloads, potentially at very high resolution, against all storage systems deployed at scale, and preferably enabling software-level data redundancy.

Secondly, both Lustre and Ceph persisted all metadata immediately on SSDs, whereas DAOS did not yet have the capability of doing so and, instead, it stored metadata and small I/O operations under 4 KiB on DRAM server-side — at that time, DAOS was still transitioning after Optane was discontinued. A newer version of DAOS should be employed and configured to immediately persist all metadata and I/O on SSDs for a fairer comparison. Nevertheless, prior work has shown that this new feature of DAOS should only have a noticeable performance impact for corner-case metadata-intensive workloads, and should in any case mostly impact only write workloads as DAOS caches metadata and small I/O operations, even if the new feature is enabled, to faster serve read operations.

In the third place, all Lustre deployments used for this analysis were set up with only one MDS (metadata server) regardless of the number of OSTs (object storage targets) deployed. However, ideally, the MDSs should be grown alongside the OSTs, for example using a ratio of 1 MDS to 8 OSTs, to ensure metadata servers do not bottleneck I/O performance.

Lastly, more advanced Ceph setups and configuration could be explored to ensure the maximum potential of Ceph is unlocked. Some ideas include deploying Ceph OSDs in a dedicated storage network; adjusting the depth of the Write-Ahead Logs in the OSDs; and adjusting the amount of DRAM used by OSDs.

Regarding the assessment of the performance benefits of object storage for the ECMWF’s operations, the NWP I/O benchmark used did not fully capture the operational contention nor access pattern, particularly when run on Lustre. The benchmark should be enhanced to better do so, or alternatively other more complex benchmarks or full operational workloads should be used, and this would likely result in a more marked performance advantage on object stores, even after the read performance issue in the POSIX I/O backends is addressed.

One limitation of this work is that it has followed a markedly empirical

approach for the performance analysis, relying mostly on analysis of bandwidths measured in benchmark runs and analysis of application-level profiling. Further in-depth analysis should be conducted, collecting abundant metrics on the server side such as queue depths and RPC counts, with the aim of providing more detailed explanations of what mechanisms may be being triggered and causing bottlenecks internally in the servers.

Also, the performance analysis has focused on rather short-lived benchmark runs of up to tens of minutes each. However, storage systems can manifest oscillation or changes in performance at longer time scales as internal buffers fill up and data structures are further populated, and this should be addressed by running benchmarks of longer duration. Likewise, the impact of storage device or node failures on storage performance should be assessed, as well as the impact of intense and short-lived I/O workloads triggered while other longer-lived workloads are active. These scenarios are common in production contexts.

As previously discussed, the new object storage adapters for the ECMWF's NWP, as currently implemented, have the writer clients persist every single data element and key-value operation immediately on non-volatile storage on the server side, as opposed to the approach followed by the POSIX adapters used currently operationally, where clients build local caches of data and indexing information which are only ensured to be persisted from time to time, when strictly necessary. Although the immediately persistent approach of the object storage adapters has some advantages, it may be unnecessarily conservative. New object storage adapters could be implemented which follow a caching approach based on that of the POSIX adapters, and this might further improve the performance and scalability of object stores for the ECMWF's operational NWP.

Finally, given the potential of object stores to provide high performance for I/O workloads involving many I/O operations and small-sized data elements, and

for less well-behaved POSIX I/O workloads, further benchmarking should be conducted to measure the likely positive impact of object storage and the new adapters on machine-learning-based NWP at the ECMWF.

Bibliography

- [1] *Timeline Of Computer History - Computers*, <https://www.computerhistory.org/timeline/computers/> (Accessed: 19 January 2024).
- [2] *Timeline Of Computer History - Memory & Storage*, <https://www.computerhistory.org/timeline/memory-storage/> (Accessed: 19 January 2024).
- [3] H. Werner Meuer, E. Strohmaier, J. Dongarra, H. Simon, and M. Meuer, *TOP500 Lists*, <https://top500.org/lists/top500/> (Accessed: 19 January 2024).
- [4] J. L. Bez, A. Dilger, D. Hildebrand, J. Kunkel, J. Lofstead, and G. Markomanolis, *IO500 Lists*, <https://io500.org/releases> (Accessed: 28 January 2024).
- [5] J.-T. Acquaviva, M. Golasowski, M. Hennecke, W. A. Jackson, T. Leibovici, J. Lüttgau, et al., *ETP4HPC SRA 6 White Paper-I/O and Storage*, English, edited by S. Neuwirth and P. Deniel, ETP4HPC SRA (2025), 10.5281/zenodo.14605692.
- [6] J. Lüttgau, M. Kuhn, K. Duwe, Y. Alforov, E. Betke, J. Kunkel, et al., “Survey of Storage Systems for High-Performance Computing”, *Supercomputing Frontiers and Innovations* **5**, 10.14529/jsfi180103 (2018) 10.14529/jsfi180103.
- [7] M. Weiland, H. Brunst, T. Quintino, N. Johnson, O. Iffrig, S. Smart, et al., “An early evaluation of Intel’s optane DC persistent memory module and its impact on high-performance scientific applications”, in *Proceedings of the international conference for high performance computing, networking, storage and analysis* (Nov. 2019), pp. 1–19, 10.1145/3295500.3356159.
- [8] P. Bauer, A. Thorpe, and G. Brunet, “The quiet revolution of numerical weather prediction”, *Nature* **525**, 47–55 (2015) 10.1038/nature14956.
- [9] S. D. Smart, T. Quintino, and B. Raoult, “A Scalable Object Store for Meteorological and Climate Data”, in *Proceedings of the platform for advanced scientific computing conference* (June 2017), pp. 1–8, 10.1145/3093172.3093238.
- [10] S. D. Smart, T. Quintino, and B. Raoult, “A High-Performance Distributed Object-Store for Exascale Numerical Weather Prediction and Climate”, in *Proceedings of the platform for advanced scientific computing conference* (June 2019), pp. 1–11, 10.1145/3324989.3325726.

- [11] N. Manubens, T. Kremer, M. Çakırçalı, C. Bradley, E. Danovaro, S. Smart, et al., *ECMWF's FDB: a Versatile High-Performance Store for Earth System Data*, <https://destination-earth.eu/event/3rd-destination-earth-user-exchange/3rd-Destination-Earth-User-Exchange-Poster>.
- [12] A. Jackson and N. Manubens, *Profiling and Identifying Bottlenecks in DAOS*, <https://www.research.ed.ac.uk/en/activities/profiling-and-identifying-bottlenecks-in-daos> DAOS User Group Meeting.
- [13] A. Jackson, M. Chaarwi, J. Lombardi, N. Manubens, and D. Hildebrand, *High-Performance Object Storage: I/O for the Exascale Era*, <https://sc24.conference-program.com/presentation/?id=tut143&sess=sess417> SC'24 Conference Tutorial.
- [14] N. Manubens, S. D. Smart, E. Danovaro, T. Quintino, and A. Jackson, “Reducing the Impact of I/O Contention in Numerical Weather Prediction Workflows at Scale Using DAOS”, in Proceedings of the platform for advanced scientific computing conference (June 2024), pp. 1–12, 10.1145/3659914.3659926.
- [15] J. Lombardi and N. Manubens, *Accelerating Storage with Optane & DAOS*, <https://events.ecmwf.int/event/169/timetable/19th-Workshop-on-High-Performance-Computing-in-Meteorology>.
- [16] N. Manubens, *Assessment of DAOS as a Backend for ECMWF's FDB*, <https://daosio.atlassian.net/wiki/spaces/DC/pages/11015454821/DUG21-DAOS-User-Group-Meeting>.
- [17] *FDB*, <https://github.com/ecmwf/fdb> GitHub repository (Accessed: 28 January 2025).
- [18] N. Manubens, T. Quintino, S. D. Smart, E. Danovaro, and A. Jackson, “DAOS as HPC Storage: a View From Numerical Weather Prediction”, in 2023 ieee international parallel and distributed processing symposium (ipdps) (May 2023), pp. 1029–1040, 10.1109/IPDPS54959.2023.00106.
- [19] N. Manubens, J. Lombardi, S. D. Smart, E. Danovaro, T. Quintino, D. Hildebrand, et al., “Exploring DAOS Interfaces and Performance”, in Sc24-w: workshops of the international conference for high performance computing, networking, storage and analysis (Nov. 2024), pp. 1340–1348, 10.1109/SCW63240.2024.00175.
- [20] N. Manubens, S. D. Smart, T. Quintino, and A. Jackson, “Performance Comparison of DAOS and Lustre for Object Data Storage Approaches”, in 2022 ieee/acm international parallel data systems workshop (pds) (Nov. 2022), pp. 7–12, 10.1109/PDSW56643.2022.00007.
- [21] A. Jackson and N. Manubens, *Performance Impacts of Replication and Sharding*, <https://daos.io/event/daos-user-group-at-sc24-dug24-DAOS-User-Group-Meeting>.
- [22] S. Neuwirth, “Accelerating Network Communication and I/O in Scientific High Performance Computing Environments”, PhD thesis (Universität Heidelberg, 2019).

- [23] J. Liu, Q. Koziol, G. F. Butler, N. Fortner, M. Chaarawi, H. Tang, et al., “Evaluation of HPC Application I/O on Object Storage Systems”, in 2018 ieee/acm 3rd international workshop on parallel data storage & data intensive scalable computing systems (pdsw-discs) (2018), pp. 24–34, 10.1109/PDSW-DISCS.2018.00005.
- [24] A. Aghayev, S. Weil, M. Kuchnik, M. Nelson, G. R. Ganger, and G. Amvrosiadis, “File systems unfit as distributed storage backends: lessons from 10 years of Ceph evolution”, in Proceedings of the 27th acm symposium on operating systems principles, SOSP ’19 (2019), pp. 353–369, 10.1145/3341301.3359656.
- [25] F. Gadban and J. Kunkel, “Analyzing the Performance of the S3 Object Storage API for HPC Workloads”, 10.3390/app11188540 (2021) 10.3390/app11188540.
- [26] J. Lofstead, I. Jimenez, C. Maltzahn, Q. Koziol, J. Bent, and E. Barton, “DAOS and Friends: A Proposal for an Exascale Storage System”, in Sc ’16: proceedings of the international conference for high performance computing, networking, storage and analysis (2016), pp. 585–596, 10.1109/SC.2016.49.
- [27] J. Soumagne, J. Henderson, M. Chaarawi, N. Fortner, S. Breitenfeld, S. Lu, et al., “Accelerating HDF5 I/O for Exascale Using DAOS”, IEEE Transactions on Parallel and Distributed Systems **33**, 903–914 (2022) 10.1109/TPDS.2021.3097884.
- [28] R. Sarpangala Venkatesh, G. Eisenhauer, S. Klasky, and A. Gavrilovska, “Enhancing Metadata Transfer Efficiency: Unlocking the Potential of DAOS in the ADIOS context”, in Proceedings of the sc ’23 workshops of the international conference on high performance computing, network, storage, and analysis, SC-W ’23 (2023), pp. 1223–1228, 10.1145/3624062.3624193.
- [29] A. Jackson and N. Manubens, “DAOS as HPC Storage: Exploring Interfaces”, in 2023 ieee international conference on cluster computing workshops (cluster workshops) (2023), pp. 8–10, 10.1109/CLUSTERWorkshops61457.2023.00011.
- [30] M. Hennecke, “Understanding DAOS Storage Performance Scalability”, in Proceedings of the hpc asia 2023 workshops, HPCAsia ’23 Workshops (2023), pp. 1–14, 10.1145/3581576.3581577.
- [31] M. Nelson, *Ceph: A Journey to 1 TiB/s*, <https://ceph.io/en/news/blog/2024/ceph-a-journey-to-1tibps/> (Accessed: 29 July 2025).
- [32] R. Raja Chandrasekar, L. Evans, and R. Wespetal, “An Exploration into Object Storage for Exascale Supercomputers”, in Cray user group (2017).
- [33] M. Hennecke, J. Olivier, T. Nabarro, L. Zhen, Y. Niu, S. Wang, et al., “DAOS Beyond Persistent Memory: Architecture and Initial Performance Results”, in High performance computing: isc high performance 2023 international workshops, hamburg, germany, may 21–25, 2023, revised selected papers (2023), pp. 353–365, 10.1007/978-3-031-40843-4_26.

- [34] R. Latham, R. B. Ross, P. Carns, S. Snyder, K. Harms, K. Velusamy, et al., “Initial Experiences with DAOS Object Storage on Aurora”, in Proceedings of the sc ’24 workshops of the international conference on high performance computing, network, storage, and analysis, SC-W ’24 (2025), pp. 1304–1310, 10.1109/SCW63240.2024.00171.
- [35] W. R. Stevens and S. A. Rago, *Advanced Programming in the UNIX Environment*, 3rd (Addison-Wesley Professional, 2013).
- [36] A. K. Paul, O. Faaland, A. Moody, E. Gonsiorowski, K. Mohror, and A. R. Butt, “Understanding HPC Application I/O Behavior Using System Level Statistics”, in 2020 ieee 27th international conference on high performance computing, data, and analytics (hipc) (2020), pp. 202–211, 10.1109/HiPC50609.2020.00034.
- [37] F. Schmuck and R. Haskin, “GPFS: A Shared-Disk File System for Large Computing Clusters”, in Conference on file and storage technologies (2002).
- [38] A. George and R. Mohr, *Understanding Lustre Internals*, https://wiki.lustre.org/Understanding_Lustre_Internals (Accessed: 29 July 2025).
- [39] P. Braam, *The Lustre Storage Architecture*, <https://arxiv.org/abs/1903.01955>.
- [40] Z. Liang, J. Lombardi, M. Chaarawi, and M. Hennecke, “DAOS: A Scale-Out High Performance Storage Stack for Storage Class Memory”, in Supercomputing frontiers: 6th asian conference, scfa 2020, singapore, february 24–27, 2020, proceedings (2020), pp. 40–54, 10.1007/978-3-030-48842-0_3.
- [41] *DAOS Architecture*, <https://docs.daos.io/latest/overview/architecture> (Accessed: 29 July 2025).
- [42] *DAOS File System*, <https://docs.daos.io/latest/user/filesystem/> (Accessed: 29 July 2025).
- [43] S. A. Weil, S. A. Brandt, E. L. Miller, D. D. E. Long, and C. Maltzahn, “Ceph: a scalable, high-performance distributed file system”, in Proceedings of the 7th symposium on operating systems design and implementation, OSDI ’06 (2006), pp. 307–320.
- [44] *Welcome to Ceph*, <https://docs.ceph.com/en/latest/> (Accessed: 29 July 2025).
- [45] *Ceph Network Configuration Reference*, <https://docs.ceph.com/en/latest/rados/configuration/network-config-ref/#general-settings> (Accessed: 29 July 2025).
- [46] *Introduction to librados*, <https://docs.ceph.com/en/latest/rados/api/librados-intro/> (Accessed: 29 July 2025).
- [47] S. Weil, *Ceph Tech Talk - Introduction to Ceph*, <https://www.youtube.com/watch?v=PmLPbrf-x9g> (Accessed: 29 July 2025).
- [48] *About Our Forecasts*, <https://www.ecmwf.int/en/forecasts/documentation-and-support> (Accessed: 28 January 2025).

- [49] ECMWF, *Supercomputer facility*, <https://www.ecmwf.int/en/computing/our-facilities/supercomputer-facility> (Accessed: 13 December 2025).
- [50] *Lustre Best Practices*, https://www.nas.nasa.gov/hecc/support/kb/lustre-best-practices_226.html (Accessed: 28 January 2025).
- [51] T. Haerder and A. Reuter, “Principles of transaction-oriented database recovery”, ACM Computing Surveys **15**, 287–317 (1983) 10.1145/289.291.
- [52] *Amazon S3 API Reference*, <https://docs.aws.amazon.com/AmazonS3/latest/API> (Accessed: 29 July 2025).
- [53] *HPC IO Benchmark Repository*, <https://github.com/hpc/ior> (Accessed: 29 July 2025).
- [54] *IO500*, <https://io500.org/about> (Accessed: 13 December 2025).
- [55] The HDF Group, *Hierarchical Data Format, version 5 [Computer Software]*, <https://github.com/HDFGroup/hdf> (Accessed: 29 July 2025).
- [56] *NEXTGenIO User Guide and Applications*, <https://ngioproject.github.io/nextgenio-docs/html/index.html> (Accessed: 29 July 2025).
- [57] A. Jackson, “Evaluating the latest Optane memory: A glorious swansong?”, in 4th workshop on heterogeneous memory systems, sc23 (2023).
- [58] *Google Cloud Landing Page*, <https://cloud.google.com> (Accessed: 29 July 2025).
- [59] *General-purpose machine family for Compute Engine*, <https://cloud.google.com/compute/docs/general-purpose-machines> (Accessed: 29 July 2025).
- [60] *Set the number of threads per core*, <https://cloud.google.com/compute/docs/instances/set-threads-per-core> (Accessed: 29 July 2025).
- [61] *Spot VMs*, <https://cloud.google.com/solutions/spot-vms> (Accessed: 29 July 2025).
- [62] *Google Cluster Toolkit*, <https://github.com/GoogleCloudPlatform/cluster-toolkit> (Accessed: 29 July 2025).
- [63] nicolau-manubens, *ecmwf-projects/daos-tests: 0.3.2*, <https://doi.org/10.5281/zenodo.13757427>, 10.5281/zenodo.13757427.

Appendix A – Performance Comparison of DAOS and Lustre for Object Data Storage Approaches

Performance Comparison of DAOS and Lustre for Object Data Storage Approaches

Nicolau Manubens

European Centre for Medium-Range Weather Forecasts
Bonn, Germany
nicolau.manubens@ecmwf.int

Simon D. Smart

European Centre for Medium-Range Weather Forecasts
Reading, United Kingdom
simon.smart@ecmwf.int

Tiago Quintino

European Centre for Medium-Range Weather Forecasts
Reading, United Kingdom
tiago.quintino@ecmwf.int

Adrian Jackson

EPCC, The University of Edinburgh
Edinburgh, United Kingdom
a.jackson@epcc.ed.ac.uk

Abstract—High-performance object stores are an emerging technology which offers an alternative solution in the field of HPC storage, with potential to address long-standing scalability issues in traditional distributed POSIX file systems due to excessive consistency assurance and metadata prescriptiveness.

In this paper we assess the performance of storing object-like data within a standard file system, where the configuration and access mechanisms have not been optimised for object access behaviour, and compare with and investigate the benefits of using an object storage system.

Whilst this approach is not exploiting the file system in a standard way, this work allows us to investigate whether the underlying storage technology performance is more or less important than the software interface and infrastructure a file system or object store provides.

Index Terms—scalable object storage, next-generation I/O, storage class memory, numerical weather prediction, DAOS, Lustre

I. INTRODUCTION

Object stores are a candidate to address long-standing scalability issues in POSIX file systems, including excessive consistency assurance and prescriptiveness [1].

Numerical Weather Prediction (NWP) usually entails object-like data access, as global weather fields are currently of the order of 1 MiB in size, relatively small if compared to traditional high-performance I/O sizes, and an advanced indexing mechanism is required for high-performance semantic discovery and access, which involves several metadata operations. Domain-specific object stores have been developed to implement this semantic indexing on traditional distributed file systems in a way that satisfies current operational NWP performance requirements [2].

With the planned resolution increases in NWP simulations, resulting in one to two orders of magnitude larger data sets, and the advent of general-purpose high-performance object stores, which are specially designed for the type of object-like operations common in NWP, adapting the domain-specific store currently in use at ECMWF becomes an increasingly appealing pathway. In a recent study, as prior research to validate such effort, we have assessed the performance that DAOS, a

high-performance object store which has been recently gaining traction, can provide together with Storage Class Memory (SCM) when tested with an ad-hoc benchmark which mimics I/O patterns in our operational NWP use case [3].

In this paper we review these DAOS performance results, and compare with corresponding performance results obtained using Lustre, one of the most popular distributed file systems in HPC, after adapting the ad-hoc benchmark to carry out the object operations on top of a file system.

This work allows us to discriminate the benefits achieved from using specific storage hardware as compared to the benefits from the object store design and implementation. It also allows us to draw conclusions of general interest on the benefits of object stores, and gives some real use-case same-hardware same-software data points for comparison of Lustre and DAOS.

II. DAOS

The Distributed Asynchronous Object Store (DAOS) [4] is an open-source high-performance object store designed for massively distributed non-volatile memory (NVM) including SCM and NVMe. It provides a low-level key-value storage interface on top of which other higher-level APIs, also provided by DAOS, are built. Its features include transactional non-blocking I/O, fine-grained I/O operations with zero-copy I/O to SCM, end-to-end data integrity and advanced data protection. The OpenFabrics Interfaces (OFI) library is used for low-latency communications over a wide range of network backends.

DAOS is deployable as a set of I/O processes or engines, one per physical socket in a server node, each managing access to SCM and NVMe devices within the socket. An engine partitions the storage it manages into targets to optimize concurrency, each target being managed and exported by a dedicated group of threads. DAOS allows reserving space distributed across targets in so-called *pools*, a form of virtual storage. A pool can serve multiple transactional object stores called *containers*. A container is a private object address space,

which can be modified transactionally and independently of the other containers in the same pool. An application first needs to connect to the pool and then open the desired container. If successfully authorised, the application obtains a handle it can use for its processes to interact with the container.

Upon creation, objects in a container are assigned a 128-bit unique object identifier, of which 96 bits are user-managed. Objects can be configured for replication and striping across pool targets by specifying their *object class*. An object configured with striping is stored in parts, distributed across targets, enabling concurrent access.

III. LUSTRE

Lustre [5] is the foremost parallel file system used at HPC site globally. It is an open-source file system, that aims to provide high bandwidth and high availability for many users across a wide range of hardware. Lustre provides a POSIX-compliant interface to distributed data storage that enables large numbers of clients to connect and use the file system concurrently.

IV. METHODOLOGY

In this work, DAOS and Lustre have been deployed on the NEXTGenIO research HPC system, exploiting the same underlying hardware, and the deployments have been benchmarked with the community-developed IOR benchmark [6] and the Field I/O benchmark.

In brief, the Field I/O benchmark consists of a pair of functions that perform writing and reading of weather fields to and from a DAOS object store, using the DAOS C API. Their design closely mimics the domain-specific object store already employed within ECMWF, and they can be combined and run in parallel in different ways, resulting in two different data access patterns of interest:

- *pattern A*: in a first phase, writer programs are run on a number client nodes (typically more than one per node), and issue a sequence of write operations. Once all writers have finished, a second phase runs, where an equal number of reader programs are executed, issuing a sequence of corresponding read operations. This pattern aims to assess the maximum write or read throughput the storage can provide to applications, mimicking a scenario where the NWP writer applications are run separately from the post-processing reader applications.
- *pattern B*: firstly, the storage is pre-populated with some data. Following this initialisation step, half of the client nodes employed for the benchmark issue a sequence of write operations, while the other half issue corresponding read operations. This pattern aims to assess the throughput storage can provide in more realistic scenarios with contention between writing and reading processes.

Due to its design, Field I/O is representative of the types of I/O workload exhibited from real NWP workflows. Typically, operational NWP workflows at ECMWF operate as in pattern B, with approximately 250 HPC nodes writing simulation

output to storage while another 250 nodes read and run post-processing tasks. However many users also run the forecasting models or post-processing applications independently in a manner that is equivalent to pattern A.

Field I/O is described in more detail in [3] along with a methodology to assess object storage performance for NWP applications, which is also adopted here. Following that methodology, the IOR benchmark has been configured so that each I/O process issues a single, large, I/O operation comprising a sequence of data parts (we refer to this mode of operation as *segments mode*). This enables assessment of the maximum achievable performance if the developed application were optimised to gather and transfer all relevant data in a single I/O operation, and provides insight on to what extent the storage server is able to exploit available network bandwidth and/or storage capability when not having to deal with new operations.

In order to execute the object-store-oriented Field I/O benchmark against POSIX Lustre, a helper library has been developed which implements the DAOS API using POSIX file system concepts. DAOS Pools have been implemented as directories hosted on the distributed file system. Containers have been implemented as directories under the corresponding pool directories. Key-Value objects have been implemented as directories under the corresponding container directory. A key is implemented as a file in the Key-Value directory, named with the key name, and a value is stored as content in that key file. Array objects are implemented as files under the corresponding container directory, named with the object ID of the Array and containing the array data.

Following this design, every write of a weather field performed by the Field I/O benchmark using the helper library will usually involve: a) write of an Array file in a Container directory exclusive for every client process, b) check existence of a Key-Value directory in a Container directory shared with all processes in the client node, c) creation and write of a Key file in a Key-Value directory shared with all processes in the client node.

A field read will usually involve: a) check existence of a Key-Value directory in a Container directory shared with all client processes, b) open and read of a Key file in a Key-Value directory shared by all client processes, c) check existence of a Key-Value directory in a Container directory shared with all processes in the client node, d) open and read of a Key file in a Key-Value directory shared with all processes in the client node, e) open and read an Array file in a Container directory exclusive for the process.

Whereas the bandwidth metric used to quantify performance in IOR runs has been the one provided by IOR itself, referred to as *synchronous bandwidth* here, a custom bandwidth metric for non-synchronised applications is used in Field I/O runs, the *global timing bandwidth*. Both metrics are described in [3].

A. NEXTGenIO

The benchmarks we present have been conducted in NEXTGenIO [7], a research HPC system composed of 34

dual-socket nodes with Intel Xeon Cascade Lake processors. Each socket has six 256 GiB first-generation Intel's Optane Data Centre Persistent Memory Modules (DCPMMs) configured in AppDirect interleaved mode, although there are no NVMe devices. Each processor is connected with its own integrated network adapter to a low-latency OmniPath fabric. Each of these adapters has a maximum bandwidth of 12.5 GiB/s.

For the Lustre benchmarking, Lustre has been deployed on 8 storage nodes (providing 16 OSTs, one per socket), plus one node devoted to the metadata service. Both the OSTs and the MDTs used in the file system mount an ext4 file system on the SCM attached to their respective sockets, providing 1.5 TB of high-performance storage per OST and MDT.

To run the benchmarks against configurable amounts of Lustre storage nodes, Lustre pools have been set up with 1, 2, 4 and 8 nodes. Before running a test, a folder is created in the file system where all test files will be generated, and the `setstripe` command is used to bind that folder to the pool with the desired number of storage nodes.

DAOS deployments have been conducted separately in an ad-hoc basis, removing and re-deploying with the desired amount of storage nodes as needed. Each node used for DAOS storage deploys a single DAOS engine per socket, using the full ext4 file system on the Optane SCM for that socket, and has access to all the cores available on the associated processor. For instance, to compare to a two-node Lustre configuration (which uses two OST nodes and one MDT node, giving 4 OSTs overall), a two-node DAOS deployment is created and provisioned for the benchmark.

Up to 16 nodes were employed to execute the benchmark client processes using both sockets and network interfaces. SCM in the client nodes was not used and did not have any effect on I/O performance.

V. RESULTS

Performance results obtained from running the described benchmarks against Lustre and DAOS deployments in NEXTGenIO are discussed next, starting with an assessment of potential achievable performance with IOR, following with real achieved performance with Field I/O without and with contention between writer and reader applications, and concluding with an assessment of the impact of file or object size in such applications.

A. IOR results, potential performance

In this test set, the IOR benchmark has been run against different amounts of Lustre and DAOS storage server nodes with the intent to analyse maximum write and read performance a client application can potentially achieve, and to analyse the behaviour of the storage performance as more server nodes are added. IOR has been run in segments mode as described above, following access pattern A.

For each server node count the benchmark has been run using as many client nodes, twice as many and, where possible, four times as many, with the aim to effectively make

use of the available bandwidth theoretically provided by the server network interfaces. For each of these combinations, the benchmark has been run with 36, 48, 72 and 96 IOR processes per client node as these were found to result in the best performance in preliminary tests, for both Lustre and DAOS. Each run has been repeated 5 times to account for variability.

The segment count has been set to 100 as it was found to be the minimum segment count that results in reduced bandwidth variability. The segment size has been set to 1 MiB, to match the object or field size in the NWP use case. This segment configuration results in files or objects of 100 MiB in size being written and read during the benchmark runs.

The results are shown in Fig. 1. Each dot represents the mean synchronous bandwidth obtained with the best performing number of client nodes and IOR process count for the corresponding server node count. Hollow dots are used to indicate cases where it was only possible to use up to twice as many client nodes as server nodes, not four times as many as in the rest of the benchmarks.

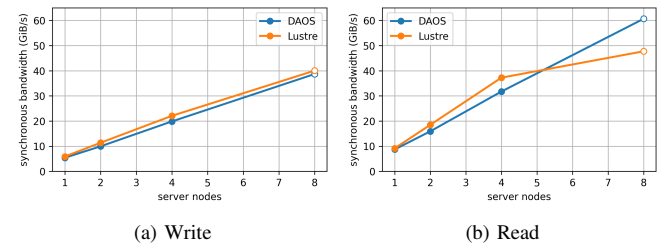


Fig. 1: Mean synchronous write and read bandwidth results for Lustre and DAOS for access pattern A with IOR in segments mode.

Lustre and DAOS perform similarly, resulting in comparable write and read benchmark bandwidths, with a similar scaling pattern. These results indicate that both storage servers and the benchmarks have been properly configured to exploit available storage and network resources, which has been further verified with monitoring of resource usage during preliminary test runs.

Slightly higher bandwidths are achieved overall with Lustre in this scenario, except in the read phase in the configuration with 8 server nodes, which was tested with only up to twice as many client nodes running the benchmark. The performance limitation in that configuration is explained by the fact that, in our test platform and with our configuration, four times as many client nodes as Lustre server nodes are required to exploit all available server interface bandwidth whereas, with DAOS, only twice as many client nodes are required. Results showing optimal client to server node ratio with Lustre have been omitted in favour of space. For DAOS, this ratio is addressed in [3].

Excluding this special case, write and read IOR bandwidths obtained with both Lustre and DAOS scale linearly. For Lustre, the benchmark bandwidth increases at a rate of approximately 6 GiB/s for write and 9 GiB/s for read per additional server node. For DAOS, the increase is of approximately 5 GiB/s for write and 7.5 GiB/s for read.

B. Field I/O results

1) *Application performance with DAOS vs. Lustre*: The Field I/O benchmark, in contrast to the IOR benchmark in segments mode, entails object-store-like I/O operations. The data elements are small, and writing or reading a single data object usually involves multiple I/O operations.

In this test set, Field I/O has been run with access patterns A and B following a similar strategy to the IOR tests above, using both Lustre and DAOS with the similar amounts of server and client nodes. In the runs here, a maximum of twice as many client nodes as server nodes have been employed for all configurations.

The benchmark has been run in its default *full* mode, and also in a mode which avoids use of DAOS containers called *no-containers* [3]. When run against Lustre, using the helper library to adapt Field I/O to POSIX file systems, every field write in the benchmark in no-containers mode will involve less metadata operations but the Array files will be written to a single directory shared by all client processes. Field reads will equally read Array files from that shared directory.

The object size has been set to 1 MiB, and the number of I/O iterations per process to 2000, to reduce the impact of potential parallel process start-up delays on bandwidth measurements. The chosen amounts of processes per client node, which have been found to result in best performance, have been 24 and 36 (slightly lower than the 36 and 48 found for DAOS). Each run has been repeated 5 times.

Results for pattern A and B are shown in Fig. 2 and Fig. 3, respectively. Note that, in both figures, Lustre results on the left side and DAOS results on the right side use a different y-axis scale.

Looking at DAOS results for pattern A, in Fig. 2 (c) and (d), we can see that Field I/O in no-containers mode performs better than the mode with containers. This is possibly due to inefficiencies in the use of DAOS containers, as discussed in [3]. The mode without containers scales linearly, and the application bandwidth increases at an approximate rate of 4.5 GiB/s write and 5.5 GiB/s read per additional server node.

Lustre results in Fig. 2 (a) show that Field I/O in no-containers mode, using the helper library to adapt to POSIX, performs poorly for write. This is likely due to performing all the Array file writes and reads in a single directory, as explained above, which suffers from Lustre contention or locking on that directory.

The full mode, which has the Array files distributed in several Container directories, performs better and reaches up to 7.5 GiB/s for write, but hits a limit at 4 server nodes. In benchmark runs with more server nodes, more client nodes are also employed, and every client node is set to execute an additional fixed amount of I/O operations. The limitation observed here is due to reaching to IOPs limits on the Lustre metadata server, which we have benchmarked at around 100 KIOPs using IOR. Measured IOPs rates for the Field I/O benchmark runs approach this limit where the scaling limit is reached. In IOR benchmarks Lustre can scale up to much larger bandwidths because there are less IOPs are involved.

Fig. 2 (b) shows that both Field I/O modes perform similarly for read, and they similarly hit a limit beyond 4 server nodes, again due to reaching maximum IOPs on the Lustre metadata server. We postulate that both modes provide similar performance due to the lack of locking/coherency required for read operations in Lustre.

For results in Fig. 3 for access pattern B, where writer applications are run concurrently with reader applications, the write and read bandwidths need to be combined for an approximate comparison with results with pattern A. With DAOS, Field I/O in no-containers mode performs remarkably well, with linear scaling and an aggregated bandwidth of approximately 50 GiB/s with 8 server nodes, higher than the separate bandwidths in pattern A.

With Lustre, the write and read performance behaviour of the full mode with access pattern B is similar to that observed in pattern A, with slightly better scaling beyond 4 nodes. The no-containers mode performs poorly not only for write but also for read, likely due to locking/coherency issues caused by concurrent writes.

In terms of achieved aggregate application bandwidth, Lustre with Field I/O pattern B in full mode reaches up to approximately 20 GiB/s with 8 server nodes, close to the read bandwidth obtained in pattern A, but far from the higher aggregate bandwidth obtained with DAOS with pattern B in any of the modes.

From the performance results for access pattern A, it can be observed that the best application bandwidths obtained with DAOS are in the same order of magnitude as those obtained with IOR, whereas with Lustre they are approximately a fifth of those obtained with IOR.

We have identified four factors that could contribute to this performance difference:

- Lustre is designed for large file I/O, and has a bottleneck in the metadata server when exposed to object-store-like applications.
- the Field I/O application, when run against Lustre, uses the helper library to adapt to POSIX, which implements a custom indexing mechanism with Key-Value directories and files. An implementation that made use of Lustre's own directory and file names for indexing would involve less file metadata operations and may perform better.
- Lustre needs four times as many client nodes as server nodes to saturate network bandwidth, but we have run the benchmarks with only twice as many.
- DAOS has been optimised for new memory technologies such as SCM and can bypass the block storage interface for some operations.

2) *Impact of object and file size*: Fig. 4 shows bandwidth results from runs of access pattern A with Field I/O in full mode with Lustre, and no-containers mode with DAOS. This time the benchmark has been run with varying object sizes of 1, 5, 10 and 20 MiB, to assess the impact of future NWP model resolution increases on I/O performance.

All tests have been run with a fixed configuration of 2 server nodes and 4 client nodes, and 100 I/O operations per client

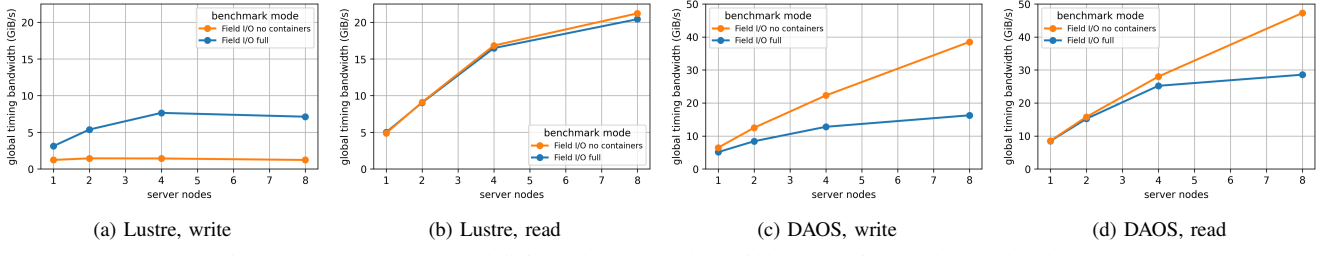


Fig. 2: Access pattern A, global timing write and read bandwidth results with the Field I/O benchmark.

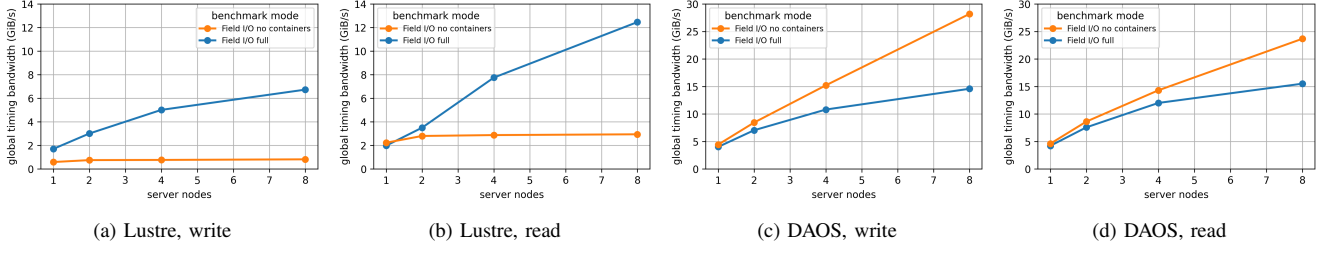


Fig. 3: Access pattern B, global timing write and read bandwidth results with the Field I/O benchmark.

process. Benchmarks are repeated 5 times, with the same client process counts as in previous Field I/O runs. The results for the 5 repetitions have been averaged, with the average bandwidth for the highest performing number of client processes per client node shown for each I/O size tested.

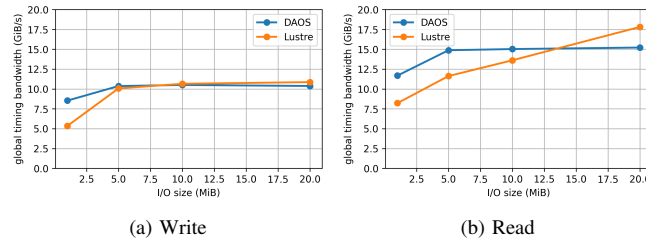


Fig. 4: Global timing write and read bandwidth results for access pattern A, with the Field I/O benchmark, using 2 server nodes and 4 client nodes.

It can be observed that increasing object or file size from 1 MiB to 5 MiB has a substantial benefit for both write and read, with both Lustre and DAOS. Beyond 5 MiB, the bandwidth stabilizes except in Lustre reading, where it continues to increase.

In this benchmark configuration, the bandwidths obtained with DAOS are higher than with Lustre when using an object or file size of 1 MiB. The two storage systems provide similar write bandwidths for larger object or file sizes. For read, DAOS performs better than Lustre with objects up to 10 MiB in size, and Lustre performs better than DAOS with larger files.

This test set could be repeated using access pattern B to investigate whether application bandwidth behaves differently as object or file size increase under write and read contention. Likewise, different server and client node configurations could be investigated as well.

VI. RELATED WORK

There has been research into object stores for high-performance I/O, including CEPH [9] and CORTX Motr [10]. However, these have so far seen less adoption for very intensive data creation or processing workloads in large-scale systems. DAOS is one of the first production-ready object storage technologies targeting HPC, with remarkable results in recent IO-500 benchmarks [11].

Science communities have investigated object stores for I/O operations [12], including using non-volatile memory [2]. These investigations have demonstrated the performance and functionality benefits, however they highlight direct porting relies on custom management of objects on storage mediums. Domain-agnostic object stores like DAOS simplify the use of NVM in production environments.

The work presented in this paper builds on previous research in the areas of exploiting object storage and NVM technologies for HPC I/O, extending understanding and knowledge on the impact of the object store approach versus the benefits of using high-performance I/O hardware. It also extends community understanding of how DAOS and Lustre perform under workload patterns common in many applications.

VII. CONCLUSIONS

Through our benchmarking and evaluation work we have demonstrated that Lustre and DAOS, using the same underlying storage hardware, can provide similar performance for large-scale bulk data operations, such as those the IOR benchmark mimics and many applications have been tuned to utilise. However, when moving to object-store-like I/O operations and workflows, DAOS shows significant performance benefits. We conclude that DAOS is a strong target for a future storage platform as it demonstrates comparative performance with traditional file systems whilst enabling object-store functionality at high-performance.

The access patterns produced with the Field I/O benchmark are not particularly specific to the NWP use case or bound to any particular file format, and therefore the findings are applicable to other use cases repeatedly writing and/or reading any objects or files with sizes in the order of 1 to 10 MiB from several processes and nodes.

The results suggest that the good performance results obtained with DAOS in the object-store-like NWP use case are not purely due to the use of high-performance storage hardware such as SCM, but also due to the design characteristics of an object store and their implementation in DAOS.

Nevertheless, performance and scalability of Lustre in this scenario should be further explored and validated by benchmarking with larger amounts of server and client nodes, and possibly implementing additional optimisations in the benchmarks to better exploit file system capabilities.

ACKNOWLEDGMENT

The work presented in this paper has been produced in the context of the European Union’s Destination Earth Initiative and relates to tasks entrusted by the European Union to the European Centre for Medium-Range Weather Forecasts implementing part of this Initiative with funding by the European Union (cost center DE3100, code 3320). Views and opinions expressed are those of the author(s) only and do not necessarily reflect those of the European Union or the European Commission. Neither the European Union nor the European Commission can be held responsible for them. This work was also supported by EPSRC, grant EP/T028351/1.

The NEXTGenIO system was funded by the European Union’s Horizon 2020 Research and Innovation program under Grant Agreement no. 671951, and supported by EPCC, The University of Edinburgh.

REFERENCES

- [1] G. Lockwood, "What's so bad about POSIX I/O?". The Next Platform 2017. <https://www.nextplatform.com/2017/09/11/whats-bad-posix-io/>
- [2] S. Smart, T. Quintino, and B. Raoult. "A High-Performance Distributed Object-Store for Exascale Numerical Weather Prediction and Climate". In Proceedings of the Platform for Advanced Scientific Computing Conference (PASC '19). Association for Computing Machinery, New York, NY, USA, Article 16, 1–11. DOI:<https://doi.org/10.1145/3324989.3325726>
- [3] N. Manubens, T. Quintino, S. D. Smart, E. Danovaro, and A. Jackson, "DAOS as HPC Storage, a view from Numerical Weather Prediction", arXiv e-prints, <https://arxiv.org/abs/2208.06752>, 2022.
- [4] Z. Liang, J. Lombardi, M. Chaarawi, M. Hennecke, "DAOS: A Scale-Out High Performance Storage Stack for Storage Class Memory" In: Panda, D. (eds) Supercomputing Frontiers. SCFA 2020. Lecture Notes in Computer Science(), vol 12082. Springer, Cham. DOI:https://doi.org/10.1007/978-3-030-48842-0_3
- [5] P. Braam "The Lustre Storage Architecture" 2019 arXiv. DOI:<https://doi.org/10.48550/arXiv.1903.01955>
- [6] "HPC IO Benchmark Repository", (2022), GitHub repository, <https://github.com/hpc/ior>
- [7] A. Jackson, M. Weiland, M. Parsons, and B. Homölle. "An Architecture for High Performance Computing and Data Systems Using Byte-Addressable Persistent Memory". In High Performance Computing: ISC High Performance 2019 International Workshops, Frankfurt, Germany, June 16-20, 2019. Springer-Verlag, Berlin, Heidelberg, 258–274. DOI:https://doi.org/10.1007/978-3-030-34356-9_21
- [8] M. Weiland, H. Brunst, T. Quintino, et al. "An early evaluation of Intel's optane DC persistent memory module and its impact on high-performance scientific applications". In Proceedings of the International Conference for High Performance Computing, Networking, Storage and Analysis . Association for Computing Machinery, New York, NY, USA, Article 76, 1–19. DOI:<https://doi.org/10.1145/3295500.3356159>
- [9] K. Jeong, C. Duffy, J. -S. Kim and J. Lee, "Optimizing the Ceph Distributed File System for High Performance Computing," 2019 27th Euromicro International Conference on Parallel, Distributed and Network-Based Processing (PDP), 2019, pp. 446-451, DOI: 10.1109/EM-PDP.2019.8671563.
- [10] S. Narasimhamurthy, N. Danilov, S. Wu, G. Umanesan, S. Chien, S. Rivas-Gomez, I. Peng, E. Laure, S. Witt, D. Pleiter, and S. Markidis. "The SAGE project: a storage centric approach for exascale computing: invited paper". In Proceedings of the 15th ACM International Conference on Computing Frontiers (CF '18). Association for Computing Machinery, New York, NY, USA, 287–292. DOI:<https://doi.org/10.1145/3203217.3205341>
- [11] A. Dilger, D. Hildebrand, J. Kunkel, J. Lofstead, and G. Markomanolis, "IO500 10 node list International Supercomputing 2021, June 2021, [online] Available:<https://doi.org/10.5281/zenodo.5171694>
- [12] S. Smart, T. Quintino, and B. Raoult "A Scalable Object Store for Meteorological and Climate Data". In Proceedings of the Platform for Advanced Scientific Computing Conference (PASC '17). Association for Computing Machinery, New York, NY, USA, Article 13, 1–8. DOI:<https://doi.org/10.1145/3093172.3093238>
- [13] MA. Vef, N. Moti, T. Süß et al. "GekkoFS — A Temporary Burst Buffer File System for HPC Applications". J. Comput. Sci. Technol. 35, 72–91 (2020). <https://doi.org/10.1007/s11390-020-9797-6>
- [14] O. Tatebe, K. Obata, K. Hiraga, and H. Ohtsuji. 2022. "CHFS: Parallel Consistent Hashing File System for Node-local Persistent Memory". In International Conference on High Performance Computing in Asia-Pacific Region (HPCAsia2022). Association for Computing Machinery, New York, NY, USA, 115–124. DOI:<https://doi.org/10.1145/3492805.3492807>
- [15] A. Miranda, A. Jackson, T. Tocci, I. Panourgias and R. Nou, "NORNS: Extending Slurm to Support Data-Driven Workflows through Asynchronous Data Staging" 2019 IEEE International Conference on Cluster Computing (CLUSTER), 2019, pp. 1-12, doi: 10.1109/CLUSTER.2019.8891014.

Appendix B – DAOS as HPC Storage: a View from Numerical Weather Prediction

DAOS as HPC Storage: a View From Numerical Weather Prediction

Nicolau Manubens

European Centre for Medium-Range Weather Forecasts, Germany
nicolau.manubens@ecmwf.int

Tiago Quintino

European Centre for Medium-Range Weather Forecasts, United Kingdom
tiago.quintino@ecmwf.int

Simon D. Smart

European Centre for Medium-Range Weather Forecasts, United Kingdom
simon.smart@ecmwf.int

Emanuele Danovaro

European Centre for Medium-Range Weather Forecasts, United Kingdom
emanuele.danovaro@ecmwf.int

Adrian Jackson

The University of Edinburgh, United Kingdom
a.jackson@epcc.ed.ac.uk

Abstract—Object storage solutions potentially address long-standing performance issues with POSIX file systems for certain I/O workloads, and new storage technologies offer promising performance characteristics for data-intensive use cases.

In this work, we present a preliminary assessment of Intel's Distributed Asynchronous Object Store (DAOS), an emerging high-performance object store, in conjunction with non-volatile storage and evaluate its potential use for HPC storage. We demonstrate DAOS can provide the required performance, with bandwidth scaling linearly with additional DAOS server nodes in most cases, although choices in configuration and application design can impact achievable bandwidth. We describe a new I/O benchmark and associated metrics that address object storage performance from application-derived workloads.

Index Terms—scalable object storage, next-generation I/O, storage class memory, non-volatile memory, numerical weather prediction, DAOS

I. INTRODUCTION

Storage performance is increasingly important for large-scale applications. This is coupled with the rise in application categories where ingestion or production of large amounts of data is common, machine learning being an obvious example. As systems scale to ever large sizes, and a subset of applications require ever large amounts of I/O bandwidth or metadata performance, there is a significant challenge to improve the capabilities of the data storage technologies being utilised for I/O operations.

Object stores, on one hand, are a candidate to address long-standing scalability issues in POSIX file systems for large-scale parallel I/O applications where an intensive use of metadata operations is required, for example if operating with small-sized data files, of the order of KiBs up to a few MiBs. These scalability issues stem from constraints imposed by POSIX file system semantics, namely metadata prescriptiveness (per-file creation date, last-access date, permissions, etc.), and excessive consistency assurance [1]. Object stores provide alternative, less restrictive, semantics to POSIX file systems and, since they have been designed from scratch, unbound from existing file system implementations or standards,

many of them have been able to follow radically different approaches.

Non-volatile memory (NVM), on the other hand, is a form of memory that offers a promising trade-off in data-intensive use-cases, with the potential to be used as NVRAM (also known as storage class memory, SCM) where performance and functionality is similar (albeit slower) to DRAM, and also heavily used in high-performance storage devices, such as NVMe drives.

The Distributed Asynchronous Object Store (DAOS) [2] is an emerging high-performance object store which features full user-space operation; use of a RAFT-based consensus algorithm for efficient, distributed, transactional indexing; and efficient byte-addressable access to NVM devices. It is being developed by Intel, and it has gained traction over the past years after consistently scoring leading positions in the I/O 500 benchmark [3].

In this paper we investigate exploiting such technologies to provide I/O functionality for applications, considering generic benchmarking on one side to evaluate what can be achieved, but also with a focus on large-scale Numerical Weather Prediction (NWP) on the other side, to evaluate whether these technologies could be a good replacement for the current HPC storage system at the European Centre for Medium-Range Weather Forecasts (ECMWF), and potentially for other applications, users, and centres.

We present a preliminary suitability and performance assessment of DAOS in conjunction with non-volatile storage hardware, conducted as a proof-of-concept, decoupled from the complex software stack currently used at the ECMWF, but specially designed to mimic the I/O characteristics. A research HPC system that is composed of nodes with 3 TiB of Intel's Optane Data Centre Persistent Memory Modules (DCPMMs) has been employed to run benchmarks and measure performance, with a number of software approaches investigated, including using the DAOS C API directly.

II. RELATED MATERIAL

There has been recent research in object store developments and deployments for high-performance I/O, including CEPH [4] and CORTX Motr [5]. However, these have so far seen less adoption for very intensive data creation or processing workloads in large-scale HPCs. DAOS, which is part of what we evaluate in this paper, is one of the first production-ready object storage technologies targeting HPC, with excellent results in recent IO-500 benchmarks [6].

The meteorological community has investigated using custom object stores for I/O operations [7], including evaluating such object store approaches using NVM technologies [8]. These investigations have demonstrated the performance and functionality benefits NVM and object storage can provide for NWP simulation I/O and data processing. When ported directly to SCM, these object stores have achieved up to 70 GB/s write bandwidth when used with SCM on a reduced set of I/O server nodes, providing confidence that SCM can be used to accelerate object storage technologies. However, direct porting relies on custom management of objects in NVM, which entails a high development and maintenance overhead and potentially limited usability for those adopting such approaches. Domain-agnostic NVM-capable object stores like DAOS simplify the use of NVM in production environments and enable implementation of high-performance user-facing tools, including domain-specific object stores, file system interfaces, programming language interfaces, and administrative tools.

Others have explored creating ad-hoc file systems on compute nodes with SCM or NVMe devices to exploit the local storage whilst providing the familiar file system interface applications are generally designed to use [9] [10] [6]. Further work has been undertaken to integrate such file systems with batch schedulers and other tools [11]. These all demonstrate the potential benefits to exploiting in-node storage for HPC applications, and the benefits to localising I/O compared to traditional parallel file systems. However, they do not provide object-centric interfaces that have been demonstrated to be beneficial for both functionality and performance for application domains such as NWP. They are still restricted to providing I/O through block-based file system approaches, which place limitations on achievable I/O performance for small I/O operations or for searching and extracting data within a large data set.

Very recent work by the authors has investigated the generic I/O performance of DAOS and Lustre on non-volatile memory systems, and has demonstrated that Lustre and DAOS can both achieve excellent I/O performance using high-performance storage hardware. However, Lustre struggles to handle the large volumes of metadata operations required to achieve high I/O bandwidth under intensive I/O workloads with small data transfer sizes. This highlights some of the potential benefits that object storage software can provide as opposed to traditional HPC file systems when looking at object-like I/O operations [12].

The work presented in this paper builds on previous research in the areas of exploiting object storage and NVM technologies for HPC I/O. However, we are looking at the requirements of production deployment, and performance in a contended and continuous system environment, with a focus on extreme-scale I/O performance. Our research introduces a new framework for benchmarking of high-performance object stores for NWP, and significantly advances the understanding of the place of DAOS in the storage landscape for HPC systems as well as explores the features, configurations, and challenges such an object store presents for large-scale parallel I/O and for the design of I/O functionality for such applications.

III. DAOS

The Distributed Asynchronous Object Store (DAOS) is an open-source high-performance object store designed for massively distributed NVM. It provides a low-level key-value storage interface on top of which other higher-level APIs, also provided by DAOS, are built. Features include transactional non-blocking I/O, fine-grained I/O operations with zero-copy I/O to SCM, end-to-end data integrity, and advanced data protection. The OpenFabrics Interfaces (OFI) library is used for low-latency communications over a wide range of network back-ends.

DAOS is deployable as a set of I/O processes or engines, generally one per physical socket in a server node, each managing access to NVM devices associated with the socket. Graphical examples of how engines, storage devices and network connections can be arranged in a DAOS system, can be found at [13].

An engine partitions the storage it manages into targets to optimize concurrency, each target being managed and exported by a dedicated group of threads. DAOS allows reserving space distributed across targets in *pools*, a form of virtual storage. A pool can serve multiple transactional object stores called *containers*, each with their own address space and transaction history.

Upon creation, objects are assigned a 128-bit unique identifier, of which 96 bits are user-managed. Objects can be configured for replication and striping across pool targets by specifying their *object class*. An object configured with striping is stored by parts, distributed across targets, enabling concurrent access analogous to Lustre file striping.

IV. WEATHER FIELD I/O

NWP is used as an exemplar application as it is a HPC use case that has significant I/O requirements, that represent production I/O workloads, and has varied I/O patterns, enabling us to evaluate a range of I/O performance implications from these varied approaches. Additionally, due to the typically small size of data units being accessed, the application benefits from an object-like I/O approach to enable both efficient I/O operations from the production applications and easy data post-processing and querying for forecast generation, research, and analysis.

At the ECMWF, our exemplar weather forecasting centre, the NWP model is run 4 times a day in 1-hour time-critical

windows using 2500 compute nodes. During each of these windows, 40 TiB of weather forecast data are generated and written by the model into the HPC storage system, and immediately read by post-processing tasks to generate derived products.

The data is generated by all model processes in a distributed manner, and it is sent through the low-latency interconnect to I/O servers, where it is aggregated. For the duration of a simulation, approximately 250 additional HPC nodes are devoted to running I/O server instances. After aggregation and data encoding, these servers forward the data to the HPC storage system.

Another 250 additional HPC nodes are devoted to running the post-processing tasks, after each step of the simulation, which read the generated output from the storage to then create derived data products.

In the described context, the I/O servers do not interact directly with the file system API. They do so via an intermediate domain-specific object store, the FDB5 [8], which is entirely software-defined. Such an object store saves any client software from implementing custom management of concurrent storage and indexing of weather fields in the file system, and enables object semantics for weather field access via a concise API.

The weather fields are the unit of data output by the model, and contain data for 2-dimensional slices covering the whole Earth surface for a given weather variable at a given time. They currently range between 1 and 5 MiB in size. Upon storage of a field, an indexing key must be provided together with the field data. A key is a set of field-specific key-value pairs that uniquely identify a field. Upon retrieval, the corresponding key has to be provided, and the field data is returned.

A. Challenges

With prospects of increasing simulation resolution and diversity of parameters modelled and output, it is expected shortly the volume of forecast data generated will reach approximately 180 TiB per time-critical window, and up to 700 TiB per time-critical window in the near future.

Therefore, the pressure on the HPC storage system will increase significantly, requiring higher throughput to maintain the time-critical and operational aspects of the service. Exploration and adoption of novel storage technologies will be key for a satisfactory implementation of the upcoming resolution increases.

B. Field I/O benchmark and object functionality

A pair of C functions have been developed to perform writing and reading of weather fields to and from a DAOS object store, using the DAOS C API. They have been developed based on the design of FDB5, the domain-specific object store already employed within the ECMWF, so that the same type of operations as in operational workflows is carried out. The diagram in Fig. 1 shows the different DAOS concepts and APIs involved in the field I/O functions.

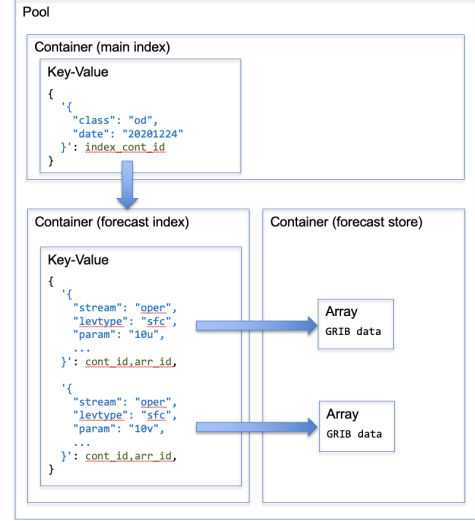


Fig. 1: Diagram of DAOS concepts and APIs involved in the weather field I/O functions developed.

At the top level a DAOS Key-Value object, in its own container, acts as a main index allowing location of the data belonging to a same model run or *forecast*. That index maps the most-significant part of the key identifying a field (e.g. ““class”: ‘od’, ‘date’: ‘20201224’”) to another DAOS container, at the lower layer. In that container is another Key-Value object that acts as a forecast index, enabling location of the data of the fields comprising a forecast. That index maps the least-significant part of the field key to a further DAOS container and a DAOS Array in that container where the data of the indexed weather field is stored.

How the developed functions perform field writes and reads using these concepts and objects is described, in a very simplified way, in Algorithms 1 and 2, respectively.

Algorithm 1: field write

```

Inputs: field key, field data
open main container
query most significant part of field key from Key-Value
if not found then
    create forecast index and store containers
    register forecast index container in main Key-Value
end
open forecast store container
write field data into new Array
open index container
update forecast Key-Value
  
```

When the field write function is called, with the binary field and its key as parameters, the most-significant part of the key is retrieved from the main Key-Value. If it exists, the indexed references to the forecast containers are retrieved and the containers are opened. If they do not exist, creation of a new pair of forecast index and store containers is attempted, with container IDs computed as md5 sums of the most-

Algorithm 2: field read

Inputs: field key
Outputs: field data
 open main container
 query most significant part of field key from Key-Value
if *not found* **then**
 | fail
end
 open forecast index container
 query least significant part of field key from Key-Value
if *not found* **then**
 | fail
end
 open store container
 read field data from Array

significant part of the key so that any concurrent processes attempting creation of the same pair of containers will avoid creation of inaccessible containers. Immediately after creation, the forecast containers are opened and the ID of the forecast store container is stored in a special entry in a newly created Key-Value in the forecast index container. Next, a reference to the forecast index container is indexed in the main Key-Value, using the most-significant part of the field key as key. Then, the binary field is written into an Array in the forecast store container, with a new object ID, and a reference to it is indexed in the forecast index Key-Value, using the least-significant part of the field key as key.

Note that when a field is written with a key that already exists in the overall store, a new Array object is created and indexed, and the previously existing one is de-referenced. No read-modify-write is performed upon re-write, and the functions do not delete de-referenced objects by design.

When the field read function is called, with the key of a field as the parameter, the most-significant part of the key is looked up in the main Key-Value. If it exists, the indexed reference to the forecast containers are retrieved and the containers are opened. Next, the least-significant part of the key is retrieved from in the forecast index Key-Value. If that is present, the indexed references to the forecast store container and Array are retrieved. Finally, the forecast store container is opened and the Array is read.

For the NWP applications we are investigating, the separation of the different Key-Values and Arrays in different containers is motivated by the need to avoid contention for the same container or indexing Key-Value object during intensive I/O workloads. This separation also allows the implementation of the different parts of the object store with different storage back-ends or on different systems.

V. METHODOLOGY

To assess the performance of DAOS, different I/O workloads have been generated and run in a research HPC system using the well-known IOR [14] benchmark and the field I/O functions. The performance of DAOS and the benchmarks

in the HPC has been analysed based on different throughput definitions discussed in subsequent sections.

A. IOR

IOR is a community-developed I/O benchmark which relies on MPI to run and coordinate parallel processes performing I/O operations against a storage system. It includes back-ends to operate with various popular storage systems, including DAOS.

IOR has been employed in this analysis with the intent to measure the throughput an application could achieve if it were programmed to operate in a traditional parallel, bulk synchronous I/O manner. That is, running a number of parallel client processes which use the high-level DAOS Array API to write or read data from a DAOS object store, all of them starting each I/O operation simultaneously, and waiting for each other to finish.

For the tests in this analysis, the IOR benchmark has been run in *segments* mode. IOR is invoked with a set of parameter values which instruct each client process to perform a single I/O operation, transferring its full data size. This is with the intent to assess the performance of a hypothetical optimised parallel application which is designed to minimise the number of I/O operations interacting with the storage. Processes in such applications issue a single transfer operation comprising all the data parts they manage, in contrast to an equivalent, non-optimised application where processes issue a transfer or even an open and a close operation for each data part.

Unless the storage is not optimised to handle large transfers or objects, this benchmark mode should give an idea of what is the maximum, ideal throughput the storage can deliver. This mode has been implemented by setting both the *-b* and *-t* IOR parameters to the size of each data part managed by each process, and *-s* to the number of data parts managed by each process. The *-i* parameter has been set to 1, and the *-F* flag (file per process) has been enabled. Each process performs the following during the benchmark execution: a) initial barrier, b) pre-I/O barrier, c) object create/open of size $t * s$ bytes, d) transfer (write or read) of $t * s$ bytes, e) object close, f) post-I/O barrier, g) post-I/O processing and logging, h) final barrier.

B. Field I/O

To gain insight on how DAOS performs in the previously outlined NWP I/O server use case, we use our custom field I/O benchmark, which mimics operational NWP I/O workflows. Here, parallel processes perform a sequence of field I/O operations using the functions previously described in the Weather field I/O section, with no synchronisation. Pool and container connections in a process are cached once initialised.

In contrast to the IOR benchmark in segments mode, the processes in this benchmark perform multiple I/O operations of smaller sizes, one for each data part. Each field I/O operation involves an Array open, transfer and close, and usually involves a few operations with Key-Value objects. We also do not enforce I/O synchronisation, as in IOR.

Fig. 2 shows a schematic representation of the processes and sequence of field I/O operations involved in an example benchmark run.

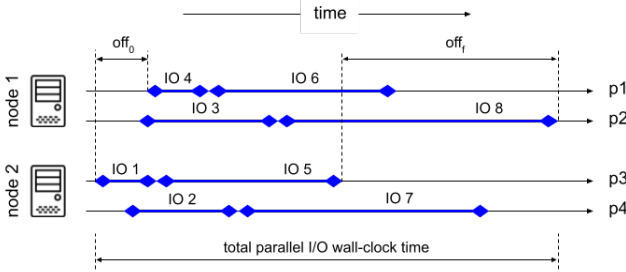


Fig. 2: Processes and I/O operations involved in an example Field I/O benchmark run.

The field I/O benchmark has been configured in three different modes for this evaluation:

- **full**: the fully-functional field I/O functions are used as described in Weather field I/O.
- **no containers**: the use of container layers in the field I/O functions is disabled with the intent to analyse any potential issues in the use of container layers. The functions create and operate with all DAOS Key-Values and Array objects in the main container.
- **no index**: the use of indexing Key-Value objects and container layers in the field I/O functions are disabled with the intent to compare with results from other benchmark modes and assess the overhead of field indexing. To preserve the ability to locate previously written fields, the field I/O functions map the field identifiers to DAOS Array object IDs by calculating a md5 sum of the identifiers. The arrays are stored and read directly from the main container.

By default, in modes with indexing enabled, each parallel process writes and reads fields indexed in its own forecast index Key-Value and therefore there should be little contention for the different objects within DAOS. The benchmark, however, can be configured to have a single shared forecast index Key-Value among all processes, inducing high contention on that Key-Value object.

The Field I/O benchmark is maintained and documented in a publicly accessible open-source Git repository [15].

C. Access patterns

The IOR and field I/O benchmarks, in each of their modes, can be further adjusted and employed as part of larger workflows to generate specific combinations of I/O workload of interest, hereafter referred to as *access patterns*. Two access patterns used in this analysis are described next.

- **A (unique writes then unique reads)**: This access pattern has two phases. Each client process performs a number of writes to new objects in the storage (single transfer to single object for IOR in segments mode). Once all writer processes have finished, a second phase begins, where another process set of the same size and distribution is executed performing an equivalent number of reads from the objects generated in

the write phase. The access pattern ends when all second-phase processes terminate.

This access pattern is designed to provide a situation where there is no contention for same fields and when there is only either write or read workloads in operation at any one time, analogous to a single large-scale application utilising the object store, or to systems where the predominate I/O patterns are only one I/O phase (writing or reading).

In this access pattern, when run with the IOR benchmark, there is no contention in Array writes or reads, as each process accesses its own Array independently from others. When run with the field I/O benchmark in any of its modes with a forecast index Key-Value per process, there is no contention in any of the forecast index or store objects, as each process writes or reads its own Key-Value and Arrays sequentially.

- **B (repeated writes while repeated reads)**: This access pattern starts with a setup phase to populate the storage with data, where half of the client processes (and thereby half the client nodes) perform a single write to a new object. Once all writer processes have terminated, the main phase begins. Half the client processes perform a number of re-writes to designated objects; simultaneously, the other half of the client processes perform the same number of reads from their designated objects. The access pattern ends when all main-phase processes terminate.

This access pattern has only been implemented with the field I/O benchmark as IOR does not allow coordination between a set of writers and a set of readers. It aims to mimic situations where one or more large-scale applications issue simultaneous writes and reads of the same objects or fields. This is the equivalent of the I/O behaviour of actual NWP and product generation workloads, or to systems with mixed applications of varying I/O workloads.

In this access pattern, when run with Field I/O in *full* or *no containers* modes with a forecast index Key-Value per process, there is no contention in Array writes or reads, but there is some contention in each forecast index Key-Value between reader and writer processes on the same object. When run in *no index* mode, the same degree of contention occurs at the Array level.

D. Parameter variation

The access patterns presented can be configured not only to run with the different benchmarks and modes, but also to use a range of parameter values. The following list summarises these parameters and the values tested in this paper.

- **number of DAOS server nodes**: 1, 2, 4, 8, 10, 12, 14, 16
- **number of client nodes**: 0.5x, 1x, 2x and 4x the amount of server nodes
- **number of processes per client node**: 1, 3, 4, 6, 8, 9, 12, 18, 24, 36, 48, 72, 96
- **number of iterations or data parts per proc.**: 100, 2000
- **object class**: S1 (no striping), S2 (striping across two targets) and SX (striping across all targets)
- **object size**: 1, 5, 10, 20 and 50 MiB

E. Throughput definitions

To quantify, compare, and discuss the performance delivered by the storage, a set of metric and throughput definitions are introduced here and applied in the Results section. During execution, the IOR and Field I/O benchmarks report timestamps for various events. Each timestamp is reported together with an identifier of the client node, process and iteration or I/O they belong to, as well as the event name. We record timestamps for: execution start, I/O start, object open start, object open end, data write/read start, data write/read end, object close start, object close end, I/O end, and execution end.

In Field I/O, *I/O start* is recorded immediately before calling the field write or read functions. In IOR it is equivalent to *object open start*.

The following derived metrics are calculated where relevant from the timestamps.

- **single iteration parallel I/O wall-clock time**: calculated as the maximum I/O end minus the minimum I/O start for a given I/O iteration across all parallel processes. This metric is only valid in benchmarks where I/O is synchronised.
- **total parallel I/O wall-clock time**: calculated as the maximum I/O end of the last I/O iteration minus the minimum I/O start of the first I/O iteration across all parallel processes. This metric is calculated separately for the write and read phases of the described access patterns, and is valid for synchronised and non-synchronised benchmarks. In the example in Fig. 2, the metric would be calculated as $t_f(IO_8) - t_0(IO_1)$.

With these derived metrics, the throughput is calculated in two different ways, outlined below. Information such as I/O size and number of parallel processes is available at analysis time and is used as input for the calculation of these throughputs.

- **synchronous bandwidth**: the sum of the sizes of the I/O operations for an iteration across all parallel processes, divided by the single iteration parallel I/O wall-clock time. The averaged result across all iterations is the synchronous bandwidth, only applicable to synchronous benchmarks (i.e. IOR).

$$\text{sync. bw.} = \frac{1}{n} * \sum_{i=1}^n \frac{\sum_{j=1}^m \text{size}(IO_{ij})}{\max_j\{t_f(IO_{ij})\} - \min_j\{t_0(IO_{ij})\}}$$

$$n = \#\text{iterations}, m = \#\text{processes}$$

IOR internally calculates the synchronous bandwidth following this definition.

- **global timing bandwidth**: the sum of the I/O sizes across all I/O operations in the workload and divided by the total parallel I/O wall-clock time.

$$\text{global timing bw.} = \frac{\sum_{i=1}^n \text{size}(IO_i)}{t_f(IO_n) - t_0(IO_1)}$$

$$n = \#\text{I/O operations}$$

It is calculated separately for the write and read phases of the described access patterns. The value of this bandwidth is

inversely proportional to global parallel I/O wall-clock time. If a benchmark performs any work between I/O iterations this will impact the global timing bandwidth measure as it will increase the total parallel I/O wall-clock time.

F. Asynchronous I/O distribution

When running patterns A or B with Field I/O, the distribution of I/O operations should be analysed and taken into account at benchmark configuration time to ensure the resulting distribution is representative of the desired access pattern. To characterise the overall distribution of I/Os, the following offsets can be measured for a benchmark run:

- **initial I/O offset** (off_0): measured separately for the write and read phases of an access pattern, calculated as the last first-iteration I/O start time minus the first I/O start time across all processes, as shown in Fig. 2.
- **final I/O offset** (off_f): measured separately for the write and read phases of an access pattern, calculated as the last I/O end time minus the first last-iteration I/O end time.
- **phase start offset** (po_0): calculated as the absolute value of the difference between the first I/O start time of the write and read phases, only applicable to access pattern B.
- **phase end offset** (po_f): calculated as the absolute value of the difference between the last I/O end time of the write and read phases, only applicable to access pattern B.

For the most accurate results, we should ensure off_0 and po_0 are not large relative to the total parallel I/O wall-clock time by adjusting access pattern configuration.

off_f may account for a large portion of the total parallel I/O wall-clock time as, for example, the storage may process operations from the various parallel processes in an unbalanced manner. Similarly, po_f may account for a large portion of the total duration of I/O (write and read) of a pattern B run, for example, as the storage may process write and read operations in an unbalanced manner.

Outside these offset time spans, there are as many in-flight I/O operations as parallel processes at any point in time during the benchmark run.

VI. RESULTS

Results obtained are discussed next, including selected system and DAOS configurations, and bandwidth calculations for the different benchmarks and access patterns.

A. Experiment environment

The benchmarks we present have been conducted using the NEXTGenIO system [16], which is a research HPC system composed of dual-socket nodes with Intel Xeon Cascade Lake processors. Each socket has six 256 GiB first-generation Intel's Optane DCPMMs configured in AppDirect interleaved mode. Each processor is connected with its own network adapter to a low-latency OmniPath fabric. Each of these adapters has a maximum bandwidth of 12.5 GiB/s. The fabric is configured in dual-rail mode, that is, two separate OmniPath switches interconnect first-socket adapters and second-socket adapters separately, respectively.

The HPC system nodes use CentOS7 as the operating system, with DAOS v2.0.1. For the majority of the tests, two DAOS engines have been deployed in each node used as DAOS server, one on each socket using the associated fabric interface and interleaved SCM devices, with 12 targets per engine.

1) *Fabric provider*: The OFI PSM2 fabric provider implements Remote Direct Memory Access (RDMA) over an Omni-Path fabric, of particular interest in the HPC system employed. However, use of PSM2 in DAOS is not yet production-ready, impeding dual-engine per node, dual-rail DAOS deployments.

Due to this, OFI's TCP provider has been used for the majority of the test runs in the analysis. TCP's use of operating system sockets instead of RDMA has an impact in transfer bandwidth between nodes, which is further detailed in IOR results and in the High-performance network section.

2) *Process pinning*: The process pinning strategy has been found to have substantial impact in I/O performance, with up to 50% reduction in performance when DAOS server engines were not optimally pinned across processors in a node, and up to 90% reduction when benchmark client processes were not optimally pinned. For best performance, each DAOS engine has been configured to pin engine processes to a single socket, and target the attached fabric interface. This has been achieved via the `pinned numa node` DAOS server configuration item. On the client side, processes have been distributed in a balanced way across sockets in each client node.

B. IOR results

In this test set, the IOR benchmark in segments mode has been run (access pattern A) with the intent to analyse the maximum write and read performance a client application can achieve.

In our initial experiment we deployed DAOS on a single server node, with one or two engines, each running on a socket of the node and using the corresponding fabric adapter (`ib0` and `ib1`, respectively). The IOR client processes have been pinned to one or two sockets (or interfaces) in one or two client nodes, as detailed in Table I. The segment count has been set to 100.

A segment size of 1 MiB has been motivated by the current weather field size at the exemplar weather centre. This segment size results in objects of 100 MiB in size being written or read by IOR. Striping has been disabled (`OC_S1`) to avoid complexity in network behaviour for the initial tests. The number of processes per client node has been set to 24, 48, 72 and 96 after verifying with several other IOR tests that process counts in that range usually resulted in higher benchmark bandwidths. Each test has been repeated 9 times for the range of client processes, and the maximum synchronous bandwidth obtained among the 36 repetitions is reported in Table I for both the write and read phases.

With a single server engine using one interface and a set of client processes using a single client interface on the first socket of the corresponding nodes (first row of the table; 1 client node), the maximum write bandwidth reaches 3 GiB/s

TABLE I: Access Pattern A, IOR Segments, 1 Server Node

server nodes	engines per server node	ifaces per client node	bandwidth (GiB/s)	
			1 client node	2 client nodes
1	1 (ib0)	1 (ib0)	3.0w / 4.2r	2.6w / 6.2r
1	1 (ib0)	2	3.0w / 7.4r	2.9w / 7.7r
1	2	2	5.5w / 7.5r	5.5w / 9.5r

and, for read, 4.2 GiB/s. When using multiple client sockets and interfaces against a single server engine on the first socket and interface (last column of first row and second row), the maximum write bandwidth still saturates at 3 GiB/s whereas the maximum read bandwidth reaches up to 7.7 GiB/s.

For the test in the last row of the table, with two DAOS engines deployed in a server node, and using both interfaces on a single client node (last row; 1 client node), the maximum write bandwidth reaches up to 5.5 GiB/s. For read, the maximum bandwidth remains at 7.5 GiB/s on a single client node, whereas it reaches up to 9.5 GiB/s with two client nodes (a total of 4 network interfaces). This indicates that more client interfaces than server interfaces are necessary to saturate server interface bandwidth for read, which is likely to be the deployment configuration of DAOS for production systems.

To further analyse the bandwidth increase when more engines and interfaces are employed, the same access pattern with identical parameters has been run with different numbers of server and client nodes, using both processors and network interfaces on each node. Using as many client nodes as server nodes has been pursued for all tested configurations to effectively make use of the available bandwidth theoretically provided by the server interfaces, and, where possible, configurations with twice or four times as many client nodes have been tested to explore if, as suggested by results in Table I, these result in higher bandwidths. A few special configurations have also been tested, for instance with less client nodes than server nodes (e.g. 2 server nodes and 1 client node), or with slightly less than double the server nodes (e.g. 10 server nodes and 18 client nodes) to explore bandwidth behaviour in unbalanced configurations. Fig. 3 shows, for each combination of server and client node count, the mean synchronous bandwidth obtained across all repetitions for the best performing number of client processes per client node.

For a single dual-engine server, the bandwidth achieved per engine is of approximately 2.5 GiB/s for write and 5 GiB/s for read. As the number of servers increases, the bandwidths increase linearly at a rate of approximately 2.5 GiB/s write and 3.75 GiB/s read for every additional engine.

It is worth noting that configurations with twice as many client nodes generally deliver best performance, both for write and for read. Setups with a substantially higher ratio (e.g. four times as many) of client nodes do not show significant increases in performance, and configurations with a slightly lower ratio show a substantial decrease in performance.

Above 8 server nodes, the scaling rate seems to decrease slightly even if using twice as many client nodes, as seen in the bandwidth results for the setup with 10 server nodes and

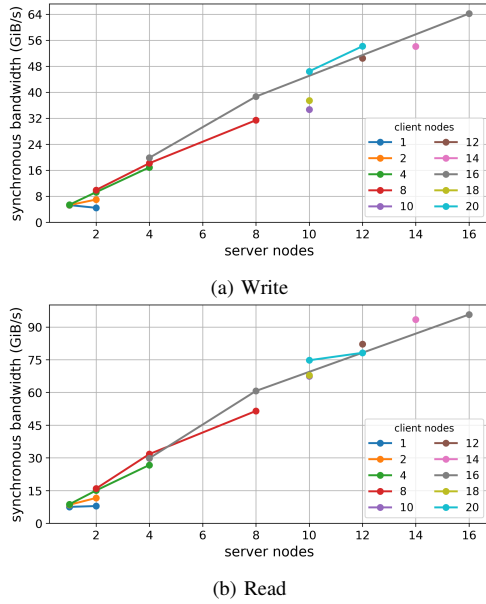


Fig. 3: Mean synchronous write and read bandwidth results for access pattern A (unique writes then unique reads) with IOR DAOS in segments mode.

20 client nodes.

The fact that the increase in read bandwidth per engine is not equal to the bandwidth achieved with a single engine is possibly due to the fact that multiple engines on both sockets in different nodes may contend to communicate through a single interface on one socket. Nonetheless, the linear increase in bandwidth with increasing engines is encouraging.

C. High-performance network

Due to the limitations encountered with the PSM2 fabric provider, we have not been able to benchmark DAOS with the highest-performance network functionality. However, it is possible to deploy DAOS with PSM2 using a single engine per server and only one socket used per client node. This restricts the usable network, processing, memory, and storage resources within nodes, but does allow comparison of TCP and PSM2 configurations of DAOS and an assessment of the impact of using a lower-performance network configuration.

We benchmarked a configuration using 4 DAOS server nodes, and up to 16 client nodes, which we tested with a number of different process counts (4, 8, 12, and 24 processes per client node). We used IOR in segments mode with the same configuration as used previously.

Fig. 4 compares both read and write performance when using the IOR benchmark with the different communication mechanisms. It is evident that PSM2 does provide higher performance than TCP, especially when scaling up the number of processes per client node. PSM2 demonstrates 10% to 25% higher bandwidth than TCP, and can also provide higher performance at lower node counts. However, it can be observed that the DAOS performance using PSM2 follows the same general patterns as with TCP communications and, whereas we expect the former would result in larger absolute bandwidths

by up to a 25%, we consider their behaviour at scale would be similar.

D. Field I/O results

We ran the Field I/O benchmark with the intent to analyse the order of magnitude and behaviour of bandwidths obtained with the field I/O functions rather than simple segment transfers; how the different field I/O modes scale; and how bandwidth behaves in access pattern B with an I/O workload similar to operational workloads.

For the rest of the tests in this paper, both sockets and network interfaces have been used on each of the nodes employed for the benchmark runs, with two DAOS engines deployed on each server node and client processes pinned to both sockets on each client node.

1) *Selection of client node and process count*: As a first parameter exploration and selection exercise, and with the intent to reduce the test parameter domain, we have run access pattern A with Field I/O, employing two server nodes and different amounts of client nodes (1, 2, 4 and 8) and processes counts (values listed in Parameter variation).

The number of I/O operations per client process has been set to 2000 to reduce the effect of any process start-up delays in bandwidth measurements. The Array object size has been set to 1 MiB, again motivated by the NWP use case.

The Key-Value objects have been configured with striping across all targets (OC_SX), and no striping (OC_S1) has been configured for the Array objects. This configuration was chosen on the assumption that Key-Values can be accessed by multiple process at a time for these benchmarks and could therefore benefit from striping across targets, whereas Arrays are never accessed by more than one process simultaneously.

Benchmark runs have been repeated 10 times. The average global timing bandwidths are shown in Fig. 5.

The results show that, both for write and read, using double the amount of client nodes as server nodes is a good trade-off, reaching high bandwidths without employing the largest amount of resources, and 36 or 48 processes per client node usually result in the best performance. Further variations of the experiment have shown that these results apply as well to pattern B and other server counts, and therefore these configuration values have been used for most of the benchmark runs reported below.

2) *Scalability of the Field I/O modes*: Access patterns A and B have been run with all modes of the Field I/O benchmark, configured for maximum contention on the indexing Key-Values. DAOS has been deployed on varying numbers of server nodes (1 to 8). Benchmarks have been repeated 10 times, using double the amount of client nodes, 36 and 48 processes per client node, and the same values for object class, object size and repetitions as above. The averaged results for the best configurations are shown in Fig. 6.

We can see from Fig. 6 that the bandwidths obtained in the mode without indexing are of the same order of magnitude and often slightly higher than those observed with IOR. This is likely due to the fact that Field I/O operations

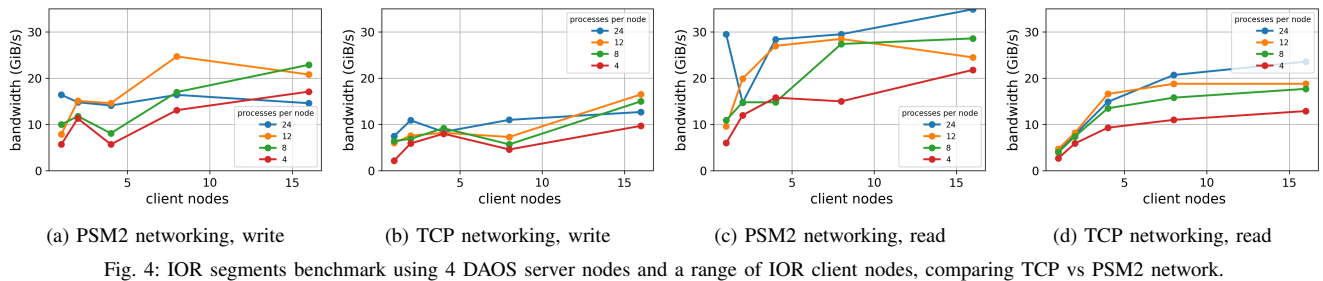


Fig. 4: IOR segments benchmark using 4 DAOS server nodes and a range of IOR client nodes, comparing TCP vs PSM2 network.

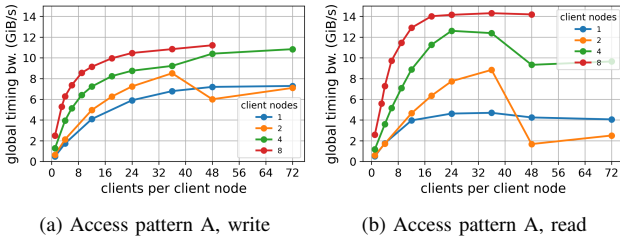


Fig. 5: Global timing write and read bandwidth results for access pattern A with the Field I/O benchmark, with two DAOS server nodes.

are spread over the duration of the benchmark run, rather than being dispatched simultaneously at every iteration as in IOR, allowing the storage to absorb them gradually. Also, the large object and transfer sizes involved in IOR may impact IOR bandwidths, although further experiments in object size are required to confirm this observation. In the full and no containers modes the bandwidths are generally lower than in the mode without indexing and IOR, as expected, due to the increased complexity and number of storage operations.

The graphs demonstrate that bandwidth scales as the number of server nodes is increased, even with the high degree of contention, with all Field I/O implementations and access patterns, with a slightly better scaling in access pattern B.

Note that in access pattern B the writers and readers run simultaneously, and therefore the write and read bandwidths should be aggregated as an approximate measurement of overall application throughput. It can be observed, if calculating the aggregated bandwidths, that there is no substantial performance degradation in access pattern B compared to pattern A, which is another encouraging result for the DAOS object store with I/O patterns such as the NWP use case.

The simplified mode of the Field I/O functions without indexing (no indexing Key-Values or containers) scales better than the two other implementations, at a rate of approximately 2.5 GiB/s for write and 3 GiB/s for read, per engine, in access pattern A. This scaling rate is similar to that observed with the IOR benchmarks, and demonstrates the capability of DAOS to perform and scale well even when, in contrast to IOR segments, separate I/O operations are issued for the different data parts managed by the client processes. In access pattern B, the increase in aggregated bandwidth for that mode is of approximately 2 GiB/s per engine, which we consider to be strong performance given the read/write contention.

For the modes with indexing, we observe the use of DAOS

containers does not have a substantial impact in Field I/O performance in this scenario. These modes scale up to 4 server nodes at a rate of approximately 1.5 GiB/s of write and read bandwidth per engine for pattern A, and 2 GiB/s of aggregated bandwidth per engine in pattern B, however the scaling rate decreases beyond 4 server nodes down to 0.5 GiB/s of aggregated bandwidth per engine.

The results shown so far have been obtained with Field I/O configured with a single shared forecast indexing Key-Value, inducing very high contention. This is however a very pessimistic scenario, and such a degree of contention is unlikely to occur in operational workloads. The complete test set has been re-run with lower contention, where each client process uses its own forecast index Key-Value, to mimic an optimistic usage scenario. The results, obtained for up to 16 server nodes, are shown in Fig. 7.

The same benchmark configuration as in the runs with high contention have been applied, also using double the amount of client nodes where possible. Due to resource limits, only 20, 14 and 16 client nodes have been used for runs with 12, 14 and 16 server nodes, respectively. These special configurations have been represented with hollow dots in the figure and, whilst the bandwidths they show are probably not as high as they would be if using double as many client nodes, they indicate a lower bound for the scalability curves at high server node counts.

The encouraging results for access pattern A show that the Field I/O implementation without containers scales remarkably well along with the mode without indexing. The full mode performs significantly worse, although it reaches higher bandwidths than in pattern A with high contention.

For access pattern B, the mode without indexing scales at a rate of approximately 2 GiB/s of aggregated bandwidth per additional engine. The full mode does not scale beyond 4 server nodes. The poor performance obtained with this mode suggests that there may be issues with the use or implementation of containers at scale, which needs further exploration.

The mode without containers in pattern B stands out, scaling at a rate of approximately 3.2 GiB/s of aggregated bandwidth per additional engine. With this mode, employing 12 server nodes, a total aggregated application bandwidth of approximately 80 GiB/s is achieved. These encouraging results demonstrate the potential of object storage and DAOS for HPC applications that can exploit such I/O patterns.

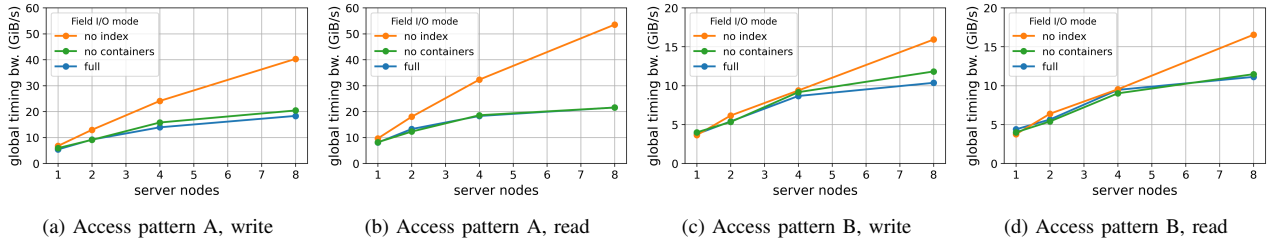


Fig. 6: Global timing write and read bandwidth results for access pattern A (unique writes then unique reads) and B (repeated writes while repeated reads) with the Field I/O benchmark, with high contention on the Key-Value objects.

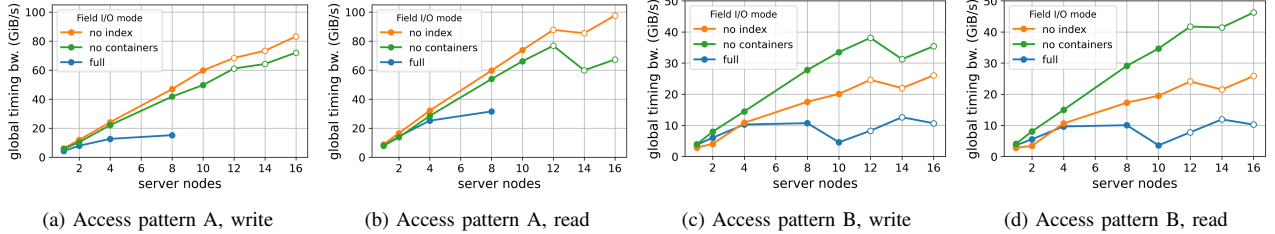


Fig. 7: Global timing write and read bandwidth results with the Field I/O benchmark, with low contention on the Key-Value objects. Hollow dots show configurations where less than twice as many client nodes as server nodes were employed.

For comparison, our reference weather forecasting centre currently uses a Lustre file system, with approximately 300 Lustre Object Storage Target (OST) nodes, each with 10 spinning disks of 2 TiB. It provides a file-per-process IOR bandwidth of up to 165 GiB/s, and a sustained application bandwidth in the order of 50 GiB/s during a typical model and product generation execution, accounting for both the write and read workload.

3) I/O distribution results: I/O offsets have been measured for all Field I/O scalability runs, as described in Asynchronous I/O distribution.

Due to the Field I/O benchmark being configured to synchronise processes at the start and perform a large number of I/O iterations per process, off_0 and p_0 have been measured to consistently range between 0% and 2% of the total parallel I/O wall-clock time, for all access patterns, Field I/O modes and server node counts.

The measured values for off_f have been found to range between 10% and 50% both for write and read phases in runs of access pattern A with different Field I/O modes and at different scales. For access pattern B, off_f ranged between 20% and 90%. Values for p_0 measured across all runs of access pattern B ranged between 0% and 20%.

The large off_f values suggest that I/O operations within a phase were processed in an unbalanced manner. This could be due to the synchronisation mechanism implemented in Field I/O (off_0 values are not always 0%), enabling some processes to initially undertake I/O with low contention from other processes, or due to how DAOS handles I/O requests.

On the other hand, lower p_0 values, together with low off_0 and p_0 values, indicate that the I/O operations in the experiments were distributed as intended according to the desired access patterns.

4) Object class and size: We also investigated the effect of object granularity and different striping configurations for the Field I/O objects. Fig. 8 shows bandwidth results from runs of access pattern A with Field I/O in its mode without containers, with object sizes 1, 5, 10, 20 and 50 MiB, and object configurations ranging from no striping (OC_S1) to striping all objects across all targets (OC_SX). Field I/O has been configured to run with no contention in the indexing Key-Values.

All tests have been run with a fixed configuration of 2 server nodes and 4 client nodes, with 36 processes per client node and 100 I/O operations per client process. Benchmarks are repeated 10 times for a range of client process counts. The results for the 10 repetitions have been averaged, with the average bandwidth for the highest performing number of client processes per client node shown for each combination of object class and I/O size tested.

It can be observed that, whilst all object class configurations result in similar performance, increasing Array object sizes from 1 to 5 MiB or 10 MiB has a substantial benefit in I/O performance for both write and read. This is a positive result for the NWP use case, which indicates that as higher-resolution data is used in the future, scaling will improve rather than deteriorate.

For configurations with no or some striping (OC_S1 and OC_S2) on the Array objects, the bandwidth plateaus or drops slightly beyond 10 MiB. This suggests that the IOR benchmarking, where we used 100 MiB objects, may not provide optimal results, although further benchmarking is required to confirm that. In configurations with maximum striping (OC_SX) on the Array objects, the read performance is consistently lower than with other configurations for all object sizes, and the write performance is similar at small object sizes but declines substantially beyond 10 MiB. This

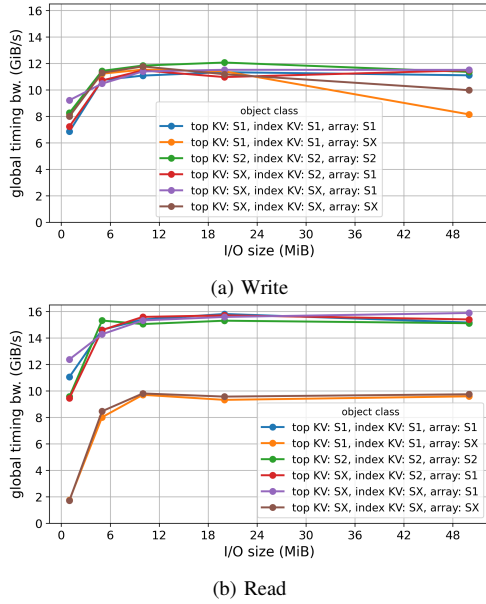


Fig. 8: Global timing write and read bandwidth results for access pattern A, with Field I/O in “no containers” mode, using 2 server and 4 client nodes.

is not surprising as striping is usually beneficial when parallel processes operate with shared objects, but DAOS objects are not shared in the Field I/O modes with indexing and without contention.

We note that all other Field I/O benchmark runs in this paper have been configured to use non-striped 1 MiB Arrays and maximum striping for the Key-Values, which Fig. 8 demonstrates is one of the best-performing configurations.

The bandwidths for access pattern B when varying object class and size, not included here, show similar behaviour, with the difference being that write and read bandwidths range from 5 to 9 GiB/s. Re-running the benchmark with larger amounts of server and clients nodes also showed similar behaviour, with no decline in write performance beyond 10 MiB, and a more notable decline in read performance beyond 10 MiB.

VII. CONCLUSIONS

DAOS has been demonstrated to provide object storage functionality meeting the demands of the weather field store currently in use for time-critical operations at the ECMWF, our exemplar weather forecasting centre. For this study, a weather field I/O benchmark has been developed and employed to evaluate if DAOS provides the required levels of consistency, functionality, and stability.

The performance of DAOS in conjunction with NVM has been tested in the NEXTGenIO research HPC system using the well-known IOR benchmark and the developed field I/O benchmark in a variety of modes and access patterns. The results demonstrate the capability of DAOS to scale linearly in throughput in applications for storage and indexing of weather fields or other relatively small data objects.

The aggregated bandwidth achieved in such applications increases at a rate of up to 3.2 GiB/s per additional socket

with SCM in the HPC system. Using up to 12 server nodes and 20 client nodes, the aggregated bandwidth reaches up to 80 GiB/s, using a sub-optimal object size. For comparison, we used a 300-node Lustre file system at our reference weather centre, which provides an aggregated bandwidth on the order of 50 GiB/s during a typical operational run.

These encouraging results, although qualified by a limited number of server and client nodes, indicate that a small DAOS system with non-volatile storage, on the order of a few tens of nodes, could perform as well as the HPC storage currently used for operations at the ECMWF, and suggest DAOS has the potential to support the next generation of weather models that will generate significantly larger amounts of data and require much larger I/O bandwidth and more intensive metadata operations.

The demonstration of strong I/O performance using a standard IOR configuration benchmarking DAOS also demonstrates that applications not adopting object store approaches or semantics are still likely to obtain good performance on a DAOS storage system, highlighting the applicability of DAOS for general HPC storage in future systems.

We note that our configuration of deploying DAOS entirely on SCM, rather than a combination of SCM and NVMe devices, may have had a positive impact on the performance DAOS achieved, but speculate that some of this benefit has been reduced by the network fabric restrictions (TCP rather than a higher-performance fabric provider) that the benchmarking has been undertaken with.

The introduced Field I/O framework opens a new area of benchmarking of high-performance object stores to assess their potential to enable I/O for next-generation NWP models. As part of this framework, we have formalised a network bandwidth measurement, global timing bandwidth, that we think more accurately represents the bandwidth achievable by mixed workloads on a shared I/O system. We consider that such benchmarking metrics will be important for ensuring user experience matches vendor deployments and procurement objectives for future I/O systems.

This preliminary assessment has showcased an example of what performance characteristics and design and configuration issues may be encountered when migrating from a high-performance distributed file system with traditional storage hardware to a high-performance object store with NVM storage, as well as the implementation of a domain-specific object store. It has shown the implementation of domain-specific object stores can result in performance benefits in certain I/O scenarios, and has helped investigate the specific requirements and the design of appropriate data layouts to use DAOS for such object stores.

ACKNOWLEDGMENT

The work presented in this paper was carried out with funding by the European Union under the Destination Earth initiative (cost center DE3100, code 3320) and relates to tasks entrusted by the European Union to the European Centre for Medium-Range Weather Forecasts. Views and opinions

expressed are those of the author(s) only and do not necessarily reflect those of the European Union or the European Commission. Neither the European Union nor the European Commission can be held responsible for them.

This work has also been contributed by the the ACROSS and IO-SEA projects, funded by the European High-Performance Computing Joint Undertaking (JU) under Grant Agreements no. 955648 and no. 955811, respectively. The JU receives support from the European Union's Horizon 2020 research and innovation programme and Italy, France, Czech Republic, United Kingdom, Greece, Netherlands, Germany, Norway.

The NEXTGenIO system was funded by the European Union's Horizon 2020 Research and Innovation program under Grant Agreement no. 671951, and supported by EPCC, The University of Edinburgh.

For the purpose of open access, Adrian Jackson has applied a Creative Commons Attribution (CC BY) licence to any Author Accepted Manuscript version arising from this submission.

REFERENCES

- [1] G. Lockwood, "What's so bad about POSIX I/O?", The Next Platform 2017. <https://www.nextplatform.com/2017/09/11/whats-bad-posix-io/>
- [2] Z. Liang, J. Lombardi, M. Chaarawi, M. Hennecke, "DAOS: A Scale-Out High Performance Storage Stack for Storage Class Memory" In: Panda, D. (eds) Supercomputing Frontiers. SCFA 2020. Lecture Notes in Computer Science(), vol 12082. Springer, Cham. DOI:10.1007/978-3-030-48842-0_3.
- [3] J. Kunkel, J. Ben, J. Lofstead, G. Markomanolis, "Establishing the IO-500 Benchmark", White Paper, 2016
- [4] K. Jeong, C. Duffy, J. -S. Kim and J. Lee, "Optimizing the Ceph Distributed File System for High Performance Computing" 2019 27th Euromicro International Conference on Parallel, Distributed and Network-Based Processing (PDP), 2019, pp. 446-451, DOI:10.1109/EMPD.2019.8671563.
- [5] S. Narasimhamurthy, N. Danilov, S. Wu, G. Umanesan, S. Chien, S. Rivas-Gomez, I. Peng, E. Laure, S. Witt, D. Pleiter, and S. Markidis. "The SAGE project: a storage centric approach for exascale computing: invited paper". In Proceedings of the 15th ACM International Conference on Computing Frontiers (CF '18). Association for Computing Machinery, New York, NY, USA, 287–292. DOI:10.1145/3203217.3205341.
- [6] A. Dilger, D. Hildebrand, J. Kunkel, J. Lofstead, and G. Markomanolis, "IO500 10 node list Supercomputing 2022", November 2022. https://io500.org/list/sc22/ten?sort=io500_mdd&direction=desc
- [7] S. Smart, T. Quintino, and B. Raoult. "A Scalable Object Store for Meteorological and Climate Data". In Proceedings of the Platform for Advanced Scientific Computing Conference (PASC '17). Association for Computing Machinery, New York, NY, USA, Article 13, 1–8. DOI:10.1145/3093172.3093238.
- [8] S. Smart, T. Quintino, and B. Raoult. "A High-Performance Distributed Object-Store for Exascale Numerical Weather Prediction and Climate". In Proceedings of the Platform for Advanced Scientific Computing Conference (PASC '19). Association for Computing Machinery, New York, NY, USA, Article 16, 1–11. DOI:10.1145/3324989.3325726.
- [9] Vef, MA., Moti, N., Süß, T. et al. "GekkoFS — A Temporary Burst Buffer File System for HPC Applications". J. Comput. Sci. Technol. 35, 72–91 (2020). DOI:10.1007/s11390-020-9797-6.
- [10] O. Tatebe, K. Obata, K. Hiraga, and H. Ohtsuki. 2022. "CHFS: Parallel Consistent Hashing File System for Node-local Persistent Memory". In International Conference on High Performance Computing in Asia-Pacific Region (HPCAsia2022). Association for Computing Machinery, New York, NY, USA, 115–124. DOI:10.1145/3492805.3492807.
- [11] A. Miranda, A. Jackson, T. Tocci, I. Panourgias and R. Nou, "NORNS: Extending Slurm to Support Data-Driven Workflows through Asynchronous Data Staging" 2019 IEEE International Conference on Cluster Computing (CLUSTER), pp. 1-12, DOI:10.1109/CLUSTER.2019.8891014.
- [12] N. Manubens, S. Smart, T. Quintino and A. Jackson, "Performance Comparison of DAOS and Lustre for Object Data Storage Approaches", 2022 IEEE/ACM International Parallel Data Systems Workshop (PDSW). DOI:10.1109/PDSW56643.2022.00007.
- [13] "DAOS Architecture", 2023. <https://docs.daos.io/latest/overview/architecture>
- [14] "HPC IO Benchmark Repository", 2022, GitHub repository. <https://github.com/hpc/ior>
- [15] N. Manubens, A. Jackson, T. Quintino, S. Smart and E. Danovaro, "DAOS weather field I/O tests", 2023, GitHub repository ecmwf-projects/daos-tests (0.1.1). DOI:10.5281/zenodo.7559332.
- [16] "NEXTGenIO User Guide and Applications", 2023. <https://ngioproject.github.io/nextgenio-docs/html/index.html>



Nicolau Manubens obtained a licentiate in informatics from the Universitat Autònoma de Barcelona in 2014, and has since worked as a software engineer at various weather and climate forecasting and research institutions. He is currently employed at the European Centre for Medium-Range Weather Forecasts and is a Ph.D. candidate at EPCC, The University of Edinburgh, doing research work on HPC storage for km-scale Numerical Weather Prediction in the context of the Destination Earth initiative.



Tiago Quintino is Head of Software Development section at the ECMWF, where they develop high-throughput specialist software supporting ECMWF's operational activity. Dr. Quintino's career spans 20 years researching numerical algorithms and developing high-performance scientific software in the areas of Aerospace and Numerical Weather Prediction. Lately, his research focuses on scalable data handling algorithms for generation of meteorological forecast products, optimising the workloads and I/O of massive data sets towards Exascale computing.



Simon Smart obtained a Ph.D. in theoretical chemistry in 2013 from the University of Cambridge, and then worked at the Max Planck Institute for Solid State Chemistry writing high-performance computational chemistry software. He has worked at the European Centre for Medium-Range Weather Forecasts since 2015, focusing on scalability and the challenges of data handling on the pathway to Exascale. He now leads the Data Management Services team, with responsibility for all of the software infrastructure underpinning data handling at ECMWF.



Emanuele Danovaro received a M.Sc. (in 2000) and a Ph.D. (in 2004) in computer science from the University of Genova. During his post-doc, he developed algorithm and compact data structures for multi-dimensional data. In 2009, he joined the Italian National Research Council as a senior researcher, working on algorithm parallelisation and leading the development of a workflow manager for meteorological applications. In 2019 he joined ECMWF and is currently responsible for the development of the high-performance data management subsystem.



Adrian Jackson is a Senior Research Fellow at EPCC, The University of Edinburgh. He has a history of research into high-performance and parallel computing, with a focus on parallel algorithms, domain decomposition, parallel I/O, and memory technologies. He collaborates with a wide range of domain scientists, from plasma physicists and radio astronomers, to CFD experts and biologists.

Appendix C – Reducing the Impact of I/O Contention in Numerical Weather Prediction Workflows at Scale Using DAOS

Reducing the Impact of I/O Contention in Numerical Weather Prediction Workflows at Scale Using DAOS

Nicolau Manubens nicolau.manubens@ecmwf.int European Centre For Medium-Range Weather Forecasts Germany	Simon D. Smart simon.smart@ecmwf.int European Centre For Medium-Range Weather Forecasts United Kingdom	Emanuele Danovaro emanuele.danovaro@ecmwf.int European Centre For Medium-Range Weather Forecasts United Kingdom
Tiago Quintino tiago.quintino@ecmwf.int European Centre For Medium-Range Weather Forecasts United Kingdom	Adrian Jackson a.jackson@epcc.ed.ac.uk The University of Edinburgh United Kingdom	

ABSTRACT

Operational Numerical Weather Prediction (NWP) workflows are highly data-intensive. Data volumes have increased by many orders of magnitude over the last 40 years, and are expected to continue to do so, especially given the upcoming adoption of Machine Learning in forecast processes. Parallel POSIX-compliant file systems have been the dominant paradigm in data storage and exchange in HPC workflows for many years. This paper presents ECMWF's move beyond the POSIX paradigm, implementing a backend for their storage library to support DAOS – a novel high-performance object store designed for massively distributed Non-Volatile Memory. This system is demonstrated to be able to outperform the highly mature and optimised POSIX backend when used under high load and contention, as per typical forecast workflow I/O patterns. This work constitutes a significant step forward, beyond the performance constraints imposed by POSIX semantics.

CCS CONCEPTS

- **Information systems** → **Distributed storage**; • **Applied computing** → **Earth and atmospheric sciences**.

KEYWORDS

High-Performance Storage, I/O Contention, Scalability, Object Storage, DAOS, Lustre, Numerical Weather Prediction

ACM Reference Format:

Nicolau Manubens, Simon D. Smart, Emanuele Danovaro, Tiago Quintino, and Adrian Jackson. 2024. Reducing the Impact of I/O Contention in Numerical Weather Prediction Workflows at Scale Using DAOS. In *Platform for Advanced Scientific Computing Conference (PASC '24)*, June 3–5, 2024, Zurich, Switzerland. ACM, New York, NY, USA, 12 pages. <https://doi.org/10.1145/3659914.3659926>

Permission to make digital or hard copies of part or all of this work for personal or classroom use is granted without fee provided that copies are not made or distributed for profit or commercial advantage and that copies bear this notice and the full citation on the first page. Copyrights for third-party components of this work must be honored. For all other uses, contact the owner/author(s).

PASC '24, June 3–5, 2024, Zurich, Switzerland
© 2024 Copyright held by the owner/author(s).
ACM ISBN 979-8-4007-0639-4/24/06.
<https://doi.org/10.1145/3659914.3659926>

1 INTRODUCTION

Numerical Weather Prediction (NWP) uses mathematical models to predict the conditions of the atmosphere and other components of the Earth system over varying forecast horizons, from hours to weeks in advance. These models include direct physical simulations and Machine Learning (ML) models[1]. Due to the diverse and vast quantities of data ingested and produced by these models, as well as the complexity of NWP workflows, NWP model runs are considered characteristic data-intensive applications. Data volumes will continue to increase substantially in the coming years, as scientific ambition drives higher model resolution and larger numbers of perturbed simulation replicas[2], and the range of downstream applications consuming forecast data is also commensurately growing. This poses a significant storage capacity requirement for current and future NWP data centres.

The challenge is further magnified by the time-critical nature of forecasting systems, driven by the sharply decreasing value of a forecast as time passes. Applications producing and consuming data run simultaneously in the HPC system, and data needs to be exchanged efficiently even under significant load and system contention.

Large distributed POSIX file systems backed by hard-drive disks (HDD) and solid-state disks (SSD) are currently the predominant high-performance storage solution in HPC systems. These file systems present limitations in highly parallel data-intensive workloads. On one hand, the POSIX file system API forces the application developer to use files and directories as the data storage units, and to think about how to distribute the data in them. The developer needs to consider concurrent access to the files and directories from several parallel processes, and implement mechanisms to ensure consistency while maintaining a sufficient level of performance. This becomes not only a source of complexity and errors in the application, but also an extremely challenging task even for an experienced programmer[3]. If multiple applications need to access the same data in the file system concurrently, all of the applications should include mechanisms to address these issues, which can be complex and costly.

On the other hand, the APIs and semantics exposed by POSIX file systems were designed decades ago when storage devices were

attached only locally to the machine rather than over the network, and the POSIX standards[4] have inherited and mandate features that can hinder performance in highly-parallel workloads. Specifically, POSIX prescribes lots of metadata to be maintained by the operating system for each file and directory; the consistency guarantees are sometimes excessive[5]; it relies on the operating system's block device interface, which enforces retrieval of entire blocks even if only a few bytes in a file are requested; and it mandates file semantics that are over-constrained and non-optimal for high write and read contention workloads on distributed systems, such that distributed locking mechanisms need to be put in place by the distributed file system implementations, causing large lock communication overheads on the client nodes[6][7][8].

The European Centre for Medium-Range Weather Forecasts (ECMWF) developed a storage library, named the FDB[9][10], which exposes a domain-specific API – described in in section 1.3 – for NWP applications to store and index weather fields according to scientifically meaningful metadata. This was built with a software backend making use of a POSIX-compliant distributed file system, handling the use and parallel access to files and directories behind the scenes and thus decoupling as best as possible the behavioural semantics required by the application domain from those provided by the file system.

More recent work has functionally split the FDB POSIX backend into *Catalogue* and *Store* backends which implement the indexing functionality and data storage capability, respectively.

Notwithstanding this work in FDB to address the challenges associated with using and managing parallel access to files and directories, the other issues associated with POSIX APIs and semantics have remained largely unaddressed for years.

Currently, the operational storage systems at ECMWF are already being used at their performance limit, and expanding them to support upcoming data volume increases of one or two orders of magnitude would be costly, or even not viable due to the unprecedented degree of contention. With the goal of enabling operational NWP to scale to such larger data volumes, ECMWF conducted a preliminary assessment[11] of a new storage technology called Distributed Asynchronous Object Store (DAOS)[12], which is a high-performance object store designed for massively distributed Non-Volatile Memory (NVM), originally developed by Intel and recently transferred to the newly formed DAOS foundation. DAOS not only offers an object store API with novel semantics which allow for server-side contention resolution, but it also reduces metadata requirements, operates fully in user-space and allows for byte-granular access to NVM storage devices. The preliminary assessment yielded promising results, but it was conducted by developing a standalone benchmark, independent from ECMWF's operational software storage stack.

This paper presents the development and evaluation of DAOS Catalogue and Store backends for the FDB. These backends were benchmarked against DAOS deployments on the NEXTGenIO prototype system[13] containing NVM distributed across the nodes. A performance comparison against identical workflows using the POSIX backends and Lustre on the same hardware is included.

1.1 Related work

Hardware and software storage technologies have proliferated in the last decade[22]. There have been many research works on how to exploit and utilise these on the path to adapting I/O to Exascale. Some have focused on the benefits of object storage as opposed to commonly used file systems and their limitations[14][20]. Others have focused on adapting I/O middleware to exploit object storage[15], and some have reported successful outcomes with DAOS specifically as a backend for I/O middleware[16][18][19] or file system APIs[17] on top of DAOS.

Object stores are increasingly present in IO-500 performance rankings[23], with some large institutions at the top after adopting object storage – mostly as a backend for the file system APIs commonly used in their applications.

Some have gone beyond file system and I/O middleware APIs and developed domain-specific object stores building on top of general-purpose object stores and low-level NVM storage libraries, and verified the benefits of that approach[21]. This includes ECMWF's previous work on the FDB5[9], which originally exploited POSIX file systems, and later was adapted to make native use of PMEM[27] and the Ceph RADOS and Cortx Motr object stores. Part of the conclusions of this work were that a PMEM backend was difficult to maintain, and RADOS, which is currently being reevaluated, did not at the time provide sufficient capabilities to implement FDB indexing. Of the remaining storage options, Motr was recently discontinued.

ECMWF has recently assessed DAOS as a potential backend for their FDB. First, a performance analysis was conducted[11] with standalone benchmark applications making native use of DAOS (Field I/O and IOR[24] with its DAOS API) showing very good performance. A dummy DAOS library was later developed which maps the DAOS API onto a file system API, and the benchmarks were run again using that library, thus exploiting Lustre deployments under the hood. DAOS showed much better performance if compared to dummy DAOS on Lustre[25]. That comparison, however, was not perfect because runs with dummy DAOS abused the file system API with massive amounts of small I/O operations rather than following file system best practices.

The work presented here describes a newly developed FDB backend which enables native FDB operation on DAOS, and discusses the implementation and performance differences between running realistic NWP I/O workflows with the new FDB backend on DAOS vis-à-vis the traditional POSIX backend on Lustre – the latter making careful and efficient use of the file system API.

1.2 Numerical Weather Prediction Data Flows

At ECMWF, the operational forecasting system is run 4 times a day in 1-hour time-critical windows. During each of these windows an ensemble of 52 perturbed model instances (members) are run across approximately 2500 compute nodes. For each of the 240 model output steps, global two-dimensional slices of data (fields) are aggregated by 2500 I/O server processes running on dedicated I/O nodes and written into a Lustre distributed file system with the FDB. Approximately 70 TiB of data are produced by the models and stored by the I/O servers during an operational run, comprising

approximately 25 million fields. 70% of the data is immediately consumed by an ensemble of post-processing tasks which run alongside the models generating derived products.

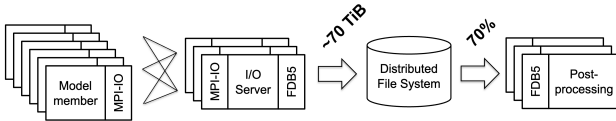


Figure 1: A simplified overview of ECMWF's operational work flow

Downstream consuming processes need to be launched as soon as their input data has been made available. Ensuring that the model, and thus the workflow controller, knows when data has been made available drives one of the primary semantic requirements of the FDB. Accomplishing this in the operational workload, under the contention of thousands of simultaneous reading and writing processes provides one of the most significant technical challenges for the FDB.

This is exacerbated by the nature of the write and read patterns. On one hand, each of the I/O server processes writes a stream of fields, which belong to a single member of the simulation. These streams contain fields for a range of simulated variables and levels in the atmosphere, with the processes producing and streaming fields for a sequence of time steps as the model progresses.

On the other hand, the post-processing tasks that consume the data are largely specified per step. That is, once step n of the forecast is completed, the post-processing for step n is launched, and those processes read data as a slice across all the output streams, but only for step n . This is essentially a transposition of the view of the data from that of the I/O server, and requires *each* of the post-processing processes to interact with *every* indexing and data output stream produced by the I/O server processes, whilst the model continues to produce and stream data for the following steps.

How this contention is handled in detail is covered extensively in an earlier paper[9]. But fundamentally, in the POSIX backends, the write pathway is optimised to the benefit of the writing processes. Each process writes its own independent indexing and data files, and maintains the transactionality required of the FDB by careful insertion of entries on the end of a table of contents file, making use of the precise semantics of the O_APPEND mode of a POSIX-compliant file system. The levels of indirection required to make the write pathway performant come at a cost to the read pathway which must access many table of contents and index files to locate the data. This read pathway has been aggressively optimised to be *good enough* for the operational purposes, with extensive index preloading, caching and pruning of the index exploration process.

A consequence of this design is that in a system with minimal contention, the write pathway is expected to perform close to the limits of the underlying file system, and the read pathway is expected to be a little slower. Once runtime contention is introduced between read and write processes, the performance impact of the internal file system lock exchanges between the storage servers and the clients required to maintain consistency is expected to be noticeable. Within DAOS, the distribution of metadata operations across all servers, server-side handling of consistency, and

the ability to undertake fine-grained I/O operations, are anticipated to significantly reduce the observed cost of this contention, leading to a benefit on a highly-contended system when running at scale.

1.3 The FDB

The FDB is a domain-specific object store for meteorological data, which sits between various data producing and consuming components in wider NWP workflows. In practice, it is a library which is compiled into these components, along with a set of management command-line tools, and configurations and data governance rules to establish a particular usage pattern. This library exists to abstract away the specific behavioural details of various underlying storage systems, and to provide a standardised API for data use.

The FDB API is metadata-driven – that is, all API actions are invoked using scientifically-meaningful metadata describing the data to be acted upon. All data objects (fields) are identified by a globally-unique metadata identifier, formed as a set of key-value pairs conforming to a user-defined schema. An example field identifier is illustrated in Listing 1.

Listing 1: An example metadata identifier of a field in FDB.

```
class = od,           stream = oper,      expver = 0001,
date = 20231201,    time = 1200,        type = ef,
levtype = sfc,      number = 13,        levelist = 1,
step = 1,           param = v
```

The schema defines not only the valid field identifier keys and values, but also how the FDB will internally split the identifiers provided by the user processes into three sub-identifiers which control how the Store backend lays out data in the storage system:

(1) **Dataset key:** describes the dataset a field belongs to. For instance, a forecast produced today starting at midday. For example, if the schema is configured to recognise class, stream, expver, date and time as dataset dimensions, the following dataset key would result for Listing 1:

```
class = od,           stream = oper,
expver = 0001,        date = 20231201,
time = 1200
```

(2) **Collocation key:** the field should be collocated in storage with other fields sharing the same collocation key. E.g.:

```
type = ef,           levtype = sfc,
number = 1,           levelist = 1
```

(3) **Element key:** identifies the field within a collocated dataset. E.g.:

```
step = 1,           param = v
```

The FDB API has precisely determined semantics. Aside from a number of administrative functions, there are four primary functions in the API, namely `archive()`, `flush()`, `retrieve()`, and `list()`. The Store and Catalogue backends are responsible for ensuring that the correct semantics are provided on top of whatever provisions are made by the underlying storage systems. In particular[27]:

- (1) Data is either visible, and correctly indexed, or not. The FDB adheres to the ACID[28] (Atomicity, Consistency, Isolation, and Durability) semantics commonly used to define database transactions.
- (2) `archive()` blocks until the FDB has taken control of (a copy of) the data. Data is not necessarily visible to consumers or persisted in storage devices at this point, but it is permitted to be.
- (3) `flush()` blocks until all data `archive()`ed from the current process is persisted into the underlying storage medium, correctly indexed and made visible and accessible to any reading process via `retrieve()` and `list()`.
- (4) Once data is made visible, it is immutable.
- (5) Data can be replaced by `archive()`ing a new piece of data with the same metadata. This second `archive()` shares the semantics of the first, such that the old data is visible until the new data is fully persisted and indexed.

2 THE DISTRIBUTED ASYNCHRONOUS OBJECT STORE (DAOS)

The Distributed Asynchronous Object Store (DAOS)[12] is an open-source high-performance object store designed for massively distributed Non-Volatile Memory (NVM), including Storage Class Memory (SCM) which resides in the memory domain of a compute node. DAOS was originally developed by Intel and has recently been transferred to the DAOS foundation[29]. It provides a low-level key-value storage interface on top of which other higher-level APIs, also provided by DAOS, are built. Its features include transactional non-blocking I/O, fine-grained I/O operations with zero-copy I/O to SCM, end-to-end data integrity, and advanced data protection. The OpenFabrics Interfaces (OFI) library is used for low-latency communications over a wide range of network back-ends.

DAOS is deployable as a set of I/O processes or engines, generally one per physical socket in a server node, each managing access to NVM devices associated with the socket. Graphical examples of how engines, storage devices and network connections can be arranged in a DAOS system can be found at [30].

An engine partitions the storage it manages into targets to optimize concurrency, each target being managed and exported by a dedicated group of threads. DAOS allows reserving space distributed across targets in *pools*, a form of virtual storage. A pool can serve multiple transactional object stores called *containers*, each with their own address space and transaction history.

The low-level key-value DAOS API is provided in the `libdaos` library, and it exposes what is commonly known as a map or dictionary data structure, with the feature that every value indexed in it is associated to two keys: the distribution (*dkey*) and the attribute (*akey*). All entries indexed under the same *dkey* are collocated in the same target, and the *akeys* identify the different entries under a same *dkey*. Listing *dkeys* and *akeys* is supported. This is an advanced API and not commonly used in third-party libraries using DAOS. High-level Key-Value and Array APIs are also provided as part of `libdaos`, both building on top of the low-level API.

The high-level Key-Value API exposes a single-key dictionary structure, where limited-length character strings (the *keys*) can be mapped to byte strings of any length (the *values*). Entries can be

added or queried with the transactional `daos_kv_put` and `daos_kv_get` API calls. Querying the size of an entry and listing keys is also supported.

The Array API is intended for bulk-storage of large one-dimensional data arrays. An in-memory buffer can be stored into DAOS or populated with data retrieved from DAOS with the transactional `daos_array_write` and `daos_array_read` API calls. These operations support targeting one or multiple byte ranges with arbitrary offset and length.

Upon creation, Key-Value and Array objects are assigned a 128-bit unique object identifier (OID), of which 96 bits are user-managed. These objects can be configured for replication and striping across pool targets by specifying their *object class*. If configured with striping, they are transparently stored by parts in different low-level *dkeys* and thus distributed across targets, enabling concurrent access analogous to Lustre file striping.

DAOS also distributes a `libbdfs`[31] library which implements POSIX directories, files and symbolic links on top of the described APIs, such that an application including this library can perform common file system calls which are transparently mapped to DAOS. `libbdfs` is, however, not fully POSIX-compliant and cannot support the FDB POSIX Catalogue backend. A FUSE daemon and interception library are also distributed by DAOS for use in existing applications using the POSIX file system API without modification.

An important feature of DAOS, if compared to POSIX distributed file systems, is that contention between writer and reader processes is resolved server-side with a lockless mechanism rather than via distributed locking on the clients.

POSIX mandates that all write and read operations must be consistent. That is, a read operation initiated right after a write operation on the same file extent must see the data being written by the write operation. And a write operation initiated right after a read operation must not modify the original data before it is fully returned to the reader. In distributed file systems these guarantees are commonly accomplished by having a distributed locking mechanism such that every process starting a write or read operation must request a write or read lock from a lock server for the target file extent before writing or reading the extent from storage, and in case of conflicting I/O the last racing process blocks until it obtains the lock it requested. Any issued set of conflicting write and read operations is thus guaranteed to be consistent and with no interruptions or failures due to I/O conflicts. Note that every lock request involves a network round-trip to the lock server.

In DAOS, instead, a Multiversion Concurrency Control (MVCC) method is used. When a write operation is issued, it is immediately persisted by the server in a new region or object in storage, with no read-modify-write operations. The new object is then atomically indexed in a persistent index, usually in low-latency SCM distributed across the DAOS servers, and the write operation returns successfully. Any subsequent read operation for that object triggers visitation of the index and returns the associated data from the corresponding storage regions across the servers. This way, writes always occur in new regions without modifying data potentially being read, and reads always find the latest fully written version of the requested object in the corresponding index entry. This mechanism not only ensures strong consistency guarantees but also avoids the use of locks and the associated overheads.

Another relevant feature of DAOS is that metadata operations are performed against all server nodes in DAOS, rather than on dedicated metadata servers which can potentially bottleneck and hinder performance at scale. Previous work by the authors[11] has demonstrated that DAOS provides a sufficient level of consistency and performance under contention in simplified NWP I/O workflows.

In terms of authentication and authorisation, the DAOS pools and containers can be configured via Access Control Lists (ACLs) to allow read-only or write-read access to different users. The client processes attach their effective UNIX user and group in every I/O operation sent to the server, and these are used to determine access permissions according to the ACLs.

3 DESIGN OF THE DAOS FDB BACKENDS

The FDB internally implements indexing functionality in what is known as a Catalogue backend, and functionality for storage (bulk write and read) of meteorological objects in a Store backend. The FDB defines abstract interfaces for these backends, such that specific Catalogue or Store instances can operate on top of a given type of storage system. If backends conform to the established interfaces and semantics, the FDB will guarantee its external API semantics. Any pair of conforming Catalogue and Store backends can then be used in conjunction even if they operate on different underlying storage systems.

Both backend interfaces define `archive()`, `flush()` and `retrieve()` methods, and a `list()` method is also defined for the Catalogue backend interface. A call to the high-level FDB API will result in internal calls to the corresponding methods in the lower-level backend interfaces. For example, an FDB `flush()` call will internally call both the Store `flush()` and the Catalogue `flush()`.

The DAOS Catalogue and Store backends have been implemented according to the design of the Field I/O benchmark, developed during ECMWF's preliminary assessment of DAOS[11]. The primary idea being to use the DAOS Key-Value and Array APIs to build an indexing structure and data store, where all contention and consistency management is handled by DAOS on the server side. A graphical representation of the different DAOS entities involved is shown in Fig. 2. All dataset, collocation or element keys are stringified for indexing by joining all values in the key with a ':' character, which can symmetrically be used to reconstruct the key.

3.1 The Store Backend

3.1.1 Interface. A Store backend implements an `archive()` method accepting a pointer to in-memory data, a dataset key, and a collocation key. The data is taken control of and optionally persisted into storage before the method returns. A field location descriptor (equivalent to a URI) is returned describing where the data is to be persisted. This location should be collocated with other fields sharing the same collocation key. The storage location must be unique, avoiding collisions with concurrent processes. `archive()` will be called repeatedly with the same dataset and collocation key, and previously archived fields must not be overwritten or modified.

The `flush()` method blocks until all data which has been `archive()`ed has been persisted to permanent storage and made accessible to external reading processes.

Given a field location descriptor, the `retrieve()` method builds and returns a `DataHandle` (a backend-specific instance of an abstract reader object), allowing the calling process to read the field from storage without knowledge of the backend implementation.

3.1.2 Implementation. Data is stored in the DAOS backend in containers identified by a stringified representation of the dataset key. When `archive()` is called, the container is created if it does not exist. Once opened for use the relevant DAOS handle is cached for the process lifetime.

Every object is `archive()`ed by a single process into its own DAOS Array object. The Array is created and opened with a unique object identifier (OID) obtained from DAOS. Allocating unique OIDs requires a round trip to the DAOS server to avoid collisions, and as such a range of OIDs are pre-allocated and cached by a process before object creation. Data is written into the array and the array closed. A unique field location descriptor to this array, also containing a length and an offset, is then returned. As this backend uses an Array for each object, the offset is always zero.

By contrast to the POSIX backend implementation, as the DAOS API immediately persists objects and makes them available, the DAOS Store correspondingly makes objects available to external readers immediately, and there is no further action to be taken in the `flush()` method. In the future, the `flush()` method may be useful if (for example) the non-blocking DAOS APIs are used in which case the `flush` method would block until those operations were complete.

Note that the input collocation key has not been used to determine data placement. In a previous version of the backend this key was used to create separate containers that collocated data, but the additional containers resulted in significant performance overheads so they have been removed. As such, all the object data associated with a single dataset key is collocated in the same container. The collocation key is nonetheless still used in the Catalogue backend for structuring the indexing information.

When `retrieve()` is called, the input field location descriptor is used to build a `DataHandle` object which reads data from the specified DAOS Array. Note that no call needs to be made to DAOS (and thus over the network to the DAOS server) to obtain the array size, as that is encoded in the field location descriptor.

3.2 The Catalogue Backend

3.2.1 Interface. A Catalogue backend has more complexity than a Store backend, not only because it addresses a more complex problem – that of maintaining a consistent index under contention – but also because it is involved in more operations, including archival, retrieval, removal, and listing. The Catalogue interface comprises more than ten methods, but only the ones required for field archival and retrieval are covered here, with some simplification.

Catalogue backends require an `archive()` method such that, given a dataset key, a collocation key, an element key, and a field location descriptor (from an earlier Store `archive()` call) the descriptor is inserted in an indexing structure, either in memory or in storage, before the method returns (with no return value). That indexing structure maps the element key to the provided associated descriptor location. This may be an internal operation, and does not guarantee persistence or visibility to reading processes. The

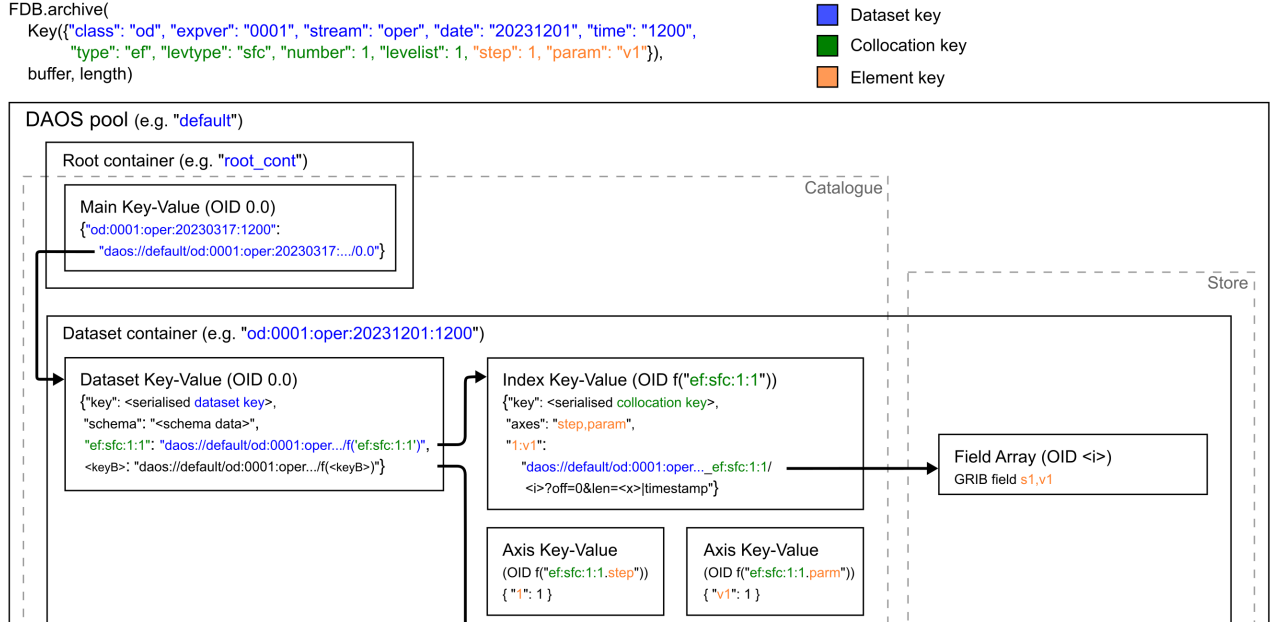


Figure 2: Diagram of DAOS entities resulting from an FDB archive call to store and index the first weather field in a simulation.

backend may make use of the dataset and collocation keys, and knowledge of the writing processes to index related information together, or separately, as makes most sense for performance on the targeted data subsystems.

`flush()` must also be implemented, which blocks until all indexed information has been persisted and made visible to any external `retrieve()`ing processes. One of the requirements is that all `flush()`ed indexing structures should also be accessible to `list()`ing processes in a reasonably efficient manner. This may require additional indexing structures to be present such that all entries can be explored from a single entry point.

The index must *always* be consistent from the perspective of an external reading process, even under read and write contention. If multiple `archive()` calls with same dataset, collocation and element keys occur, the older data should be replaced by newer in a transactional manner from the perspective of any reading processes.

The `retrieve()` method must return the field location descriptor given the dataset, collocation and element keys for a field. This can then be passed as an argument to the Store `retrieve()` method to retrieve the actual data. It is important to note that, due to the potential for the use of the FDB as a cache in a larger data infrastructure, failing to find a field is not an error and results only in no data being returned.

The `list()` method, although not covered in detail here, must return a list of field identifiers and location descriptors matching a partial request comprising spans of possible key values (i.e. not necessarily specifying all keys required for an identifier according to the schema). Making this listing possible and efficient added further constraints on the implementation approaches and choices.

3.2.2 Implementation. The DAOS Catalogue backend is built using a network of DAOS Key-Value objects to construct a navigable

index of the stored fields. To make the data explorable, a Key-Value object identified with OID 0.0 is built, as a single point of entry, in a configured root container. Below this, each dataset is assigned its own container. Inside this container a first level (dataset) Key-Value object, also with OID 0.0, maps collocation keys onto the second level (index) Key-Value object, which in turn maps element keys onto data location descriptors.

In parallel with this, a set of Key-Value objects (the Axis Key-Values) is built per index Key-Value, describing the span of values indexed in it. One Key-Value object is created for each element key component to act as set containing all the values written at that level. This can be used to improve the efficiency of the read process.

When `archive()` is called the root pool and container are opened. If the (stringified) dataset key is not found in the root Key-Value object, the dataset container is created (with the same name as used in the Store backend), and populated with a dataset Key-Value object at OID 0.0. An entry is placed in the root Key-Value mapping the dataset key to the (URI of the) dataset Key-Value. As there is a meaningful overhead to handling pools and containers, once any have been opened they are cached for the lifetime of the process.

The collocation key is handled in the same manner. If the (stringified) collocation key is not found in the dataset Key-Value object a new Key-Value is created identified by the collocation key, and an entry added to the dataset Key-Value mapping the collocation key to the URI of the index Key-Value. Otherwise, the identified Key-Value is used. An entry is then added to index Key-Value mapping the element key to the supplied field location description.

After `archive()` has returned, the indexing information has already been persisted and the indexed fields have been made visible to reader processes. There is no further action to be taken in the `flush()` method.

Concurrent processes writing or reading fields with same dataset and collocation keys will contend on a same index Key-Value, which can have a noticeable performance overhead. It is therefore advisable to configure the FDB schema such that as few parallel processes as possible share the same keys, as is done in the NWP I/O workflows considered in this paper. Alternatively, it would be possible to extend this design such that each writing process uses its own unique Key-Value, in a similar way to the POSIX catalogue backend, although this would significantly increase implementation complexity.

The root and dataset Key-Values in this implementation primarily make the fields efficiently findable and listable. By having its own container, entire datasets can be easily and efficiently removed, facilitating the use of the FDB as a rolling archive.

When `retrieve()` is called, the root pool and container are opened. The dataset key is looked up in the root Key-Value to identify the corresponding container and dataset Key-Value. The collocation key is then looked up in this dataset Key-Value to identify the index Key-Value in the same way. Finally the element key is looked up in the index Key-Value and, if found, the field location descriptor is returned.

The `list()` method makes use of the information stored in the Axis Key-Values. The Axis object is compared against the query and the index Key-Value is skipped if nothing contained in it matches the query. As axis information is cached in the calling process, it may become out of date and need to be purged, but the FDB guarantees that any fields written before the last `flush()` will be correctly visible to any tasks started after.

The transactionality of the `daos_kv_put` and `daos_kv_get` operations on the Key-Value objects is critical to ensuring consistency of indexes under `archive()` and `retrieve()` contention, and to ensuring that such contention is resolved on the DAOS server.

Although any concurrent writer and reader processes interact with the root and dataset Key-Values, contention on these Key-Values is avoided by caching the relevant entries in the reader process pathway, and excessive load from `archive()`ing processes can be avoided by using only a few different dataset and collocation keys in every writer's lifetime. These approaches and design decisions mean that index Key-Values remain as the objects where most of the contention occurs.

4 PERFORMANCE ASSESSMENT

Performance and scalability tests have been carried out comparing the new DAOS FDB backend to the existing POSIX backend using DAOS and Lustre installed on the same hardware resources. The same test configurations were also run through the Field I/O benchmark[11], a standalone benchmark tool developed to evaluate the performance of DAOS without involving the full complexity of ECMWF's I/O stack while reproducing the I/O operations and patterns the DAOS backend requires.

4.1 Test system

Tests have been carried out on NEXTGenIO[13], a research HPC system composed of 34 dual-socket nodes with Intel Xeon Cascade Lake processors. Each socket has six 256 GiB first-generation Intel® Optane™ Data Centre Persistent Memory Modules[32][33]

(DCPMs) configured in AppDirect interleaved mode. There are no NVMe devices. Each processor is connected via its own integrated network adapter to a low-latency OmniPath fabric. Each of these adapters has a maximum bandwidth of 12.5 GiB/s.

The fabric is configured in dual-rail mode. That is, a separate network for each processor socket on a node, meaning there are two high performance networks per node. The HPC system nodes use CentOS7 as the operating system, with DAOS v2.4.

For the DAOS benchmarking, DAOS has been deployed on different numbers of storage nodes with a single DAOS engine per socket (i.e. two per node), using the full ext4 file system on the Optane SCM for that socket. Each socket uses the associated fabric interface and interleaved SCM devices, with 12 targets per engine. DAOS does not support using PSM2, a low-latency communication protocol implementing RDMA on OmniPath. Instead, it was configured to use the TCP protocol.

Lustre has been deployed as well on different numbers of storage nodes, with one OST per socket, plus one node devoted to the metadata service. Both the OSTs and the MDTs used in the file system mount an ext4 file system on the SCM attached to their respective sockets, providing 1.5 TB of high-performance storage per OST and MDT, with servers and clients connected using the high performance PSM2 communication library.

Up to 20 nodes have been employed to execute the benchmark client processes using both sockets and network interfaces. SCM in the client nodes was not used and did not have any effect on I/O performance.

4.2 Benchmark

`fdb-hammer` is an FDB performance benchmarking tool provided in the FDB Git repository[10], which can be built alongside the other FDB command-line tools.

`fdb-hammer` takes a single GRIB field, supplied on the command line, and uses its encoded metadata as a template to generate a sequence of fields to be archived, retrieved or listed. `fdb-hammer` processes are independent without synchronisation with any other parallel processes. In this manner it simulates the behaviour of model I/O server processes which write independent streams of data to the FDB, and the behaviour of post-processing tools which also read independently. It creates an “I/O pessimised” benchmark – i.e. a worst possible case for I/O as all relevant computation has been removed.

`fdb-hammer` is configured with a series of command line arguments (including `--class`, `--expver` and `--nlevels`) specifying the span of metadata to be iterated during the run. Most significantly `--nsteps` controls the values of the `step` keyword in the metadata and therefore, if `fdb-hammer` is invoked in its archive mode, it also controls the number of times `flush()` is called and the number of fields written in sequence between flushes.

A number of benchmark scripts[34] have been used which invoke `fdb-hammer` in parallel at different scales to mimic I/O patterns in ECMWF's operational workflow. Each of the invoked `fdb-hammer` processes outputs timestamps and profiling statistics which are aggregated to produce the following results.

4.3 Methodology

The methodology in this performance analysis is based on ECMWF's DAOS preliminary assessment with Field I/O[11]. It considers:

- (1) How bandwidths should be calculated
- (2) Different I/O patterns of interest
- (3) How to optimise benchmark and system parameters for performance and reproducibility
- (4) How to scale the storage system and benchmark runs

Regarding (1), bandwidth calculations are made from the total volume of data transferred (written or read) and the time elapsed between the first benchmark I/O start time to the last benchmark I/O end time. This is known as *global timing bandwidth*.

Regarding (2), only *access pattern A* (as defined in [11]) has been considered. A writing phase is run first, where *fdb-hammer* is run in parallel from a number of parallel processes in its archive mode, and each process archive()s a sequence of fields with different metadata identifiers. Following this, *fdb-hammer* is executed in *retrieve()* mode from the same number of processes. There is no contention between writers and readers as they run sequentially, and so it is referred to as *no w+r contention* hereafter.

A variant of that access pattern has also been considered, in which a writer phase is run initially to populate the storage, and then a writer and a reader phase are run simultaneously. In this variant there is contention between writers and readers but, in contrast to the *pattern B* defined in [11], the processes write and read a sequence of fields with different metadata rather than repeating the same metadata. This pattern is referred to as *w+r contention*.

Considering (3) Optimising the benchmark and system parameters, given such a wide possible parameter space, has been challenging. The parameter optimisation strategy outlined in [11] has been followed in this analysis. Firstly, an appropriate run length is determined. The benchmark is run against a fixed system with fixed configuration, only varying the number of fields to be written per process, which is increased progressively until the variability in bandwidth measurements becomes small (less than 5%). This helps balance test reproducibility whilst also keeping runtimes as short as possible.

After this, the client-to-server node ratio and the number of benchmark processes per client node are varied to find the point of diminishing returns, where the server connections approach saturation and adding additional client nodes or processes has little benefit. Note that each additional process added increases the overall I/O size of the benchmark as the fields written per process is now fixed.

Once these parameters are fixed, the I/O startup timestamps are the analysed to ensure that all processes in the benchmark are really working in parallel. If this is not true, the startup processes of the benchmark should be modified, the number of fields written needs to be increased further to minimise the impact of startup time, or explicit I/O startup synchronisation needs to be implemented.

Following this, the backend specific parameters can be tested and optimised, including in this case DAOS object class, Lustre file striping, FDB schema optimisations, and others.

Regarding (4), the number of nodes employed for the storage system can be increased progressively, and the benchmark can be

run at each scale with a corresponding number of client nodes (according to the selected client-to-server-node ratio), with all access patterns of interest. The bandwidths obtained for the sequence of steps will provide insight into the scaling behaviour for the different access patterns, as more resources are employed for the storage system and the benchmark application.

5 RESULTS

5.1 Parameter Optimisation

Following the described methodology, *fdb-hammer* was run first with the DAOS backends with *no w+r contention*, from 16 NEXTGenIO nodes, each node executing 32 parallel *fdb-hammer* processes, and with a DAOS system deployed on 8 nodes. The size of the fields written and read was set to 1 MiB.

Writing 2000 fields per process was found to reduce variance in bandwidth measurements down to approximately 5%. Each *fdb-hammer* process was configured to make these 2000 iterations correspond to 10 steps, 10 parameters, and 20 model levels for a single dataset and member. 2000 fields per process was also found to be suitable with the POSIX backend running on Lustre deployed on 8+1 nodes. Despite this, occasional outlier benchmark runs were observed varying by more than 10% from the mean when using the POSIX backend. To identify any potential further outliers, all tests in this paper were repeated 3 times. In the end outliers were found to be very rare and were not analysed further, and the 3 bandwidth results for each test were averaged.

Once the tests were fixed at 2000 fields per process, they were repeated, varying the client-to-server-node ratio and the number of benchmark processes per client node. The results for both the DAOS and the POSIX backends are shown in Fig. 3.

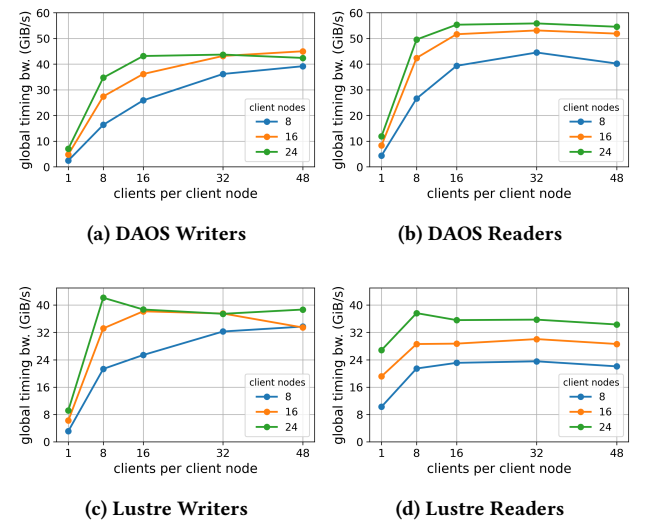


Figure 3: Bandwidth results for *fdb-hammer/DAOS* (8 server nodes; top row) and *fdb-hammer/Lustre* (8+1 server nodes; bottom row) runs. No w+r contention.

For both DAOS and Lustre runs, a client-to-server-node ratio of 3 (i.e. 24 client nodes for the 8-server-node setup) does not result in

significantly higher bandwidths compared to a ratio of 2, whereas a ratio of 2 results in substantially higher bandwidths than those obtained with a ratio of 1. This suggests a ratio of 1 is not sufficient to saturate the server-side network interface cards. A ratio of 2 has been chosen for most of the tests in the rest of the analysis.

Regarding client process counts, bandwidths generally saturate at 16 or 32 processes per node. Lustre bandwidths saturate at lower client process counts, probably because Lustre is using the PSM2 protocol – which implements Remote Direct Memory Access (RDMA) over the OmniPath network adapters – for efficient communications, whereas DAOS uses the TCP protocol. This issue is analysed in more detail in [11].

Where 8 or more server nodes have been employed, process counts of 16 and 32 have been used for all DAOS and Lustre tests. Where fewer than 8 server nodes were employed, process counts of 32 and 48 were chosen as they were found to result in the highest bandwidths.

The tests were then re-run at the largest scale allowed by the test system (20 client nodes and 12 server nodes, 12+1 for Lustre), and the timestamps output by the benchmark were analysed to identify any potential delays in I/O start up across processes. The detail of the methodology followed to address this can also be found in [11]. No substantial delays were identified.

At this point, other relevant configuration options were tested using the *no w+r contention* pattern with 20 client nodes and 12 server nodes (12+1 for Lustre). A DAOS object class of OC_S1 for DAOS Arrays resulted in the best performance, as anticipated in the preliminary assessment[11], likely due to the relatively small field size in conjunction with the large number of processes accessing them concurrently in a benchmark run. For the FDB schema, it was found to be optimal to have the `number` and `levelist` identifiers at the collocation level for the DAOS backend, as shown in Fig. 2. This results in each process writing or reading from an exclusive set of index Key-Values, minimising contention. Having these dimensions at the element level performed best for the POSIX backend as writing processes already maintain independent indexes there.

It was not as straightforward to apply this optimisation methodology as this report might suggest. The DAOS backends were improved a few times, and configuration flaws were discovered and fixed both for the server and the benchmark, resulting in the procedure being repeated multiple times. Some examples of improvements and flaws that led to starting over were optimisations in the DAOS backends to avoid Array size checks in the read pathway; use of Arrays without attributes for more efficient opening and

creation in the write pathway; increasing the configured number of OIDs allocated per `daos_cont_alloc_oids` call in the DAOS backends; properly pinning client processes to both sockets to fully exploit the network interface cards; and using different releases of DAOS with varying performance.

5.2 Short Scaling Tests

Tests were run both with and without write/read contention to characterise the performance scalability of the system. The number of DAOS and Lustre server nodes employed for the fdb-hammer runs were increased gradually from 1 to 16 (plus one in Lustre deployments for the metadata server), preserving a client-to-server-node ratio of 2 where possible. The results are shown in Fig. 4, with DAOS bandwidths in dark blue, Lustre bandwidths in orange, and results obtained with the Field I/O benchmark[11] in light blue which provide insight on the bandwidths that should be achievable with the DAOS backends.

For configurations with 10 or fewer server nodes the client-to-server-node ratio of 2 was satisfied. With 12 server nodes only 20 client nodes were available, and above this a client-to-server-node ratio of 1 was used due to the limited nodes available in the system. These reduced configurations, which obtain a lower bandwidth than the server nodes could provide, have been marked in the figure with hollow dots. For the *w+r contention* runs, half of the client nodes were employed as writers and the other half as readers

The DAOS and the Lustre backends perform fairly similarly, with DAOS generally achieving slightly higher bandwidths except when writing in the absence of any contention where Lustre performs best. It is encouraging that the DAOS backends attain similar bandwidths to those observed in Field I/O runs.

Results for both backends scale well but sub-linearly as the number of server nodes increases. Although the sharp decline in bandwidth at higher server node counts was expected (due to the reduced client node counts) this does not fully explain the gentle plateauing which was also observed in the Field I/O results. That plateauing was unexpected because nearly identical runs had been performed a few months ago (those reported in [11], Fig. 7), and no performance decline was observed then. This change in scaling behaviour in Field I/O runs is most likely due to a DAOS version upgrade from v2.0.1 in [11] to v2.4 in this paper. We can also see from the results that DAOS provides improved performance compared to Lustre in the scenario with contention, especially for writer tasks, except where the ideal client-to-server node ratio was not fulfilled.

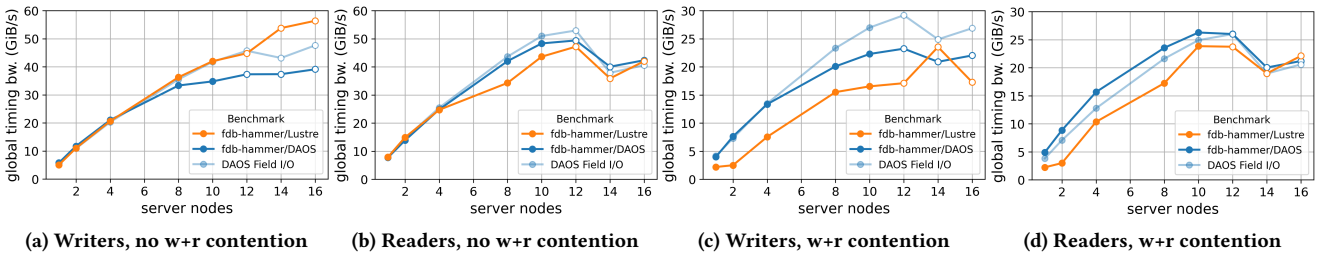


Figure 4: Bandwidths observed in short fdb-hammer and Field I/O runs without and with write/read contention.

To get further insight into the performance characteristics of the DAOS backend, profiling information was collected from `fdb-hammer` for some of the runs with 12 server nodes, which is analysed and summarised in Fig. 5. Whereas most of the time was spent in `daos_array_write` and `daos_array_read` calls, which is a good sign that the transfer of data across the network and persisting into storage devices predominated, a significant amount of time is spent in one-off establishment of DAOS pool and container connections, as well as in other pool operations and other one-off FDB overheads, particularly in the `fdb-hammer` writers. These overheads should become less significant in operational workloads where the processes operate for time periods one or two orders of magnitude longer than in the short `fdb-hammer` runs tested.

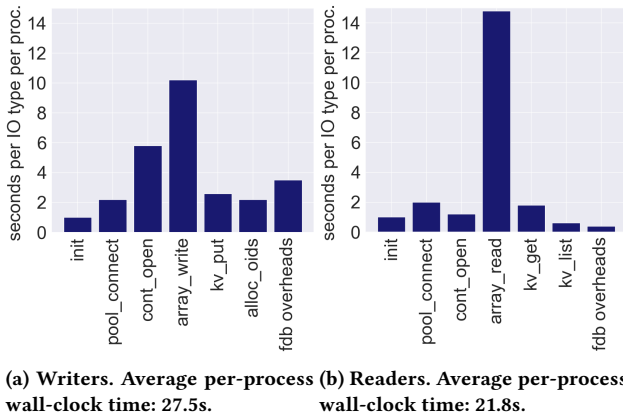


Figure 5: Profiling results for fdb-hammer/DAOS runs (12 server and 20 client nodes; 32 processes per client node).

5.3 Longer Scaling Tests

The scalability assessment was repeated using longer runs of 10,000 fields per process, to attempt to minimise the impact of the one-off overheads and analyse something more reflective of a real I/O workload. Each `fdb-hammer` process was configured to use 100 steps, 10 parameters, and 10 model levels for a single dataset and member. The results are shown in Fig. 6.

The longer runs scale essentially linearly in most configurations as more server nodes are added. It is interesting to see how all three benchmarks perform very similarly for (a), write with *no w+r contention*, achieving similar bandwidths to the IOR/DAOS benchmarking performed on the same system and reported in [11]. This indicates that all three benchmarks are making efficient use of the underlying storage in the absence of contention.

For (b), read with *no w+r contention*, the DAOS backend again shows very good scalability reaching close-to-IOR bandwidths. The POSIX backend performs significantly worse, and this is due to the design choices made in that backend to benefit write performance at the expense of read performance, as explained in Section 1.3.

`fdb-hammer` with the DAOS backends generally reaches slightly higher bandwidths than were achieved with Field I/O. This is due to some optimisations implemented in the FDB DAOS backends which were not implemented in Field I/O, particularly the use of

`daos_array_open_with_attrs` on write and avoiding unnecessary `daos_array_get_size` calls on read.

In (c) and (d), with *w+r contention*, DAOS performs remarkably well with nearly linear scaling, whereas Lustre shows 50% lower bandwidths with a marked performance decline starting at 4 server nodes, presumably due to file locking overheads.

These excellent results demonstrate that the new object store semantics and contention resolution mechanisms in DAOS can enable high I/O performance at scale in ECMWF's operations and potentially in other applications with strong I/O contention.

Although the full contention and the reader view transposition in operational NWP, described in Section 1.2, could not be reproduced exactly in the benchmarking reported here (mostly due to the non-synchronised nature of `fdb-hammer`), they were partially captured in both DAOS and Lustre runs. We expect that a full reproduction of such contention would result in lower Lustre bandwidths relative to DAOS, as the locking overheads would become more prominent.

For the reported *no w+r contention* long runs with the DAOS and POSIX backends, `fdb-hammer` was also run in its `list()` mode to compare the listing performance of both backends. `fdb-hammer` was configured to list all indexed fields for the first step archived in the write phase, and executed from a single node. Listing with the POSIX backend was consistently double as fast as with the DAOS backend, for all server node configurations. This is explained by the fact that the POSIX backend collocates all indexed field identifiers and locations for a same collocation key in a single file per process, and these files are loaded by the listing backend with a single read operation per file. In the DAOS backend, instead, every single indexed field location needs to be retrieved with a `daos_kv_get` operation, inflicting a large amount of I/O operations and causing strain on the DAOS server.

6 CONCLUSION

This work has demonstrated the feasibility of implementing Catalogue and Store backends for the FDB making use of DAOS, and presenting the same external semantics and API as the existing FDB backends. The performance of the new backends was tested, and we present a series of comparative scaling curves against our existing implementations running on top of a Lustre parallel file system on the same hardware.

Although implementing the same API, the new backend has some special characteristics. Most notably it immediately persists and makes data visible rather than waiting until explicit `flush()` calls, and all data are indexed together rather than in one index per writing process. These should allow more aggressive workflow optimisation, and should support better scaling of read and listing semantics going forward. It is worth noting that obtaining optimal performance required adjusting the data schema, and thus the structure of the data indexing, between the backends.

The most relevant metrics obtained for operational NWP are the performance and scaling of runs with I/O patterns matching those in the forecast pipeline, with contention between simultaneously active readers and writers. Under these conditions, the DAOS backends have demonstrated higher throughput and better scaling than runs carried out using the POSIX backends on top of Lustre, on the same hardware. This argues strongly that the combination

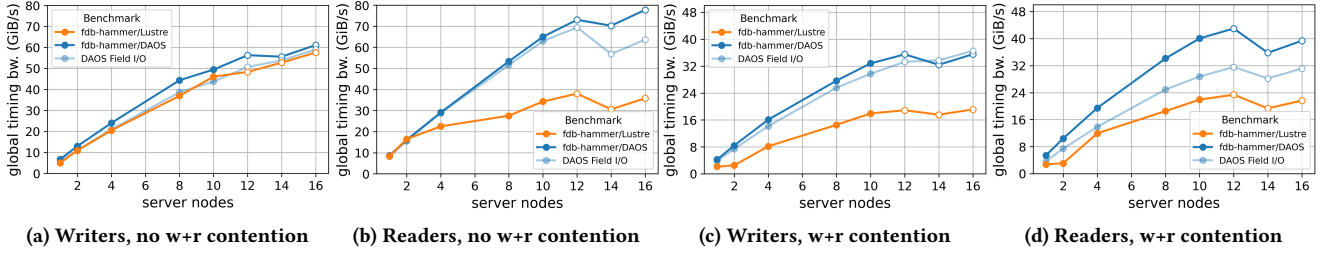


Figure 6: Bandwidths observed in long fdb-hammer and Field I/O runs without and with write/read contention.

of the object storage semantics in DAOS, and the existence of the Key-Value objects in which contention is resolved locally on the DAOS server, give performance benefits over the mechanisms that can be built on top of distributed POSIX file systems.

The performance of the new DAOS backends tracks very closely to that of the Field I/O benchmark, which mimics the I/O approach used. This strongly confirms that the implemented backends are performing as expected, in line with the design aspirations.

The methodology applied in the performance analysis is well defined, and in particular provides good guidance on how to approach the parameter optimisation required when exploring such an extensive parameter domain. It is sufficiently general that it can be used to guide assessment of other I/O systems and developments.

We are thrilled by the outcome of this work, which has demonstrated the potential of DAOS for ECMWF and NWP workloads, and potentially for any other data-intensive workloads requiring relatively small object sizes or a high degree of contention. This opens new doors for ECMWF to consider a wider range of storage systems for operations in the future. In the immediate future we expect to test DAOS and the FDB backends on larger systems with an I/O configuration more closely matching actual operational use. Beyond this work, we are actively involved in research to enhance and extend high-performance workflows with semantically driven data movements and access, which this research will contribute to[35–38].

ACKNOWLEDGMENTS

The work presented in this paper was carried out with funding by the European Union under the Destination Earth initiative (cost center DE3100, code 3320) and relates to tasks entrusted by the European Union to the European Centre for Medium-Range Weather Forecasts. Views and opinions expressed are those of the author(s) only and do not necessarily reflect those of the European Union or the European Commission. Neither the European Union nor the European Commission can be held responsible for them.

This work has also been contributed to by the ACROSS and IO-SEA projects, funded by the European High-Performance Computing Joint Undertaking (JU) under Grant Agreements no. 955648 and no. 955811, respectively. The JU receives support from the European Union's Horizon 2020 research and innovation programme and Italy, France, Czech Republic, Greece, Netherlands, Germany, Norway.

The NEXTGenIO system was funded by the European Union's Horizon 2020 Research and Innovation program under Grant Agreement no. 671951, and supported by EPCC, The University of Edinburgh. Adrian Jackson was supported by UK Research and Innovation under the EPSRC grant EP/T028351/1.

For the purpose of open access, Adrian Jackson has applied a Creative Commons Attribution (CC BY) licence to any Author Accepted Manuscript version arising from this submission.

REFERENCES

- [1] "About Our Forecasts", 2024. <https://www.ecmwf.int/en/forecasts/documentation-and-support>
- [2] P. Bauer, A. Thorpe, and G. Brunet, "The Quiet Revolution of Numerical Weather Prediction", *Nature* 525, 47–55 (2015). <https://doi.org/10.1038/nature14956>
- [3] "Lustre Best Practices", 2024. https://www.nas.nasa.gov/hecc/support/kb/lustre-best-practices_226.html
- [4] "The Open Group Base Specifications Issue 7, 2018 edition", 2024. <https://pubs.opengroup.org/onlinepubs/9699919799/2018edition/>
- [5] G. Lockwood, "What's so bad about POSIX I/O?", *The Next Platform* 2017. <https://www.nextplatform.com/2017/09/11/whats-bad-posix-io/>
- [6] A. K. Paul, O. Faaland, A. Moody, E. Gonsiorowski, K. Mohror, and A. R. Butt, "Understanding HPC Application I/O Behavior Using System Level Statistics", 2020 IEEE 27th International Conference on High Performance Computing, Data, and Analytics (HiPC), Pune, India, 2020, pp. 202–211, doi: 10.1109/HiPC5069.2020.00034.
- [7] F. Schmuck, and R. Haskin, "GPFS: A Shared-Disk File System for Large Computing Clusters", 2002. https://www.usenix.org/legacy/publications/library/proceedings/fast02/full_papers/schmuck/schmuck_html/index.html
- [8] A. George, and R. Mohr, "Understanding Lustre Internals", 2024. https://wiki.lustre.org/Understanding_Lustre_Internals
- [9] S. Smart, T. Quintino, and B. Raoult, "A Scalable Object Store for Meteorological and Climate Data". In Proceedings of the Platform for Advanced Scientific Computing Conference (PASC '17). Association for Computing Machinery, New York, NY, USA, Article 13, 1–8. DOI:10.1145/3093172.3093238.
- [10] "FDB", 2024, GitHub repository. <https://github.com/ecmwf/fdb>
- [11] N. Manubens, T. Quintino, S. D. Smart, E. Danovaro, and A. Jackson, "DAOS as HPC Storage: a View From Numerical Weather Prediction", 2023 IEEE International Parallel and Distributed Processing Symposium (IPDPS), St. Petersburg, FL, USA, 2023, pp. 1029–1040, doi: 10.1109/IPDPS54959.2023.00106.
- [12] Z. Liang, J. Lombardi, M. Chaarawi, and M. Hennecke, "DAOS: A Scale-Out High Performance Storage Stack for Storage Class Memory", In: Panda, D. (eds) Supercomputing Frontiers. SCFA 2020. Lecture Notes in Computer Science(), vol 12082. Springer, Cham. DOI:10.1007/978-3-030-48842-0_3.
- [13] "NEXTGenIO User Guide and Applications", 2024. <https://ngioproject.github.io/nextgenio-docs/html/index.html>
- [14] J. Liu, Q. Koziol, G. Butler, N. Fortner, M. Chaarawi, H. Tang, S. Byna, G. Lockwood, R. Cheema, K. Kallback-Rose, D. Hazen, and Mr. Prabhat, "Evaluation of HPC Application I/O on Object Storage Systems", 2018. 24–34. 10.1109/PDSW-DISCS.2018.00005.
- [15] J. Lofstead, I. Jimenez, C. Maltzahn, Q. Koziol, J. Bent, and E. Barton, "DAOS and Friends: A Proposal for an Exascale Storage System", SC '16: Proceedings of the International Conference for High Performance Computing, Networking, Storage and Analysis, Salt Lake City, UT, USA, 2016, pp. 585–596, doi: 10.1109/SC.2016.49.
- [16] A. Jackson, and N. Manubens, "DAOS as HPC Storage: Exploring Interfaces", Proceedings of 3rd Workshop on Re-envisioning Extreme-Scale I/O for Emerging

- Hybrid HPC Workloads (REX-IO), 2023
- [17] M. Hennecke, "Understanding DAOS Storage Performance Scalability", 2023. In Proceedings of the HPC Asia 2023 Workshops (HPC Asia '23 Workshops). Association for Computing Machinery, New York, NY, USA, 1–14. <https://doi.org/10.1145/3581576.3581577>
- [18] J. Soumagne, J. Henderson, M. Chaarawi, N. Fortner, S. Breitenfeld, S. Lu, D. Robinson, E. Pourmal, and J. Lombardi, "Accelerating hdf5 i/o for exascale using daos", 2021. IEEE Transactions on Parallel and Distributed Systems 33, 4 (2021), 903–914.
- [19] R. S. Venkatesh, G. Eisenhauer, S. Klasky, and A. Gavrilovska, "Enhancing Metadata Transfer Efficiency: Unlocking the Potential of DAOS in the ADIOS context". In Proceedings of the SC '23 Workshops of The International Conference on High Performance Computing, Network, Storage, and Analysis (SC-W '23). Association for Computing Machinery, New York, NY, USA, 1223–1228. <https://doi.org/10.1145/3624062.3624193>
- [20] A. Aghayev, S. Weil, M. Kuchnik, M. Nelson, G. R. Ganger, and G. Amvrosiadis, "File systems unfit as distributed storage backends: lessons from 10 years of Ceph evolution". In Proceedings of the 27th ACM Symposium on Operating Systems Principles (SOSP '19). Association for Computing Machinery, New York, NY, USA, 353–369. <https://doi.org/10.1145/3341301.3359656>
- [21] R. R. Chandrasekar, L. Evans, and R. Wespertal, "An Exploration into Object Storage for Exascale Supercomputers". Cray User Group 2017.
- [22] J. Lüttgau, M. Kuhn, K. Duwe, Y. Alforov, E. Betke, J. Kunkel, and T. Ludwig, "Survey of storage systems for high-performance computing", 2018. Supercomputing Frontiers and Innovations. 5. 31–58. 10.14529/js?180103.
- [23] A. Dilger, D. Hildebrand, J. Kunkel, J. Lofstead, G. Markomanolis, S. Ihara, and H. Nolte, "IO500 10 node list Supercomputing 2023", November 2023. <https://io500.org/list/sc23/ten-production>
- [24] "HPC IO Benchmark Repository", 2024, GitHub repository. <https://github.com/hpc/ior>
- [25] N. Manubens, S.D. Smart, T. Quintino, and A. Jackson, "Performance Comparison of DAOS and Lustre for Object Data Storage Approaches", 2022. IEEE/ACM International Parallel Data Systems Workshop (PDSW), 7–12.
- [26] "Access to Archive Datasets", 2024. <https://www.ecmwf.int/en/forecasts/access-forecasts/access-archive-datasets>
- [27] S. Smart, T. Quintino, and B. Raoult, "A High-Performance Distributed Object-Store for Exascale Numerical Weather Prediction and Climate". In Proceedings of the Platform for Advanced Scientific Computing Conference (PASC '19). Association for Computing Machinery, New York, NY, USA, Article 16, 1–11. DOI:10.1145/3324989.3325726.
- [28] B. Medjahed, M. Ouzzani, and A. Elmagarmid, "Generalization of ACID Properties", 2009. Cyber Center Publications. Paper 97. <http://docs.lib.psu.edu/ccbpubs/97>
- [29] "DAOS Foundation", 2024. <https://foundation.daos.io>
- [30] "DAOS Architecture", 2024. <https://docs.daos.io/latest/overview/architecture>
- [31] "DAOS File System", 2024. <https://docs.daos.io/v2.4/user/filesystem/>
- [32] D. Waddington, M. Kunitomi, C. Dickey, S. Rao, A. Abboud, and J. Tran, "Evaluation of intel 3D-xpoint NVDIMM technology for memory-intensive genomic workloads". In Proceedings of the International Symposium on Memory Systems (MEMSYS '19). Association for Computing Machinery, New York, NY, USA, 277–287. <https://doi.org/10.1145/3357526.3357528>
- [33] A. Jackson, "Evaluating the latest Optane memory: A glorious swansong?", 2023. 4th Workshop on Heterogeneous Memory Systems (HMEM 2023), SC23.
- [34] N. Manubens, A. Jackson, T. Quintino, S. Smart and E. Danovaro, "DAOS weather field I/O tests", 2024, GitHub repository ecmwf-projects/daos-tests (0.2.0). DOI:10.5281/zenodo.10699254.
- [35] "Destination Earth", 2024. <https://destination-earth.eu>
- [36] "Warm World", 2024. <https://warmworld.de>
- [37] "OpenCUBE", 2024. <https://horizon-opencube.eu>
- [38] "European Pilot for Exascale", 2024. <https://eupex.eu>

Appendix D – Exploring DAOS Interfaces and Performance

Exploring DAOS Interfaces and Performance

Nicolau Manubens

*European Centre for Medium-Range
Weather Forecasts (ECMWF)*
nicolau.manubens@ecmwf.int

Johann Lombardi

DAOS Foundation

Simon D. Smart

ECMWF

Emanuele Danovaro

ECMWF

Tiago Quintino

ECMWF

Dean Hildebrand

Google

Adrian Jackson

*EPCC, The University of
Edinburgh*

Abstract—Distributed Asynchronous Object Store (DAOS) is a novel software-defined object store leveraging Non-Volatile Memory (NVM) devices, designed for high performance. It provides a number of interfaces for applications to undertake I/O, ranging from a native object storage API to a DAOS FUSE module for seamless compatibility with existing applications using POSIX file system APIs.

In this paper we discuss these interfaces and the options they provide, exercise DAOS through them with various I/O benchmarks, and analyse the observed performance. We also briefly compare the performance with a distributed file system and another object storage system deployed on the same hardware, and showcase DAOS' potential and increased flexibility to support high-performance I/O.

Index Terms—object storage, DAOS, I/O interfaces, I/O performance, HPC, cloud, Lustre, Ceph

I. INTRODUCTION

The Distributed Asynchronous Object Store (DAOS) [1] is a novel software-defined object store designed for high-performance Input-Output (I/O) to distributed Non-Volatile Memory (NVM) devices. It currently provides a relevant alternative to traditional POSIX distributed/parallel file systems in an HPC context after having scored top positions in recent editions of the I/O 500 [2].

Distributed file systems need to be used carefully by applications to achieve optimal storage performance and ensure consistency of stored data under contention between reading and writing processes. Even then, there is a concern that these systems may not scale to extreme workloads due to fundamental design aspects, including metadata prescriptiveness, sustained involvement of the operating system, block-level operation, distributed locking to ensure client cache coherency, and potentially centralised metadata serving [3] [4] [5] [6].

DAOS was designed from the ground up with these concerns in mind, and addresses them by having low metadata requirements on objects, operating fully in user space, providing byte-addressable access to data, implementing lockless contention resolution, and serving metadata in a fully distributed manner across all storage server nodes.

There are different interfaces provided for applications to interact with a DAOS system.

One of them is the libdaos library which provides an object storage API. This includes Array functionality, intended

for bulk storage of large one-dimensional data arrays, and dictionary-like Key-Value functionality. Key-Values provide a mapping between keys (limited-length strings) and values (arbitrary-length data) that can be queried. Key-Value and Array objects must be created within a DAOS container, which provides an isolated object namespace and transaction history. Upon creation, objects are assigned a 128-bit unique object identifier (OID), of which 96 bits are user-managed. The sharding, replication, and erasure-coding of these objects can be controlled by specifying their object class on creation. If configured with any of these options, they are transparently stored entirely or by parts across different storage devices and nodes thus enabling efficient concurrent access.

Because porting existing POSIX I/O applications to libdaos is a daunting task, DAOS also provides the libdfs library which implements POSIX directories, files and symbolic links on top of the libdaos APIs. An application using this library can perform common file system calls which are transparently mapped to DAOS, with only minor modifications required. libdfs is not fully POSIX-compliant but supports the majority of existing POSIX-based applications.

A DAOS FUSE (file system in user space) daemon (DFUSE) is also provided which allows users to mount and expose a DAOS system through the standard POSIX infrastructure, enabling existing POSIX applications to operate on DAOS without modification. The DFUSE mount command supports several options, e.g. to specify the number of FUSE and event queue threads [7], or to configure caching of file system data and metadata in the client nodes.

DFUSE can show limited performance under intensive small I/O workloads due to many round-trips required between kernel and user space. For these cases, an I/O interception library (IL), also provided with DAOS, can be used to forward operations directly to libdfs and reach optimal performance.

In this paper we present results from DAOS deployed on Google Cloud Platform (GCP) Virtual Machines (VMs; also referred to as instances or nodes) with locally attached NVMe SSDs, exercising the DAOS system through the available interfaces using a number of benchmark applications. We also tested the data protection features DAOS supports. With the obtained measurements, we analysed the performance and scalability of the different interfaces and options.

II. METHODOLOGY

To analyse the performance DAOS can provide when accessed via the different available interfaces, we deployed DAOS on GCP instances with locally attached NVMe SSDs and ran a selection of benchmark applications, introduced in II-A, on separate instances. When run, the benchmarks output timestamp information that we used to calculate bandwidths and compare and discuss performance.

All selected benchmarks first execute a write phase followed by a read phase, and can be configured to run across multiple processes and nodes. Some benchmarks (e.g. IOR) can be configured such that each parallel process performs bulk I/O to a single object or file. As this I/O pattern executes small amounts of metadata operations and generally requires little logic to be triggered in the storage system, such benchmarks typically reach the maximum I/O bandwidths the storage system — in this case DAOS — can provide. We ran these benchmarks with DAOS data protection disabled, measured the achieved bandwidth, and compared this to the raw bandwidths available from the underlying storage and network hardware (as measured with lower-level tools).

Some of the benchmarks or configurations can trigger more complex I/O workloads with smaller object sizes or performing more metadata or Key-Value operations, and we used these to gain insight into the strengths and weaknesses of the storage system when under more realistic or complex workloads.

There are many options and parameters which may be adjusted when deploying DAOS on the server VMs and running the benchmarks on the client VMs, for which we made use of support from DAOS and Google Cloud experts. For the exploration of parameters in the benchmark runs, we tested every benchmark with different client node and process counts to determine the maximum achievable bandwidth, as outlined in [8] and [9]. We then ran all benchmarks using the optimal node and process counts against DAOS servers deployed on increasing numbers of instances, to assess the scalability of DAOS and the benchmarks. Finally, we reran some of the benchmarks with DAOS data redundancy enabled.

Each benchmark run took between 1 and 20 minutes of wall-clock time, depending on the scale, thus providing insight on short-term performance rather than long-term stability.

We applied a common bandwidth definition for the calculation of all bandwidths reported in III: the amount of data transferred (written or read) divided by the wall-clock time elapsed between the start of the first I/O operation and the end of the last I/O operation. Each and every test was repeated 3 times, and the average and standard deviation of the measured bandwidths are shown in the figures for each test.

A. Benchmarks

1) *IOR* [10]: is a popular open-source I/O benchmark developed by the HPC community, originally intended to measure the I/O performance of parallel file systems, but expanded over time with new I/O backends to support operation on other storage systems like DAOS and Ceph. It runs as a parallel MPI application, where the concurrent processes create a file

or object each, wait for each other, and commence issuing a sequence of write or read operations. IOR can be configured to have all processes operate against a single shared file, a file per process, to adjust the number and size of operations per process and their distribution in the file, and to reproduce other common I/O patterns and approaches.

2) *HDF5* [11]: is a library for efficient storage of complex and voluminous data sets used in a range of disciplines, and supports features such as data compression and encryption. HDF5 operates, by default, on POSIX file systems, but has adaptors to support operation on other storage systems including DAOS [12]. The IOR benchmark has a backend that uses HDF5, allowing benchmarking of HDF5 approaches with IOR. When IOR is run with the HDF5 backend on POSIX, a file is created per writer process, where the process metadata, indexing information, and data are stored. If the DAOS adaptor is enabled, a DAOS container is created per writer process, and the data from every write operation stored in a separate object in the container. This makes the HDF5 approach with IOR a more complex set of I/O patterns than those performed when using POSIX or DAOS backends.

3) *Field I/O* [13]: is a standalone benchmark tool developed by ECMWF to evaluate the performance a DAOS system can provide for Numerical Weather Prediction (NWP) operations at the centre, without involving the full complexity of their operational I/O stack. It runs as a set of independent processes, each writing and indexing a sequence of weather variables, or fields, into DAOS with a combination of libdaos Array and Key-Value operations. If configured in read mode, the processes retrieve the same sequence of fields by querying the Key-Values and reading the Array data. Field I/O processes write each field in a separate Array, and store indexing information in a set of Key-Values — some of them exclusive to the process, and some of them shared amongst all processes.

4) *fdb-hammer* [14]: is a benchmark tool to measure the performance of ECMWF's domain-specific object store, the FDB [15]. FDB implements transactional and efficient weather field storage and indexing on a number of storage systems, including POSIX file systems, DAOS, and Ceph. FDB exposes a scientifically meaningful API for applications to archive and retrieve weather fields without requiring knowledge of the underlying storage system, effectively abstracting it away.

fdb-hammer runs as a set of independent processes, each archiving or retrieving (depending on the selected access mode) a sequence of weather fields via FDB. When run with FDB's DAOS backend, *fdb-hammer* uses a set of libdaos Arrays and Key-Values to store and index the weather fields, in a similar way as Field I/O. When run with FDB's POSIX backend, *fdb-hammer* writer processes create a pair of files each, which are expanded incrementally with indexing information and field data, respectively. Writer processes accumulate small chunks of data in client memory, that are persisted periodically into the file system in large blocks to achieve optimal write performance, with the aim of avoiding throttling ECMWF's NWP model in operations. Reader processes repeatedly open and read, for every field in the sequence, the corresponding

files containing the index and field data, resulting in substantial metadata and small I/O operation workloads.

B. Test system

All tests were conducted on Google Cloud Platform (GCP) infrastructure. For the DAOS deployments we used VMs of a custom type [16] n2-custom-36-153600, each with 36 logical cores, 150 GiB of DRAM, 6 TiB of local NVMe SSDs distributed in 16 logical devices, and a 50 Gbps network adaptor.

The benchmarks were run in VMs of type n2-highcpu-32, each with 32 logical cores, 32 GiB of DRAM, and a 50 Gbps network adaptor. To exploit all available network bandwidth, we carefully pinned the benchmark processes evenly across all available cores, and configured all VMs with Simultaneous Multi-Threading (SMT) [17] enabled.

DAOS v2.4.1 libraries were installed both on the server and client side. The DAOS deployments had a single engine deployed per server VM, and each engine was configured to deploy 16 DAOS targets [18] in the VM — one per available NVMe SSD. DAOS was configured to use the DRAM in the VMs for metadata storage as there was no Storage Class Memory in these VMs.

Although GCP provides generic VMs, not necessarily hardware-tailored purely for HPC, it makes an excellent standard testbed to analyse software-side performance and scalability of storage systems such as DAOS. The same overall behaviour should be expected on systems using similar technology.

III. RESULTS

A. Hardware Bandwidth

The raw bandwidth of the NVMe SSDs on server instances for bulk I/O was measured by mounting each of the 16 drives in one of the instances as an ext4 file system and then running the `dd` command in parallel for all of them, first writing and then reading 1000 blocks of 100 MiB. The measurements showed 3.86 GiB/s of aggregate write bandwidth and 7 GiB/s of aggregate read bandwidth.

`iperf` was used to measure raw network bandwidth between client and server instances, which was found to match the expected 50 Gbps (6.25 GiB/s) in both directions.

These measurements indicated that every additional DAOS server instance employed in a DAOS deployment could at best provide an additional 3.86 GiB/s for write, limited by the SSD bandwidth, and 6.25 GiB/s for read, limited by the network.

B. API performance comparison

We deployed a DAOS system on 16 nodes with NVMe and ran IOR with the libdaos and libdfs backends, and with the POSIX backend on DFUSE and DFUSE with interception, varying client node and process count. IOR was configured to have each parallel process run a sequence of 10000 I/O operations (write or read) each of 1 MiB in a single Array or file per process. We selected an object class of SX (sharding across all targets) for the libdaos Arrays and files and directories in libdfs and DFUSE, as this was found to perform best. For DFUSE mounts, we configured 24 FUSE threads and 12

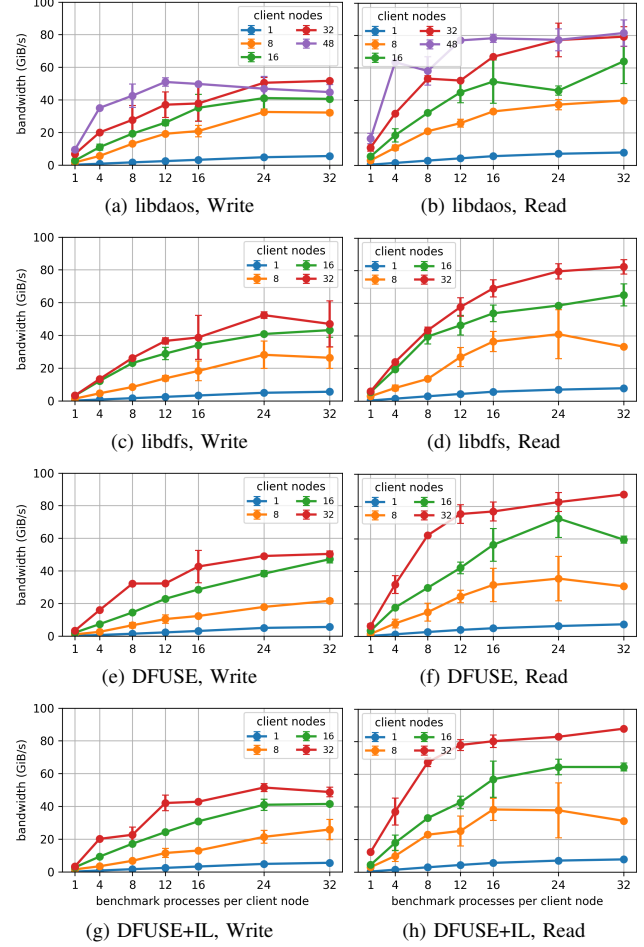


Fig. 1: Client node and process count optimisation results for IOR with the different DAOS APIs, against a 16-node DAOS instance.

event queue threads, and disabled all caching. The results are shown in Fig. 1.

Although there are slight differences in the performance behaviour with respect to the process count — i.e. the libdaos backend achieves higher bandwidths at lower process counts — all APIs generally behave similarly and can reach bandwidths of nearly 60 GiB/s for write and 90 GiB/s for read. These bandwidths are very close to the calculated optimum of 61.76 GiB/s for write and 112 GiB/s for read. 16 client nodes, that is, a ratio of 1-to-1 client-to-server nodes, are generally sufficient to approach the best bandwidths.

It is worth noting that the DFUSE interception library does not bring much benefit with the selected I/O size of 1 MiB. The benefit becomes very noticeable for smaller I/O sizes, as shown in Fig. 2, comparing the amount of I/O operations per second (IOPS) reached with DFUSE and DFUSE with IL using an I/O size of 1 KiB.

We then ran similar tests using the more complex benchmarks, including IOR with the HDF5 backend using POSIX through DAOS DFUSE with interception, IOR with the HDF5 backend configured with the DAOS adaptor operating natively on libdaos, and Field I/O and fdb-hammer both operating na-

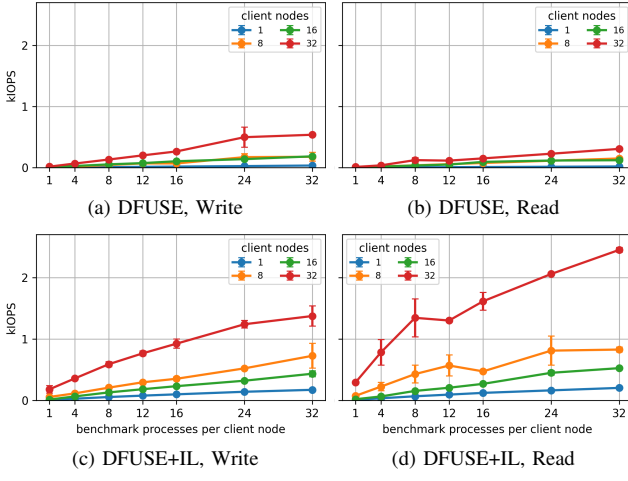


Fig. 2: Client node and process count optimisation results for IOR on DFUSE and DFUSE+IL with 1KiB I/O size, against a 16-node DAOS instance.

tively using libdaos. All were configured to perform equivalent I/O workloads as in previous IOR tests, that is, performing 10k I/O operations of 1 MiB per process. While HDF5 on POSIX uses a file per process, the rest of the applications use a separate DAOS Array for every I/O. We found the optimum object classes to be SX for files in HDF5 on POSIX and objects in HDF5 on libdaos; SX for Key-Values and S1 for Arrays in Field I/O; and S1 both for Key-Values and Arrays in fdb-hammer. The results are shown in Fig. 3.

Fig. 3 (e), (f), (g) and (h) show that both the Field I/O and fdb-hammer benchmarks perform very well, with similar I/O performance compared to the simple IOR runs. This is a great result showing that DAOS enables performance at scale even if using relatively small transfer and object sizes, and performing many Key-Value operations. The two benchmarks perform an average of 10 Key-Value operations (put or get) for each of the 10k objects accessed by each process, to provide a domain-appropriate index of the data written.

The bandwidth of the read mode in Field I/O increases linearly as the processes count is increased. This scaling is inferior to that shown by fdb-hammer. This is likely explained by the fact that fdb-hammer contains optimisations to avoid object size checks prior to every read operation, and Field I/O does not implement these.

HDF5 runs on DFUSE and libdaos, in Fig. 3 (a), (b), (c) and (d), show inferior bandwidths than the rest of the benchmarks, particularly HDF5 on libdaos. Similar runs for HDF5 on libdaos against a 4-node DAOS system, in Fig. 4 (c) and (d), show that HDF5 on libdaos can approach optimal hardware performance similarly to IOR on libdaos as shown in Fig. 4 (a) and (b). This points to a potential scalability issue in the HDF5 DAOS adaptor, as it can perform well at small scale but not at large scales. The scalability issue is likely to lie in the fact that the adaptor uses a DAOS container per parallel writing process, and this harms performance at large scales in DAOS as demonstrated in [8].

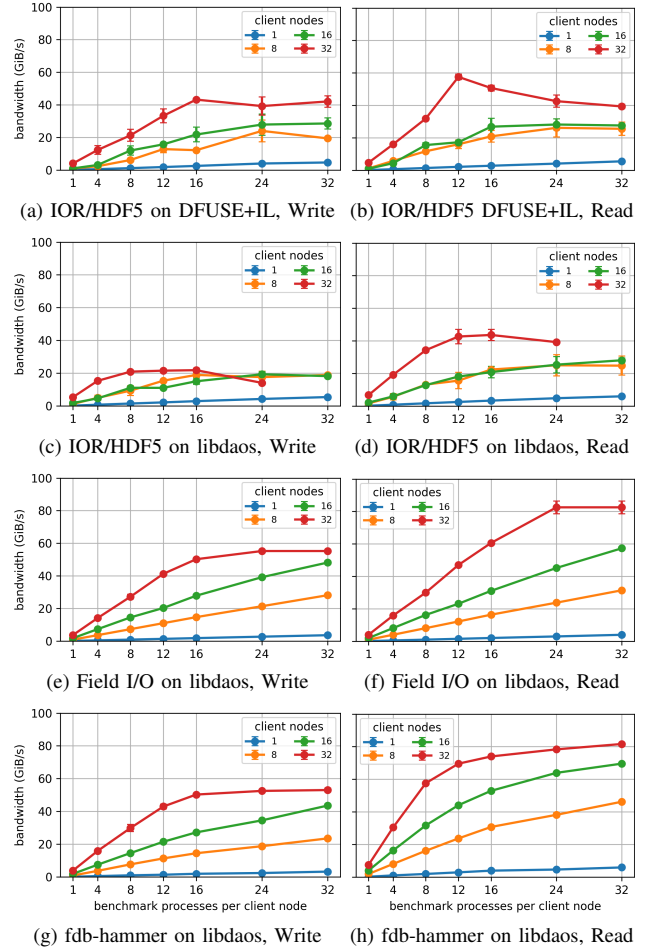


Fig. 3: Client node and process count optimisation results for the different DAOS applications, against a 16-node DAOS instance.

C. Scalability of DAOS and the APIs

We ran all benchmarks using the optimal client node and process counts, as determined in the previous section, against DAOS deployments on increasing numbers of nodes. The results, in Fig. 5, show that DAOS — when used via all APIs — and most applications can scale approximately linearly up to 24 DAOS server nodes, reaching close to ideal performance.

HDF5 on DFUSE reaches approximately half the performance and seems to stop scaling beyond 16 server nodes, but it should be noted that this application was designed for POSIX and ported with zero effort or tuning other than the adjustment of the DFUSE file object class. HDF5 on libdaos performs worse and stops scaling beyond 4 DAOS server nodes, and this is likely due to the discussed container scalability issue.

Nevertheless, this comparison between HDF5 on DFUSE and HDF5 on libdaos makes an excellent example of the benefit of running POSIX applications on DFUSE directly. They may not achieve optimal performance, but they can reach substantial performance with zero porting effort, exceeding the performance that a full libdaos porting would provide if not following all DAOS best practices [19].

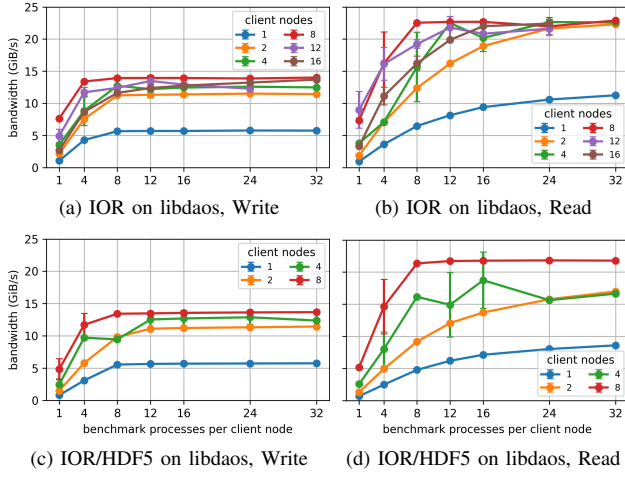


Fig. 4: Client node and process count optimisation results for IOR on libdaos and IOR/HDF5 on libdaos, against a 4-node DAOS instance.

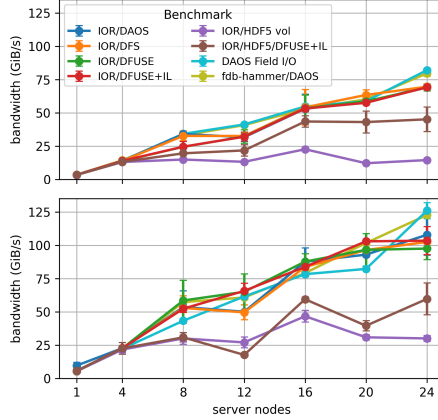


Fig. 5: Write scalability (top) and read scalability (bottom) of the DAOS APIs and applications, with no redundancy.

D. Performance of DAOS redundancy

We ran optimisation tests similar to those in Fig. 1 and Fig. 3, against a 16-node DAOS system, this time using 2+1 erasure-coding, preserving the same sharding configuration as in previous tests. Some of the most relevant results for the erasure-code tests are shown in Fig. 6.

As expected, erasure-coding did not harm read performance, with all tested benchmarks reaching the same read bandwidths as before. For write, the maximum bandwidths achieved are close to 40 GiB/s, that is, two thirds of the bandwidths obtained with no redundancy enabled. This is essentially optimal relative to the hardware available, as for an erasure-code configuration of 2+1, an additional 50% of data volume needs to be written, using 50% more NVMe device bandwidth.

For these tests, directories in libdfs and Key-Values in Field I/O and fdb-hammer were configured with a replication factor of 2 rather than with 2+1 erasure-coding, as it can be inefficient to perform erasure-coding on indexing entities that are being constantly modified.

Similar tests with a replication factor of 2 for both the Arrays/files and Key-Values/directories, not included here,

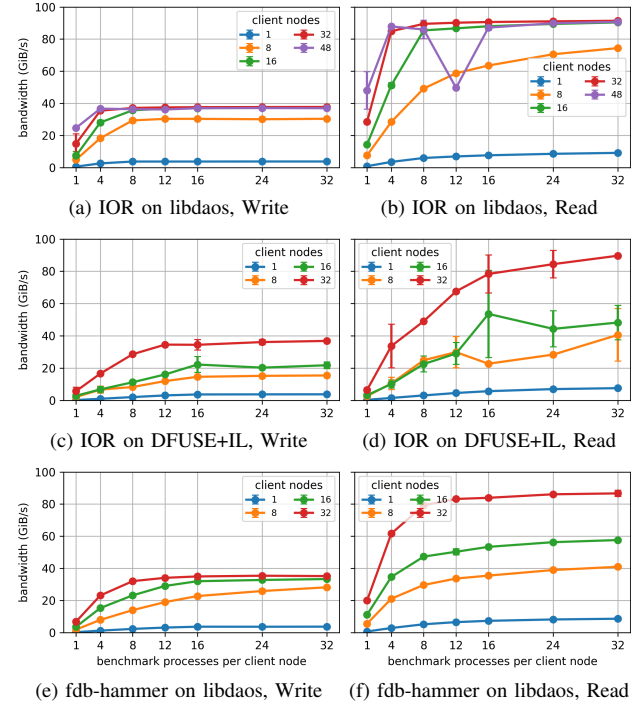


Fig. 6: Client node and process count optimisation results for IOR and fdb-hammer against a 16-node DAOS instance with EC 2+1.

showed similarly optimal results, with read bandwidth unaffected, and write bandwidths halved reaching up to 30 GiB/s.

E. Comparison to POSIX file system performance

We deployed a Lustre distributed file system on 16 NVMe nodes with identical hardware to the DAOS deployment, having 16 Object Storage Targets (OSTs) [20] deployed on each, plus an additional node with a single NVMe drive where a Metadata Service (MDS) [21] was deployed. Lustre was configured with no data protection enabled. We ran IOR and the fdb-hammer benchmarks, configured to use their POSIX backends, against this Lustre system.

IOR results, not included here, showed Lustre can also reach close to optimal hardware performance for large file-per-process I/O. Results for fdb-hammer tests, also using a file per process with striping across 8 OSTs and a stripe size of 8 MiB, are shown in Fig. 7.

These results show that fdb-hammer can reach close to IOR bandwidths for write, as fdb-hammer and its POSIX backend are optimised for write. fdb-hammer readers, however, only reach up to 40 GiB/s, and this is explained by the increased metadata workload, which Lustre and file systems in general are not optimised for. fdb-hammer on libdaos performing small I/O, however, can reach close to optimal performance for both write and read, as shown in Fig. 3 (g) and (h).

F. Comparison to Ceph object store performance

Ceph [22] — another open-source object store designed for data protection on commodity hardware, popular in Cloud environments — was deployed on 16 NVMe nodes, with

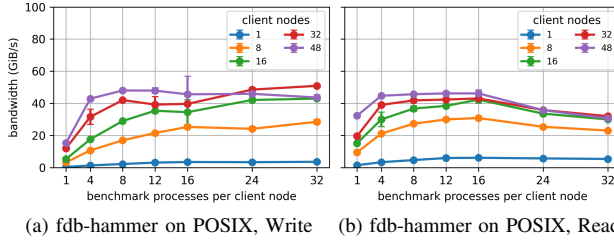


Fig. 7: Client node and process count optimisation results for fdb-hammer runs on POSIX, against a 16+1-node Lustre instance.

16 Object Storage Daemons (OSDs) [23] per node, plus an additional node with no NVMe where a Ceph Monitor [24] was deployed. Ceph was configured with no data protection. We ran IOR and fdb-hammer configured to use their Ceph backends, both making use of the librados library for direct operation with the core object storage functionality of Ceph.

IOR results using an object per process, not included here, showed Ceph could only reach up to 25 GiB/s for write and 50 GiB/s for read — roughly a half of the corresponding results for DAOS and Lustre. This IOR performance difference is explained on one hand because Ceph cannot shard objects across OSDs unless enabling erasure-code or replication, whereas IOR on DAOS and Lustre did benefit from sharding even if data protection was disabled. On the other hand, we configured Ceph with the recommended maximum object size of 132 MiB, and adjusted the IOR processes to perform each only 100 I/O operations of 1 MiB to fit in the per-process objects. This prevented IOR processes sustaining I/O to their assigned object for very long, thus not saturating the system. Configuring Ceph for larger object sizes is discouraged and resulted in low write performance.

fdb-hammer runs on Ceph, for which results are shown in Fig. 8, reached higher bandwidths of up to 40 GiB/s for write and 70 GiB/s for read. The number of Ceph Placement Groups (PGs) [25] was optimised, with the optimum value found to be 1024, to achieve balanced object placement across OSDs, and thus best performance. This performance increase with respect to IOR is explained by the fact that fdb-hammer processes perform 10k I/O operations of 1 MiB each, with a separate Ceph object for every I/O. This results in many objects being placed in a balanced way across PGs and thus efficiently exploiting all server bandwidth, and enables processes to sustain I/O for longer and saturate the system. The achieved performance, however, is only approximately two thirds of the ideal hardware bandwidth and significantly lower than the fdb-hammer bandwidths when run against DAOS.

These results indicate that Ceph can provide reasonable, albeit suboptimal, performance for applications using small object sizes, and is not designed to support high performance for large object sizes. These performance limitations could become more marked at larger scales.

Results for fdb-hammer runs on 32 client nodes against DAOS, Ceph and Lustre instances, extracted from Fig. 3 (e) and (f), Fig. 7, and Fig. 8, are shown superimposed in Fig. 9 for direct comparison of the reachable bandwidths with an

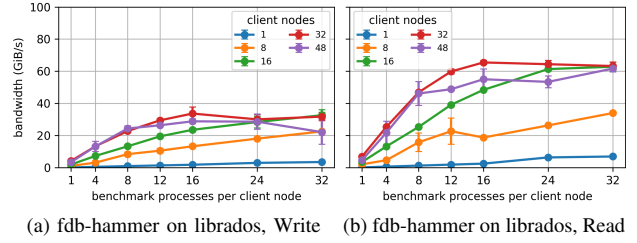


Fig. 8: Client node and process count optimisation results for fdb-hammer runs on librados, against a 16+1-node Ceph instance.

application such as fdb-hammer, operating with small-sized data units, optimised for the three storage systems.

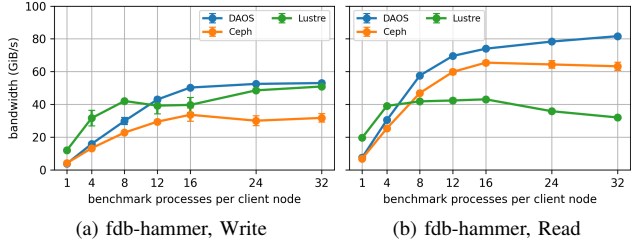


Fig. 9: Results for fdb-hammer runs on 32 client nodes against deployments of DAOS on 16 nodes, Ceph on 16+1 nodes, and Lustre on 16+1 nodes.

IV. CONCLUSIONS

This work has demonstrated that DAOS on NVMe and all DAOS interfaces perform and scale very well, at least up to the scale tested and with an I/O size of 1 MiB — much smaller than any distributed file system could support while preserving high performance.

Applications making direct use of libdaos can perform and scale equally as well if following certain best practices for high performance. Even though HDF5 on DFUSE and HDF5's DAOS adaptor do not perform or scale as well as the rest, they have demonstrated that running existing POSIX applications on DFUSE can give reasonable performance with zero porting effort, and indeed better than porting to libdaos when best practices are not followed with that interface.

We have also demonstrated DAOS can support replication and erasure coding without degrading performance more than is strictly required given the underlying hardware, although it unavoidably implies a reduction in total storage capacity.

Finally, this work has briefly compared DAOS performance to Ceph and a distributed POSIX file system, and demonstrated the potential of DAOS as storage for HPC systems, as it is the only option that can provide high performance both for large I/O as well as for metadata and small I/O workloads. This can give more freedom for applications to perform I/O as desired without requiring a major redesign to adapt to specific well-performing I/O patterns.

ACKNOWLEDGMENT

For the purpose of open access, the authors have applied a Creative Commons Attribution (CC BY) licence to any Author Accepted Manuscript version arising from this submission.

REFERENCES

- [1] Z. Liang, J. Lombardi, M. Chaarawi, and M. Hennecke, "DAOS: A Scale-Out High Performance Storage Stack for Storage Class Memory", In: Panda, D. (eds) Supercomputing Frontiers. SCFA 2020. Lecture Notes in Computer Science(), vol 12082. Springer, Cham. DOI:10.1007/978-3-030-48842-0_3.
- [2] A. Dilger, D. Hildebrand, J. Kunkel, J. Lofstead, G. Markomanolis, S. Ihara, and H. Nolte, "IO500 10 node list Supercomputing 2023", November 2023. <https://io500.org/list/sc23/ten-production>
- [3] A. K. Paul, O. Faaland, A. Moody, E. Gonsiorowski, K. Mohror, and A. R. Butt, "Understanding HPC Application I/O Behavior Using System Level Statistics", 2020 IEEE 27th International Conference on High Performance Computing, Data, and Analytics (HiPC), Pune, India, 2020, pp. 202-211, doi: 10.1109/HiPC50609.2020.00034.
- [4] G. Lockwood, "What's so bad about POSIX I/O?". The Next Platform 2017. <https://www.nextplatform.com/2017/09/11/whats-bad-posix-io/>
- [5] A. George, and R. Mohr, "Understanding Lustre Internals", 2024. https://wiki.lustre.org/Understanding_Lustre_Internals
- [6] F. Schmuck, and R. Haskin, "GPFS: A Shared-Disk File System for Large Computing Clusters", 2002. https://www.usenix.org/legacy/publications/library/proceedings/fast02/full_papers/schmuck/schmuck_html/index.html
- [7] "DAOS File System", 2024. <https://docs.daos.io/v2.4/user/filesystem/#dfuse-daos-fuse>
- [8] N. Manubens, T. Quintino, S. D. Smart, E. Danovaro, and A. Jackson, "DAOS as HPC Storage: a View From Numerical Weather Prediction", 2023 IEEE International Parallel and Distributed Processing Symposium (IPDPS), St. Petersburg, FL, USA, 2023, pp. 1029-1040, doi: 10.1109/IPDPS54959.2023.00106.
- [9] N. Manubens, S. D. Smart, E. Danovaro, T. Quintino, and A. Jackson, "Reducing the Impact of I/O Contention in Numerical Weather Prediction Workflows at Scale Using DAOS", 2024 Proceedings of the Platform for Advanced Scientific Computing Conference (PASC '24). Association for Computing Machinery, New York, NY, USA, Article 12, 1–12. <https://doi.org/10.1145/3659914.3659926>
- [10] "HPC IO Benchmark Repository", 2024, GitHub repository. <https://github.com/hpc/ior>
- [11] The HDF Group. "Hierarchical Data Format, version 5 [Computer software]", <https://github.com/HDFGroup/hdf5>
- [12] J. Soumagne et al., "Accelerating HDF5 I/O for Exascale Using DAOS," in IEEE Transactions on Parallel and Distributed Systems, vol. 33, no. 4, pp. 903-914, 1 April 2022, doi: 10.1109/TPDS.2021.3097884
- [13] N. Manubens, A. Jackson, T. Quintino, S. Smart and E. Danovaro, "DAOS weather field I/O tests", 2024, GitHub repository [ecmwf-projects/daos-tests](https://github.com/ecmwf-projects/daos-tests) (0.2.0). DOI:10.5281/zenodo.10699254.
- [14] "fdb-hammer.cc", 2024, GitHub repository file. <https://github.com/ecmwf/fdb/blob/master/src/fdb5/tools/fdb-hammer.cc>
- [15] S. Smart, T. Quintino, and B. Raoult. "A High-Performance Distributed Object-Store for Exascale Numerical Weather Prediction and Climate". In Proceedings of the Platform for Advanced Scientific Computing Conference (PASC '19). Association for Computing Machinery, New York, NY, USA, Article 16, 1–11. DOI:10.1145/3324989.3325726.
- [16] "General-purpose machine family for Compute Engine", 2024. <https://cloud.google.com/compute/docs/general-purpose-machines>
- [17] "Set the number of threads per core", 2024. <https://cloud.google.com/compute/docs/instances/set-threads-per-core>
- [18] "DAOS Storage Model", 2024. <https://docs.daos.io/v2.0/overview/storage/>
- [19] A. Jackson and N. Manubens, "Profiling and identifying bottlenecks in DAOS", DAOS User Group 2023 https://www.research.ed.ac.uk/files/392151952/DUG23_FDB_DAOS.pdf
- [20] "Lustre Object Storage Service (OSS)", 2024. [https://wiki.lustre.org/Lustre_Object_Storage_Service_\(OSS\)](https://wiki.lustre.org/Lustre_Object_Storage_Service_(OSS))
- [21] "Lustre Metadata Service (MDS)", 2024. [https://wiki.lustre.org/Lustre_Metadata_Service_\(MDS\)](https://wiki.lustre.org/Lustre_Metadata_Service_(MDS))
- [22] "Welcome To Ceph", 2024. <https://docs.ceph.com/en/reef/>
- [23] "Ceph-OSD – Ceph Object Storage Daemon", 2024. <https://docs.ceph.com/en/latest/man/8/ceph-osd/>
- [24] "Ceph-Mon – Ceph Monitor Daemon", 2024. <https://docs.ceph.com/en/latest/man/8/ceph-mon/>
- [25] "Placement Groups", 2024. <https://docs.ceph.com/en/latest/rados/operations/placement-groups/>

Appendix: Artifact Description/Artifact Evaluation

Artifact Description (AD)

V. OVERVIEW OF CONTRIBUTIONS AND ARTIFACTS

A. Paper's Main Contributions

- C_1 Demonstration that DAOS on NVMe and all DAOS interfaces can perform and scale very well with an I/O size of 1 MiB.
- C_2 Demonstration that applications making direct use of libdaos can also scale very well, although HDF5 on libdaos or DFUSE does not scale so well.
- C_3 Demonstration that DAOS can support replication and erasure coding without degrading performance more than is strictly required.
- C_4 Demonstration that, compared to Lustre and Ceph, DAOS is the only option that can provide high performance both for large I/O as well as for metadata and small I/O workloads.

B. Computational Artifacts

A_1 <https://doi.org/10.5281/zenodo.13757427>

Artifact ID	Contributions Supported	Related Paper Elements
A_1	C_1, C_2, C_3, C_4	All figures

VI. ARTIFACT IDENTIFICATION

A. Computational Artifact A_1

Relation To Contributions

This artifact includes scripts and configuration, all contained in the `google` directory (all other directories are irrelevant to the analysis in this paper), to deploy Lustre and Ceph on NVMe on Google Cloud, as well as to deploy an auto-scaling Slurm cluster of client nodes to run benchmarks against DAOS, Lustre and Ceph deployments. Scripts and configuration to deploy DAOS systems are property of Google Cloud and have not been made publicly available.

The artifact also includes scripts and configuration to build and run the I/O benchmarks in the Slurm cluster to reproduce all tests reported in the paper.

Therefore, this artifact can reproduce all tests necessary to verify all contributions (C_1, C_2, C_3, C_4) of this paper.

Expected Results

IOR on libdaos, libdfs, DFUSE and DFUSE+IL, and Field I/O and fdb-hammer against DAOS, should perform and scale very well up to 24 NVMe server nodes. IOR on HDF5 on libdaos and DFUSE+IL should perform and scale worse.

Using a DAOS replication factor of 2 or erasure-coding of 2+1 should not harm read performance, and should reduce write performance down to a half for replication and two thirds for erasure-coding.

IOR against Lustre should perform as well as IOR against DAOS deployed on equivalent amount of NVMe server nodes. fdb-hammer against Lustre should perform as well as against DAOS for write, and worse than DAOS for read.

IOR against Ceph should perform significantly worse than IOR against DAOS deployed on an equivalent amount of NVMe server nodes. fdb-hammer against Ceph should reach bandwidths approximately two thirds as high as those observed for fdb-hammer against DAOS.

Expected Reproduction Time (in Minutes)

The Artifact Setup is expected to require 360 minutes, not including the time required to follow and manually execute the steps of the build procedure or to set up the Google Cloud account and quota. This is because a number of images need to be built for the different storage systems and the Slurm cluster, and also because the deployment of these complex systems takes a substantial amount of time until ready. Additionally, because the testing is performed on preemptible virtual machines, the deployment of these systems may need to be repeated several times before all tests are completed.

The Artifact Execution can require approximately 20000 minutes of wall-clock time. For every data point in every figure in the paper, three test repetitions need to be run, each requiring between 1 and 10 minutes of wall-clock time.

The artifact analysis can require approximately 1000 minutes of wall-clock time, as many log files need to be processed to calculate the bandwidth measurements, and the figures need to be generated.

Artifact Setup (incl. Inputs)

Hardware: The tests are run entirely in Google Cloud infrastructure, using virtual machines of type n2 and c2, some of them (the server machines) with locally attached NVMe SSDs. This artifact includes configuration resources which specify and provision the exact type of resources required.

Software: The required software packages include DAOS, Ceph, Lustre, Slurm, MPI, IOR, HDF5 and its DAOS adaptor, Field I/O, and fdb-hammer. These — except Slurm and MPI — are introduced in the paper. The version numbers employed for the analysis have all been hard-coded in the build and install scripts in this artifact, which fetch all sources or binaries from public repositories.

Datasets / Inputs: The benchmarks in this paper generally do not require special input files, as they generate random data to be written or read from the different storage systems. Where benchmarks require input configuration or seed data files, they have been included in this artifact.

Installation and Deployment: As performed by the scripts included in the artifact.

Artifact Execution

The following steps need to be followed to execute this artifact.

- Obtain a Google Cloud Platform account.
- Install Google Cloud SDK (last tested with v488.0.0), go (last tested with v1.22.1), Terraform (last tested with v1.9.4) and hpc-toolkit (last tested with v1.38.0).
- Clone this artifact.
- Run the scripts to provision the different storage systems (one at a time) and the Slurm client cluster, available in the artifact under `google/ceph/deployment/deploy.sh`, `google/lustre/deployment/deploy.sh`, and `google/slurm/deploy.sh`, respectively.
- Open an ssh connection to the Slurm controller node with `gcloud compute ssh`.
- Clone this artifact under `$HOME/daos-tests` in the controller node.
- Locate the master test script, in function of the storage system and benchmark to be tested, available in the artifact under `google/<storage system>/<benchmark>/access_patterns/A.sh`.
- Adjust the master test script with the amounts of server nodes (specified in the `servers` variable), client nodes (specified as a vector via the `C` variable) and processes per client node (specified as a vector via the `N` variable) to test with. The amount of I/O iterations per process and test repetitions can also be adjusted (via the variables `WR` and `REP`), but are generally set to 10k and 3 by default, respectively. For IOR tests, the IOR APIs to test with can also be adjusted via the `API` variable. For DAOS tests, the object class can be adjusted via the `OC` variable.
- Change directories to the `google/<storage system>` directory, and invoke the master script with `source <benchmark>/access_patterns/A.sh`.
- When executed, a master script performs the following tasks:
 - check that the storage system is available
 - spin up the required Slurm client nodes
 - build and/or install the client software if not present
 - execute the benchmark in a loop for all configured client node and process counts, APIs, object classes, and repetitions
- All test output is stored in a directory hierarchy under `google/<storage system>/runs`.

Artifact Analysis (incl. Outputs)

For every test run, the timestamp reported before the first I/O and the timestamp reported after the last I/O across all parallel processes have to be extracted from the log files for that run, and the time difference between the two calculated. The total amount of data written or read by all processes in the test run is then divided by the time in seconds obtained in the previous step, resulting in a bandwidth measurement in bytes per second. The average and standard deviation of the bandwidths for the three repetitions for every test are calculated and used as data point for the figures.